A COMPARATIVE STUDY OF HAND-HELD MAGNETIC SUSCEPTIBILITY INSTRUMENTS

By

Deng Ngang Deng

A thesis submitted in partial fulfillment
of the requirements for the degree of
Master of Science (MSc) in Geology

The Faculty of Graduate Studies
Laurentian University
Sudbury, Ontario, Canada

THESIS DEFENCE COMMITTEE/COMITÉ DE SOUTENANCE DE THÈSE
Laurentian Université/Université Laurentienne
Faculty of Graduate Studies/Faculté des études supérieures

Title of Thesis
Titre de la thèse A COMPARATIVE STUDY OF HAND-HELD MAGNETIC SUSCEPTIBILITY INSTRUMENTS

Name of Candidate
Nom du candidat Deng, Deng

Degree
Diplôme Master of Science

Department/Program
Département/Programme Geology

Date of Defence
Date de la soutenance October 24, 2014

APPROVED/APPROUVÉ

Thesis Examiners/Examinateurs de thèse:

Dr. Richard Smith
(Supervisor/Directeur de thèse)

Dr. Andrew McDonald
(Committee member/Membre du comité)

Mr. Bill Spicer
(Committee member/Membre du comité)

Dr. Randy Enkin
(External Examiner/Examinateur externe)

Approved for the Faculty of Graduate Studies
Approuvé pour la Faculté des études supérieures
Dr. David Lesbarrères
M. David Lesbarrères
Acting Dean, Faculty of Graduate Studies
Doyen intérimaire, Faculté des études supérieures

ACCESSIBILITY CLAUSE AND PERMISSION TO USE

Abstract

A study to compare six magnetic susceptibility (MS) instruments (the KT-10 supplied by Terraplus Inc., RT-1 produced by Fugro, SM30 produced by ZH Instruments, MS2K & MS2C produced by Bartington Instruments and MPP-EMS2+ probe produced by GDD Instruments (denoted as GDD)) was conducted to characterize the equipment on the basis of their accuracies, resolution, reproducibility, ease of use and response to drift. MS data were collected on BQ core from 3 holes, NQ core samples, 2 rock samples and 2 calibration samples at the Vale office in Thompson, Manitoba. The results show that the GDD and MS2K are most affected by temporal drift whereas the KT-10 and MS2C gave more repeatable results. The MS2C, MS2K and GDD generally gave higher susceptibility readings than the rest of the meters. It was also noted that measurements on the flat face of half-core samples were always higher compared to measurements on their respective whole core samples. There is a correlation between instruments, frequencies and sensitivities, but no relationship between frequencies of operation and temporal drift.

Keywords

Magnetic susceptibility instruments, measurements, temporal drift, instrument accuracy, data quality, quality control protocols, calibration standards, Terraplus' KT-10, GDD's MPP probe, Fugro's RT-1, ZH's SM30, Barrington's MS2C, MS2K & MS3, Bartsoft, correlations, lower limits of accuracy, sensitivity, frequency dependence, instrument design, sensing area, sensor size and inductive coil.

Acknowledgement

The author would like to sincerely thank the research partners: NSERC, Vale, Sudbury Integrated Nickel Operations, a Glencore Company, KGHM International, Wallbridge Mining and The Centre for Excellence in Mining Innovation (CEMI) for their financial support throughout the course of this research. Without their funding, this research would have not been a success. Many thanks go to Vale for giving me the time to attend classes and permission to use their core and rock samples.

I am very grateful to my thesis advisory committee: Dr. Richard Smith, Mr. Bill Spicer and Dr. Andy McDonald for their continuous support and quick feedbacks. Their professional guidance, coaching and criticism were exceptional and have significantly improved the quality of the thesis and expanded the scope of my project. I would also like to thank Desmond Rainsford of the Ontario Geological Survey for sharing his expertise and for suggesting invaluable techniques during data analysis.

Special thanks to Vale's Thompson Brownfield Exploration, especially Robert Stewart and Graeme Gribbin for giving me the space to keep my research equipment and for allowing me to maintain my office for studies even after I transferred to the Mine. I also acknowledge all the technical assistance offered by Brian Parson during data collection and processing. Many thanks also go to Christine Giroux and Andrew Mackie for processing downhole probe data (noted as BSS -02B data).

I would also like to thanks my friends and relatives especially Chol Dakbai Ngang, Dhieu Magot Piok, Martha Adhieu Gideon Dau, Brigadier Achiek Ajith Joh, Aluou Ajak Aluou, Ngor Lueth Madit, Ajah Garang Mathiang, sister Ann Apajok Malith, Riak Mach Riak, mama Ajoh Jong Aruor, David Sidebottom, David Chol Mayen, Machar Buol Deng, Buol Achiek Ngong, Alier Abuol Jok, Atong Mach Aduot, Mangar Abuoi Athiek, Deng Duoi Ngarawang, Asni Mekonnen, Kuol Majak Anyieth,

uncle Panchol Ajak, Matthews Chol Deng Kuir, Liliane Vicente, Duot Ateny Nyieth, Bol Ateny Nyieth, Ajok Magok, Rev. Aguto Majok, uncle Achuoth Kuckon Achuoth, uncle Kur Mayen Alier, Malou Del Malou, Ajak Mabut Ajak, James Kuol Pat, Kuol Achiek Kuot, Jacob Awan Reng, Deng Kuol Madoot, Wuoi Athieu Mach, aunty Yar Lukuach Mach, Mach Agor Guem, Peter Mathiang Ngong, David Panchol Alier, Jok Kuol Mayom, Mama Keth Anyang, Mama Abuk Majok, Martha Achol Biar, Bor community in Australia, Yom Panchol Wel, late aunt Akuol Malou Akol, Mabior Gai Deng, Panther Kuol Aguto, koko Akuch Deng Diing, Ajak Malual Jok and Kuol Diing Deng. Without your support, words of wisdom and encouragement, I would have not come this far. Thank you

Last but not least, I thank my father Mr. Ngang Deng Gai and my mother Rev. Rebecca Ateny Kuol Lueth for raising me and my siblings in the most harmonious family and for their tremendous investment in my education. Thank you dad for sharing your experiences with me, especially those that emphasized the importance of education. My utmost appreciation goes to my beloved wife Yom *Mawut Gai Ayuel Yuot*, for her love, patience, support and encouragement during this research.

Dedication

To:

My lovely

Son: Ajak Deng Ngang

Wife: Yom Mawut Gai Ayuel

Parents: Mr. Ngang Deng Gai and Rev. Ateny Kuol Lueth

Siblings: Akoi, Aguet, Akuot, Nyiel, late Ajak, Gai, Diing, Konuong, late Deng Jr. & Deng A.

Declaration

I, **Deng Ngang Deng**, declare that the master's thesis entitled "**A Comparative Study of Hand-Held Magnetic Susceptibility Instruments"** is no more than 100,000 words in length including quotes and exclusive of tables, figures, appendices and references. It contains no material that has been submitted previously, in whole or in part, for the award of any other academic degree or diploma other than the cited literature. I strongly declare that this thesis is solely my own work.

I also declare that this master's thesis is an academic document that focuses purely on scientific and technological advancement, hence its findings are not endorsement of any of the products studied. I, the author, declare that I do not have any connection with any of the companies that produce or supply the devices whatsoever.

Signature: *Deng Ngang Deng* Date: 30*st November, 2014*

Table of Contents

List of Tables

Table 51: Calculated means, standard deviations, percent coefficient of variations, range and variance that were used in assessing the suitable modes in each instrument; data was obtained from borehole 1301020

Table 52: Shows the averaged MS data collected on KT-10 calibration sample using all instruments, except MS2C because of the shape and size of the sample

Table 53: Shows data collected using the six hand-held MS instruments and the BSS-02B probe used with the IFG interface box

Table 54: Show MS measurements collected using KT-10 meter on KT-10 calibration sample. The data was used to assess the two modes and the pin option

LIST OF FIGURES

Chapter 1: Introduction

1.1 Introduction

Numerous studies involving physical property measurements of rocks and unconsolidated soils have been undertaken in the past five decades (Zhao, 1996; Airo et al., 2011; Dearing et al., 1996; Borradaile and Henry, 1997; McFadden and Scott, 2013; Potter, 2005; Lee and Morris, 2013; Retallack et al., 2003; Schibler et al., 2002; Enkin et al., 2012, Oniku et al., 2008 and Girault et al., 2011). The physical properties measured usually include but are not limited to conductivity, density, magnetic susceptibility (MS), temperature, porosity and permeability.

MS measurements correlate with resources (sulphide mineralogy and even oil and gas) as well as other natural occurrences (McDowell et al., 2007; Potter, 2005 and Borradaile and Henry, 1996). In the early 2000s, a test for nickel-grade estimation using MS probes in blast-holes was performed in Sudbury Ontario by McDowell et al. (2007). The measurements showed a direct correlation between nickel grade and the MS values in low sulphide zones (figure 1B). This use of MS as an exploration tool complements the use of conductivity probes (McDowell et al., 2007), which have traditionally been used in blast-holes to delineate ore zones in a mine area (McDowell et al., 2004), but did not show a correlation in this case (figure 1A).

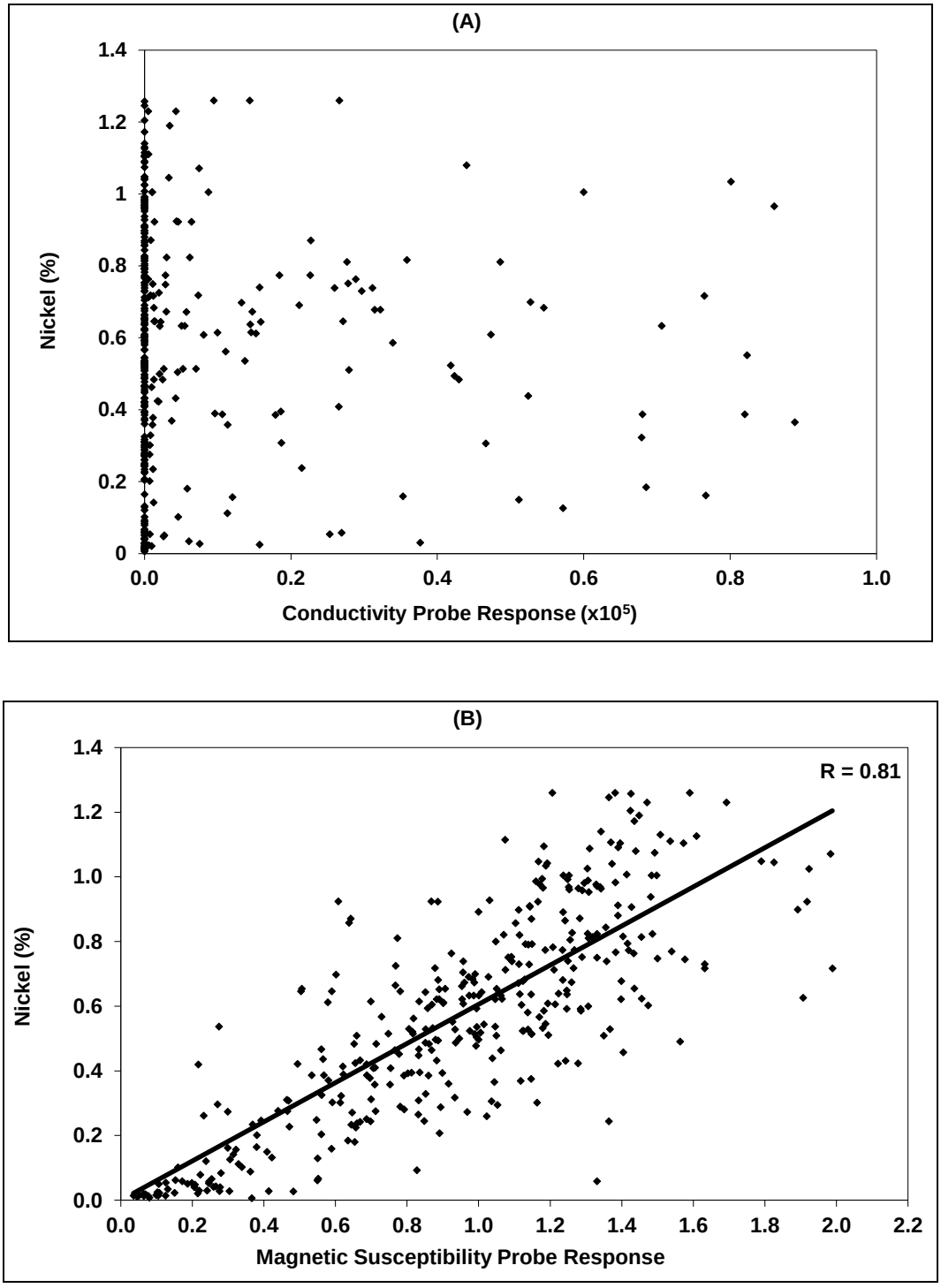

Figure 1: A) Nickel grade plotted against conductivity and B) magnetic susceptibility. In this case, magnetic susceptibility measurements show a correlation, whereas conductivity does not (After McDowell et al., 2007).

Airo et al., (2011) presented petrophysical properties of the Outokumpu deep drilling program conducted between 2003 and 2010. The results showed a magnetic anomaly in serpentinized ultramafic that could be delineated using MS measurements. This observation is similar to the findings in Zhao (1996), which reported the magnetic signature of serpentinized peridotite samples obtained from Ocean Drilling Program's Leg 149 sites 897 and 899.

Other uses of MS measurements are environmental assessment and the testing of soil magnetism (Dearing et al., 1996; Girault et al., 2011; McFadden and Scott, 2013). Dearing et al., (1996) studied MS values for topsoil and other geochemical and geological data to characterize the types of soils across England. Girault et al., (2011) used low-field MS measurements and effective radium concentration to characterize soil samples from Nepal. McFadden and Scott (2013) carried out an experiment on how soil MS affect the success of electromagnetic induction by studying 43 samples from the United States, Puerto Rico, Iraq and Afghanistan. The results of these studies show MS measurements as a cheap but effective means of understanding soil magnetic properties.

The increased interest in acquiring physical property measurements has triggered a demand for better instruments to measure these physical quantities accurately and efficiently. There are numerous instruments for measuring data: wireline probes and hand-held devices. However, each manufacturer has a particular objective when designing their instruments so the specifications and measurement procedures will be different.

In the case of MS meters, the variations in coil size and operating frequency and electronic design, influence the meter's reaction to factors such as thermal or temporal drift, change in ambient magnetic

field as well as the device's resolution and sensitivity. To assess the characteristics of each meter requires consistent procedures in order to evaluate the accuracy and reproducibility of the equipment. One way of evaluating the instruments is to measure the susceptibility of calibration samples with known MS readings; another way is to take measurements on a wide variety of samples.

A comprehensive understanding of physical properties of a rock (Smith et al., 2012) is important to mineral exploration. However, the physical property measurements are as good as the instrument that measured them. This is because the accuracy and precision of each instrument affect the result being measured. Bad results can lead to poor interpretation and poor conclusions.

1.2 Research objectives

This project aims to compare six handheld magnetic susceptibility meters on the basis of their accuracy, reproducibility, resolution and susceptibility to drift. Experience with the instruments also allows an assessment of the ease of use of the instruments and their suitability for different tasks. In addition a downhole conductivity and magnetic susceptibility probe (BSS-02B), manufactured by *Bartington Instruments*, was used to collect MS measurements from one of the three selected holes, to provide a seventh set of measurements.

1.3 Methodology

Specimens were selected from Vale exploration drill core and outcrop (flat and freshly cut surfaces) in the Thompson Nickel Belt. The drill-core and outcrop samples encompass a wide range of rock

types from weakly magnetic quartzite to highly magnetic massive sulphides, iron formation and serpentinized ultramafic. This provided a wide range of MS values over which the instruments can be tested. The standard calibration samples (the KT10 calibration pad and MS2C calibration rod) were also used to compare each instruments' reproducibility and the relative differences between the values obtained using different instruments.

Quality control protocols were observed during data collection. These included taking at least 5 readings at each point and then calculating the average and standard deviation; ensuring there was no metallic or magnetic material within 50 ft of the sensor during the measurement; and collecting data at the same location (point on the core or sample) using different meters. In addition, instruments were calibrated daily. Any deviation from manufacturer's stated values were noted and used to calculate daily standard deviations.

After measurements were compiled, various analyses were undertaken: drift analyses, measures of central tendency, and measures of dispersion and correlation cross-plots. This was then followed by integrated interpretation of the results. Conclusions are drawn and recommendations made.

Chapter 2: Rock magnetism

2.1 Introduction to magnetic susceptibility

Magnetic susceptibility (MS) is defined as a parameter for each sample that quantifies the ease with which the material in the sample can be magnetized. For any given material, the MS (also denoted χ) is given as

$$\chi = \mathbf{M}/\mathbf{H}, \quad (1)$$

where **M** is the magnetization induced as a consequence of an applied field **H** (A/m).

The MS is a dimensionless quantity, so it is normally given the units (SI) when the magnetization and the applied magnetic fields are in A/m. Another dimensionless unit for MS measurements is cgs, which differs from SI by a factor of 4π. To better understand the reasons why rocks have magnetic susceptibility, we shall review rock magnetism in the following section.

2.2 Magnetic properties of rocks

Contrasts in magnetic properties in different rocks arise due to variations in the concentrations and types of magnetic grains present (Hrouda et al., 2009; Oniku et al., 2008; Searl, 2008) and the size of those mineral grains. These authors conclude that in general the MS is largely a measure of the content of magnetite (Fe_3O_4) and its solid solution ulvöspinel (Fe_2TiO_4). Other minerals such as monoclinic pyrrhotite and ilmenite are also magnetic and can result in a large MS readings (Hroud et al., 2009). Stronger MS result from greater concentrations of these minerals. The tables 1a - d below give the MS measurement for various minerals.

Table 1a - d: MS of minerals modified after Hrouda (2009), Bleil and Petersen (1982), Kropaček (1971) and Krs and Kropaček (1987). Only the minerals of interest have been presented in these tables. The symbol * indicates a value for that mineral is not in the referenced data.

1a): sulphides

1b)

minerals	**Formula**	**SI [10^{-6}]**
Pyrite	FeS_2	-6.3 to 63
Galena	PbS	-33 to 9.3
Chalcopyrite	$CuFeS_2$	308 - 411
Cobaltite	CoAsS	553 - 157892
pyrrhotite	$Fe_{(1-x)}S$ (x = 0 to 0.2)	*

Oxides

Minerals	**Formula**	**SI [10^{-6}]**
Spinel	$MgAl_2O_4$	30
Rutile	TiO_2	107
Hematite	Fe2O3	1300 – 7000
Chromite	$FeCr_2O_4$	2827 – 7069
Ilmenite	FeTiO3	8042
Maghemite	γ-Fe_2O_3	Up to 3000000
Jacobsite	MnFe2O4	50000 – 3000000
Magnetite	Fe_3O_4	3000000

1c) Carbonates and graphite

Minerals	**Formula**	**SI [10^{-6}]**
Aragonite	$CaCO_3$	-15.0
*Graphite	C	-177
Calcite	$CaCO_3$	-13.1
Dolomite	$CaMg(CO_3)_2$	11.3
Siderite	FeCO3	2770 – 3170

1d) Silicates

Silicates	**Formula**	**SI [10^{-6}]**
Quartz	SiO_2	-15.4
Orthoclase	$KAlSi_3O_8$	-13.7
Forsterite	Mg_2SiO_4	-12.6
Opal	$SiO_2 \cdot nH_2O$	-12.9
Muscovite	$KAl_2(AlSi_3O_{10})(F,OH)_2$	36-711
Enstatite	$MgSiO_3$	121
Phlogophite	$KMg_3AlSi_3O_{10}(F,OH)_2$	176-281
Actinolite	$Ca_2(Mg,Fe)_5Si_8O_{22}(OH)_2$	490
Augite	$(Ca,Na)(Mg,Fe,Al,Ti)(Si,Al)_2O_6$	555-1111
Clinopyroxene	$(Ca,Mg,Fe,Al)_2(Si,Al)_2O_6$	613
Hornblende	$(Ca,Na)_{2-3}(Mg,Fe,Al)_5(Al,Si)_8O_{22}(OH,F)_2$	746-1368
Staurolite	$Fe^{2+}{}_2Al_9O_6(SiO_4)_4(O,OH)_2$	790 -1590
Biotite	K(Mg,Fe)3AlSi3O10(F,OH)2	873-3040
Epidote	$Ca_2Al_2(Fe^{3+};Al)(SiO_4)(Si_2O_7)O(OH)$	1010
Diopside	$MgCaSi_2O_6$	1319
Hedenbergite	$FeCaSi_2O_6$	2783
Riebeckite	$Na_2Fe^{2+}{}_3Fe^{3+}{}_2Si_8O_{22}(OH)_2$	3016
Ferrosilite	$FeSiO_3$	3670
Orthopyroxene	$(Mg,Fe)_2Si_2O_6$	3700
Fayalite	Fe_2SiO_4	4976

One aspect of these tables is that for some minerals, e.g. Augite, there is a range of values given. In other cases, there is a single value. In the former case, the specific distribution of values within the range is not specified. For example, it is unclear if the values are spread uniformly across the range, or are clustered tightly about a mean. In the cases when there is only one value, it is not specified whether there was only one sample that was measured or because all samples have this value. From these tables, it is possible the magnetic properties of rocks could be used to discriminate minerals within rocks and possibly the rocks themselves. However, knowing the susceptibility alone does not

define the mineral uniquely. For example a reading close to 1000 x 10^{-6} SI could be one of many minerals. For a rock, low and high susceptibilities would not necessarily define the minerals in the rock, but more likely the value is indicative of the percentage of magnetite in the rock. However, the susceptibility of a rock can be used to help geologists and geophysicists explore for mineral deposits.

Generally, materials which are strongly magnetic are either **ferromagnetic or ferrimagnetic** (with large positive MS values) e.g. magnetite and pyrrhotite. On the other hand, minerals with negative MS are **diamagnetic** and include calcite, quartz, orthoclase, graphite and forsterite (a Mg-bearing Olivine). There are also **paramagnetic** minerals with positive but low susceptibilities, which include rutile, biotite, pyroxenes, olivine among others. There are also **anti-ferromagnetic** materials, where the positive and negative magnetic moment within the mineral would cancel out to zero but the spin results in positive moderate magnetic susceptibility (e.g. Hematite).

According to Ivakhnenko (2012) diamagnetic substances reduce the density of magnetic field lines, and weakening the applied fields; whereas paramagnetic, ferrimagnetic, anti-ferromagnetic and ferromagnetic materials reinforce the density of magnetic field lines and create a stronger force. Since magnetite is the dominant source of strong magnetism in rocks, the rock susceptibility measurements cannot be higher than that of a pure monomineralic magnetite grain with approximately 3 SI (Hrouda, 1986 and Heider et al., 1996). Therefore, measurements above 3 SI should be inspected for potential sources of errors.

.

Enkin et al. (2012) further demonstrated how rocks could be grouped on the basis of their magnetic responses: magnetite and paramagnetic rocks have susceptibilities in the ranges of 10^{-2} SI and 10^{-4} SI respectively, whereas pure quartz and pure carbonates are diamagnetic and can give susceptibilities which could be as low as -15 x 10^{-6} SI.

2.3 Rocks characterization using magnetic susceptibilities

A rock, defined as an aggregate of minerals, combines elements or compounds in a given ratio. The second order mineralogy, grain size and atomic structures determine the rock's petrophysical properties such as density, porosity, permeability, conductivity and magnetic susceptibility. These properties can be measured directly or remotely and analyzed to predict the economic potential of an area. Despite its non-uniqueness, the MS measurements can be used to characterize rocks.

Potter (2005) demonstrated the use of MS measurements to estimate permeability and porosity of sediments in an oilfield in conjunction with gamma ray wireline logs. He suggested that the application of MS would allow for easy and cost effective way of characterizing sedimentary basins.

Another contribution to the advancement of MS as an emerging technology is described by Hrouda et al. (2009). The paper presented the influence of ***metamorphism***, ***metasomatism*** and ***alteration*** on the magnetic properties of a rock and how these processes can be mapped. This follows the generalization that susceptibility in fresh volcanic rock is controlled by variations in titanomagnetites and any change in the chemistry of these minerals during alteration (or metamorphism) can result in a measurable change in their MS. For example, increasing **metamorphism** leads to decreasing MS values due to the breakdown of magnetite but quickly increases once again when pyrite (a diamagnetic mineral) changes to pyrrhotite (a ferrimagnetic mineral). Hrouda et al. 2009 discussed how they used these subtle changes to trace metamorphic zones and isograds.

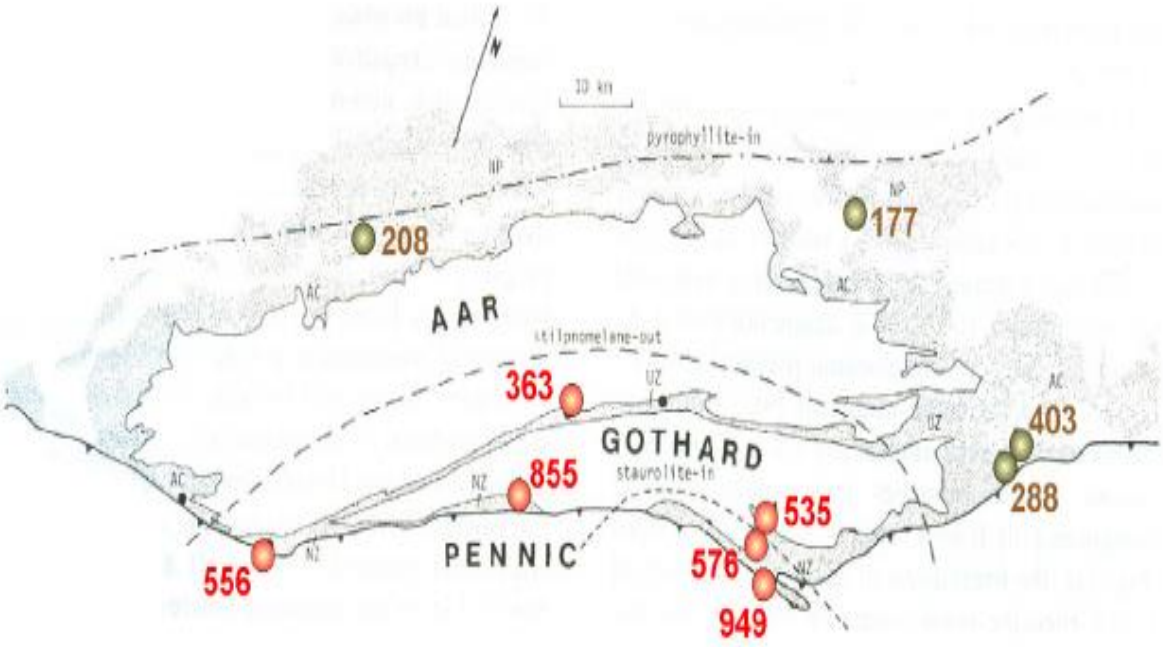

Figure 2: Variation of magnetic susceptibilities with metamorphic zones in black shales of the Swiss Alps. Higher magnetic susceptibilities in red indicate appearance of new metamorphic pyrrhotite. Adapted from Rochette (1987) as cited in Hrouda et al. (2009). The author of this thesis assumes the magnetic susceptibilities shown in the diagram have a factor of 10^{-6} SI

M**etasomatism** and **alteration** also have bearings on the rocks chemistry and their magnetic susceptibilities. This is because the processes such as ***fenitization*** (alkaline metasomatism) and ***serpentinization*** of ultrabasic rocks form magnetite, which boost the rock's magnetism, whereas ***carbonitization, propylitization*** and ***spilization*** destroy titanomagnetites, thus resulting in a decrease in the susceptibility of the rock (Hrouda et al., 2009).

MS measurements were also used to log the drill holes on IODP Expedition 304 that investigated igneous rocks below the sea-floor (Searl, 2008). The continuous MS measurements enabled high

resolution characterization of minute lithological variations and changes in alteration downhole, hence allowing the identification of minor differences in the geology with depth. Searl (2008) reported high MS readings in locations where primary and secondary magnetite concentrations are high and low readings in zones where magnetite has been altered to ilmenite.

2.4 Use of Magnetic Susceptibility in aeromagnetic data processing

The MS is a very important constraint in the inversion and interpretation of magnetic anomaly (Lowe and Anderson, 2002). This is accomplished by selecting a three-dimensional region of interest in the subsurface and dividing it into large number of discrete rectangular prismatic cells, each with a constant MS and magnetization (Lelièvre, 2003). The MS of these cells are then adjusted to assist in the interpretation of magnetic-anomaly.

In general, magnetic properties depend on the quantities of oxides and sulphides present in a rock. Therefore, higher quantities of magnetite and pyrrhotite in a rock will translate to higher MS readings.

Chapter 3: Geological setting

3.1 Introduction to geology of the Thompson Nickel Belt

The Thompson Nickel Belt (TNB) is a northeast trending belt with a width of 2-35 km and an exposed strike length of about 200 km in northern Manitoba. The covered parts of the belt are inferred from magnetic interpretation to be stretching as far as South Dakota below the Paleozoic and Mesozoic sedimentary cover (Bleeker, 1991, cited in Lawley, 2007) (figure 3). The TNB belt is sandwiched between the Superior and the Churchill provinces of the Precambrian Canadian Shields (Paktunc, 1984a; Bleeker, 1991; Layton-Matthews et al., 2007; Macek et al., 2004; Lawley, 2007; Vanos, 2008). The belt is estimated to be about 1.9 billion years old and it is associated with the Trans Hudson Orogeny.

3.2 Lithostratigraphy

The belt comprises of an Archean basement and the Ospwagan Group of metasediments, which consists of conglomerates, carbonates, schists, quartzite, iron formation and metavolcanic flows (Deng, 2012). These rocks have been intruded by amphibolites, pegmatite and moderate to highly serpentinized ultramafics. The metasediments are grouped into the Manasan, Thompson, Pipe and Setting formations and the metavolcanic unit has been named the “Bah Lake Assemblages” (Macek, pers. communication, 2011, Macek et al., 2004).

3.2.1 Archean basement

The basement rocks are highly deformed and metamorphically layered Archean gneisses overlain by the Ospwagan Group (metasediments and the metavolcanic Bah Lake assemblage) of the TNB. According to Macek et al., (2004) and Zwanzig et al. (2007), the Archean consists of quartzofeldspathic gneiss, biotite gneiss, feldspar-augen gneiss, amphibole-bearing agmatite and migmatite. Usually, these groups of gneisses have low MS readings of 10^{-4} SI (*from this thesis data, unpublised*). These weak susceptibilities reflect low amount of ferrimagnetic minerals in the Archean gneisses.

3.2.2 Ospwagan Group of metasediments

Above the Archean basement are the metasedimentary sequences of the Ospwagan Group classified into the following formations:

i. Manasan formation

ii. Thompson formation

iii. Pipe formation

iv. Setting formation

The **Manasan formation** is composed of two members, a light beige and well laminated M1 quartzite and a poorly sorted M2 metaconglomerate (Layton-Matthews, 2001; Macek et al., 2004 and Deng, 2012). The M2 member consists of argillaceous wacke and mudstone that have been subjected to varying grades of metamorphism along the belt. The MS of the M1 quartzite is very low but it still shows weak paramagnetism contrary to diamagnetism in pure quartz. The M2 metaconglomerate was not intersected in the studied holes; hence no measurements are available to assess its susceptibility.

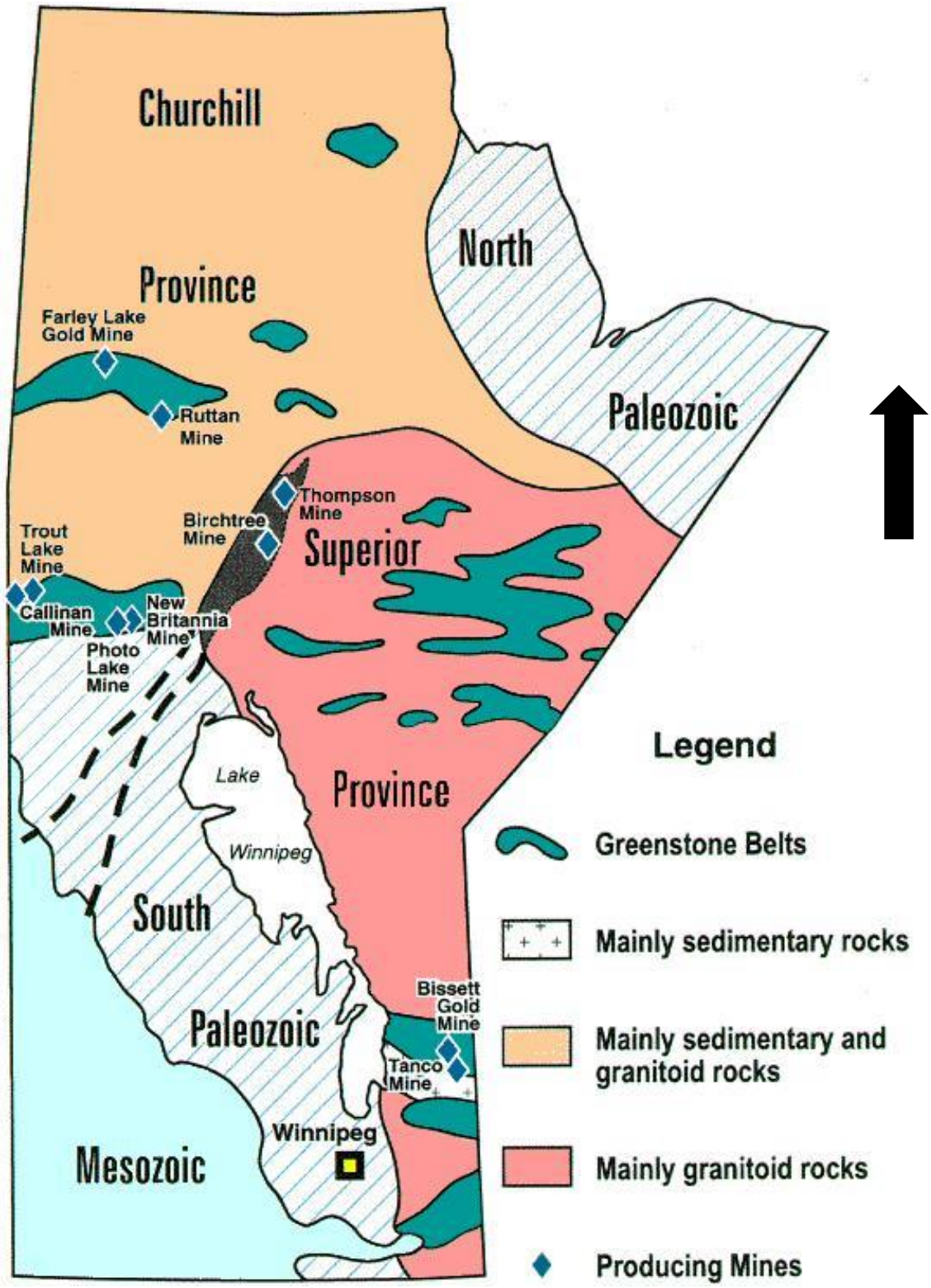

Figure 3: Provincial map of Manitoba showing the location of the Thompson Mine, Thompson Nickel Belt. The dashed lines show the inferred extension of the belt. Adapted from http://geology.about.com

Above the Manasan Formation is a group of calcareous metasediments of the **Thompson Formation**. It is recognizable texturally by its blotchy and soapy textures and the intercalation of calc-silicates with chert bands. Its mineralogy consists of olivine, diopside, carbonates, quartz and biotite. Like the Manasan formation and the Archean, the Thompson formation has very low quantities of magnetic minerals, hence very low MS (~3 x 10^{-4} SI) as measured during this research.

The **Pipe formation** is made of successions of pelitic & semi-pelitic schists, quartzite and iron formations. They are grouped into three members: P1, P2 & P3. The P1 member consists of two sub members, the iron formation containing graphitic sulphides and chert (Layton-Matthews, 2001 and Deng, 2012), which are overlain by a reddish fine-grained and thinly laminated micaceous schist sub member (Zwanzig et al., 2007). On top of these P1 beds is the P2 member of the Pipe formation. It is composed of pelitic schists with microcrenulations and distinctive kink bands and sometimes siliceous facies of black chert that are consider as stratigraphic markers (Deng, 2012). These pelitic schists are also intruded by ultramafics. All the nickeliferous sulphides and nickeliferous ultramafics in the Thompson Nickel Belt are found in this sequence.

The magnetic properties of this formation depend on the amount and type of sulphides, the degree of serpentinization of the ultramafic, and the amount of magnetite in the iron formation. The uppermost member of the Pipe Formation is P3, which is comprised of cyclic layers of quartzite and silicate-facies iron-formation and has a vague contact with the P2 member. The contact between P2 and P3 consists of pelite, calcium carbonate precipitate and iron sulphide. The massive sulphides (especially monoclinic pyrrhotite-rich massive sulphides) and magnetite-rich iron formations behave as ferrimagnetic units in the studied core and samples.

The uppermost metasedimentary sequence of the Ospwagan Group is the **Setting formation**. Deng (2012) describes this formation as metaturbidite overlying P3 sequence and consists of sillimanite-phlogophite-garnet schist and rhythmically layered leucocratic quartzite. It shows low to moderate MS except in a few locations where barren, pyrrhotite dominated, sulphides are emplaced in it.

Above the Setting formations are the metavolcanic flows of the **Bah Lake (BL) assemblage**. The assemblage consists of ultramafic and mafic lava flows that capped the Setting formation (Bleeker, 1991; Zwanzig et al., 2007; Deng, 2012). This sequence is rarely encountered at the Thompson mine as well as in the selected core and samples used in this research. Therefore, less attention will be paid to it when it comes to the discussion of the magnetic properties of the studied specimens.

3.3 Metamorphism and alteration

The rocks of the Thompson Nickel Belt have been subjected to metamorphic conditions estimated at 6-7 kbar and 700-750 ºC during the Hudsonian Orogeny (1870 Ma) (Bleeker, 1991, SRK Consulting, 2006). The metamorphic grades observed in and around the Thompson Mine range from lower (muscovite-quartz) to upper amphibolite facies (or sillimanite-K-feldspar grade in sediments) and were associated with retrograde metamorphism (Bleeker, 1991).

According to Layton-Matthews (2001) the ultramafic rocks of the TNB show two metamorphic assemblages that reflect the original igneous rocks' compositions. These trends are (i) hydration of olivine in metadunite in which olivine serpentinization determine the tie-line between olivine and

serpentine and (ii) hydration of metaperidotites in which serpentinization and amphibolization of pyroxenes dominate. Layton-Matthews (2001) resolved that the main ferromagnesian silicate minerals in the TNB's ultramafic minerals were serpentine, tremolite, hornblende and olivine. He also concluded that the presence of high amounts of serpentinized olivine and less abundance of unserpentinized olivine means strong hydration. These conclusions were supported by Deng (2012) who studied thin petrographic sections at Birchtree 140 ultramafic (located in Birchtree Mine's P2 schist formation). In general, the hydration process can be described as:

Olivine + water = serpentine + magnetite + brucite (2)

This process will increase the MS because it generates magnetite as one of its products. Other processes that have altered rock chemistry in the belt are: carbonate alteration, chlorite alteration and breakdown of serpentine into talc and carbonate (Layton-Matthews, 2001).

As discussed earlier in chapter 2, the metamorphic conditions, the type and degree of alteration in the TNB, would influence the amount of titanomagnetites and other magnetic minerals present in its rocks. Therefore, the MS measurements collected on the selected drill-holes reflect the interplay of all these factors plus any primary magnetite.

3.4 Location of the specimens

MS measurements used in this study were collected from BQ core from three drill-holes (1301020, 1301080 and 1301240). The three drill-holes were testing the Thompson Extension, which is a subset of the Thompson Mine deposit. The stratigraphy in this zone is reversed as a result of regional tectonic events. As a result, basement is normally intersected at the top of the drill-hole.

Each of the three drill-holes was (1) logged by geologists and (2) the continuous magnetic susceptibilities were collected using a downhole MS probe (BSS-02B) manufactured by Bartington Instruments. This instrument is not among the devices being studied in this project but its data will be used for cross-reference. The geological logs from each of the drill holes are described below

Drill hole: 1301020

Geological logs show three stratigraphic sequences intersected by the drill hole. These include Archean gneisses, Pipe and Setting formations. The missing units were either eroded away or have been boudinaged during regional and local tectonism.

The Archean gneisses have been intruded by amphibolites and pegmatite, which are not shown in the schematic presentation of the stratigraphy in figure 4. The gneiss, amphibolites and pegmatite are usually weak paramagnetic rocks with susceptibility around 10^{-4} SI as measured using the KT-10 meter.

The Pipe formation shows only two of the three members, the biotite-sillimanite schists, sulphide bearing schist (P2) and the magnetite-rich iron formation (P3). In addition, it has been intruded by mineralized serpentinized ultramafic and pegmatite. It has also undergone structural deformation as indicated by two sheared zones on either side of the ultramafic. This iron formation (P3) hosts the most significant magnetic rocks in the stratigraphic section with susceptibility in the range of 10^{-3} – 10^{-2} SI. The geological unit intersected at the bottom of the hole is the Setting formation, which is a quartzite cross-cut by pegmatite.

Drill-hole: 1301080

The geology of this drill hole is similar to the one encountered in 1301020 except (1) there are no ultramafic rocks intersected in the P3, (2) the shear zone is in the Archean, (3) the extent of mineralization in P2 shows significant width and grade, and (4) the hole ended in an aplite.

Drill-hole: 1301240

This borehole went through Archean gneisses, Manasan formation quartzite, Thompson formation skarn, P2 – schist, mineralized schist and massive sulphide and Setting formation quartzite and schist. These lithologies have all been cross-cut by pegmatite and amphibolite dikes. There is a fault characterized by broken schist and quartzite and carbonate-chlorite alteration that was intersected in the Setting formation. High MS measurements are associated with the mineralization in the P2.

The schematic cross-sections shown in figure 4 and 5 are not "refined" i.e. they only show stratigraphic units and some of the small units were ignored for geological modelling purposes. A good example of a figure showing more detailed lithological information is figure 6, which display all the lithologies including those displayed in figure 4 & 5. For exploration purposes, the P3 lithologies (iron formation, schist and quartzite) are all lumped into the Setting formation.

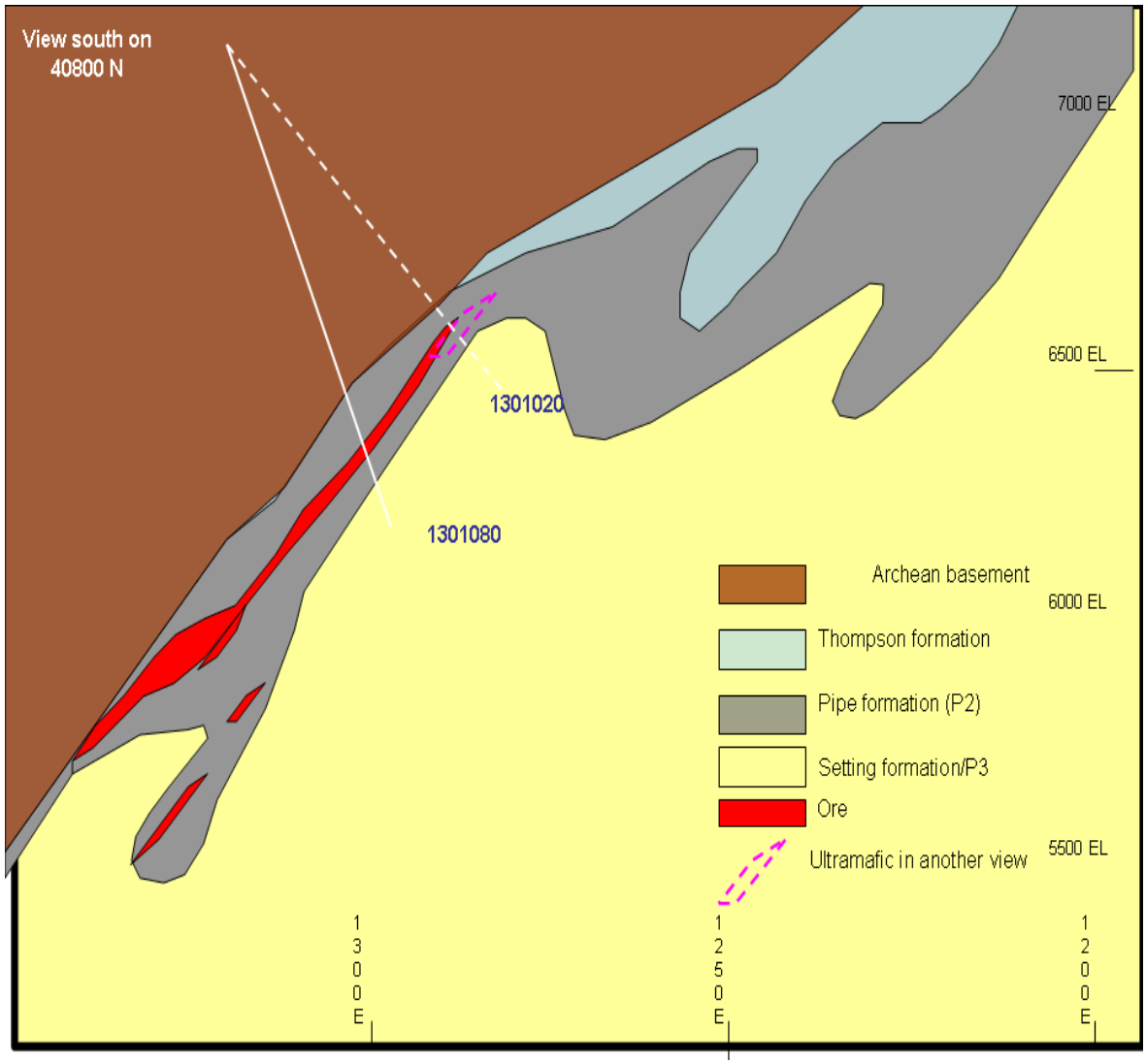

Figure 4: Schematic cross-section of the stratigraphy showing the geology around the boreholes: 1301020 and 1301080. The view to the South on 40800 N has influence on what can be seen on this section. It shows no indication of ultramafic rock intersected by 1301020. This is because that intersection is on a different northing. Vertical scale is in feet

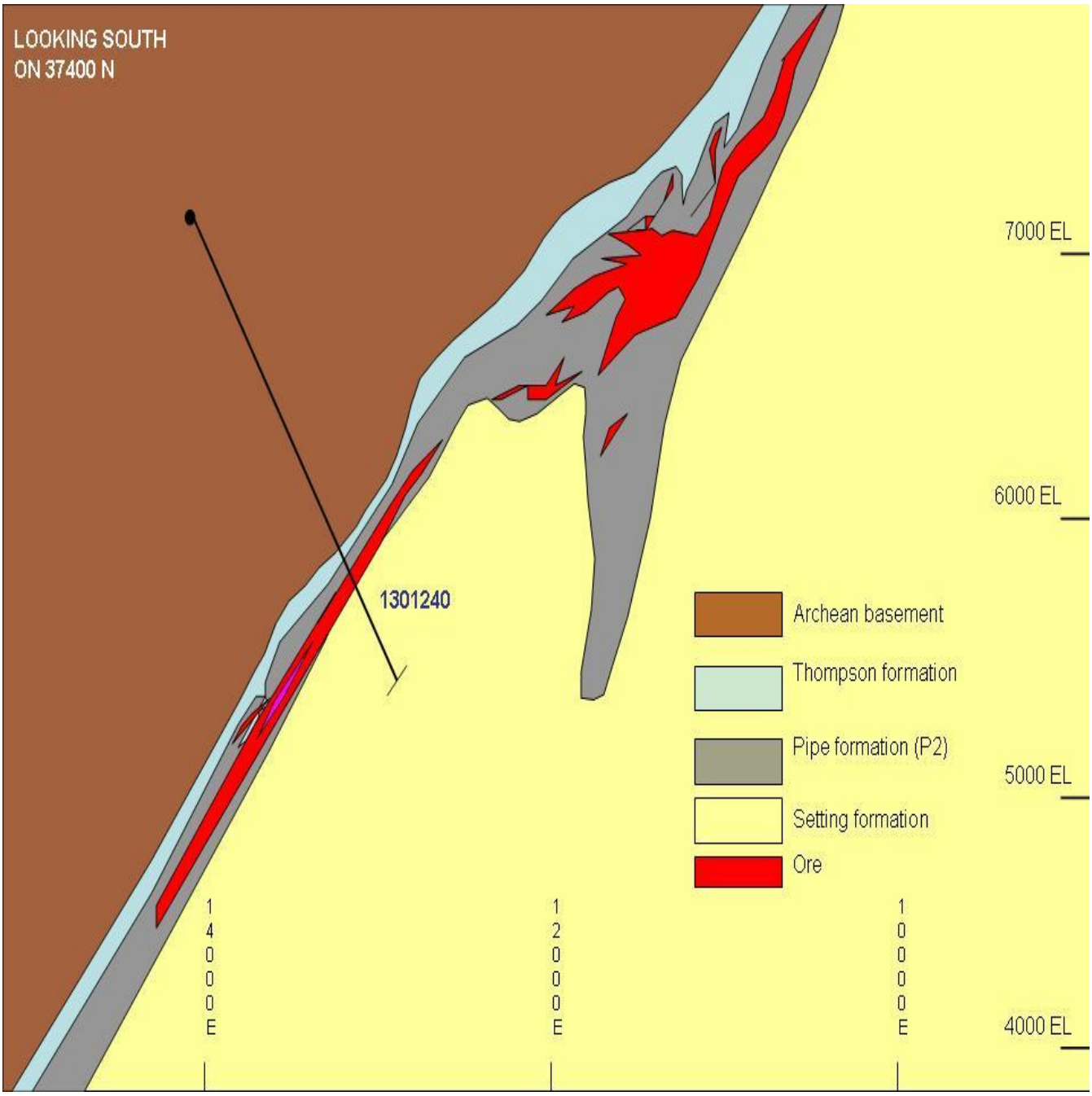

Figure 5: The simplified schematic cross-section showing the geology of 1301240. In between the Archean and Thompson formation is a thin section of Manasan quartzite. It is also imperative to note that amphibolites, pegmatites and a fault have not been shown. Vertical scale is in feet

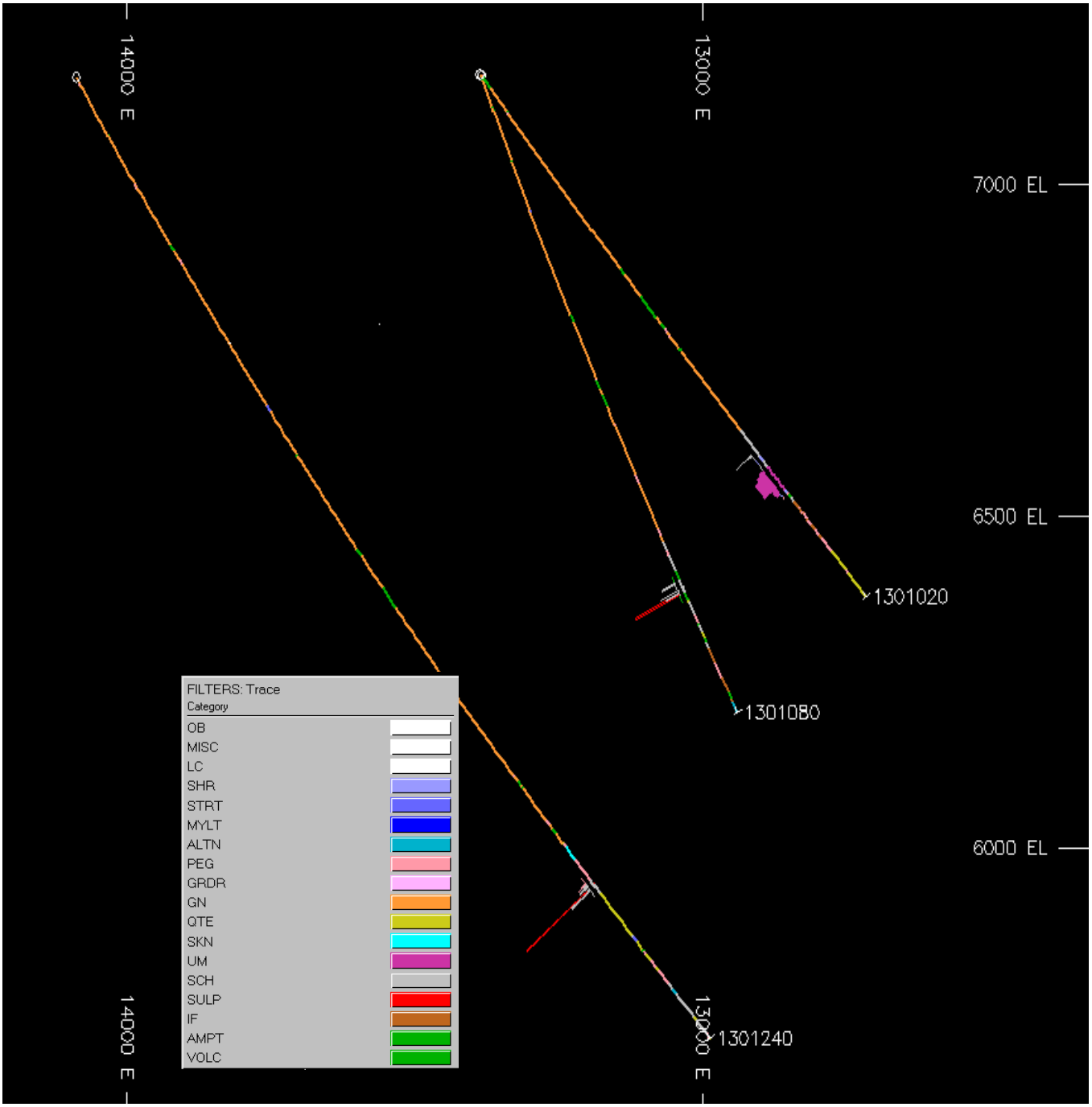

Figure 6: Detailed stratigraphic representation of the three drill-holes shown in figures 5 and 6 and which core was used in this research. The bar graphs indicate areas of sulphide mineralization and ultramafic. The most important abbreviations in the above figure are GN for gneiss, SKN for skarn, SCH for schist, SULP for sulphide, IF for iron formation, ALTN for alteration, QTE for quartzite, PEG for pegmatite, AMPT for amphibolite MYLT for mylonite and SHR for shear. Vertical scale is in feet

Chapter 4: Instruments

4.1 Introduction

There are numerous types of hand-held magnetic susceptibility (MS) meters that have been developed for the purpose of measuring the MS of rock samples. However, the accuracy, reliability and repeatability of the individual instruments are poorly known. Also, different instruments have different measurement procedures, which could impact on the accuracy and the time required to acquire data. The motivation for this research is to determine the strengths and weaknesses of the some of these instruments and to recommend the appropriateness of each device to a given target or task.

This chapter reviews six magnetic susceptibility meters and one magnetic susceptibility downhole probe, which are used in this study. Each instrument is described in terms of its operating principle, modes of operation, physical quantities measured (table 2), data downloading and storage, and accompanying accessories.

Table 2: Summary of specifications from all the six MS instruments. MS = magnetic susceptibility, cond => conductivity.

	Fugro RT-1	**Terraplus KT-10**	**GDD MPP-EMS2+**	**Bartington MS2K**	**Bartington MS2C**	**ZH SM30**
Physical quantities	MS	MS/cond	MS/cond	MS	MS	MS
Number of modes	2	3	4	2	2	6
Sensing area (mm^2)	N/A	3318	N/A	491	4072	1964
Software	N/A	GeoView	PDA software	Bartsoft	Bartsoft	SM30 software
Operating frequency (kHz)	0.75	10	N/A	0.93	0.565	8
Resolution	10^{-4}	10^{-6}	10^{-6}	10^{-6}	10^{-6}	10^{-7}

4.2 The KT-10

KT-10 is a portable hand-held MS meter made by Terraplus Inc., a geophysical equipment supplier in Canada. It has been used at many locations around the globe to measure susceptibilities on outcrops, float (Hroud et al. 2009) and on drill core. The manufacturer claim a well-developed internal self-correcting system that corrects for thermal drift.

Modes of acquisition

There are three modes of data acquisition for the KT-10: ***measure***, ***measure core*** and ***scanning***. It is worth noting that recent developments have seen the manufacturer discontinued the functionality of the ***measure core*** mode and the same task that used to be performed by ***measure core*** mode is now executed using ***measure*** mode.

Figure 7: The KT10 magnetic susceptibility meter and a KT-10 calibration sample.

If quick scanning of a sample is required, the ***scanning mode***, which records up to 20 readings per second, can be used. This allows rapid data collection, thus saving time and resources. However, the quality of the data is compromised in this mode and it is not recommended if the measured data are required for precise scientific or exploration purposes. In this research, only ***measure mode*** was used to collect measurements on the BQ & NQ core and smooth flat surfaces.

The KT-10 meter can also be used with a pin. This is a small sensor that is attached to the device to allow measurements to be recorded on small rock samples or outcrops with uneven surfaces (Hroud et al. 2009; Terraplus KT-10 manual). The pin ensures the coil is triggered at the same height above the sample (Enkin, pers. com, 2014). Since this research was carried out on even surfaces – core, freshly cut rocks, and standard samples, the pin option was not necessary. A few tests were conducted with and without the pin and the results are shown and discussed in the result section.

Measured parameters

The KT-10 version used in this research records MS only but there is another version (KT-10 S/C) that records both susceptibilities and conductivities. In addition both the KT-10 and KT-10 S/C record the time, voice signature and location. The voice signature is a KT-10 functionality that allows the user to verbally record any information about the collected data that could be used in describing or interpreting the results.

Physics of the measurement

The instrument uses an inductive coil. When a sample is brought into the sensor's magnetic field the self-inductance of the coil is changed and this results in a change in the resonant frequency of the circuit. This frequency change is converted to a MS value and displayed on the screen or stored in device memory.

The manufacturer notes that temperature deviations from the recommended range could have adverse effects on the accuracy of the measurements. These temperature dependence effects are minimized by (1) taking readings in free space before and after taking measurements and (2) using a self-correcting system, an advanced algorithm, in the instrument to correct for any deviations associated with temperature changes (Terraplus KT-10: User's Guide, Rev. 16). The meter can also be set on audio output, which help in locating areas of high magnetic susceptibilities

Accessories and software

The KT-10 comes with a set of accessories, which include batteries, battery charger, pins, instructional manual, carrying case, connecting USB cable, Bluetooth for a GPS link and for downloading the data onto a PC. Beside data transfer, the USB cable is also used to upgrade the software. The instrument also comes with GeoView software and geousb.exe USB software. The former provides an algorithm for data analyses and the latter facilitates data transfer between the instrument and the PC.

The KT-10 Calibration Pad

The KT-10 calibration standard was designed by GEORADiS and supplied by Terraplus Inc. It is one of the three standards used in this research, each of which is a material with a known nominal MS. The standard we have has a magnetic susceptibility value of 36.2 x 10^{-3} SI, as determined by the manufacturer. This calibration test was carried out in 2011 and was assigned a serial number 2011/50. Compositionally, the sample is made of Mn-Zn ferrite compacted with a mudstone (www.westernex.com.au). The top surface of the standard pad is 165.13 cm^2 (figure 7).

Data transfer

The internal memory has a storage capacity that can keep up to 2000 readings and there is also a capability to optionally recorded spoken comments for each reading. To transfer measurements to the PC, a USB cable is used. When the readings are transferred successfully, the file is stored in ASCII format in a database or in an Excel spreadsheet for later analyzes. A sample spreadsheet generated is shown in table 3

Table 3: Data file downloaded from the KT10 meter

ID	Date	Time	Type	Pin	Error	Diameter of core	MeasTime	TriggerTime	Kappa	Altitude
1378	7/20/2013	0:11:46	1	0	0	36mm	120	74	56.5	0
1379	7/20/2013	0:12:39	1	0	0	36mm	94	43	57.016	0

4.3 The GDD

MPP-EM2S+ Probe (referred to as GDD in this research) is a multi-parameter system produced by GDD Instrumentation Inc. of Quebec, Canada. It consists of a handheld gun-shaped probe and a pocket-size HP pocket computer (figure 8). The designers claim that it is one of the most advanced and accurate geophysical tools if their recommendations and operational procedures are followed with precision.

Modes of acquisition

There are three modes of data acquisition in the probe. These are ***manual, automatic and graph*** modes. In **manual** mode, sampling is activated when the "display" button is pressed whereas **automatic** mode is set to collect measurements at intervals ranging from 0.1 - 60 seconds in a continuous mode and is able to collect up to 10 readings per second (GDD user's manual). In graph mode, the instrument displays the measurements graphically. This provides a visual aid for the operator to spot where there is more magnetic material in the specimen(s) under investigation. However, such data was not useful in this research because numerical values are needed to allow comparison of the probe with the other meters being studied. In this research, data collection was performed using the manual mode.

Data transfer, archiving and plotting

Data can be transferred to a computer via USB serial cable or using wireless Bluetooth. In this research a connecting cable was used. Once the data is transferred, it is then archived either as an Excel or a text file. The information in the file includes the metadata (sample identification code, date, time,

depth) and their associated measured values (table 4). These files can be imported into other software for further analyses or processed using GDD data processing software that comes with the system.

Table 4: Example of the main columns of the data downloaded from the GDD probe. SID – Sample identification

SID	Position	U	Core diameter	U	HF_Response	Scpt:0.001_SI	Cond:Mhos/m
130109	187	m	36	mm	0	2.17	0
130109	192	m	36	mm	0	2.17	0

Figure 8: GDD MPP-Probe (left) for measuring MS. It is connected to a HP palm computer (right) where data is recorded and saved for later use.

Accessories and software

The probe comes with a handheld computer and accessories. These accessories include batteries (AA batteries & Li-ion batteries), connecting and downloading cables and Microsoft's ActiveSync 4.5 software. When this software is installed on a PC or laptop, it allows easy transfer of data files from the hand-held computer to the PC and plotting of graphs during data reduction.

4.4 The Bartington Instruments' sensors

Two Bartington Instruments' hand-held sensors: MS2C & MS2K were used in this research. They were supported by the MS3 meter and other accessories.

The MS2C is a loop sensor with an internal diameter of 72 mm that measures volume MS. Its capability is restricted to cylindrical or semi-cylindrical samples because other shapes or cylinders of greater diameter than the sensor's internal diameter do not fit into the MS2C. Only core samples of given sizes can be studied with this meter, thus the sensor cannot be used on outcrops.

The MS2C designers have indicated that the instrument gives less reliable measurements when the core is conductive (Bartington user's manual) and care must be taken if quality data is anticipated. This limits it use in massive sulphides.

The handheld MS2K sensor is designed to measure the volume MS on moderately flat and smooth surfaces. I tested this claim on a whole core (cylinder) and then split the same core into half and compare the two results.

MS3

The MS3 meter (figure 11) is designed to connect to all the sensors manufactured by Bartington Instruments for measuring MS. The MS3 meter superceeds the MS2 meter. The MS3 is controlled by a Windows computer, to which it is connected by a USB cable. The requirement for a windows computer means that the sensor, meter and computer are more bulky and hence the system is not intended for use in the field.

Physics of the measurements

MS measurements are a result of changes in the amplitude of a low-frequency magnetic field. When a susceptible rock is brought near the sensor's field, a magnetic field is induced in the sample. The resultant total magnetic field is therefore a function of the primary field and the induced magnetizations. The amplitude therefore increases or decreases depending on whether the induce magnetization reinforces or opposes the sensor's magnetic field (Bartington user's manual). This frequency change is recorded and converted to the MS readings by the instrument.

Figure 9: MS2K sensor and its disk-shaped calibration sample.

Figure 10: MS2C sensor and a cylindrical shaped calibration sample.

Figure 11: MS3 magnetic susceptibility meter.

Bartsoft

Bartsoft is a Windows software application developed by Bartington Instruments for used with the MS3 meter. It allows the MS3 to be connected to a PC or laptop and enables the user to control the

meter and to download the results and display them on the screen. The software has special features that can be customized to save time. It is also claimed by the manufacturers that the software automatically corrects for thermal drift (www.bartington.com) by using a linear interpolation of the sample-free frequency before and after the measurement.

Other accessories

Bartington Instruments' MS meters are accompanied by calibration samples and communication cables. The calibration pad and cylinder for the MS2K and the MS2C respectively are used in this research as quality control tool.

Data transfer, plotting and archiving

Once the data is collected and stored in Bartsoft compatible files, it is then transferred into Excel spreadsheet format where further analyses and data presentations can be undertaken. Sometimes data processing is performed within Bartsoft.

4.5 The RT-1

The RT-1 is a portable hand-held MS meter produced by an Australian company, Fugro Instruments. It uses a procedure that involves zeroing the meter in air (like the KT-10 and the SM30). A short warm-up time limits the amount of wait time and allow efficient data acquisition.

It has been observed that the meter only records moderate to high susceptibilities, giving zeros for any value less than 1.0×10^{-4} SI. Therefore, it is not suitable for investigating rocks with very low paramagnetic or diamagnetic susceptibility measurements. It is also worth noting that the

manufacturer points out that measurements obtained during data collection are “apparent” MS measurements. To acquire “true” susceptibility values, designers advised that a core correction factor should be applied by the user to convert these apparent susceptibilities into the more acceptable values. This is done automatically in the KT-10 and GDD; once the core size is indicated values are corrected.

Core size correction factor

Since core size varies depending on the dimension of the drill rod use, it is necessary to correct for any discrepancy that are likely to arise. Table 5 below gives a summary of the drill core correction factors proposed by the manufacturer. However, it is not clear if these correction factors are the same as used by other instruments.

Figure 12: Shows Fugro Instruments' RT1 magnetic susceptibility meter.

Table 5: Drill core correction factors and the diameter of each core size. Adapted from: Fugro RT-1, 2011 user's manual

Core	Diameter (mm)	Correction factor
AQ	27	1.82±0.02
BQ	33	1.77±0.02
NQ	48	1.51±0.02
HQ	62	1.44±0.02
PQ	85	1.24±0.02

Modes of acquisition

Data collection is performed in two modes: ***scanning and step modes***. In ***scanning mode***, continuous readings are displayed on the screen and are stored once the measure button is pressed. On the other hand, ***step mode*** only records a single reading at a time and only displayed readings once the measure button has been pressed. In either mode, the measured values are displayed on the screen both numerically and as a bar graph. Moreover, both modes produce a beeping sound that monitors peak susceptibilities (Fugro User's manual, 2011).

Physics of the measurements

The susceptibility is measured using the concept of electromagnetic induction in a receiver coil. The RT-1 has two coils positioned perpendicularly to each other in the detector head (sensor). After

initializing the meter in free air, the induced voltage in the receiver coil is set to zero. When a rock sample is brought close to the sensor coils, it induces a voltage proportional to the MS of the sample (Fugro user's manual, 2011); this voltage is used to estimate the MS of that sample. The low frequency of operation will mean that the meter will in theory not be strongly impacted by conductive material.

Data transfer, plotting and archiving

The device has an internal memory where the readings are stored in groups of 100s. Each individual reading is flagged with a symbol denoting comments on the reading e.g. whether errors (E) or bad readings (x) were incurred. In table 6 below, the results were all good hence no flags were recorded.

Table 6: Sample metadata obtained from RT-1 meter. The flag has no error or poor quality symbols in the flag column.

Memory	Value		Flag
M01-67	41	x10-5 SI	.
M01-68	40	x10-5 SI	.
M01-69	40	x10-5 SI	.

Once the data is stored in the meter's memory, it is then transferred to a PC as an Excel file via Bluetooth. Sometimes the Bluetooth functionality fails due to technical issues. This has happened on several occasions during this research. When such failures occur, it is important to know how to resolve it effectively. This involves disconnecting the Bluetooth adapter from the computer and removing it from the control panel, then reconnecting and reinstalling it every time it fails. If data transfer is successful, the file is saved in an Excel spreadsheet where plotting and presentation of the MS values are performed. Note that the data in the RT-1 is automatically stored in device memory unless the operator decides to delete it.

Accessories and software

The RT-1 comes with Bluetooth adapter, Bluetooth installation software and a user's instruction manual. Unlike other devices, it has no special software. Excel is used for data processing which is easy and cost effective.

4.6 The SM30

The SM 30 magnetic susceptibility (MS) meter is a hand-held pocket-sized device manufactured by ZH instruments. Like other susceptibility meters, the SM30 can measure rock MS on outcrops and on core samples.

Modes of acquisition

SM30 meter has six modes of operation, which include ***basic modes A & B, extrapolation, interpolation, scanning and averaging modes***. These modes differ from one another by the number and sequence of steps taken to acquire the measurements. The choice of the mode to use depends on the interest of the user.

The sequences are:

- ✓ ***Pickup step*** – frequency change near the rock
- ✓ ***Compensation step*** – frequency change in free air & away from the rock.

Subtracting **compensation** from **pickup** readings gives the susceptibility measurements, which are then displayed on the screen (user manual, 2009). An assessment of the above mentioned modes is presented below.

Basic modes A and B operate on similar principles except that mode B is four times faster than mode A (SM 30 user's manual, 2009) and I did not find any advantage of using mode A over mode B during this research. The results of the above mentioned modes will be compared and interpreted in later chapters where the strengths and weaknesses of each instrument is discussed in greater detail. In the following paragraphs, I will provide a general overview of all modes listed above.

Physics of the measurements

This meter [SM30] has an induction coil enclosed at the bottom left-hand side of the cuboid box (SM30 user's manual, 2009). When measurements are taken, the change in the instrument's frequency depends largely on the distance between the rock and the sensor (SM 30 user's manual, 2009) and the type of rock.

When a rock specimen is brought to the sensor's magnetic field, the inductance of the coil changes and this changes the resonant frequency of the circuit. The change in frequency is then converted into MS that is displayed on the LCD screen.

In both A and B modes, there are two steps: the measurement or pickup (f1) and compensation (f2) in that order. These modes assume no thermal drift between the two readings (steps) and that the second reading is representative of the compensation. However, the data becomes susceptible to thermal drift especially when the rock has a very low MS (user's manual, 2009). Therefore, failure to correct for any drift may results in non-repetitive results. The susceptibilities in these modes are therefore computed as the differences between f2 and f1 measurements in equation 3 (user's manual, 2009)

$$\text{Susceptibility} = \text{constant} \times (f2 - f1) \qquad (3)$$

The extrapolation and interpolation modes are different. Although they both involve three steps to solve for the thermal drift (one pickup and two compensation steps), they differ in the sequences of those steps. For instance, extrapolation mode follows the following operational sequences: pickup (f1) – compensation (f2) – compensation (f3) steps; whereas interpolation mode has: compensation (f1) – pickup (f2) – compensation (f3). Susceptibility calculations in these two modes are summarized below assuming equal time intervals between each measurement.

Figure 13: Front view of SM30 susceptibility meter.

For the extrapolation mode the thermal drift from the second to the third measurement is $f_3 – f_2$. If the same drift is assumed back to the first pickup measurement, then the drift component at the time of the first measurement is $2f_2$-f_3. Subtracting the actual reading (rock plus drift at the first measurement) gives the formula for the corrected value when the drift is corrected by extrapolation. This is described by equation 4.

Susceptibility = constant * $(2f_2 - f_1 - f_3)$ (4)

Using the interpolation method, the first measurement f_1 is a drift measurement, the second is a sample measurement and the last is another drift measurement. Interpolating between (i.e. averaging) the first and third measurements estimates the drift at the time of the second measurement $½(f_1+f_3)$. Subtracting the second measurement gives $½(f_1+f_3)-f_2$, or equivalently

Susceptibility = constant $*(-½)$ $(2f_2 - f_1 - f_3)$ (5)

The scanning mode allows acquisition of continuous measurements up to 20 pickups. Its sequence is compensation – ***n*** pickups – compensation whereby ***n*** represents the number of intervening pickups or measurements, a number that can be specified between 1 and 20 (user's manual, 2009). It is the quickest mode to obtain a large dataset over a short period of time but it is also affected by drift and its data can't be treated with as much confidence as the measurements with individual drift compensations. Table 7 summarizes the steps taken in each mode to acquire magnetic susceptibility measurements using the SM30 sensor.

Averaging mode records up to 20 pickups between compensation steps, similar to ***scanning mode,*** except the output is a single value that is an average of all the values measured. It sequences include compensation – n pickups – compensation and the automated calculation of an average reading. This output is put into memory register, where it is can be downloaded for later use.

Device memory

The SM30 meter has 250 memory spaces known as **registers (**written as **R_1, R_2, R_3.....R_{250}**). Measurements are saved in these registers in an incremental sequence but it is possible to save readings in a lower **R_{n-1}** than the preceding one, especially if the first reading was saved in the **R_{250}** register.

This may arise when the operator browses the memory registers and forget to go back to the last **R** with a saved measurement. This situation can be avoided, but requires careful procedures are followed so that the order of the readings are not mixed. To minimize such mistakes, the operator should wait until the memory is full or the acquisition is completed before browsing the memory. If there is a need to check the registers in the middle of data acquisition, the user **MUST** be mindful of the consequences and come back to the last reading taken before taking any more measurements.

Table 7: The six modes used in the SM30 and the sequences associated with each mode. It also gives the lowest resolution that the meter can detect in each mode. Users are advised not to confuse steps in the Interpolation for those in the Extrapolation mode as this can cause troubleshooting errors and compromise data quality

	Object measurement & init.	**Object measurement & init.**	**Object measurement & init.**	**Resolution (SI Units)**
Basic modes A & B	Rock Press left button	Free air Press left button	--------- ---------	10^{-6}
Extrapolation mode	Rock Press left button	Free air Press left button	Free air Automatically	10^{-7}
Interpolation mode	Free air Press left button	Rock Press left button	Free air automatically	10^{-7}
Scanning mode	Free air Press left button	Rock n-times Press left button	Free air Press right button	10^{-6}
Average mode	Free air Press left button	Rock n-times Press left button	Free air Press right button	10^{-7}

Data transfer, plotting and archiving

Data downloading was performed using a RS-232 cable connected to the computer via an external serial port. This RS-232 serial port is not available on all computers, so some effort is required, either in finding a computer with this type of port, or an external RS-232 to USB converter. Users are therefore advised to test the compatibility of the cable with their computer and perhaps download a test file before embarking on a large project, especially if the work is in remote areas where computer accessories are difficult to obtain.

Table 8: Data output of the SM30 Basic B mode

/RAW/POINT/NR.	/RAW/POINT/VALUE	/REGISTERS/POINT/NR./#AGG	/REGISTERS/POINT/VALUE	/REGISTERS/POINT/VALUE/#AGG	/UNITS/@USC
1	-0.00295	1	0.084	0.084	10-3Si
1	-0.00295	2	0.085	0.085	10-3Si
1	-0.00295	3	0.082	0.082	10-3Si

4.7 The BSS-02B

The BSS-02B Sonde used in this study is a downhole MS probe manufactured by Bartington Instruments that can be used with other conductivity probes made by IFG instruments to simultaneously record conductivity and MS at the rate of up to 20 readings per seconds. The intervals over which the measurements are taken downhole are determined by the speed of the winch. Technical description of the system is summarized in its manual

"*The BSS-02B magnetic susceptibility Sonde is intended to be used for prospection of magnetic minerals and stratigraphic correlation to depths of 6000 m. The operating frequency is chosen to be sufficiently low to avoid interference from rock conductivities and the circuitry is temperature compensated to minimize thermally induced drift. The region of detection is situated 160 mm from the tip of the pressure-equalized housing. The detector features a single focused coil arrangement to achieve a single response to strata. The detection region has a full-width-half-maximum response of 25mm and measurements are digitized at a rate of approximately 20 per second giving a theoretical maximum logging rate of 0.5 m per second. The tool is calibrated for operation in 50 mm diameter unclad boreholes. Larger diameter holes can be logged where the angle of the borehole assures de-centralization*……"

This instrument is not a principal instrument in this study but its data will be used to create a continuous downhole profile for comparison with readings from other equipment. The data were collected and processed by the Vale Exploration team. I was able to get only the corrected dataset.

4.8 Instruments calibration

Calibration is defined as the set of operations that establish, under specified ambient conditions, the relationship between values indicated by the measuring instrument and the corresponding known values of a measurand (UNIDO, 2006). If all the instruments used in this study are properly calibrated, they should all give the same reading on the same sample. Calibration samples (measurands) can also be used to check that there has not been a long term drift or malfunction of the instrument by making periodic measurements of that calibration sample.

There are various ways of calibrating instruments. For instance, some instruments are calibrated by specialists in specialized facilities. Others are calibrated using accessory calibration standards with known nominal measurements e.g. the MS2C calibration cylinder or the KT-10 calibration pad.

Some instruments have automated internal systems that can achieve a similar purpose by zeroing the drift, but this is not a complete recalibration, as there can still be a scaling error or an offset.

In this research Terraplus' KT-10 and Bartington Instruments' MS2K & MS2C were recalibrated using their respective standard samples and their measurements of the reference sample were checked against the known value at the beginning of each day of work. The SM30, GDD Probe and the RT-1 meters have self-zeroing internal systems that were exploited to reset them.

Chapter 5: Data Acquisition

5. 1 Introduction

The data used in this study was acquired using core samples from three BQ and two NQ boreholes, two rock samples (dolomite and ultramafic picrite) from the Thompson Nickel Belt and the calibration samples manufactured by GEORADiS and Bartington Instruments. Specific locations, where MS measurements were collected, were identified and clearly marked on the core and on the outcrop specimens. The calibration samples also have recommended points were measurements are taken.

Figure 14: Shows an example of core from borehole 1301020. The X marks indicate locations where measurements were taken using the six magnetic susceptibility instruments.

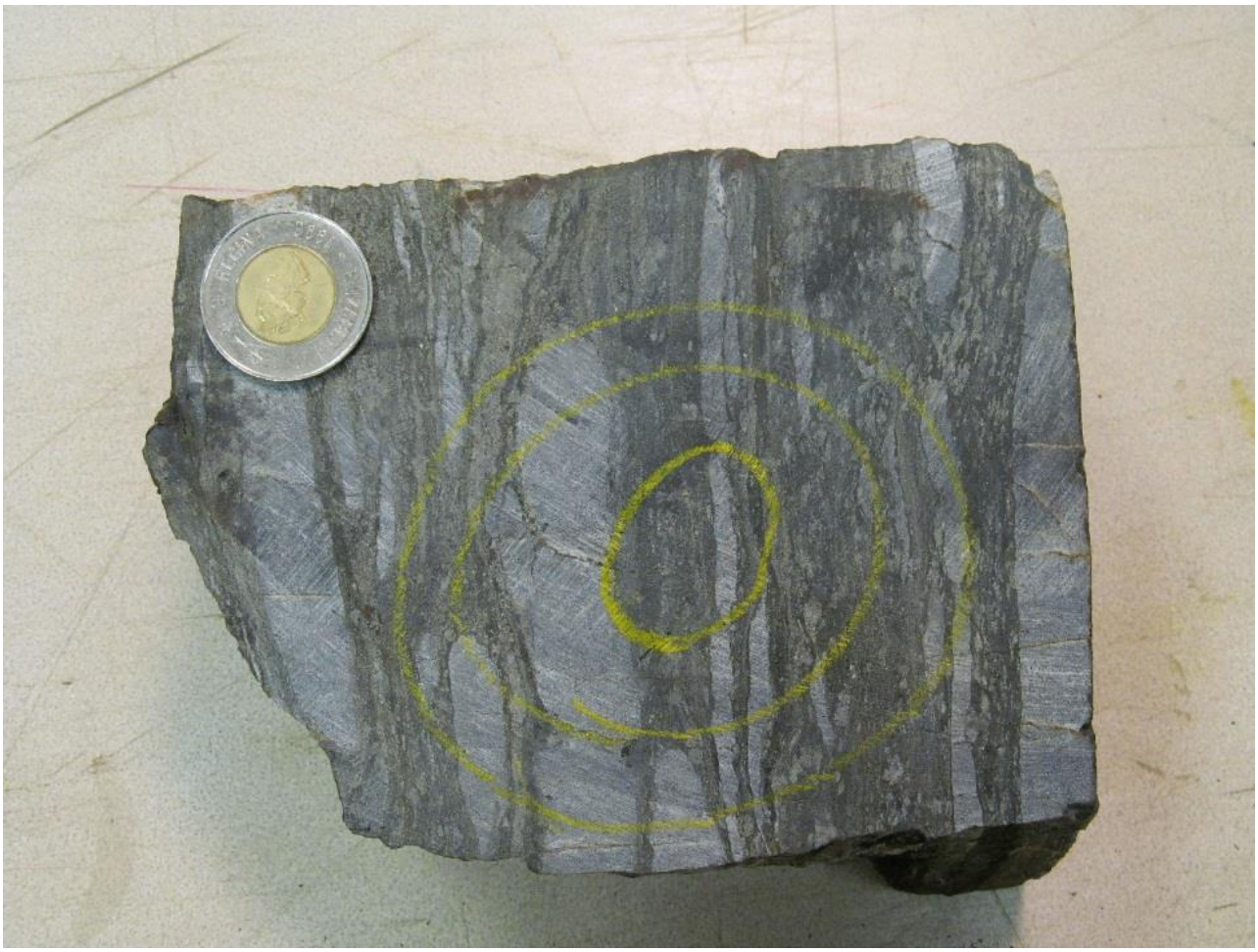

Figure 15: Shows an ultramafic picrite (example of flat surface rock samples used in this research). The area marked with yellow circles indicates point where measurements were taken. This common location was used to enhance repeatability. Note that this particular sample is heterogeneous, so selecting an appropriate location is difficult.

The location for measurements recording (with yellow circles) was selected on ultramafic picrite. The inhomogeneity of the mineralogy in this region makes it an appropriate representation of an outcrop that could be found in the field. The outcrop samples were chosen to meet three objectives: (1) provide wide range of MS measurements (low in dolomite & high in ultramafic picrite), (2) to demonstrate the variations in mineralogy in typical field sample and (3) test the effect of drift on instruments when used on a flat sample.

It is important to note that variations in the type and amount of mineral grains being sensed in each measurement is not a function of time. Changes in the measured value might be due to small changes in position resulting in changes in the magnetic minerals sensed. Typically this will result in the measured values oscillating about the median or mean value. On the other hand, a unidirectional change in MS readings, either decrease or increase of MS with time, is attributed to instrument drift.

Figure 16: Split or half NQ core used in this research. The cut surface shows a network of sulphide matrix that is almost uniform throughout.

MS measurements were generally taken on whole core (curve surface), but when the core was split, measurements were also taken on the flat surface to compare the measurements and assess the effect of temporal drift associated with each of the samples.

The following subsections discuss how the data was acquired, the quality control and quality assurance protocols and the operational procedures involved with each instrument studied.

5.2 Data Acquisition

The data used in this research were acquired between April and July 2013 at the Vale Exploration office in Thompson, Manitoba, Canada. Except for the calibration samples, all other specimens used were obtained with permission from Vale.

Generally, the MS measurement procedure involved holding the sensor against the rock surface in the case of the KT-10, SM30, MS2K, MPP-EMS2+ probe and RT-1 meters or inserting the sample inside the hollow cylinder for MS2C sensor. The measurements are then taken. However, a sensor must not be pressed too hard on the rock as it might cause mechanical shock to the inductive coil, which might result in erratic measurements. The measurements were collected on the core, which were boxed in core tray as shown in figure 14. The surrounding core were not moved, hence their impact on the measurements was present in all of the instrument used except the MS2C, which required that a sample be removed from the core box and placed inside the hollow cylinder.

Three BQ boreholes (1301020, 1301080 and 1301240) studied have intersected various lithologies with different susceptibilities as discussed in chapter two and three. These lithological units provided a wide range of measured values, which permit a comprehensive assessment of the range of sensitivities of the instruments.

At the start of the project, a large dataset was collected from measurements at 9 locations on 1301020 core. This was accomplished by taking 20 repeated measurements at each of the marked points using each MS instruments discussed in chapter 4. In the case where the instrument has more than one usable mode of operation, each mode was used (where possible) to record the same number of measurements. All data were backed up in individual files. These measurements were then used to characterize the

modes of operation of each instrument and the best mode was then chosen and used throughout the rest of the data collection season (table 9).

The chosen mode was then used to acquire more data on the boreholes 1301080 and 1301240; NQ samples (massive sulphide and schist), rock samples (dolomite and serpentinized ultramafic picrite) and the two calibration samples.

The NQ core samples include biotite – phlogophite – sillimanite – quartzofeldspathic P2 schist and a semi-massive sulphide. One spot was marked on each of the two NQ samples. It was on those marked points that the MS measurements were collected. Note that the NQ samples were not in a core tray, thus I was able to test the instruments without influence from surrounding core.

In addition, the NQ samples were cut into halves and their MS measurements were recorded again on the freshly cut surface. This provided some grounds for assessing the effect of (1) using half instead of whole core, (2) a flat surface instead of cylindrical whole core and (3) quantifying the discrepancies between the three sets of measurements (whole core, half core flat side, half core cylindrical side).

Moreover, a dolomite and a serpentinized ultramafic picrite, sampled during the TNB field trip in 2012, were used to check how the readings from each instrument vary when used on "outcrops". To better understand the fluctuation, each instrument, except MS2C, was used to record up to 130 readings at the spot marked with a circle in figure 15. The results were used to investigate whether instruments such as the MS2K give better results on outcrops than on core.

Lastly, data were collected on Terraplus' KT-10 calibration standard and Bartington Instruments' MS2C calibration cylinder; the MS2K calibration sample is too small to be used with other instruments besides MS2K meter. The samples have a known nominal MS measurement as in the calibration report by their manufacturers. All instruments were used to record 80 - 100 readings on the KT-10 calibration standard, except the MS2C, as this instrument requires a cylindrical sample of a given diameter, not exceeding 72 mm. Hence the shape of the KT-10 calibration standard does not fit in the MS2C sensor. The same number of measurements was collected on the MS2C calibration cylinder. The dataset from these two standard samples would answer four questions (1) how the values from each instrument deviate from the standard averages, (2) how much drift is evident over the time taken to take the 80-100 readings, (3) how much drift occurs over a number of months, and (4) whether there is any given sample that could to be called an absolute "standard" for use with all the instruments.

5.3 Quality Control and Assurance

Quality of measurements is a necessity and must be met for the measurements of any study to be accepted as a true representation of the value being measured. The need to generate more reasonable and less erroneous data is very important (UNIDO, 2006). This means that the choice of instrument to use for a given study must consider the required accuracy, resolution and precision. Eisenhart (1963) described precision in association with reliability, reproducibility and repeatability of measurements. Generally, poor quality data could have both legal and operational consequences when used to arrive at major decisions. It is therefore the responsibility of the operator to ensure the production of "good" quality data by limiting human and instrumental errors.

Quality control techniques allow the user to determine whether the measured values are within the range of allowable errors and are true and reasonable estimates of the quantity being measured.

Several papers, discussed below, have presented guidelines for acquiring quality data using MS meters.

The physical property measurements in the Nechako Basin of central British Columbia identified common sources of errors and how they could be minimized (Andrews et al., 2011). It was observed that samples larger than the sensor tend to have better accuracy than smaller ones, a point which was also echoed by Searl (2008), who studied core samples from the Integrated Ocean Drilling Program (IODP). For accuracy and precision controls, Andrews et al. (2011) recommended taking susceptibility readings on samples that are larger or at least the same size as the sensor. They also suggested taking at least 3 readings and calculating the averages.

Enkin et al. (2012) discusses rock physical property measurements and suggested standard procedures necessary for achieving a quality dataset; specifically MS measurements should be made on a whole and dried core (also in Searl, 2008). Drying the core is suggested to remove ions that might affect the magnetic behaviour of the rocks. All core and samples used in this study were dry and the surrounding environment was moisture free. Enkin et al. (2012) recommend taking several measurements and taking the geometric averages as opposed to medians.

Schibler et al. (2002) discusses comparability and reproducibility of MS measurements collected by two independent teams using the Bartington MS2 meter in combination with the MS2D sensor, a surface scanning coil. In their attempt to minimize discrepancies cause by handling errors, they followed the following procedures (1) the data was collected at similar spots for all the instruments, (2) the sample length was maintained and was greater than the sensor's and (3) the vicinity was cleared

of any known magnetic interference. Cross-plots and linear regressions allowed the authors to determine the correlation between the two Bartington instruments. Finally, the tabulation of means and standard deviations was used to evaluate how stable, reliable and reproducible results were.

In this research, attempts were made to ensure the production of high quality data by deploying standard quality control and quality assurance (QA/QC) protocols. These measures included (1) following designers instructions and recommendations on the use of the equipment, (2) taking at least 5 readings at a similar (marked) spot and computing the average and median susceptibility measurement at that point, (3) ensuring a magnetically safe surrounding i.e. without any magnetic material within 50 ft of the sensor, (4) collecting data at the same location (point on the core or sample) using different meters, (5) calibrating or zeroing the equipment before readings were taken, (6) avoiding the use of heavily altered or weathered rock samples, (7) taking readings on the calibration samples with each instrument (where applicable) at the beginning of each day of data collection and plotting the result to assess the drift over time, (8) using statistical and visual assessments to determine the quality of the measurements and (9) ensuring the sample length is greater than the sensor. The relevance of the outlined procedures will be revisited in the data reduction and interpretation chapters that follow.

Chapter 6: Data reduction

The focus in this research is to compare the instruments based on their repeatability, susceptibility to drift, sensitivities and lower limits of accuracy. The analysis undertaken therefore focussed on achieving these objectives. The following subsections discuss each of the methods involved during data processing.

6.1 Geometric Reduction

Geometric reduction is a require procedure in the analyses of physical property measurements and interpretation of geological structures and lithologies. Some of the instruments, such as GDD, MS2K, MS2C and KT10, have internal algorithm that apply correction based on core size.

If the instrument did not apply the geometric correction automatically, then no additional correction is applied. Data such as that acquired in this thesis could be used to derive geometric correction factors.

6.2 Choosing "the most suitable" modes

The choice of the mode of operation to be used in each case was based on several factors. The main factors included (1) accuracy and resilience to temporal drift (2) the type of data it generates (e.g. graph modes were avoided because the research needed numerical values for further analyses) and (3) the ease of operation. Note that the KT-10 measure-core mode was inactive.

Data was collected on the KT-10 calibration sample and on core from borehole 1301020. The core samples were selected to have a wide range of susceptibilities as the instruments performance might

be a function of measured value. All modes of operation in each instrument were used where applicable. The collected data from each instrument's modes were presented on plots as a function of repeated measurements to permit the visual assessment of accuracies and the effect of drift.

The data were also analyzed using measures of central tendency: means, median, range, variance and coefficient of variation. The calculations were done in Excel with each lithology (of 1301020) treated separately.

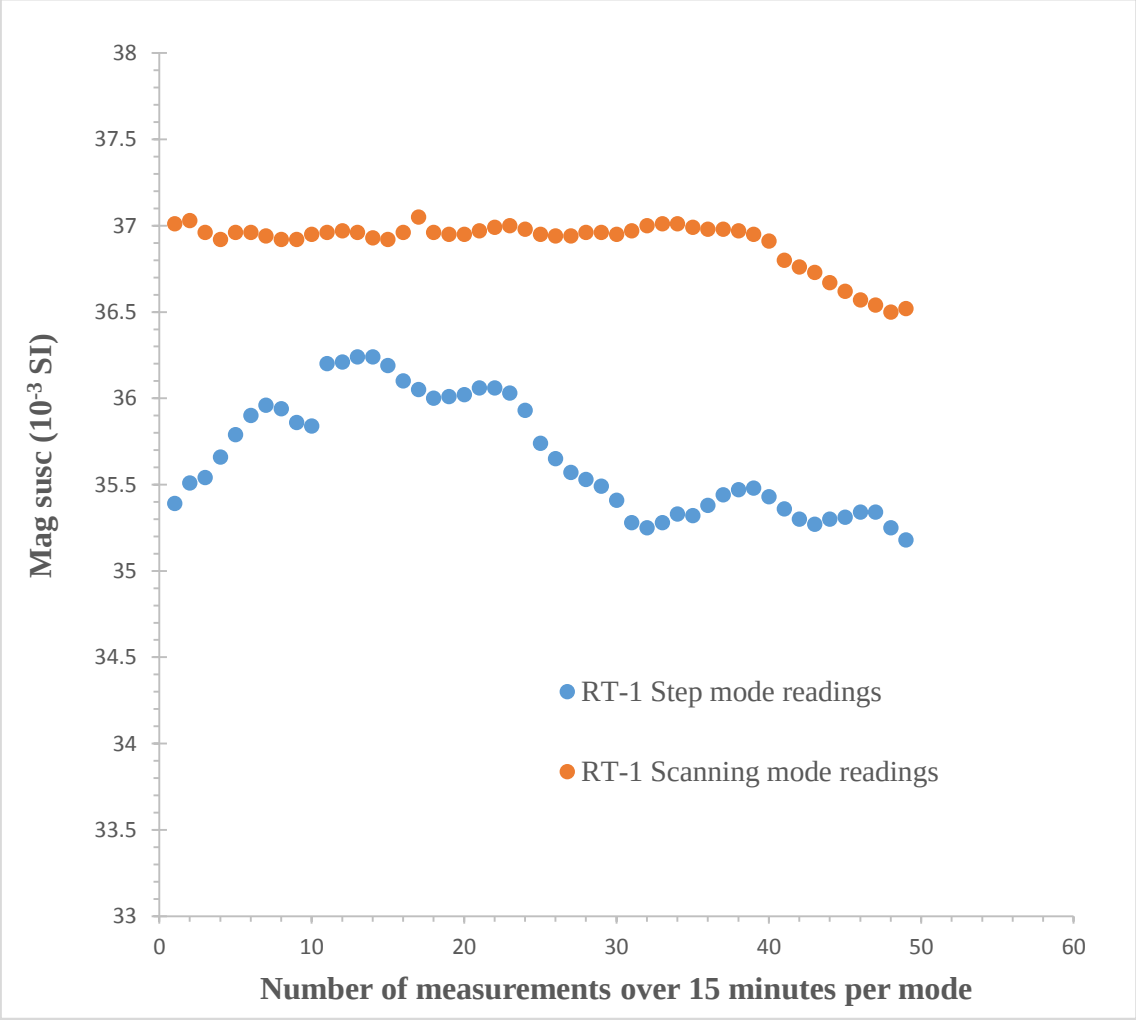

Figure 17: Test of RT-1's *Step and scanning modes* on KT-10 calibration sample.

RT-1's two modes of operation, ***Step and scan***, were used to record 49 readings each on the KT-10 calibration sample. The results were plotted as shown in figure 17. The results show that scanning mode provides results that are more reproducible than step mode. Therefore, the scanning mode was chosen as the better option for this instrument to be used through the rest of the study. The RT-1 was tested on other samples, with similar results. None of the modes measures weak magnetic susceptibility values, so measurements of weak paramagnetic or diamagnetic materials could not be acquired.

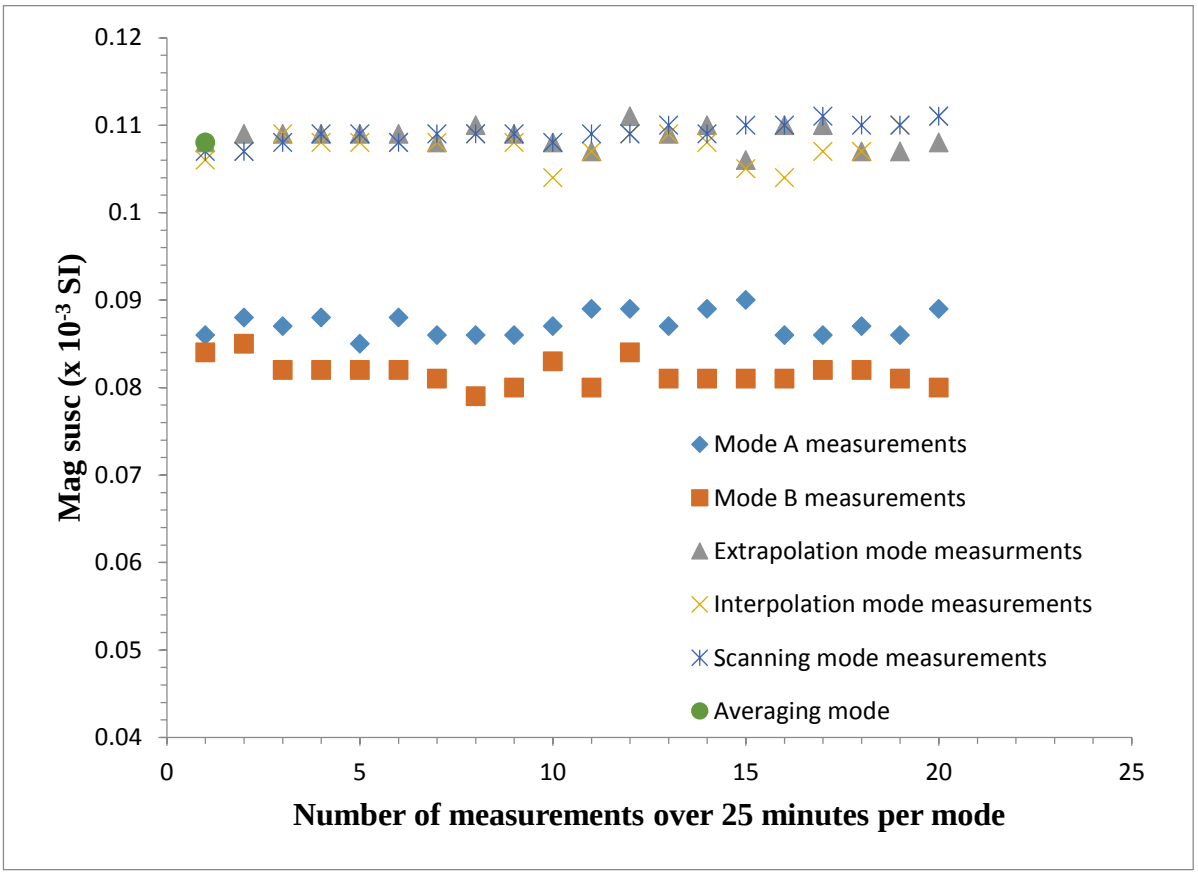

Figure 18: Shows measurements taken in Archean gneiss using the six SM30 modes.

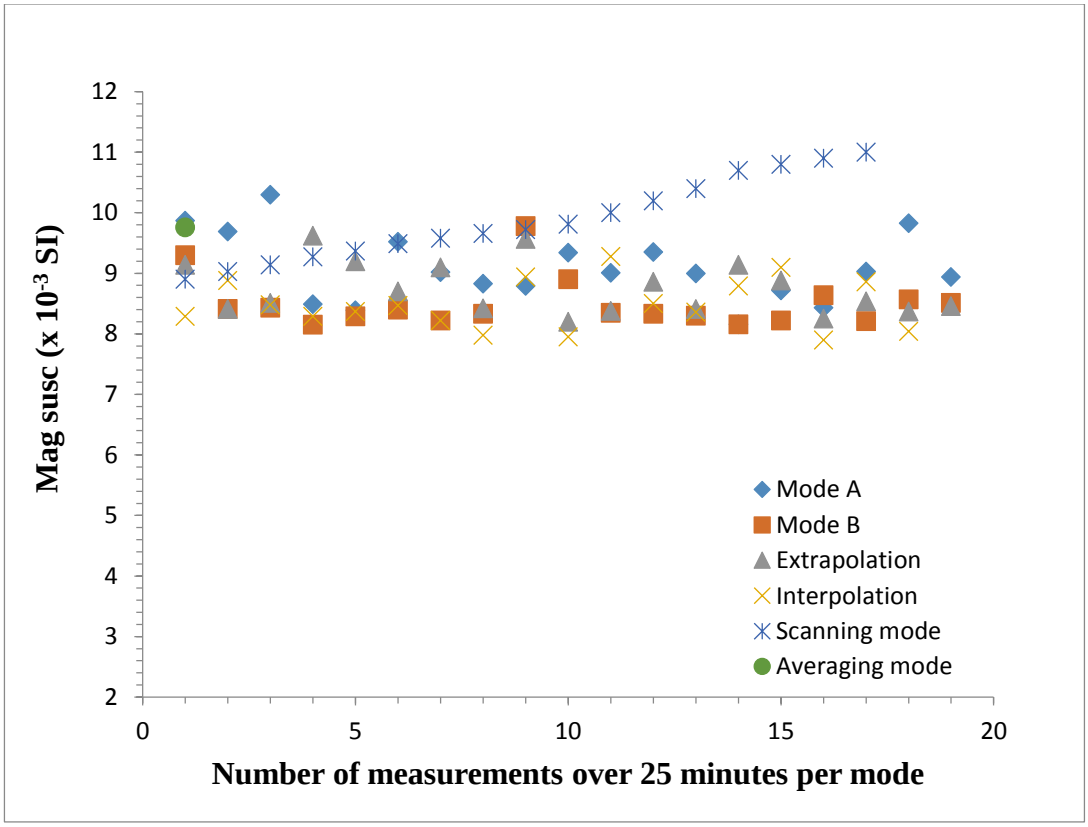

Figure 19: Measurements recorded on mineralized peridotite using the six SM30 modes.

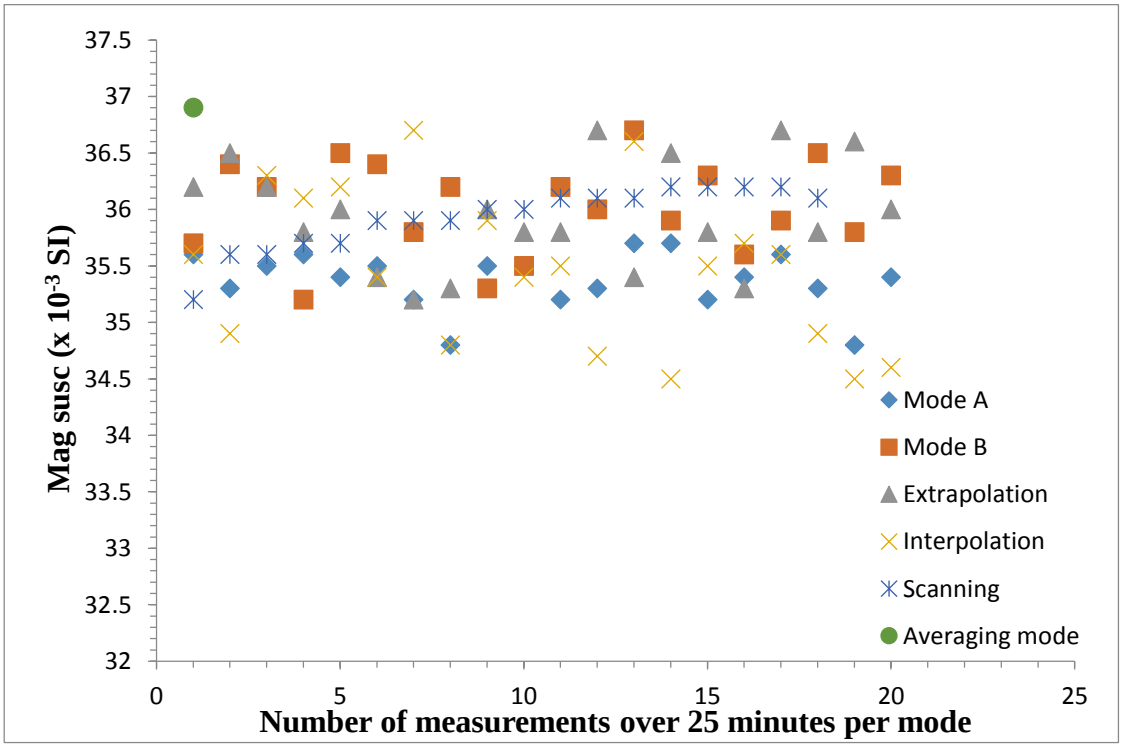

Figure 20: Show measurements on mineralized serpentinite using the six SM30 modes

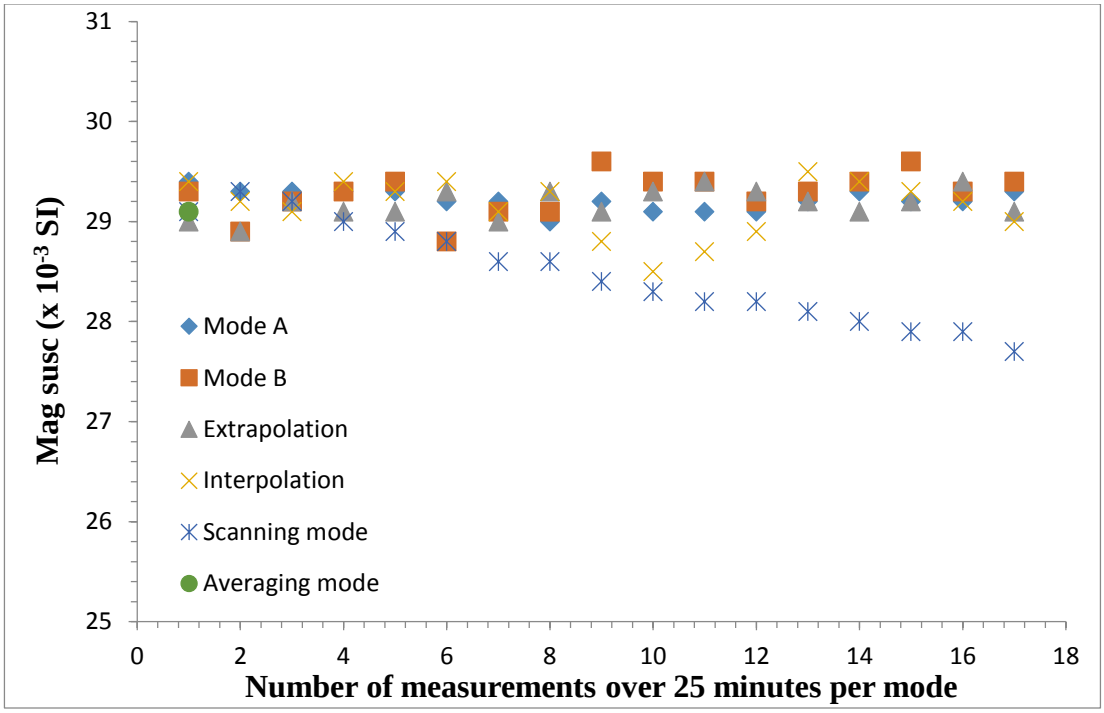

Figure 21: Measurements on serpentinized ultramafic using the six SM30 modes

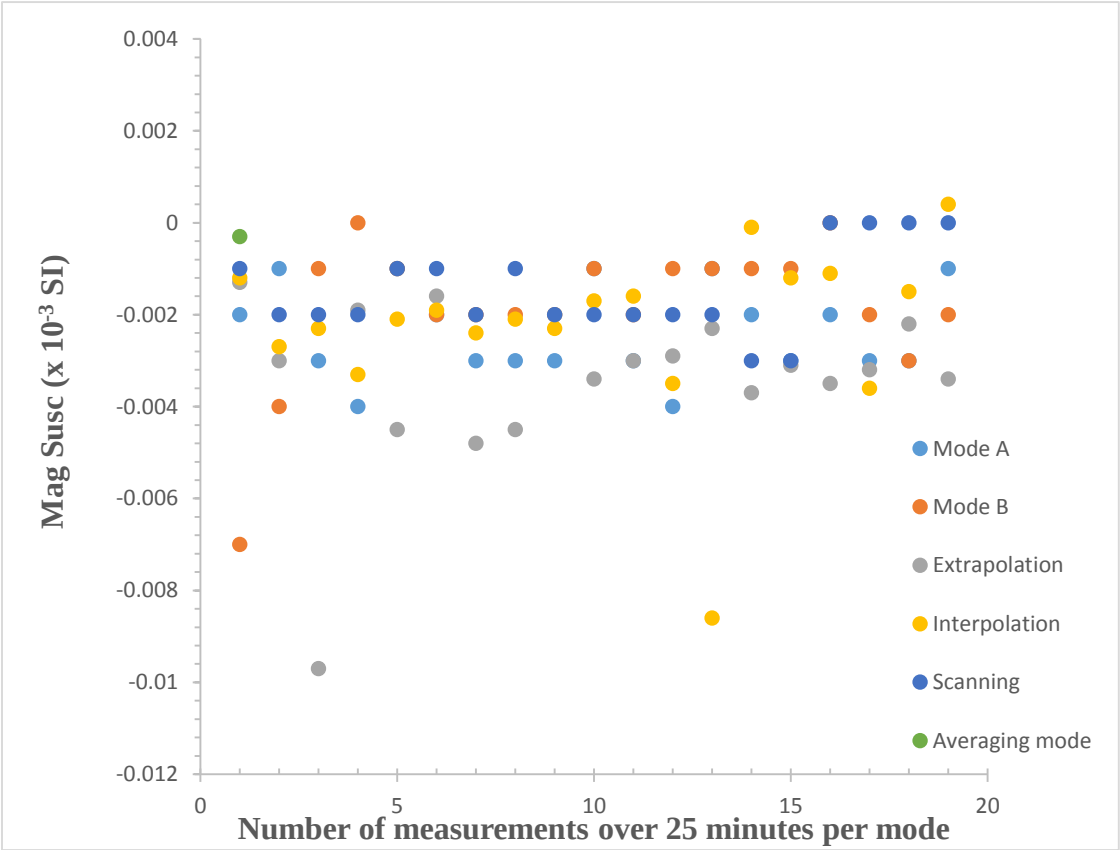

Figure 22: Measurements on quartzite core using the six SM30 modes.

The SM30 was tested on five samples with a wide range of susceptibility values. The plots for these are shown in figures 18 – 22, using the six modes of acquisition provided by the SM30. It is observed that ***scanning mode*** shows a high susceptibility to drift. It is observed that mode B is the least affected by drift of all the modes. The averaging mode's measurements are higher relative to the other modes' measurements except in figure 19 and 21 where it is almost equal to the first values of each mode. In figure 22 the measurements are erratic and non-reproducible and very small when measured in all 6 modes. The ***Basic mode B*** was chosen because (1) it is the most reliable mode of the 6 modes and (2) it is four times faster than ***Basic mode A.*** The specifications listed in table 6 implies that the interpolation and extrapolation mode give better readings for small susceptibilities (down to $1x10^{-7}$ SI), however, this claim was not verified in the weakly susceptible samples.

Two steps were taken to choose the KT-10's mode of operation. Firstly, there are three modes – ***measure, measure core and scanner***, among which one was to be chosen. However, the ***measure core*** option was disabled by the manufacturer. That means only two modes were available for use. The data obtained using these two modes using the KT-10 calibration sample was plotted in figure 23. Secondly, there was a need to decide whether to use the meter with a pin or without a pin. The results for these cases when measurements are made on the KT-10 calibration sample were plotted in fig. 24.

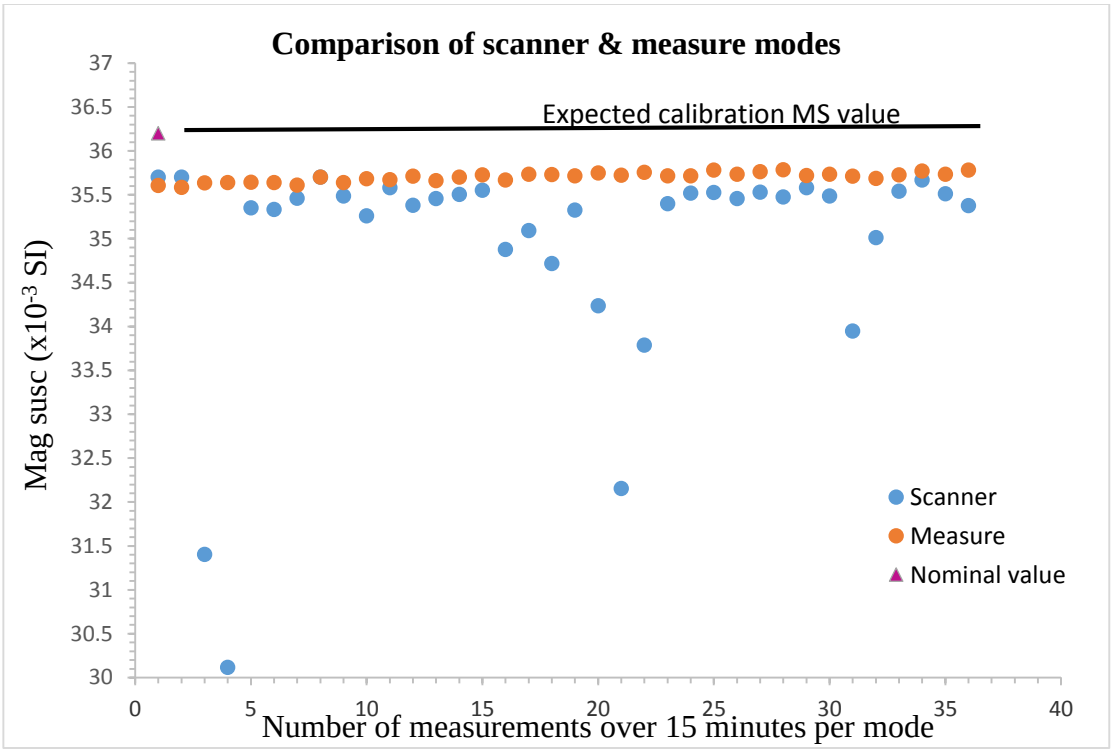

Figure 23: Comparison of the KT-10's scanner and measure modes. Measurements were recorded on the KT-10 calibration sample

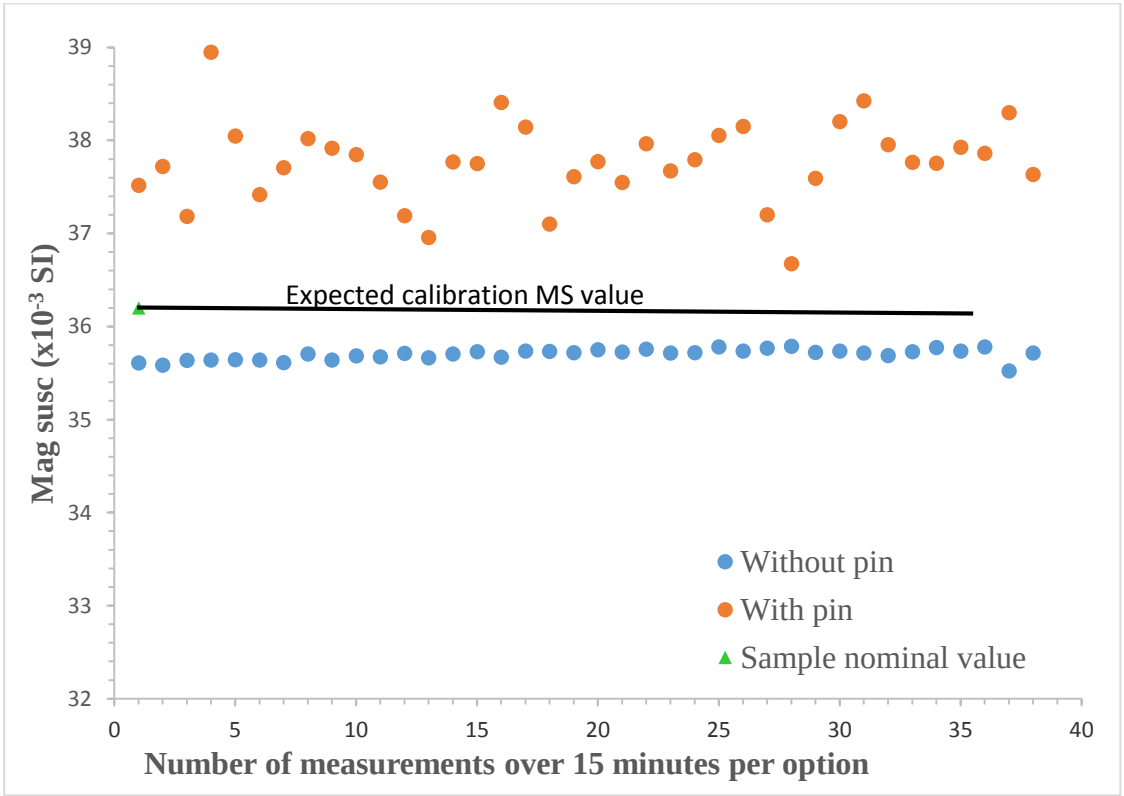

Figure 24: Comparison of the KT-10 measurements collected with pin and without pin in measure mode.

The results in figure 23 show greater fluctuation in the ***scanner mode than*** the ***measure mode***. Figure 24 also indicates significant variations in the measurements measured with a pin than those recorded without a pin. Further observation shows the pin's measurements were always higher compare to those recorded without a pin and were also larger than the sample's nominal value. Therefore, the results favor the measure mode and a no-pin-option. This measure mode was also found to give consistent results when used on weak paramagnetic samples. However, none of the modes (and pin or no pin options) give reliable results with diamagnetic samples (negative susceptibility measurements).

There are two modes that can be selected for the MS2K and MS2C when data are acquired using the Bartsoft software (Automatic and manual modes). The GDD has four modes: ***manual, continuous, graph and single reading.*** These modes are setup in the pocket HP computer that comes with the probe. In both Bartington and GDD instruments, I selected manual modes for practical reasons: (1) a desire to control when and where the measurements were taken and (2) the ease of operation. As a result, table 9 was generated with all the chosen modes highlighted in red.

Table 9: Shows instruments' modes of operation. One mode (in red) was chosen as the preferred mode in each instrument for the requirements of this study.

KT10 Modes	**RT-1 Modes**	**GDD Modes**	**MS2C Modes**	**MS2K Modes**	**SM30 Modes**
- Measure (without a pin) - Measure core - Scanner	- Step - Scan	- Manual - Continuous - Graph -Single reading	- Manual -Automatic	- Manual - Automatic	- Mode A - Mode B - Extrapolation -Interpolation -Scanning -Averaging mode

6. 3 Drift Analysis

Measurements dependent on frequency changes in an inductive-coil circuit are easily affected by drift (Lee and Morris, 2013). Although the manufacturers' quality control & assurance procedures were performed to minimize drift, some drift was still observed during the time of data collection, which usually took about 15 to 25 minutes per mode of operation. Having selected the mode of operation for each instrument, I undertook further analyses to quantify the observed temporal drift in these modes. Figure 25 – 30 show the figures generated as part of drift testing on a mineralized peridotite sample (a moderately paramagnetic rock).

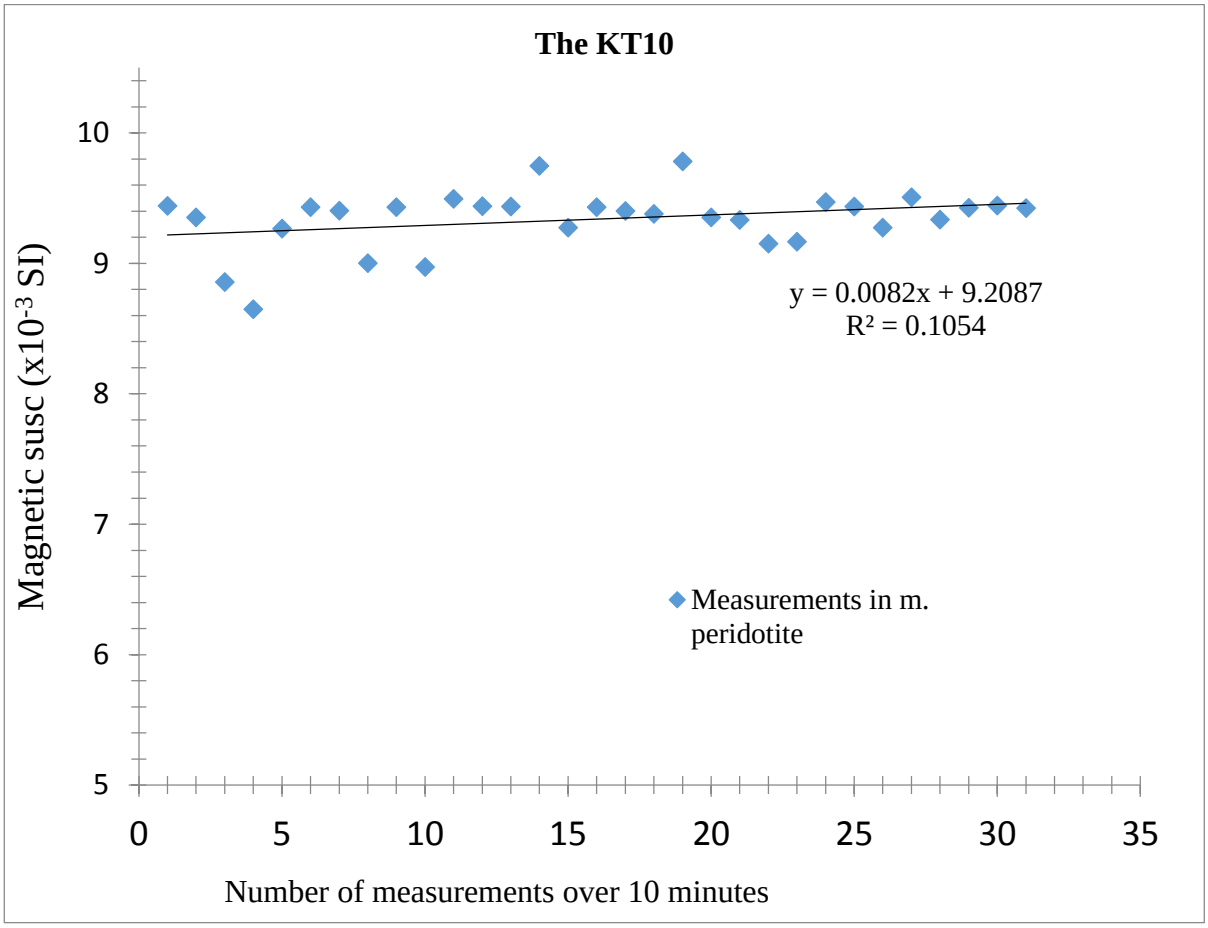

Figure 25: Plots of MS measurements on a mineralized peridotite sample from the 1301020 core.

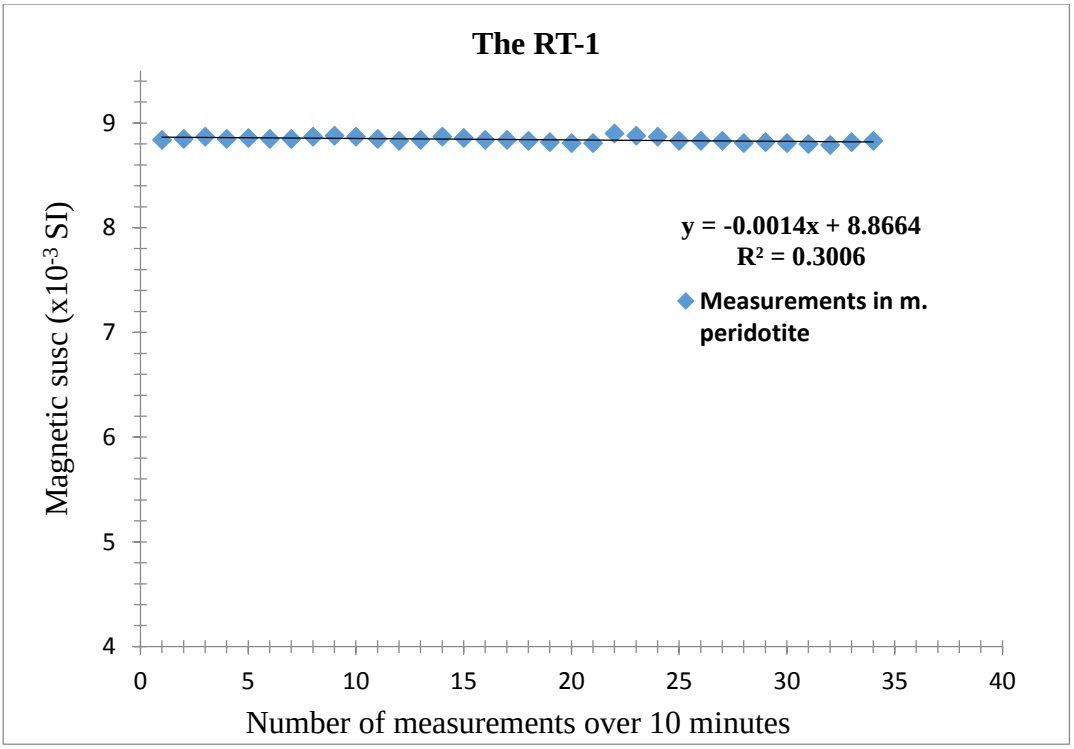

Figure 26: Plot of MS measurements on a mineralized peridotite sample from the 1301020 core.

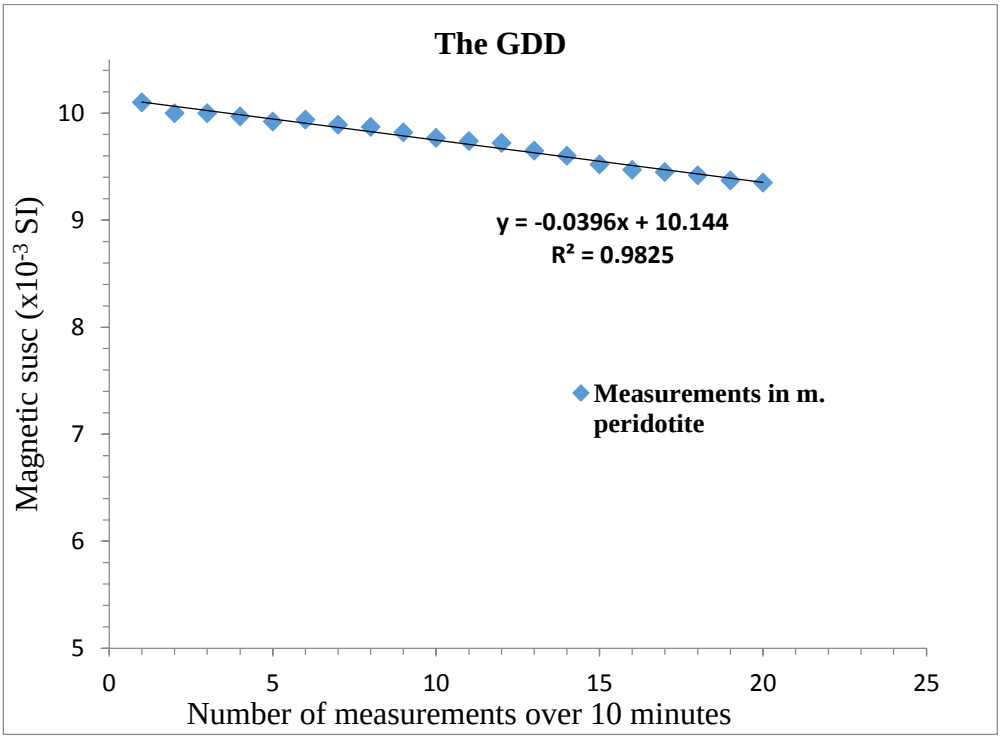

Figure 27: Plots of MS measurements on a mineralized peridotite sample from the 1301020 core.

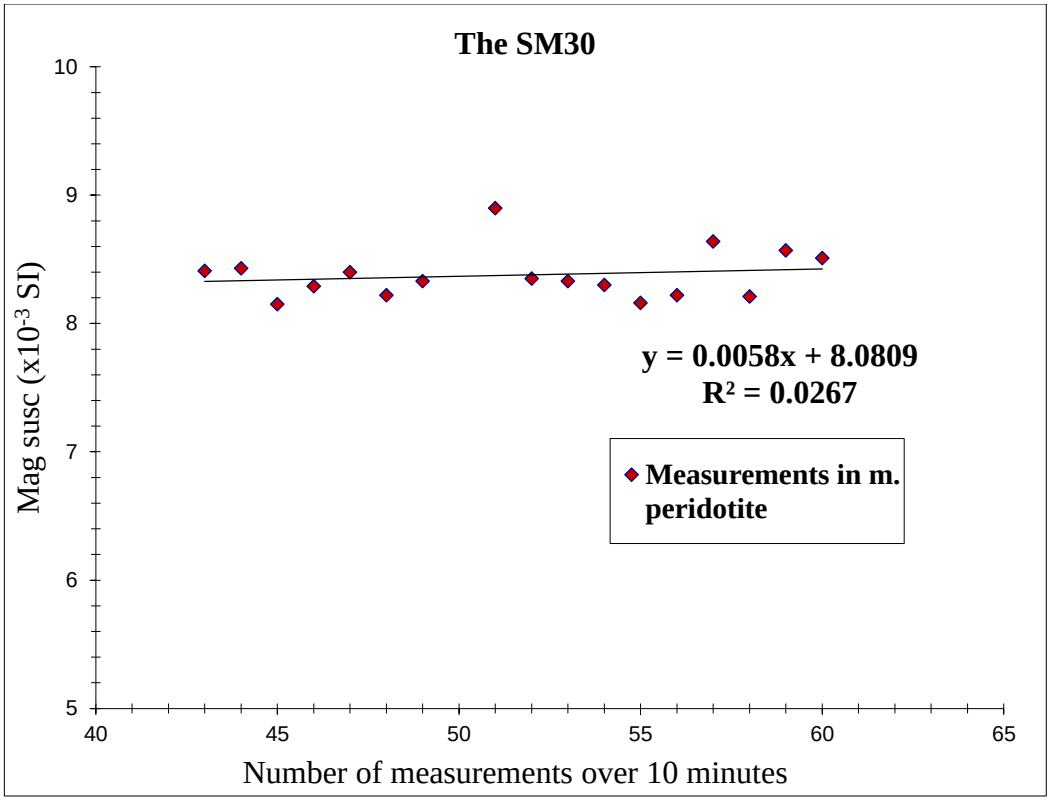

Figure 28: Plot of MS measurements on a mineralized peridotite sample from the 1301020 core. The samples started at 42 because 1-41 were used to record measurements in form a different mode

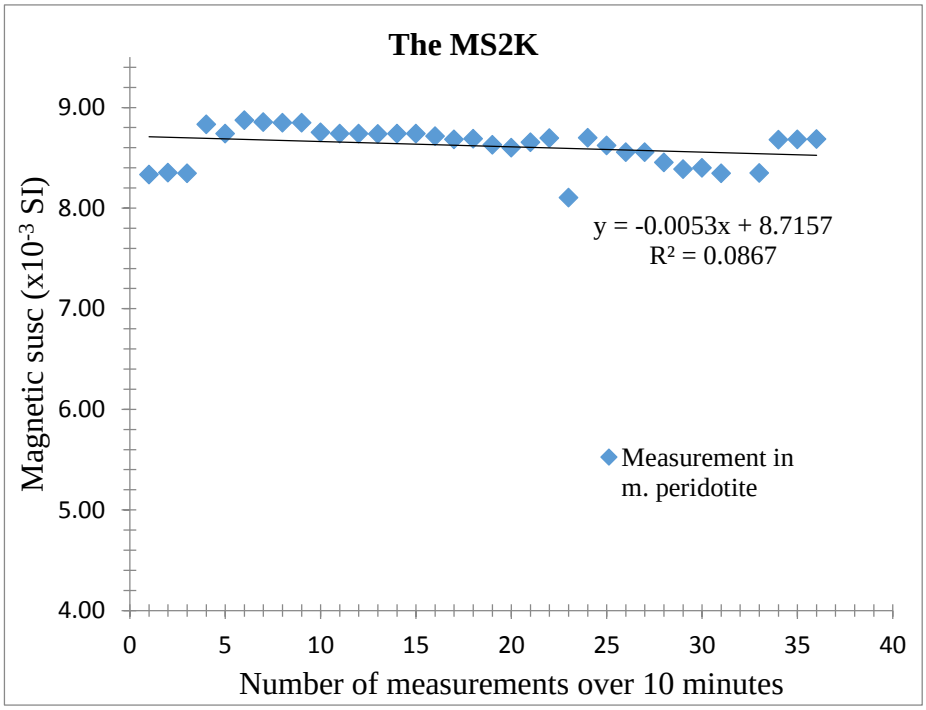

Figure 29: Plot of MS measurements on a mineralized peridotite sample from the 1301020 core.

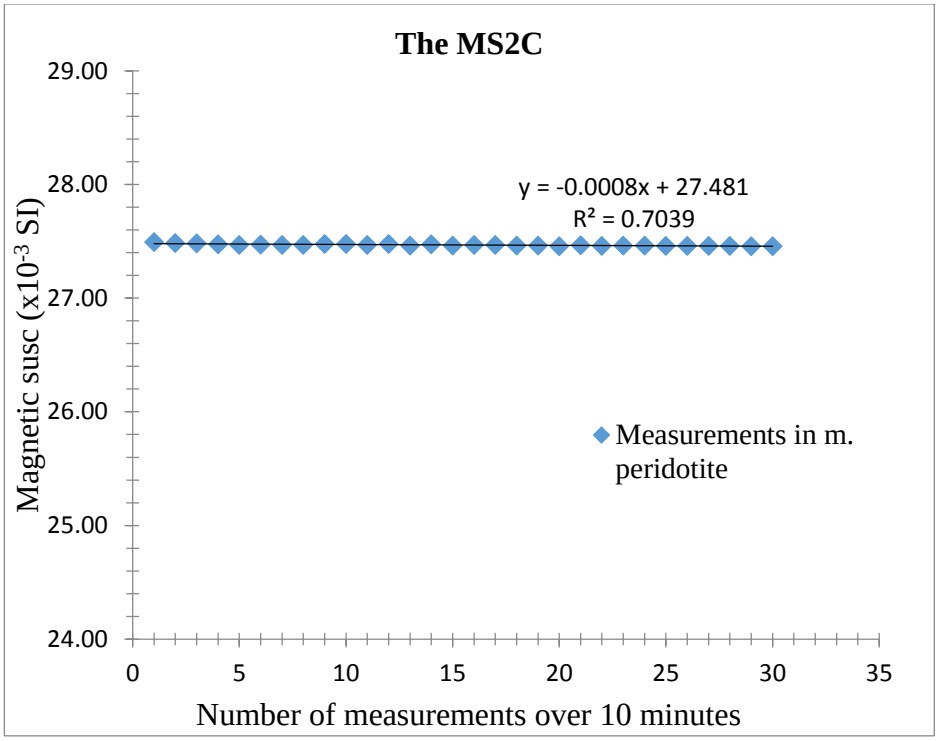

Figure 30: Plot of MS measurements on a mineralized peridotite sample from the 1301020 core.

From the results above, the MS2C and RT-1 show less fluctuation in their measurements relative to the other instruments and a very slight negative drift. The other instruments show greater scatter and the GDD and MS2K show significant drift. The drift is characterized by the slopes shown in table (10) below

Table 10: The slopes obtained from the six MS measurements on mineralized peridotite sample (moderately paramagnetic sample) from the 1301020 core

	RT-1	KT-10	GDD	MS2K	MS2C	SM30
Slope (x10^{-3} SI)	0.0014	0.0082	-0.0396	-0.0053	-0.0008	0.0058

Further drift analyses were performed using the data collected on the KT-10 calibration sample, other rock samples (ultramafic picrite and dolomite) and NQ size (whole and split) core samples: schist and semi-massive sulphide. The measurement on whole and split core was triggered by the need to test

drift on flat surfaced samples and cylindrical samples and (2) the need to monitor the drift on weak and strong magnetic materials.

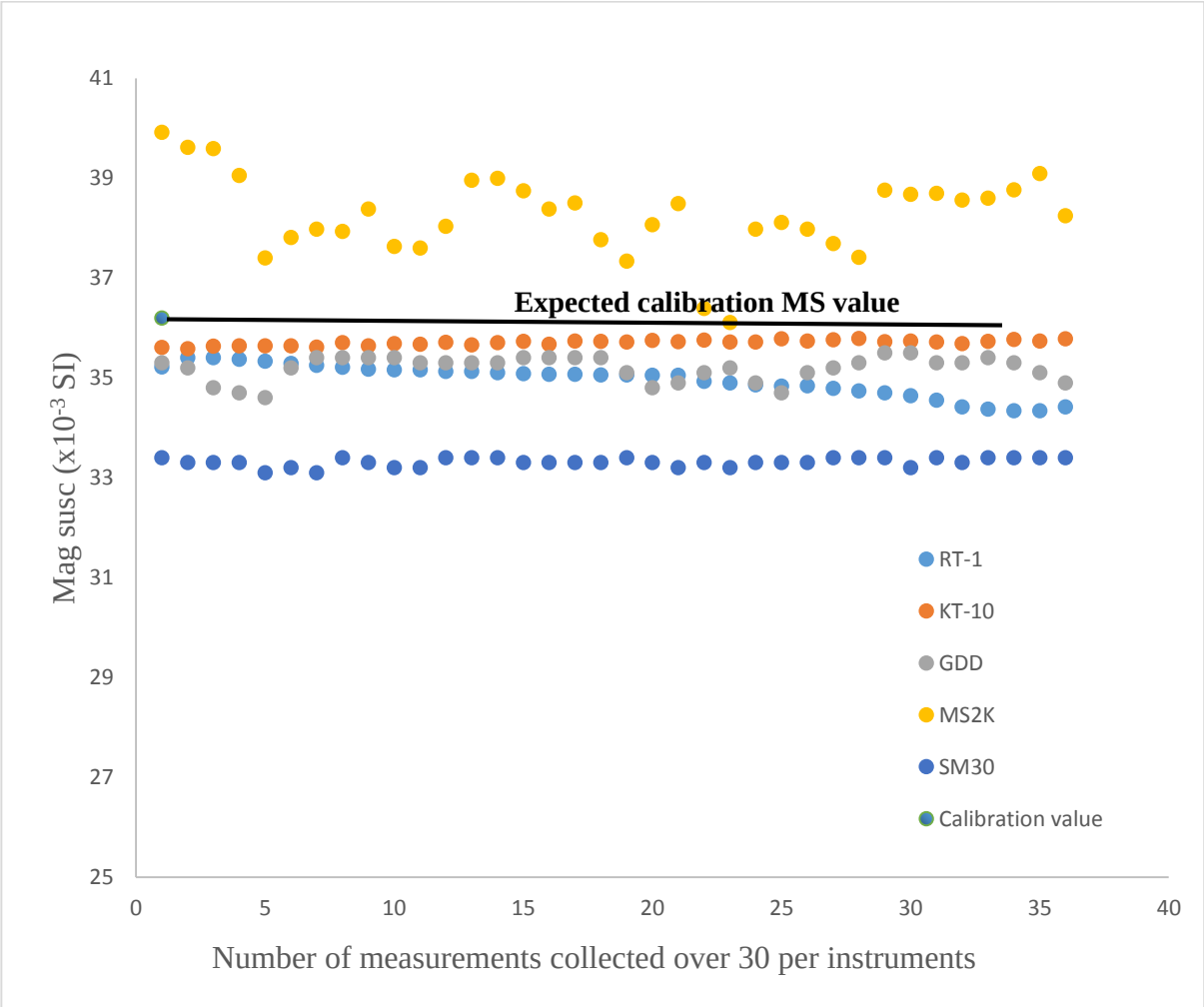

Figure 31: Comparison of magnetic susceptibility instruments on the KT-10 calibration sample.

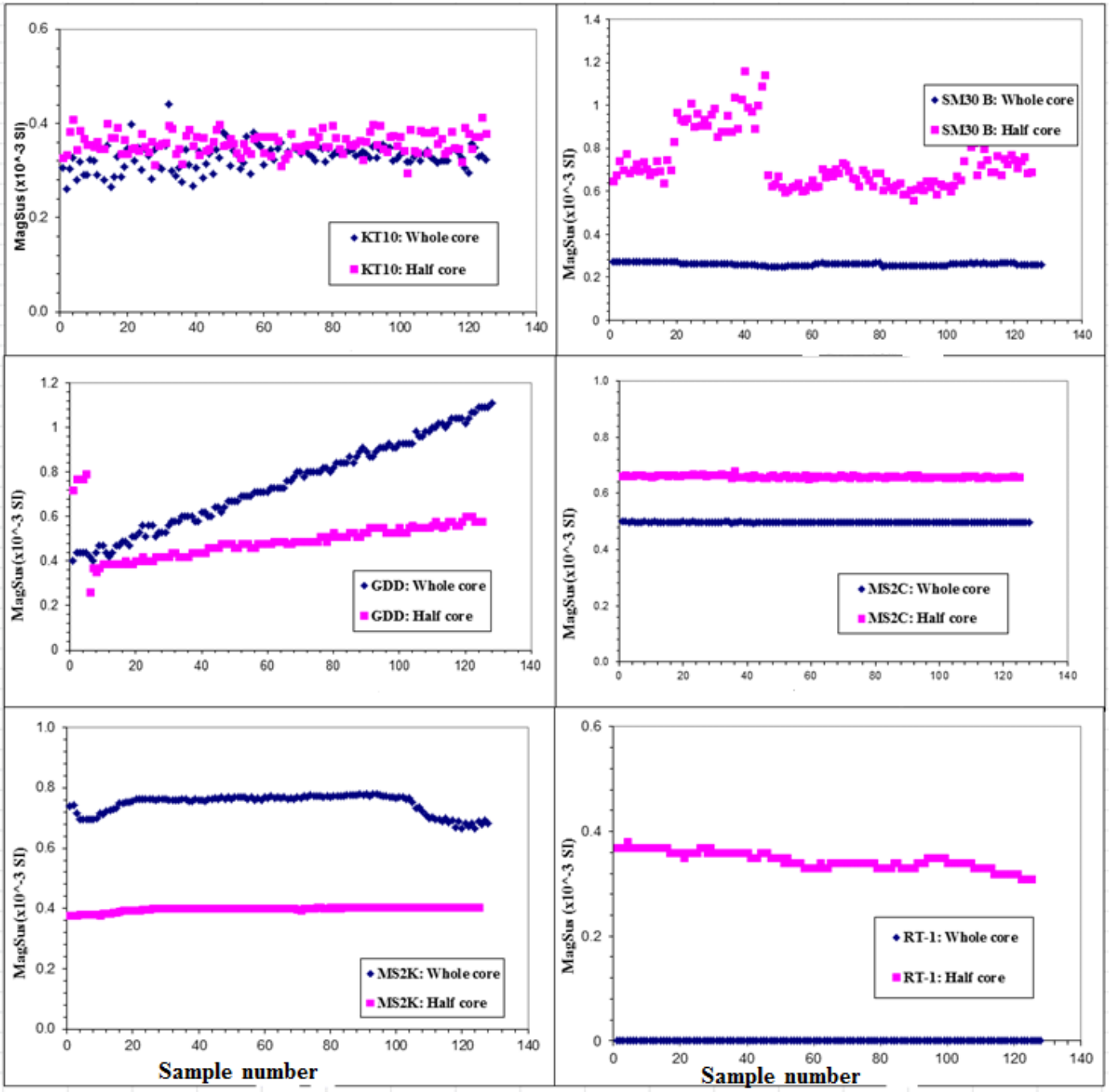

Figure 32: Repeat magnetic susceptibility response on whole and split core - schist. Changes with sample number indicates drift over 30 minutes of data collection per instrument.

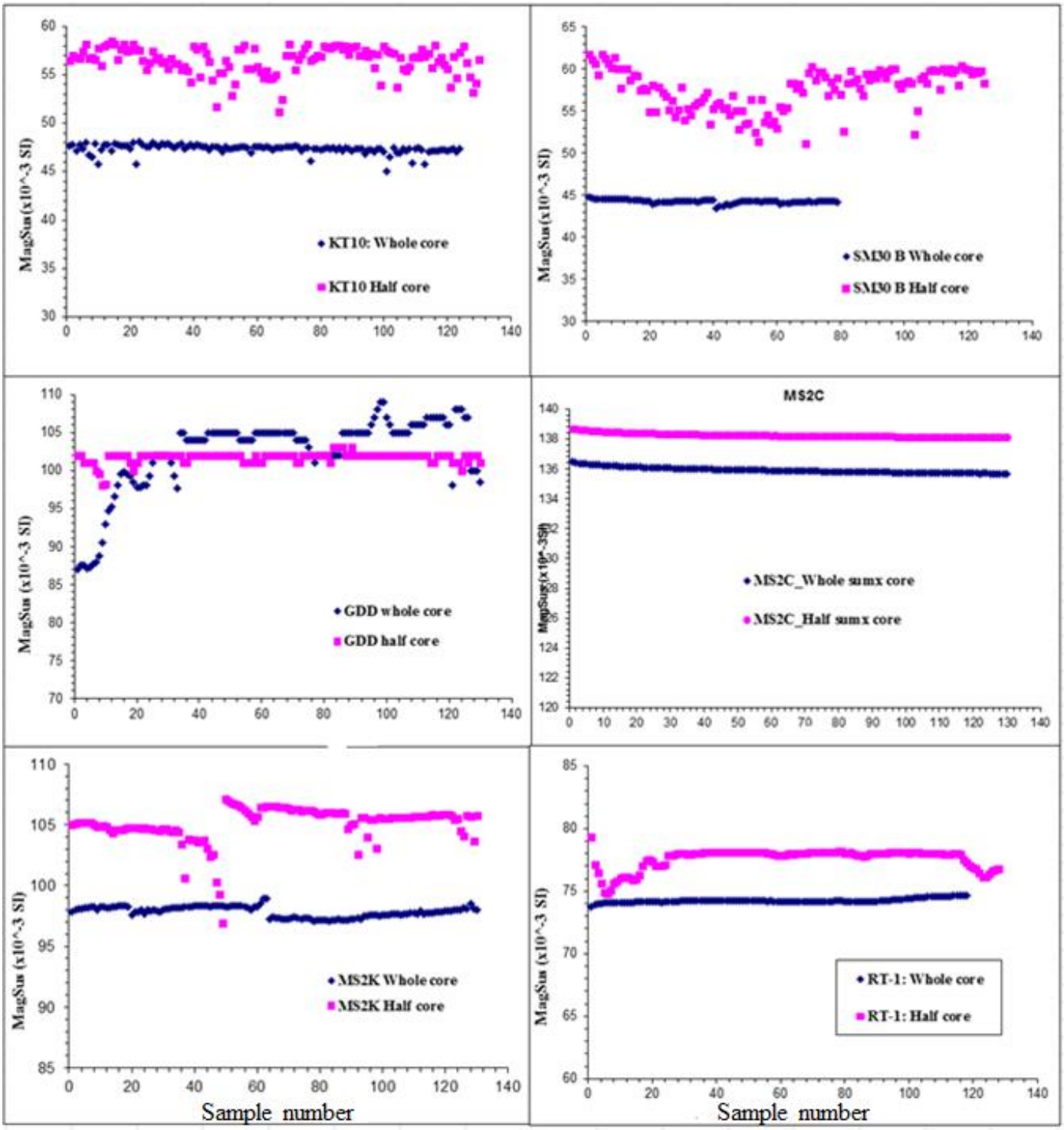

Figure 33: Repeat magnetic susceptibility measurements on whole (dark blue) and split (purple) semi-massive sulfide core. Changes with sample number indicates drift over 30 minutes of data collection per instrument.

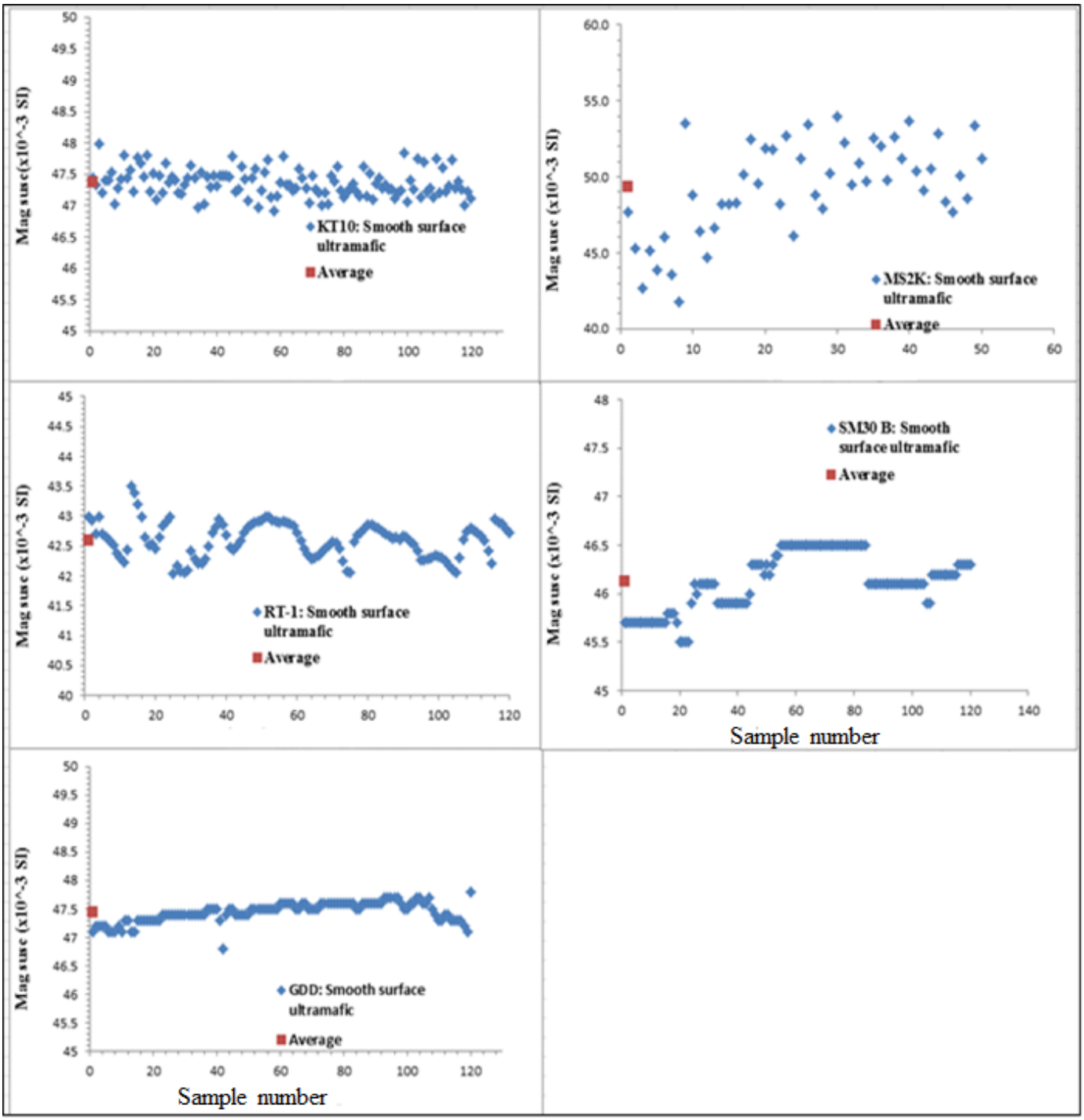

Figure 34: Comparison of magnetic susceptibility response on ultramafic picrite. Changes with sample number indicates drift over 30 minutes of data collection per instrument.

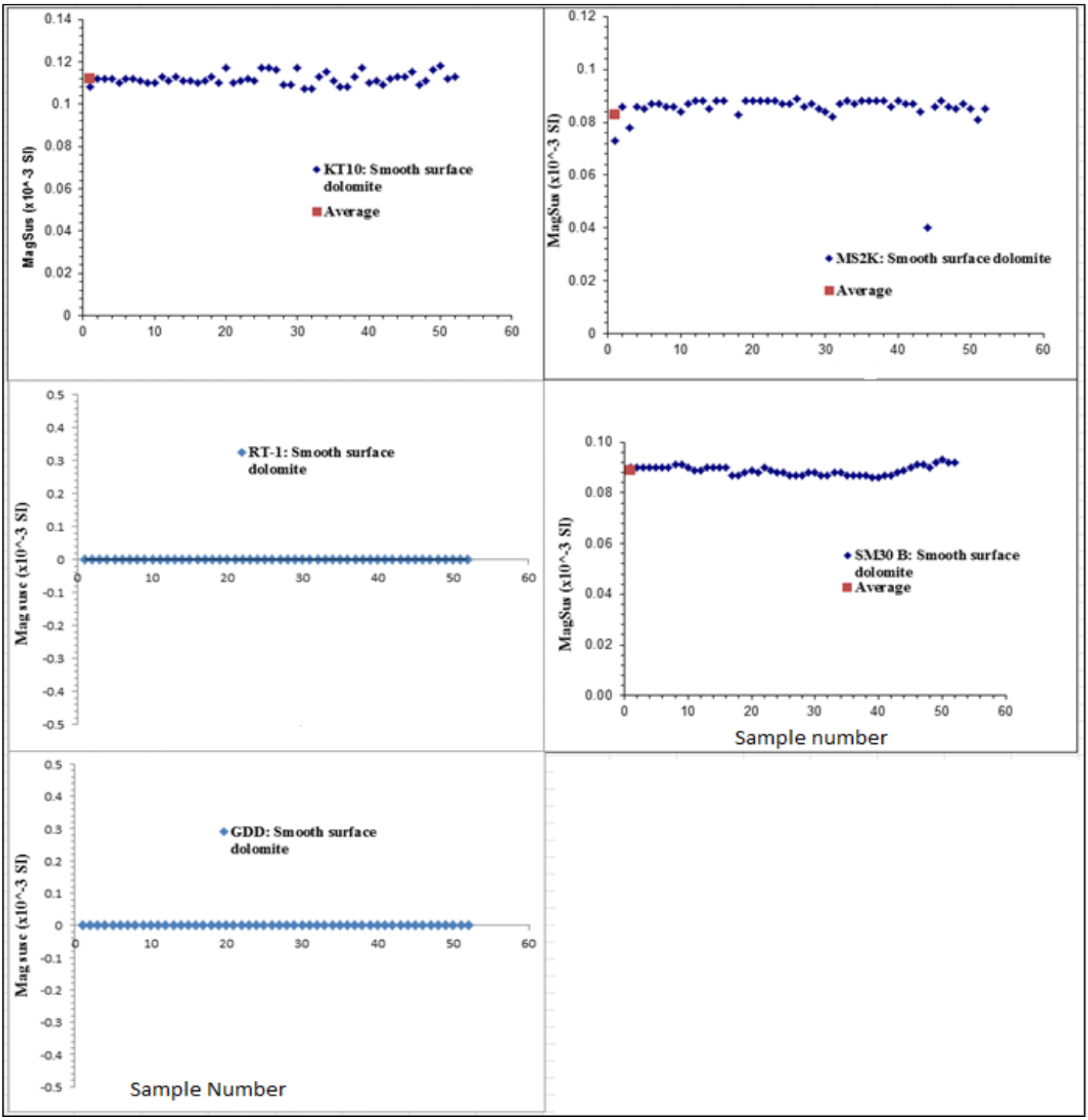

Figure 35: Comparison of magnetic susceptibility response as measured on dolomite sample.

Table 11: Slopes, which demonstrate the magnitude of the temporal drift in figure 32

Schist	RT-1 ($x10^{-3}$ SI)	KT-10 ($x10^{-3}$ SI)	GDD ($x10^{-3}$ SI)	MS2K ($x10^{-3}$ SI)	MS2C ($x10^{-3}$ SI)	SM30 ($x10^{-3}$ SI)
Whole core	-	0.0002	0.0054	-0.0002	-0.00001	-0.00007
Half core	-0.0004	0.00004	0.0011	0.0001	-0.00006	-0.0014

Table 12: Slopes, which demonstrate the magnitude of the temporal drift in figure 33

Semi-massive Sulfide samples	RT-1 ($x10^{-3}$ SI)	KT-10 ($x10^{-3}$ SI)	GDD ($x10^{-3}$ SI)	MS2K ($x10^{-3}$ SI)	MS2C ($x10^{-3}$ SI)	SM30 ($x10^{-3}$ SI)
Whole core slope	0.0037	-0.0046	0.0888	-0.0048	-0.0047	-0.0042
Half core slope	0.0062	-0.0046	0.0043	0.0104	-0.0032	0.0125

Table 13: Slopes, which demonstrate the magnitude of the temporal drift in figure 34

	RT-1 ($x10^{-3}$ SI)	KT-10 ($x10^{-3}$ SI)	GDD ($x10^{-3}$ SI)	MS2K ($x10^{-3}$ SI)	MS2C ($x10^{-3}$ SI)	SM30 ($x10^{-3}$ SI)
Ultramafic slope	-0.0013	-0.0013	0.0028	0.1224	-	0.0048

In figure 31, the MS2K measurements vary significantly compared to the rest of the measurements. According to the plot in figure 31, the KT-10 and SM30 give the most stable measurements of all the devices. The mean of the value measured by the MS2K are higher than the nominal calibration value by 1.8 x 10^{-3} SI whereas the SM30 measurements are 2.9 x 10^{-3} SI lower. The KT-10 measurements are less than the nominal calibration value by 0.5 x 10^{-3} SI. However, all these values are within 10% of the nominal value. The observations in figure 35 show the results from the mineralization peridotite (figure 25 – 30), which show fluctuations in the KT-10 and SM30 measurements and more stable results from the MS2C.

Figure 32 and 33 show the results obtained from taking measurement on whole and split NQ core samples – schist and semi-massive sulphide respectively. In both figures, the KT-10 and MS2C show the least drift, while the GDD shows greater drift (tables 11, 12 and 13). The KT-10 and SM30 show the greatest scatter, while the MS2K and RT1 show some scatter. The split semi-massive sulphide sample clearly show higher MS values in all instruments (except the GDD) while the schist sample gives mixed results (some have high readings in whole core compared with split core and vice versa). It is also noted that the RT-1 shows a zero reading on whole core and non-zero readings on split core as shown in figure 32.

Comparing the values of figures 32 and 33, it can be seen that the MS2K, MS2C and GDD give higher magnetic susceptibility readings compared to the RT-1, KT-10 and SM30. This observation is consistent with most of the acquired data through the study season.

The results on the ultramafic picrite sample show the most stable measurement (least affected by temporal drift) with the KT-10 (figure 34) amongst the five instruments used. Perhaps the variability is a reflection of the homogeneity of the ultramafic picrite and the dolomite samples. The variability of the KT-10 on cut and uncut core (figure 32) might be a reflection of the way that core was cut.
Figure 35 show measurements on the dolomite sample. This sample has a lower susceptibility, with the RT-1 and GDD giving readings of zero, while the other instruments gave non-zero readings. The readings from this sample are below the detection limits of the GDD and RT-1. There is a little more variability in this low susceptibility case, with the readings differing by about 15%. The KT-10 show the most stable results among the three non-zero measurements. In figure 34 and 35, the MS2C was not used because the shape and size of the sample (non-cylindrical shape) did not fit in the hollow MS2C sensor.

Drift over the data acquisition season

The data were collected between the months of April and July, 2013. During this time, measurements on the KT-10 calibration sample were recorded using each instrument at the beginning of each work day. These measurements were then displayed on scatter plot and their variation over the three months analyzed. The results were as shown below (figure 36).

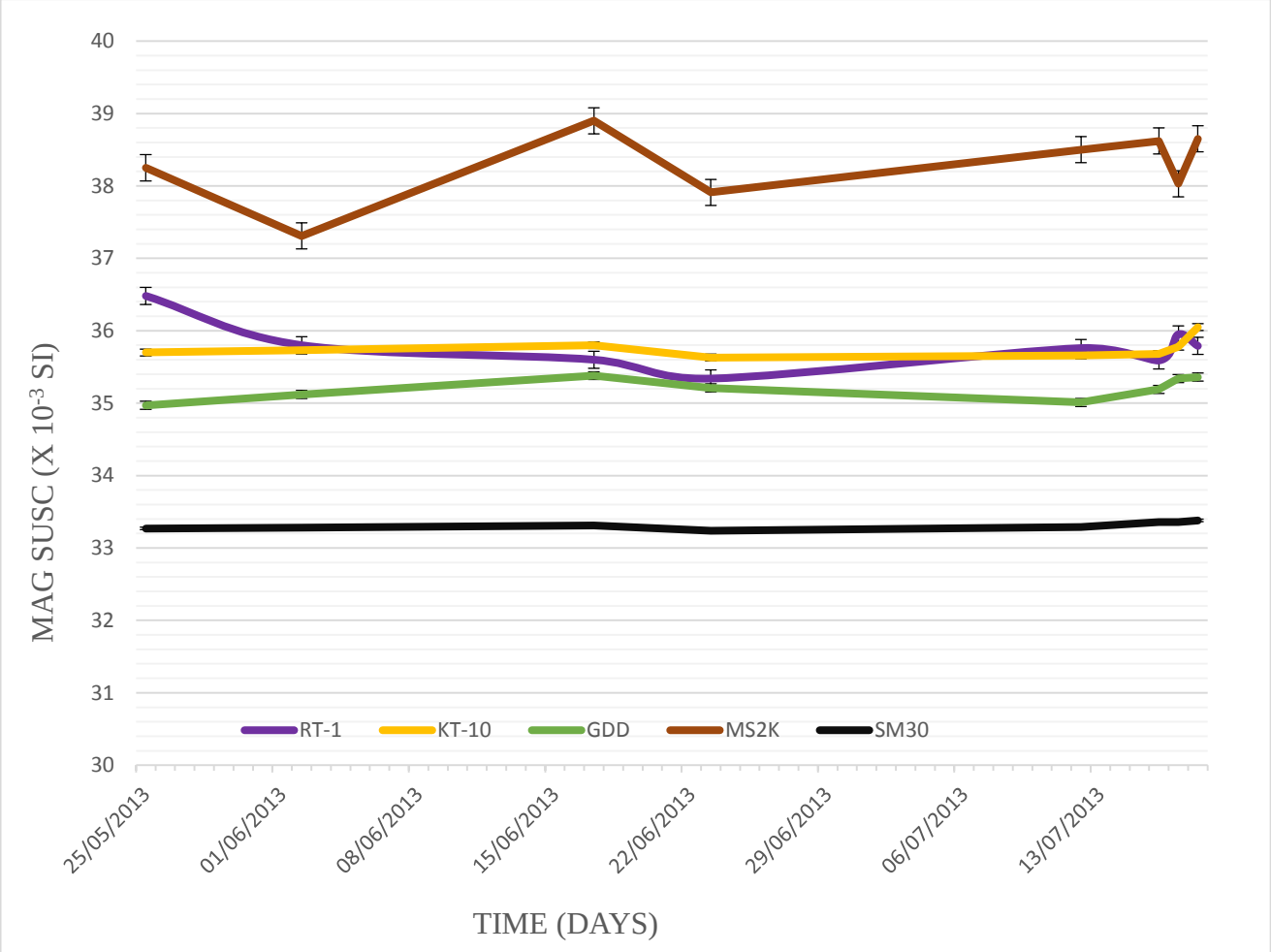

Figure 36: Comparison of the drift of the magnetic susceptibility instruments over three months with error bars. The measurements were recorded using each instrument on the KT-10 calibration sample with a nominal value of 36.2 x 10^{-3} SI.

It was observed that measurements collected with MS2K fluctuate the most over three months and SM30 and KT-10 show more stable results over that period. The temporal variation is of the order of

3% or less, which is acceptable for this study. There were no data collected with the MS2C because of the sample size could not permit the use of the MS2C meter.

6.4 Statistical methods

All of the data collected for this research (discussed in previous chapter) were analyzed using the statistical techniques presented in Kume (1987). These include measures of central tendency, measures of dispersion and measures of association.

Measures of central tendency

These are statistical methods use to define the center of the data and include mean, median and modes. The mean is the average value of the data; median is the value that falls in the middle of the data if it is ordered from smallest to the largest; and the mode is the value that is most common in the dataset. In this thesis, the means and the medians are used, as they present the simplest techniques to calculate central tendencies of data. For example, the averaged measurements on the KT-10 and MS2C calibration samples were calculated and presented in table 14

Table 14: Mean values taken on Terraplus' KT10 calibration pad and the MS2C calibration rod. The values in red are the optimal values reported by the manufacturers. The symbol * indicates measurements not taken.

Samples	Nominal values	KT10	RT1	MS2K	MS2C	SM30	GDD
	($x10^{-3}$ SI)	($x10^{-3}$ SI)	($x10^{-3}$ SI)	($x10^{-3}$ SI)	($x10^{-3}$ SI)	($x10^{-3}$ SI)	($x10^{-3}$ SI)
KT10 cal. sample	**36.2**	35.7	34.96	38.26	*	33.31	35.190
MS2C cal. sample	**10.68**	4.32	3.72	4.09	11.04	4.22	3.980

Errors

Percentage errors were calculated by taking the difference between the sample's nominal value and the averaged readings from this study (table 14) normalized by known nominal value. The errors were calculated as a percentage and tabulated in table 15.

Table 15: Errors calculated from the tables of measurements whose means are presented in table 14

Samples	**KT10** (%)	**RT-1** (%)	**MS2K** (%)	**MS2C** (%)	**SM30** (%)	**GDD** (%)
KT10 cal. sample	-1.37	-3.44	5.68	-	-7.98	-2.790
MS2C cal. sample	-59.51	-65.14	-61.66	3.36	-60.52	-62.780

Measures of dispersion

Dispersion is a term that describes how a set of repeated measurements varies from the central value. The measures of the magnitude of dispersion in datasets include

i. **Range (R)** – is the difference between the smallest (min) and the largest (max) values of any given datasets.

$$R = Max - Min \quad (6)$$

ii. **Variance (V)** - is defined as the mean of the square of the difference between individual data and the averaged measurements. This statistical method determines how far apart the measurements are scattered. Equation 7 is the formula used in this research to determine the sample variance.

$$V = \frac{1}{n}\sum_{i=0}^{n}(x_i - \bar{x})^2 \quad (7)$$

iii. **Standard deviation** (S) –This is a statistical methods used in determining the diversity of the dataset in the same units as the measurement. It was calculated by taking the square root of the variance.

$$S = \sqrt{V} \quad (8)$$

iv. **Coefficient of variation (CV)** – is a quantity derived by dividing the sample standard deviation by the sample mean. It is expressed mathematically as shown in equation 9 below (Wolfram Math World, www.mathworld.wolfram.com)

$$C.V. = \frac{Standard\ Deviation}{mean} \quad (9)$$

After calculating the range, variance, standard deviation and coefficient of variation from the data used to derive the values in table 14 and 15, the results were as shown in table 16 below.

Table 16: Measures of dispersion as calculated from the data collected on KT-10 and MS2C calibration samples. The symbol * indicates data was not collected due to sample size and shape

Measure	Samples	KT10	RT1	MS2K	MS2C	SM30	GDD
Range (x10^{-3} SI)	MS2C	0.570	0.150	0.169	0.012	0.230	0.270
	KT10	0.203	1.060	3.806	*	0.300	0.900
Variance (x10^{-3} SI)	MS2C	0.018	0.002	0.003	0.000	0.002	0.004
	KT10	0.003	0.099	0.647	*	0.008	0.060
Standard deviation (x10^{-3} SI)	MS2C	0.134	0.039	0.051	0.003	0.043	0.066
	KT10	0.053	0.314	0.900	*	0.094	0.246
Coefficient of variation	MS2C	0.031	0.010	0.012	0.000	0.010	0.017
	KT10	0.001	0.009	0.024	*	0.003	0.007

The averages presented in table 14 and the percent errors in table 15 show small difference from the nominal values obtained by the manufacturers during their calibration. On the KT-10 calibration sample it is observed that MS2K gives an averaged value that is about 6% too high, while the SM30 gives a value that is 8% too low. When measurements were taken on MS2C calibration sample, it is noticed that all instruments, except MS2C, gave values 60% too low. This is associated with the curved geometry of the sample's surface.

In table 16, the results from the measures of dispersion are tabulated. It is observed that KT-10 measurements on KT-10 calibration sample show the lowest range, variance, standard deviation and the coefficient of variation whereas the MS2K gives the highest range, variance, standard deviation and the coefficient of variation. There were no measurements recorded with the MS2C to compare it with the other instruments. The measurements on the MS2C calibration sample show the KT-10 as having the highest range, variance, standard deviation and the coefficient of variation while MS2C show the lowest parameters of the measures of dispersion.

Measures of Association

Measures of association are statistical coefficients that demonstrate the strength of the relationship between two variables (www.stasticssolutions.com) for measurements on a large number of different samples. The most common measure of association is the correlation coefficient (R-squared or R^2). This parameter measures the degree of agreement between two or more datasets. In this thesis, the two variables were plotted on correlation diagrams and the R^2 calculated. The value used to characterize the reading for each sample could be the mean or the median. It was not yet clear which of these two to use, so the measured of association were calculated for both and compared.

Correlation using the averaged values

The averaged values from each instrument on all 71 samples were compared on correlation diagrams. On each axis, the value plotted is the logarithm (base 10) of the magnetic susceptibility (x 10^{-3} SI), so a value of 0 corresponds to $1x10^{-3}$ SI and a value of -2 to $1x10^{-5}$ SI. The following subsection presents correlation diagrams (figures 37 to 42) and discusses the results.

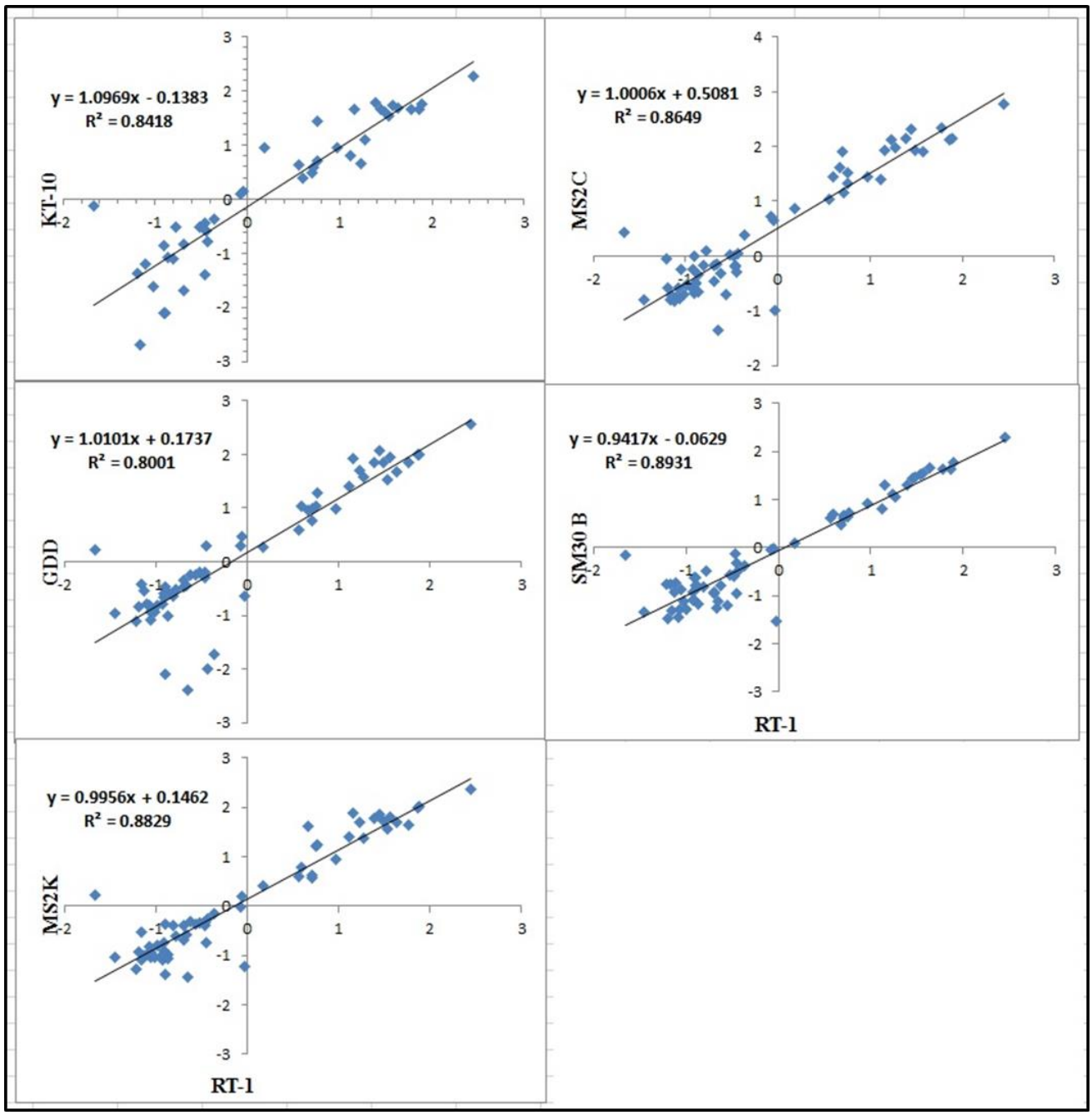

Figure 37: Correlation analysis of the averaged MS values obtained from the tested sensors vs RT-1.

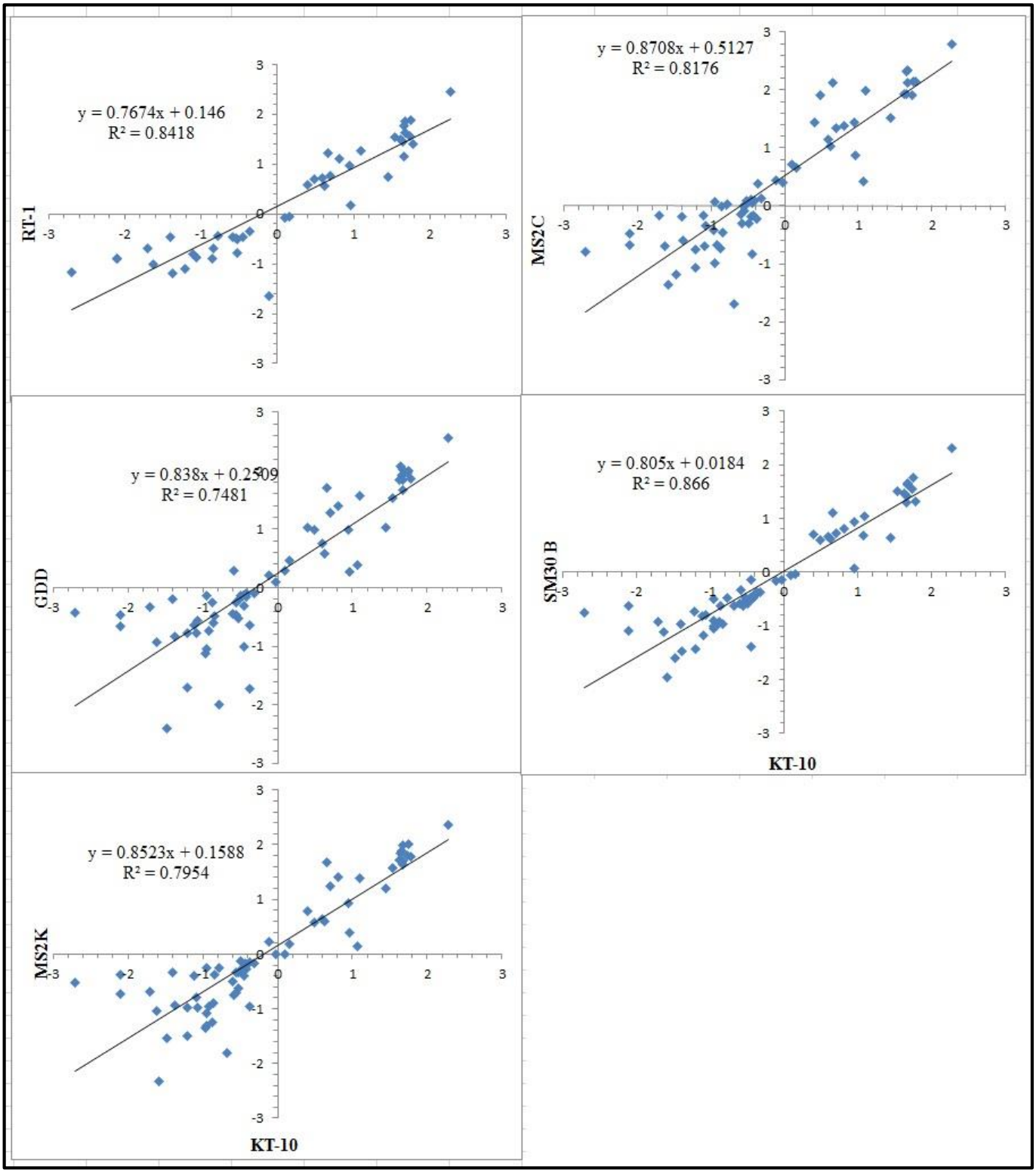

Figure 38: Correlation analysis of the averaged MS values obtained from the tested sensors vs KT-10.

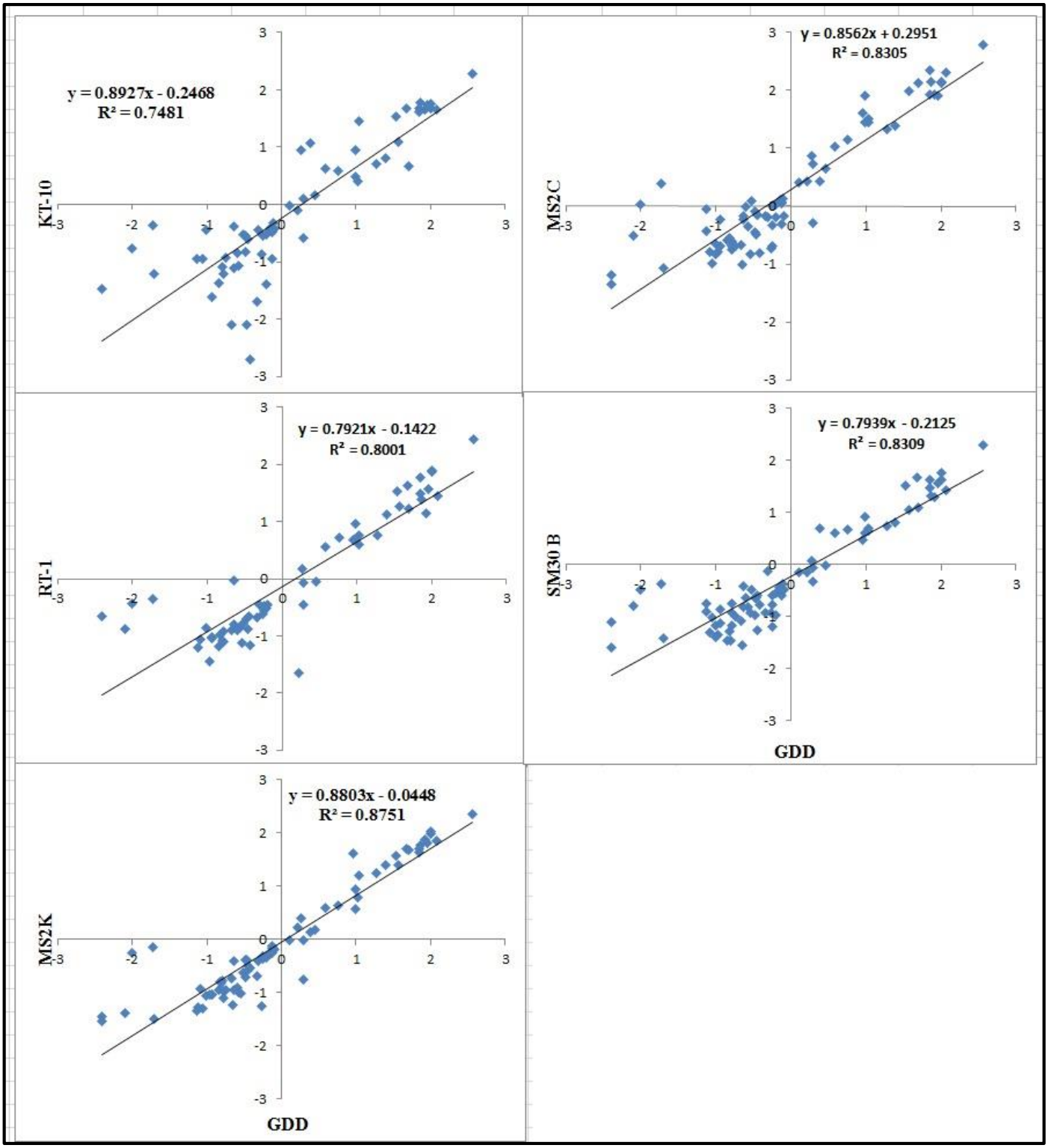

Figure 39: Correlation analysis of the averaged MS values obtained from the tested sensors vs GDD.

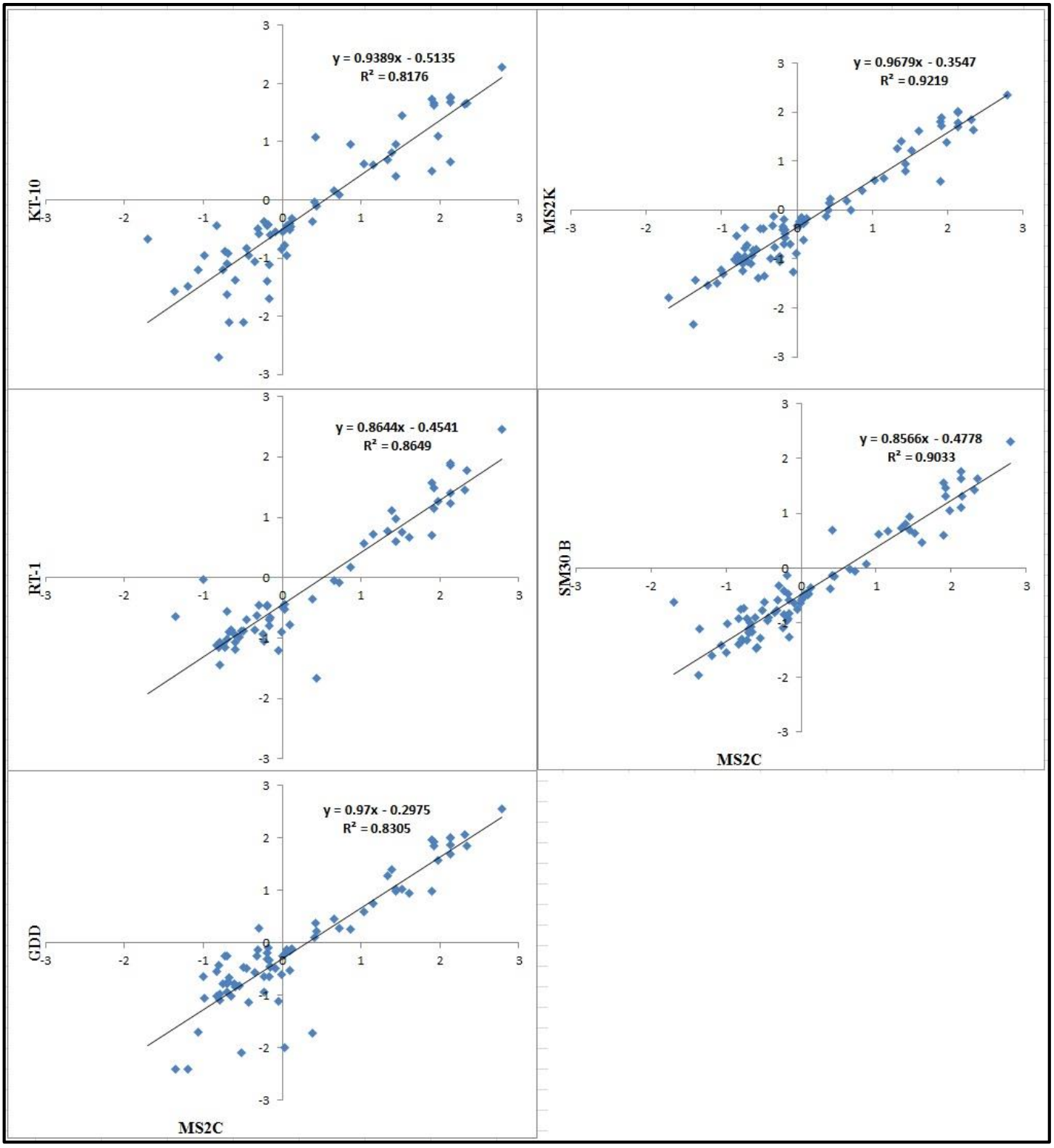

Figure 40: Correlation analysis of the averaged MS values obtained from the tested sensors vs MS2C

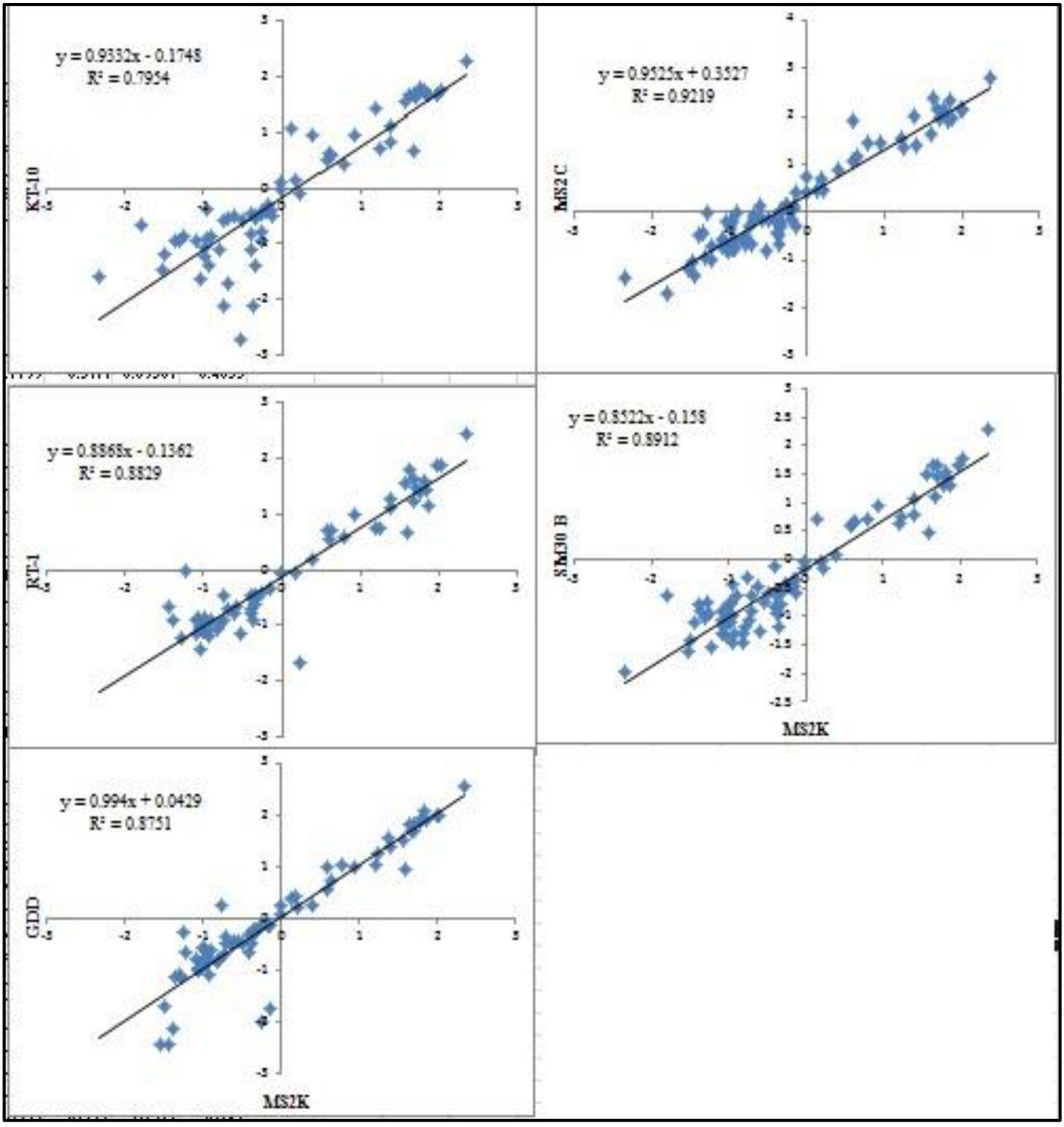

Figure 41: Correlation analysis of the averaged MS values obtained from the tested sensors vs MS2K.

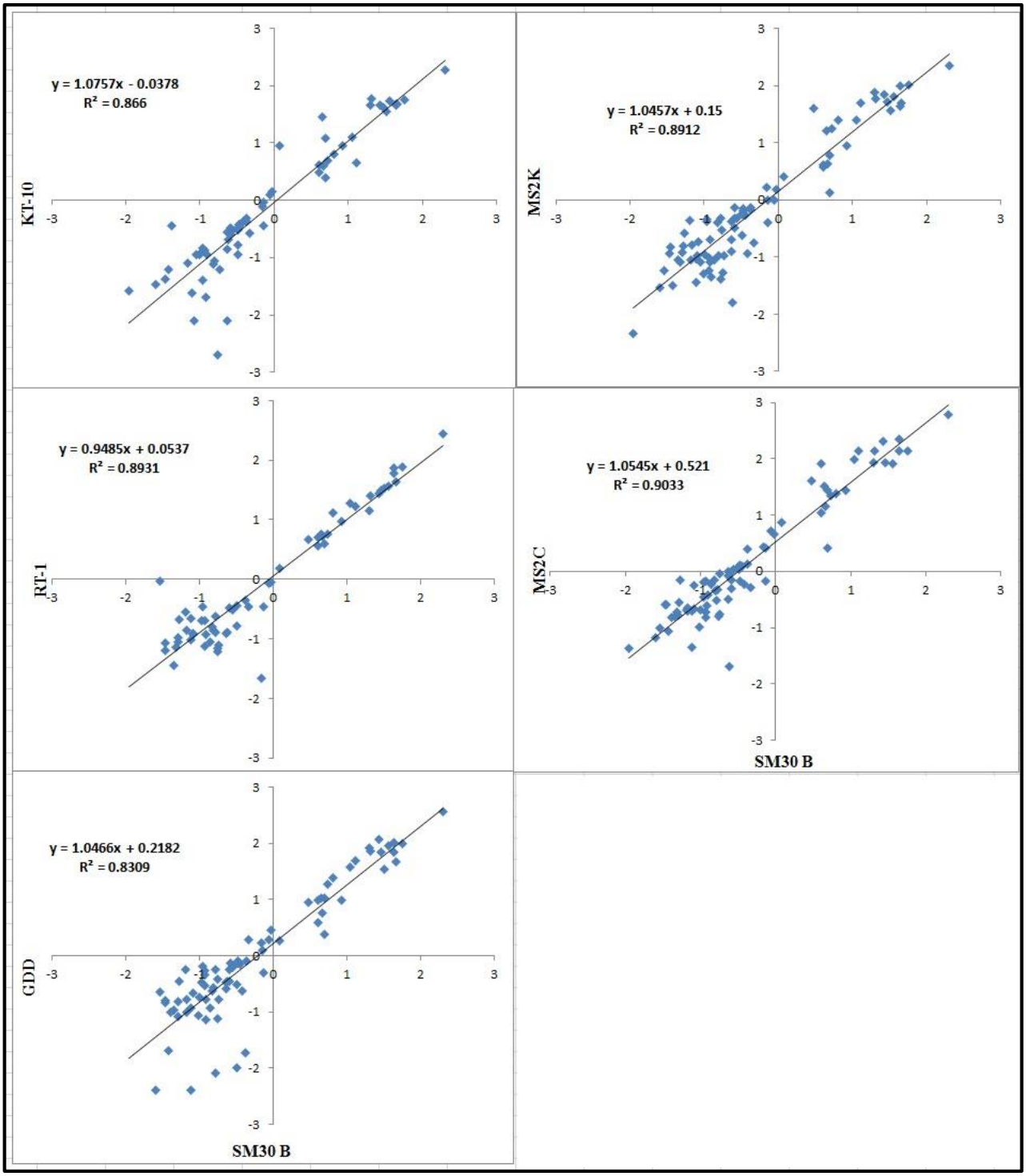

Figure 42: Correlation analysis of the averaged MS values obtained from the tested sensors vs SM30

The slopes, intercepts and R-squared were tabled as shown in table 17, 18 and 19 respectively. If there is a perfect correlation, the slope and R^2 will be one and the intercept value at zero.

Table 17: Slopes of the logarithmic correlation diagrams shown in figure 37 – 42. The rows are the instrument on the y axis and the columns the x axis. Red values are slopes greater than 1, greens are slopes close to 1 and blues are the lowest values

Slopes						
	KT10	RT1	GDD	MS2K	MS2C	SM30 B
KT10	1	1.0969	0.8927	0.9332	0.9389	1.0757
RT1	0.7674	1	0.7921	0.8868	0.8644	0.9485
GDD	0.838	1.0101	1	0.994	0.97	1.0466
MS2K	0.8523	0.9956	0.8803	1	0.9679	1.0457
MS2C	0.8708	1.0006	0.7939	0.9525	1	1.0545
SM30 B	0.805	0.9417	0.8562	0.8522	0.8566	1

Table 18: Intercepts of lines of "best fit" in the correlation diagrams in figure 37 – 42. The rows are the instrument on the y axis and the columns the x axis.

Intercepts						
	KT10	RT1	GDD	MS2K	MS2C	SM30 B
KT10	0	-0.1383	-0.2468	-0.1748	-0.5135	0.0378
RT1	0.146	0	-0.1422	-0.1362	-0.4541	0.0537
GDD	0.2509	0.1737	0	0.0429	-0.2995	0.2182
MS2K	0.1588	0.1462	-0.0448	0	-0.3547	0.15
MS2C	0.5127	0.5081	0.2951	0.3527	0	0.521
SM30 B	0.0184	-0.0629	-0.2125	-0.158	-0.4778	0

Table 19: R-squared values denoting how the degree of correlation between measurements plotted in figure 37 - 42. The rows are the instrument on the y axis and the columns the x axis. Red values show the closest correlation between MS2K and MS2C

R – squared						
	KT10	RT1	GDD	MS2K	MS2C	SM30 B
KT10	1	0.8418	0.7481	0.7954	0.8176	0.866
RT1	0.8418	1	0.8001	0.8829	0.8649	0.8931
GDD	0.7481	0.8001	1	0.8751	0.8305	0.8309
MS2K	0.7954	0.8829	0.8751	1	0.9219	0.8912
MS2C	0.8176	0.8649	0.8305	0.9219	1	0.9033
SM30 B	0.866	0.8931	0.8309	0.8912	0.9033	1

Correlation using the median values

The results in the previous section are now compared with the correlation diagrams (figures 43 to 48) generated by taking the median MS for each sample and each instrument.

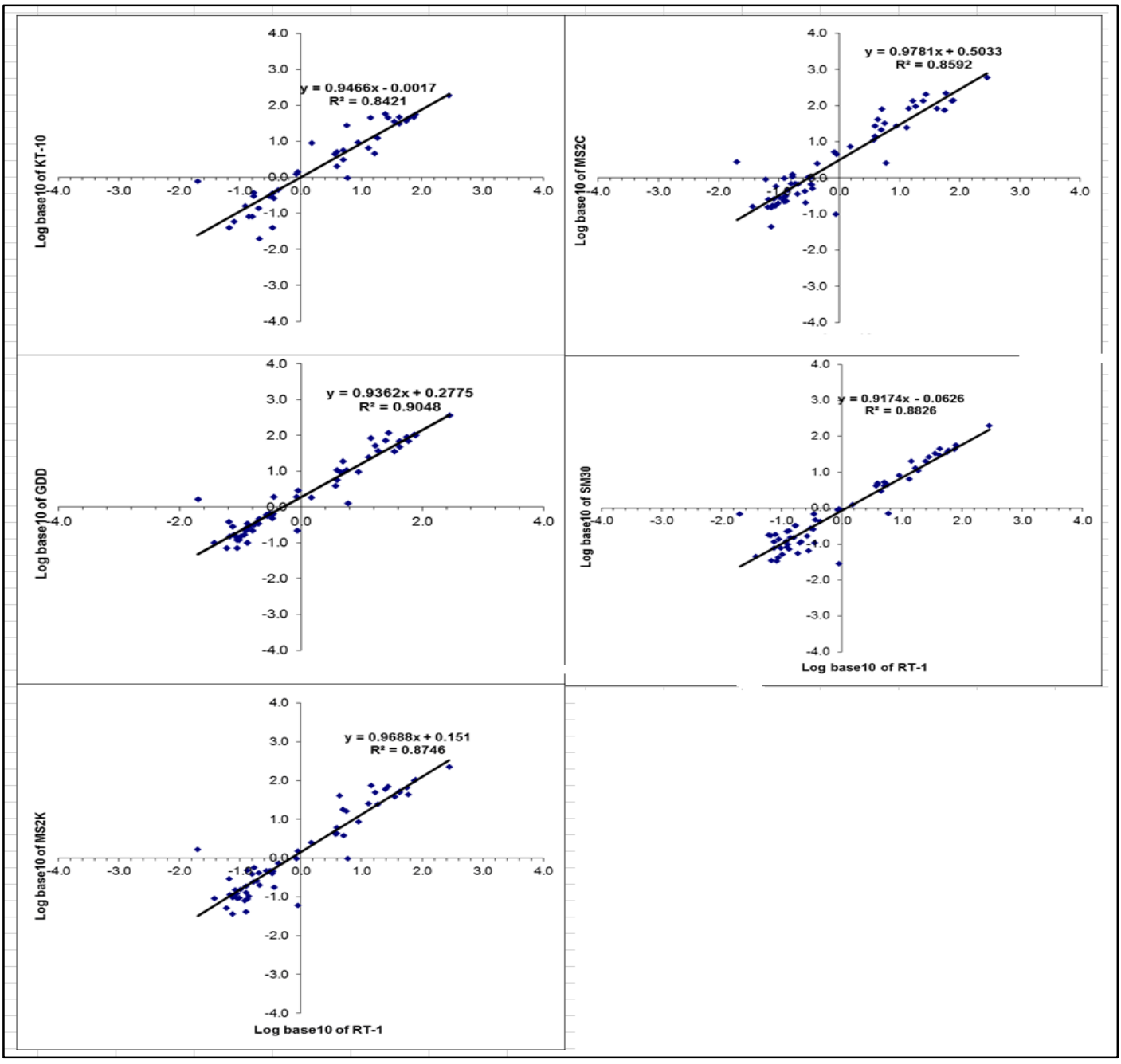

Figure 43: Correlation analysis of the median MS values obtained from the tested sensors vs RT-1.

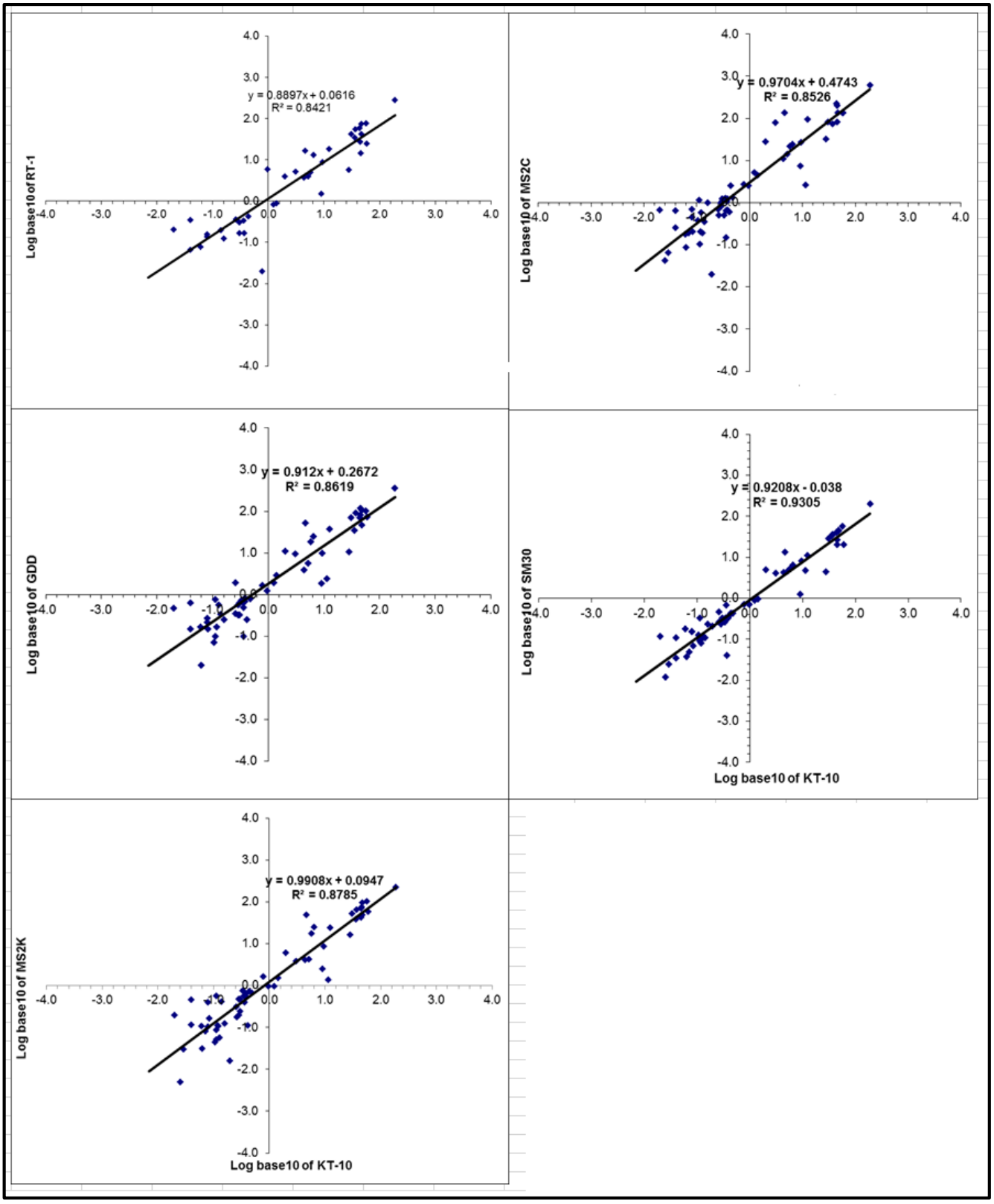

Figure 44: Correlation analysis of the median MS values obtained from the tested sensors vs KT-10.

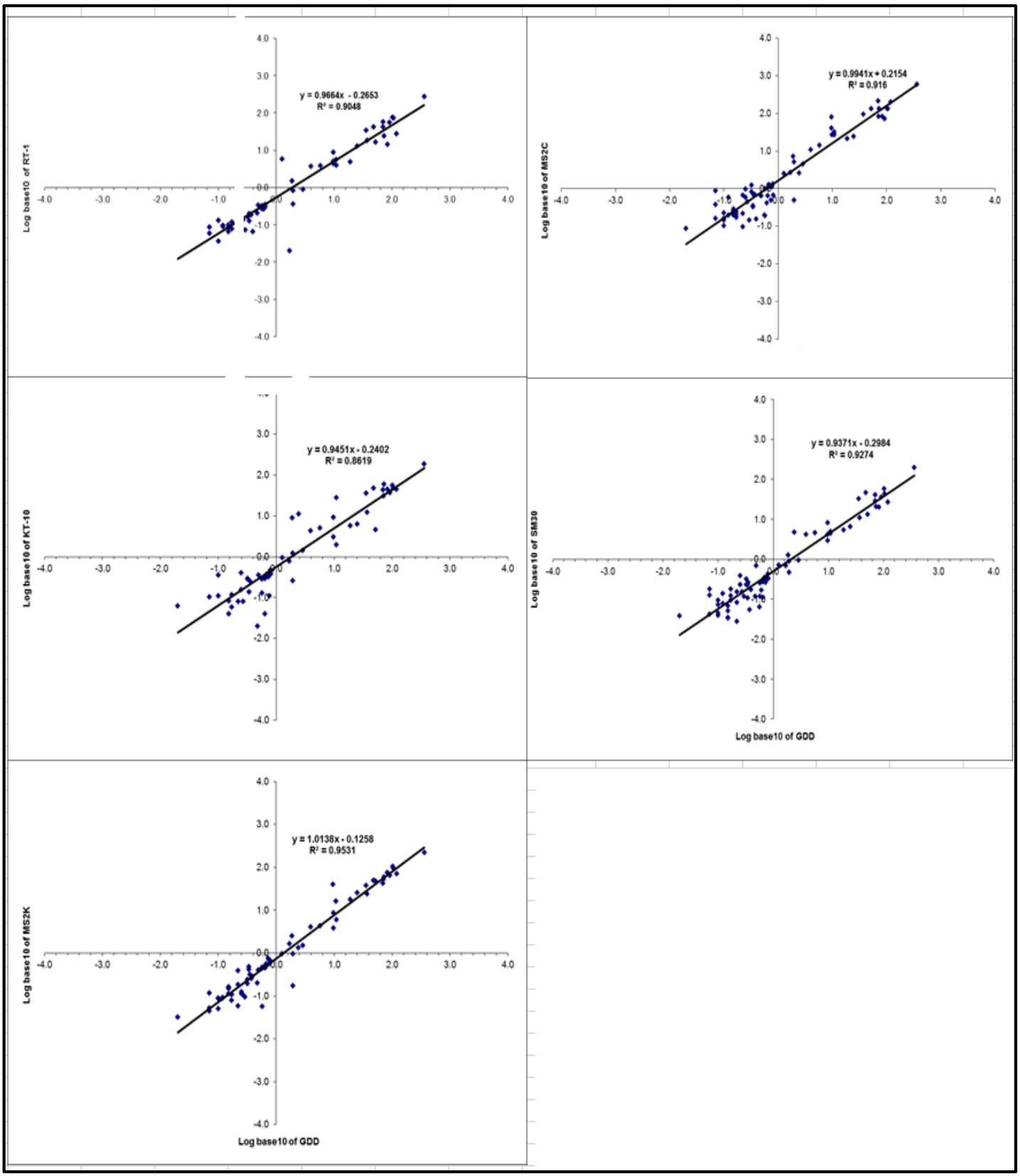

Figure 45: Correlation analysis of the median MS values obtained from the tested sensors vs GDD.

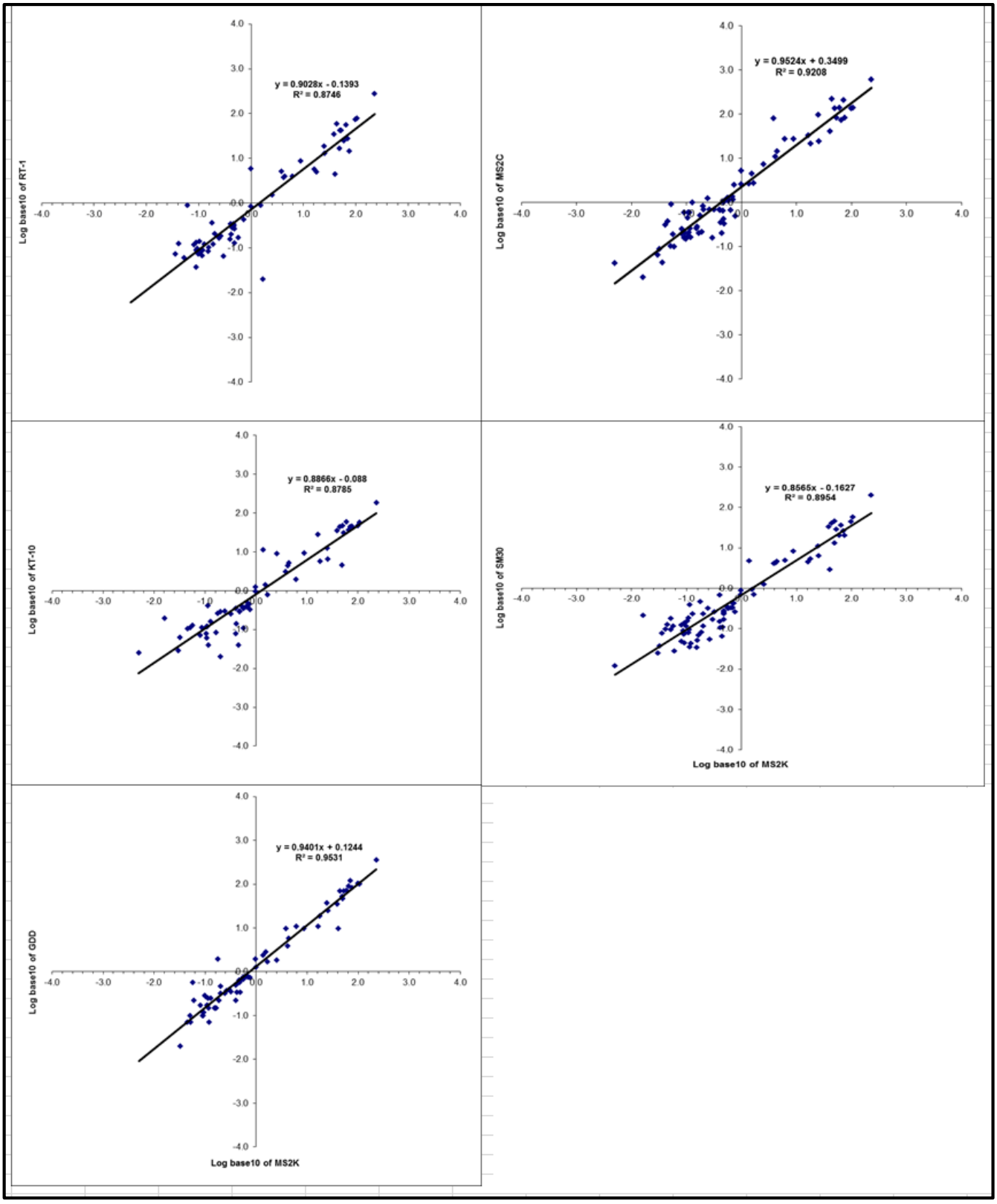

Figure 46: Correlation analysis of the median MS values obtained from the tested sensors vs MS2K.

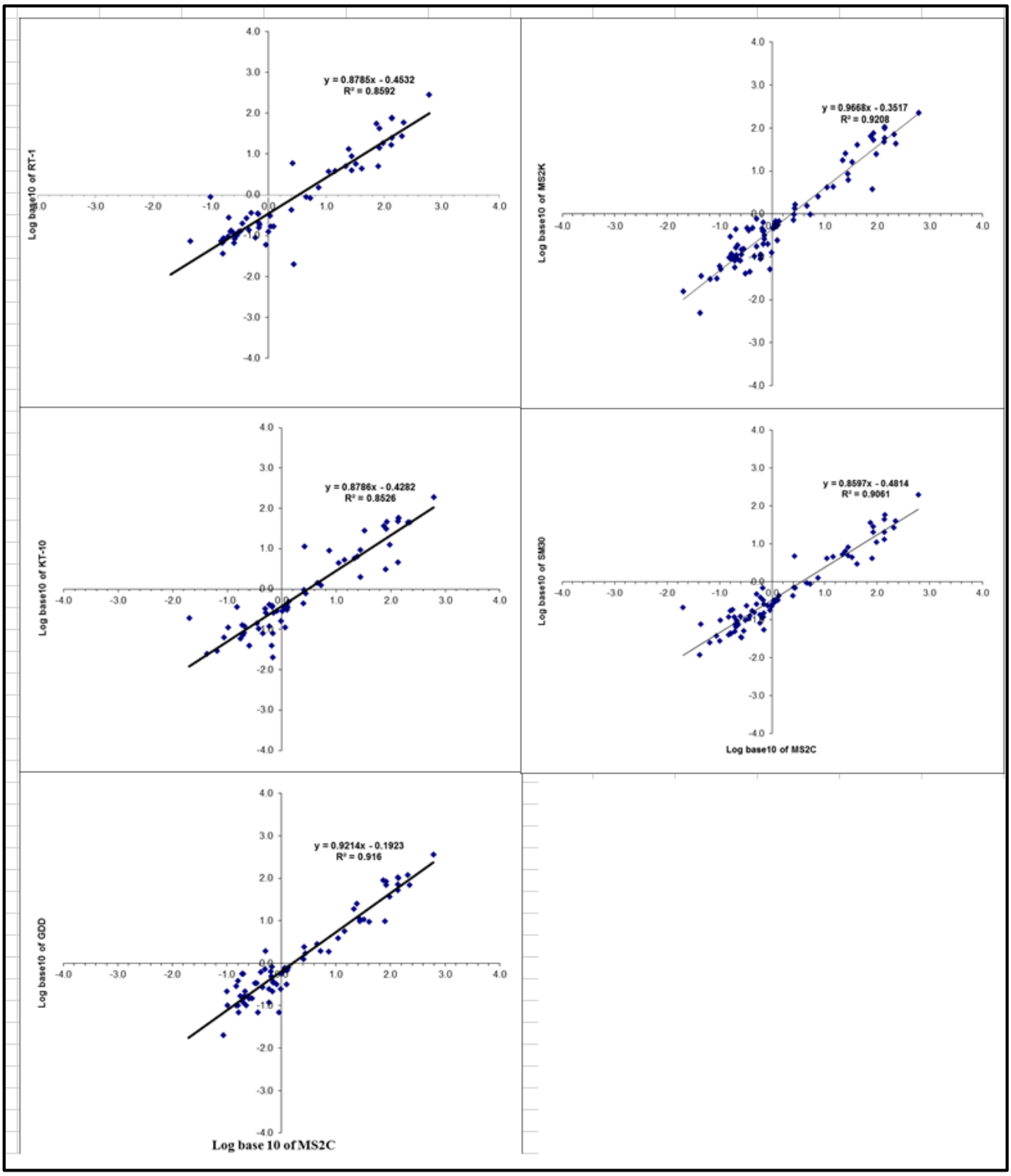

Figure 47: Correlation analysis of the median MS values obtained from the tested sensors vs MS2C.

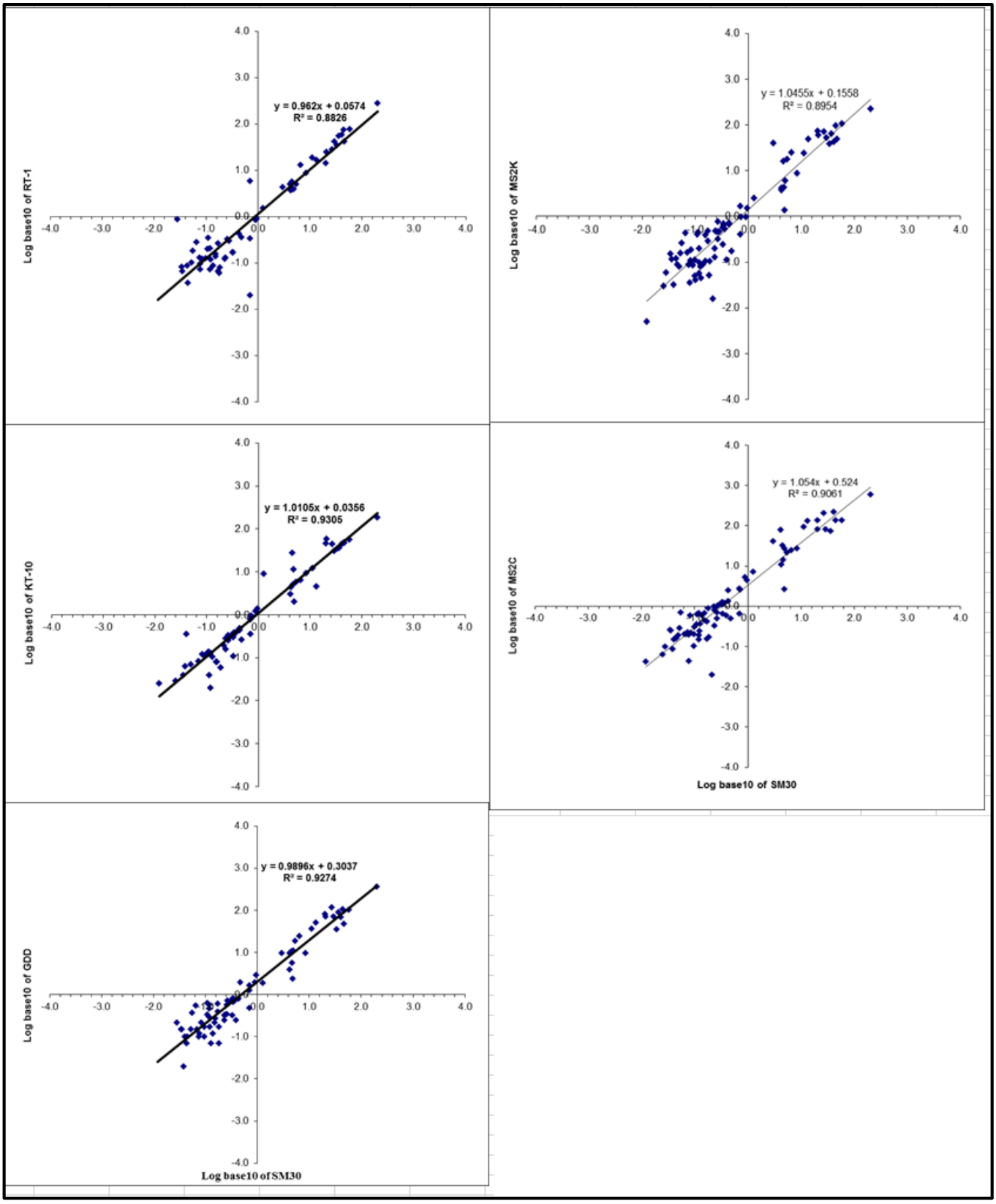

Figure 48: Correlation analysis of the median MS values obtained from the tested sensors vs SM30

Table 20: Show the slopes of the logarithmic correlation diagrams of the medians in figure 43 – 48. The rows are the instrument on the y axis and the columns the x axis.

Slopes						
	KT-10	RT-1	GDD	MS2K	MS2C	SM30B
KT-10	1	0.8897	0.912	0.9908	0.9704	0.9208
RT-1	0.9466	1	0.9362	0.9688	0.9781	0.9174
GDD	0.9451	0.9664	1	1.0138	0.9941	0.9371
MS2K	0.8866	0.9028	0.9401	1	0.9524	0.8565
MS2C	0.8786	0.8785	0.9214	0.9668	1	0.8597
SM30B	1.0105	0.962	0.9896	1.0455	1.054	1

Table 21: Show the intercepts of the logarithmic correlation diagrams of the medians in figure 43 – 48. The rows are the instrument on the y axis and the columns the x axis.

Intercepts						
	KT-10	RT-1	GDD	MS2K	MS2C	SM30B
KT-10	0	0.0616	0.2672	0.0947	0.4743	-0.038
RT-1	-0.0017	0	0.2775	0.151	0.5033	-0.0626
GDD	-0.2402	-0.2653	0	-0.1258	0.2154	-0.2984
MS2K	-0.088	-0.1393	0.1244	0	0.3499	-0.1627
MS2C	-0.4282	-0.4532	-0.1923	-0.3517	0	-0.4814
SM30B	0.0356	0.0674	0.3037	0.1558	0.524	0

Table 22: Show the R-squared of the logarithmic correlation diagrams of the medians in figure 43 – 48. The rows are the instrument on the y axis and the columns the x axis.

R-Squared						
	KT-10	RT-1	GDD	MS2K	MS2C	SM30B
KT-10	1	0.8421	0.8619	0.8785	0.8526	0.9305
RT-1	0.8421	1	0.9048	0.8746	0.8592	0.8826
GDD	0.8619	0.9048	1	0.9531	0.916	0.9274
MS2K	0.8785	0.8746	0.9531	1	0.9208	0.8954
MS2C	0.8526	0.8592	0.916	0.9208	1	0.9061
SM30B	0.9305	0.8826	0.9274	0.8954	0.9061	1

The slopes intercepts and R^2 values for the median values are tabulated in tables 20, 21 and 22 above. When comparing two instruments on a correlation plot, if the two instruments are giving identical readings, then the data points will all lie on a straight line with a slope of 1, an intercept of zero and an R^2 of 1.

When the slopes (Table 17 and 20) in a specific row and column are less than 1.0, then the instrument in that row is giving readings that do not increase as quickly as those from the instrument in the corresponding column. On the other hand, slopes of greater than one imply that the instrument in the row is giving readings that increase more quickly than the readings from the instrument in the column. One might expect the slopes of instrument A vs instrument B to be the inverse of instrument B. However, this is not the case, perhaps due to the logarithms being calculated or perhaps there exist some bias in the least square routine used in Excel. This might also be caused by the smaller readings contributing less to the misfit, but because the smaller readings are more erratic, they have an erratic impact on the slopes. Hence, the significance of the slopes in the tables have not been interpreted in detail. Usually, the slopes are closer to 1 when the median values are being compared.

The intercept (Table 18 and 21) is a measure of instrument bias at low values of susceptibility. In this case the intercepts of instrument A vs B is the negative of instrument B vs A, so the values might be more reliable. However, there are no clear trends in these values, except that the KT-10 and SM30 appear to have a consistent positive intercept in averaged data but consistently negative when the median is used for analysis. The MS2C shows consistent negative intercepts in averaged values and positive in median values. This contradiction in the two analyses is beyond the scope of this research and further statistical studies would be required to understand this.

The R^2 values in Tables 19 and 22 is a measure of the quality of agreement or lack of scatter. In this case the values are independent of whether instrument A is plotted against B or vice-versa. The fits are generally mediocre in table 19 (averaged values) and generally good in table 22 (median). In many cases (table 18), the fit at large values (upper right quadrant) is good, but in the lower left quadrant is poor. A good example of this is the RT-1 and the SM30 (figure 43). This suggests that most instruments give more reliable results for susceptibilities greater than $1x10^{-3}$ SI, but poorer results for smaller susceptibilities. The best fit is between the MS2C and MS2K (R^2=0.92), which shows less scatter in the lower quadrant (figure 47). In table 22, all instruments, except the KT-10 have good correlations with the GDD ($0.90 \leq R^2 \leq 0.95$). Ignoring the mixed results from the intercepts, the median values show better correlation amongst instruments compare to the correlation when the averages are used.

6.5 Lower limits of accuracy and range of values

This analysis aims at increasing our understanding of the lower limit of accuracy of each instrument so that the operator can predict when the instrument is likely to start giving unreliable readings. The means or medians and the coefficient of variations calculated in the previous sections of this thesis are used to estimate the lower limit. However, only medians vs Coefficient of variations are presented below, as similar results were obtained with the means. I have also estimated the maximum and minimum values measured on all samples in this study to estimate a range of values that can be measured with each instrument. This range might have been different had different samples been measured.

Lower limit of accuracy

The lower limit of accuracy is estimated by generating plots of coefficient of variations against the median values (each on logarithmic scales) and the results were presented in figures 49 to 54 for the six instruments.

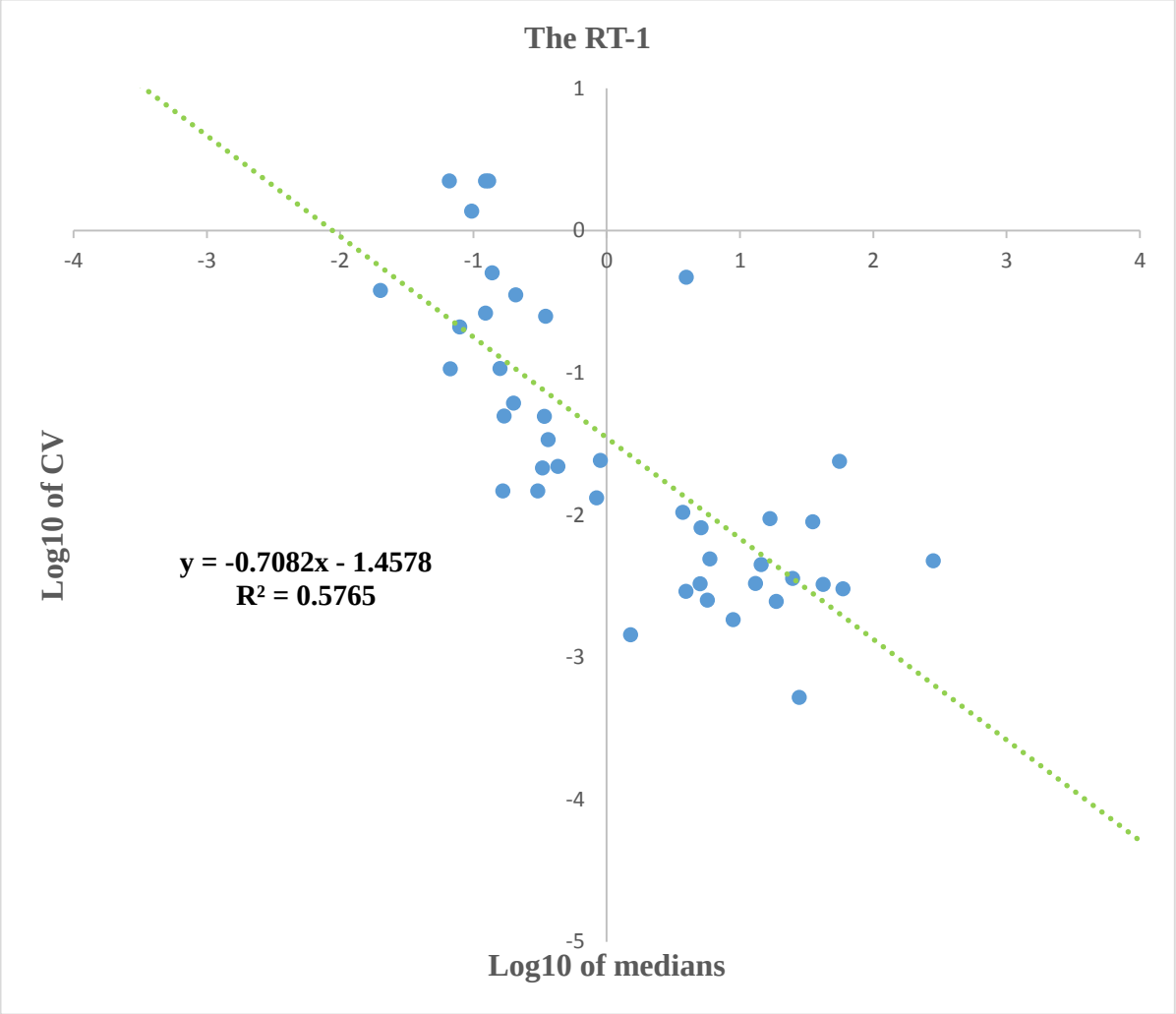

Figure 49: Log_{10} plot of coefficient of variations (standard deviation/means) against log_{10} of median MS measured with RT-1.

RT-1 readings (figure 49) are unreliable (CV > 0.1 or even > 1.0) when the median MS is less than 0.1 x 10^{-3} SI. The readings are reliable (with CV < 0.1) when the median value is greater than 0.1 x

10^{-3} SI. On this plot, the minimum median value is 0.02 x 10^{-3} SI; and the maximum median value 280 x 10^{-3} SI.

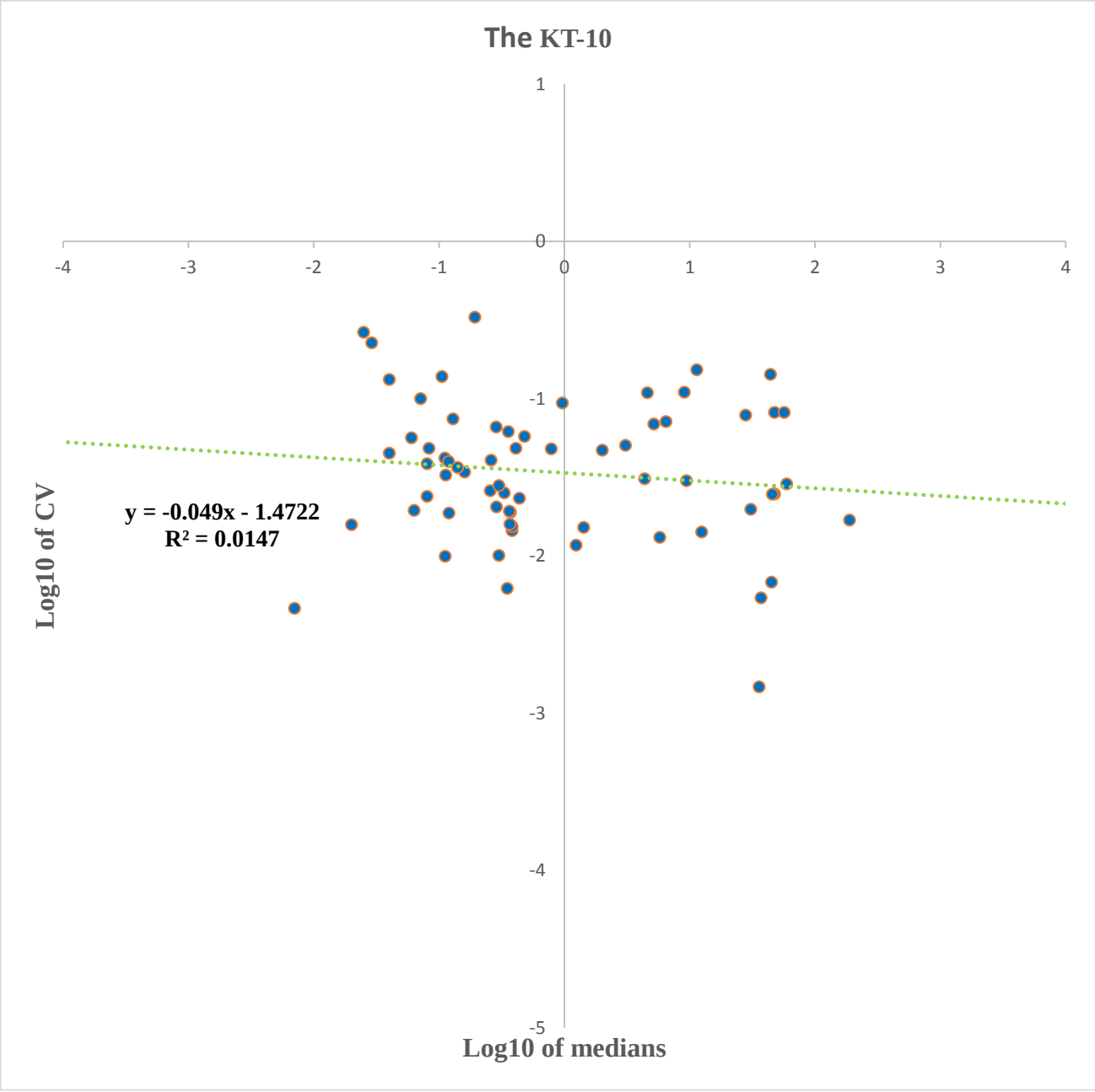

Figure 50: Log_{10} plot of coefficient of variations against log_{10} of median MS measured with KT-10.

KT-10 readings are reliable, with the CV being less than 0.1 for most values of the MS. The minimum and maximum median values measured with the KT-10 are 0.007 $x10^{-3}$ and 186 $x10^{-3}$ SI respectively.

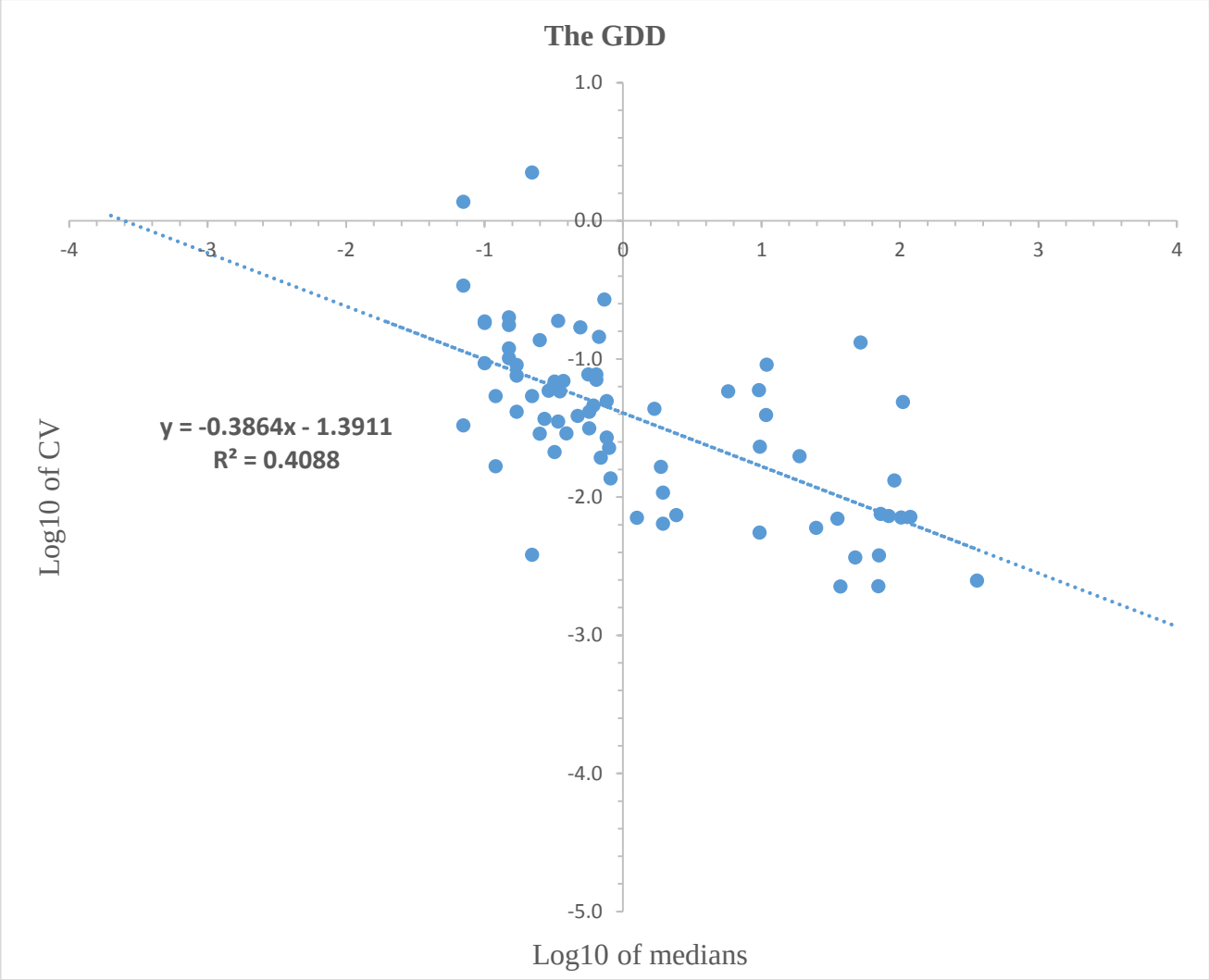

Figure 51: Log_{10} plot of coefficient of variations against log_{10} of median MS measured with GDD.

The GDD readings are unreliable (CV > 1) when the median MS is less than about 0.2 x 10^{-3} SI. The readings are generally reliable with CV < 0.1 when the median value is greater than 0.15 x 10^{-3} SI. The minimum median value measured is 0.07 x 10^{-3} SI; and the maximum median value 360 x 10^{-3} SI.

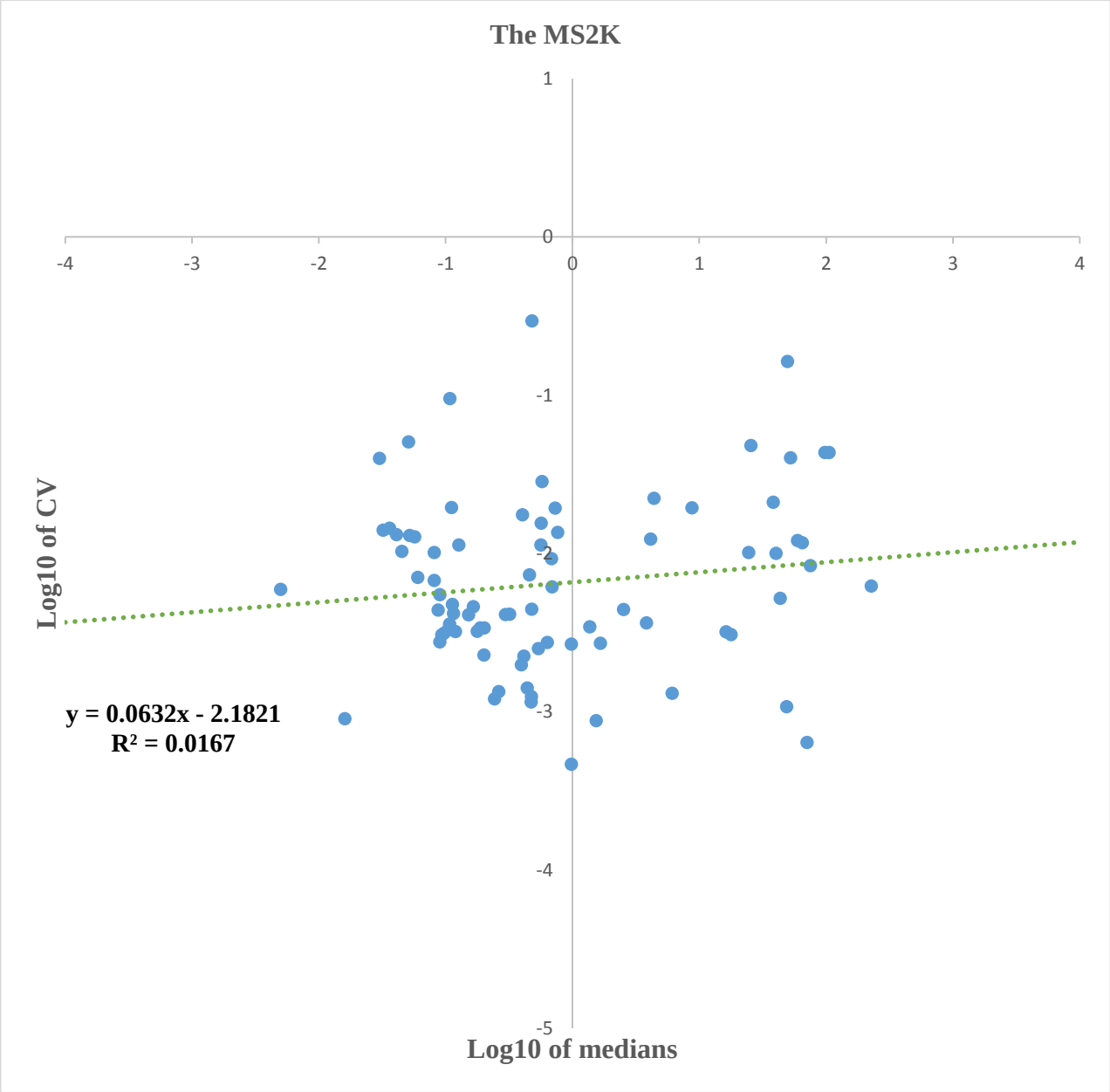

Figure 52: Log_{10} plot of coefficient of variations against log_{10} of median MS measured with MS2K.

The MS2K has no CV values greater than 1, so there are no unreliable readings. Virtually all readings have a CV less than 0.1, so the MS2K gives very reliable readings over the whole measurement range from a minimum of 0.005 x 10^{-3} to a maximum of 230 x 10^{-3} SI.

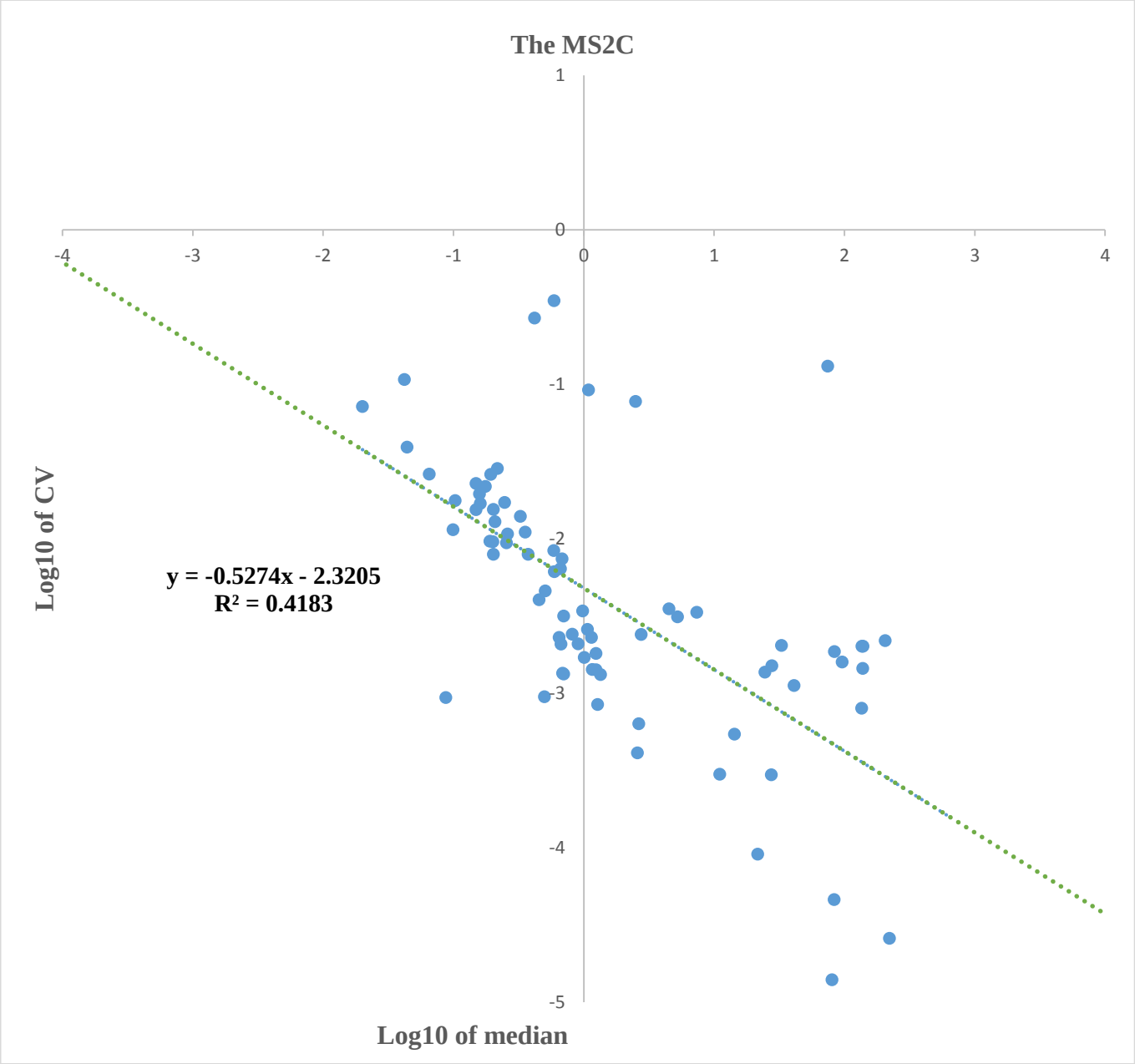

Figure 53: Log_{10} plot of coefficient of variations against log_{10} of median MS measured with MS2C.

Although the MS2C shows the CV increasing as the median value decreases, there are no CV values greater than 1, so there are no unreliable readings. Virtually all readings have a CV less than 0.1, so the MS2C gives very reliable readings over the while measurement range from a minimum of 0.02 x 10^{-3} to a maximum of 220 x 10^{-3} SI.

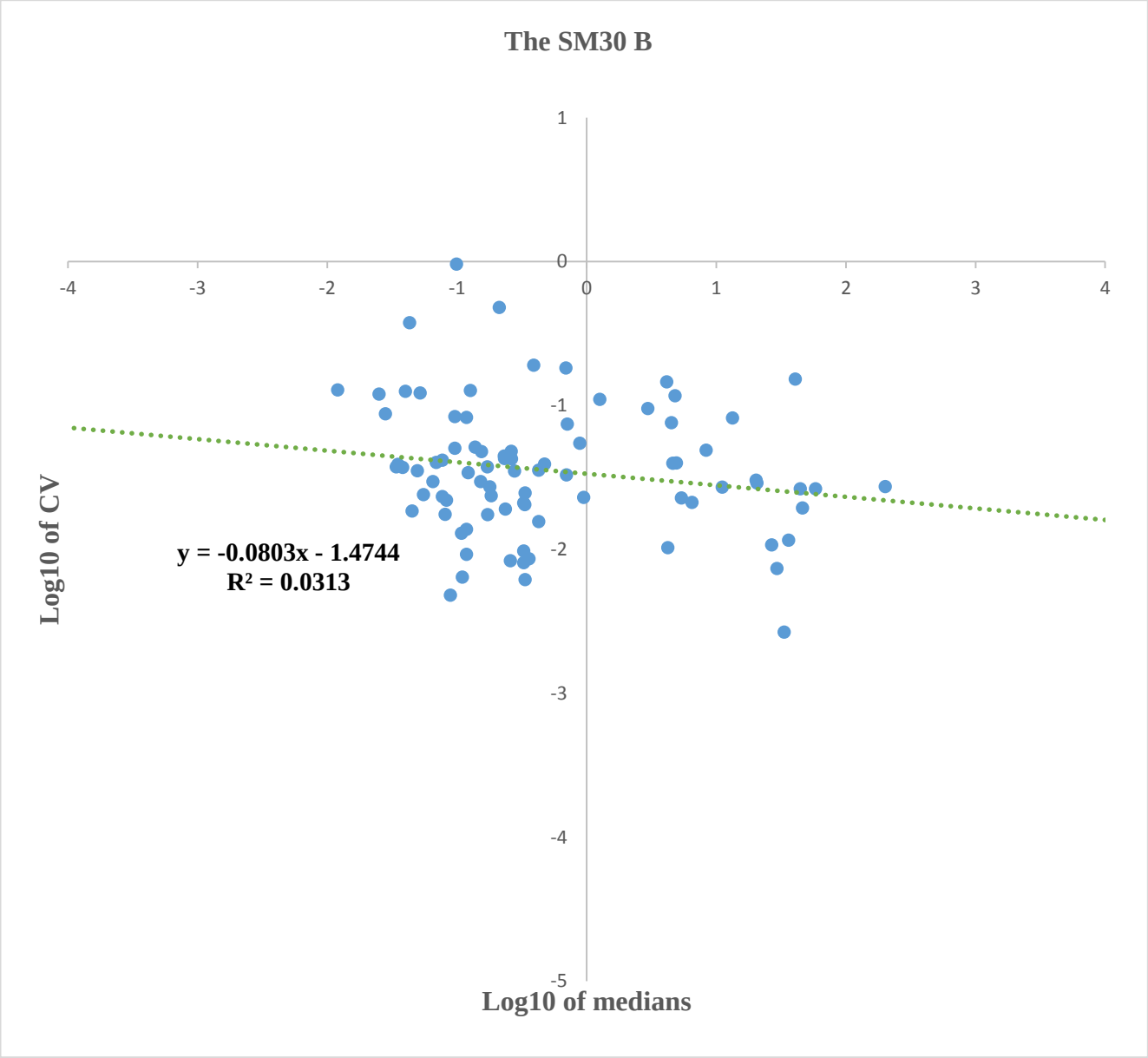

Figure 54: Log_{10} plot of coefficient of variations against log_{10} of median MS measured with SM30

The SM30 has no CV values greater than 1, so there are no unreliable readings. The CV is generally below 0.1 when the median MS is more than 0.02 x 10^{-3} SI; but it is rarely above 0.1 when the mean MS is greater than 1 x 10^{-3} SI. The minimum median value is 0.01 x 10^{-3} and the maximum value is 200 x10^{-3} SI.

Table 23: Shows the summary of lower limit of accuracy for each of the instruments and the maximum values measured (medians).

Instrument	Minimum absolute value measured	When CV>1	When CV> 0.1	Maximum value measured
RT-1	0.02 x 10^{-3} SI	0.1 x 10^{-3} SI	0.1 x 10^{-3} SI	280 x 10^{-3} SI
KT-10	0.007 x 10^{-3} SI	-	0.007 x 10^{-3} SI	186x 10^{-3} SI
GDD	0.07 x 10^{-3} SI	0.2 x 10^{-3} SI	0.15 x 10^{-3} SI	360 x 10^{-3} SI
MS2K	0.005 x 10^{-3} SI	-	0.005 x 10^{-3} SI	230 x 10^{-3} SI
MS2C	0.02 x 10^{-3} SI	-	0.02 x 10^{-3} SI	220 x 10^{-3} SI
SM30	0.01 x 10^{-3} SI	-	0.02 or 1 x 10^{-3} SI	200 x 10^{-3} SI

For the RT-1, the CV increases as the MS decreases, with errors becoming greater than 10% when the median MS is less than 0.1 x 10^{-3} SI. When the readings are less than 0.1 x 10^{-3} SI, they are unreliable as the CV is greater than the MS. The range of reliable values from the instrument for this project was from 0.1 to about 300 x 10^{-3} SI

For the KT-10, the CV appears to be uniformly high across the whole range of values but generally less than 1 in both mean and median plots. When the MS is greater than 1 x 10^{-3} SI, the CV is typically less than 0.1, but when the MS is less than 1 x 10^{-3} SI, some larger CVs are observed. The range of reliable measured values is from 0.007 x 10^{-3} SI to 186 x 10^{-3} SI.

The GDD plot is similar to the RT-1; the CV increases as the MS decreases, with errors becoming greater than 10% when the MS is less that 0.2 x 10^{-3} SI. When the measurements are less than 0.2 x 10^{-3} SI, they are unreliable as the CV is greater than the MS. The range of reliable values from the instrument for this project was from 0.2 x10^{-3} to 360 x 10^{-3} SI.

The MS2C shows a CV that increases as the MS decreases. However, except for two samples, the CVs remain less than 0.1, so the readings are generally reliable. The range of reliable measurements is from 0.02 x 10^{-3} to 220 x 10^{-3} SI.

The MS2K shows large scatter in the CVs, but broadly speaking they are uniform across the whole range of MS. The CVs are virtually all less than 0.1, and average 0.01, so the readings are generally reliable. The range of reliable measured median MS is from .005 x10^{-3} to 225 x 10^{-3} SI.

The plot for the SM30 is similar to the KT-10, with uniform CVs across the whole range of values. As with the KT-10, the largest CVs occur when the MS is less than 1 x 10^{-3} SI. The range of reliable measured values is from 0.01 x10^{-3} to 200 x10^{-3} SI.

In general the plots suggest poor accuracy when measurements are very low. To confirm this observation, I plotted the measurements recorded on a quartzite sample from borehole 1301020, which shows very low values and diamagnetic signature in most of the instruments (figure 55).

The erratic behaviour of low susceptibilities observed is well supported in figure 55, which shows that all instruments, except GDD and RT-1 that have zero readings, have measurements that are affected by various degrees of erratic measurements.

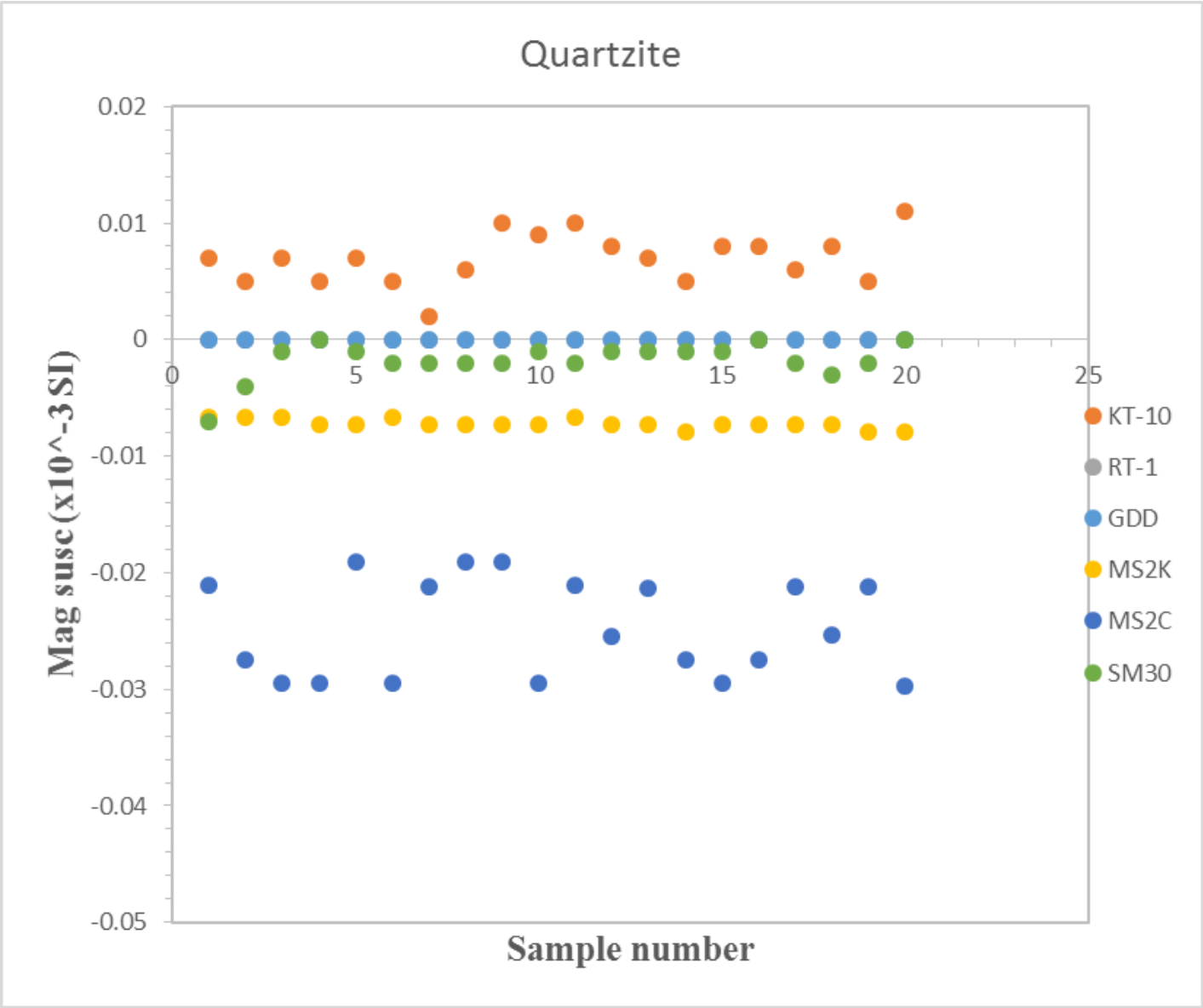

Figure 55: MS measurements of diamagnetic quartzite in borehole 1301020.

6.6 Comparison with BSS-02B Downhole probe

Physical property data were collected by lowering the multi-sensor IFG probe, which also houses the magnetic susceptibility probe (BSS-02B) as one of the sensors, in borehole 1301240. As the probe moves downhole, both magnetic susceptibility (from BSS-02B) and conductivity (from the other IFG sensor) readings are recorded at a depth sampling rate determined by the speed of the winch. The

measurements were collected every 0.05 ft to a depth of 1600 ft, the maximum length of the armored steel logging cable that links the probe and winch.

Digital data from the BSS-02B probe is transmitted to the IFG interface box, where it is converted into ASCII format and stored into memory registers. After collection, the data was downloaded to a laptop for storage using an RS-232 serial cable. The data was sent to Sudbury, Ontario for depth correction and QA/QC checks.

The readings of interest are those collected by the probe at the same depth that samples were collected for measuring with the other six instruments. Since multiple borehole samples were recorded at the depth of interest, the 4 adjacent readings were averaged to obtain a representative MS value at the depth that measurements were collected with the hand-held instruments.

The combined downhole plots of all the instruments' measurements plotted on a logarithmic scale was created as a function of depth and the lithological units were added onto the plot. The measurements are presented in figure 56.

It was observed that the magnetic susceptibility of the borehole probe are close to or within the envelope of the variable measurements acquired from the other instruments. The exception was near the bottom of the hole (-1580 feet) where the borehole measurements were low compared to the other instruments. This was at a location, where the conductivity measured from the BSS-02B was high. This occurred in zones that include semi-massive to massive sulfide, magnetite bearing iron formation and mineralized ultramafic.

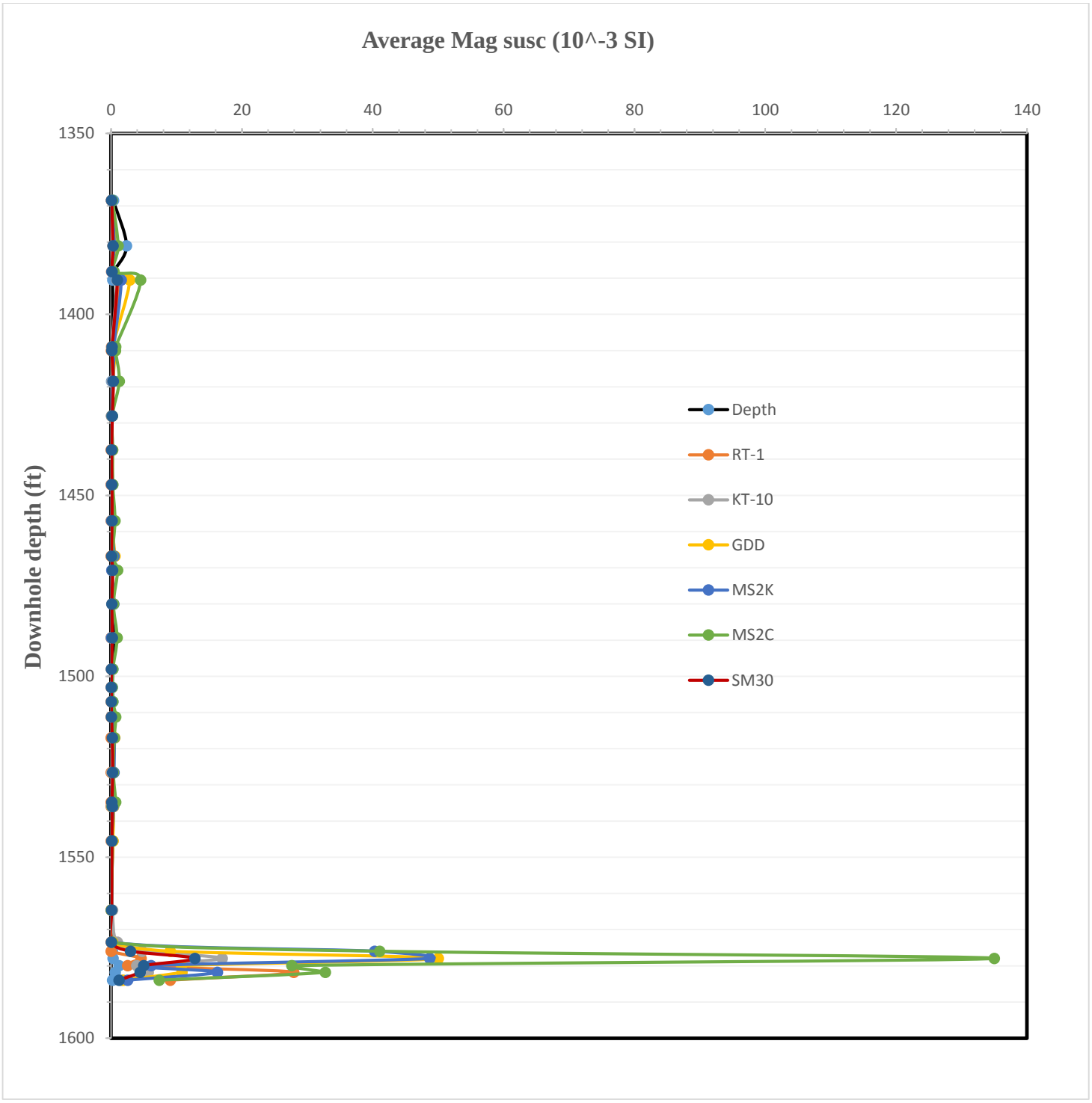

Figure 56: Comparison of BSS-02B downhole probe's data and the six instruments used in this research. The MS readings were plot against the depth (ft). Data from borehole 1301240.

The plots above demonstrated that hand-held meters can be used to generate comparable quality MS readings as the BSS-02B downhole probe. However, it was observed that areas of conductive lithologies show some discrepancy as the MS in BSS-02B tends to be very low (not clear in the above due to the scale). Given the broad range of frequencies and measurements techniques used by the hand-held instruments, and that they all gave consistently higher values, we conclude that borehole probe gives values which are too small. This is most likely due to the conductivity impacting the BSS-02B measurement.

Chapter 7: Integrated Interpretation

7.1 Modes selection

The choice of the most appropriate mode of operation for each instrument was determined after each of the operational modes were tested on samples with a range of MS values. The mode selected was that judged to give data of high quality suitable for meeting the research goals of this project. These goals were the comparison of the instruments' accuracies, range of sensitivities, resolution and the degree to which the instruments are affected by temporal drift. Some modes (e.g. scanning mode) are inappropriate for repeated measurements on the same sample. For other projects, different goals would influence the choice of the most appropriate mode of operation for each instrument. It is therefore imperative for operators to assess the strengths of the available modes and compare this with the goals of the project before choosing a specific mode.

For the SM30, tests showed that mode B was better than basic mode A, scanning, interpolation and extrapolation modes. The less reliable modes are strongly discouraged unless the readings are needed for rough estimation of the MS. The less reliable modes for the SM30 and KT-10 are the scanning modes. However, the ***scan mode*** in the RT-1 gives more stable measurements than its ***step mode***. In the MS2K, MS2C and GDD, the single point measurements were used as these were more appropriate for the project than the graph or continuous modes.

The choice whether or not to use the pin in the KT-10 is dependent on the type of surface the measurements is being made on. It might be useful when irregular surfaces are tested or very local focussed measurements are required; however, the pin readings were more erratic and the pin sensor does not give any comparative advantage over the pin-less KT-10 sensor when used on regular

surfaces such as core and cut samples. The higher measurements recorded with the pin on the calibration sample are greater than the known susceptibility, suggesting some bias.

The chosen modes generated data that meet the standard required for good quality as (e.g. figure 56 and many of the diagrams presented in chapter 6). However, all instruments give erratic measurements to some extent when values are small and negative (Figure 55). This suggests that not all of the modes are capable of recording reliable measurements in weakly susceptible rocks.

7.2 Factors that might influence your choice of instrument

Temporal drift

The analyses show that the smaller sensor coils instruments, GDD and the MS2K, have measurements that were highly affected by the temporal drift whereas the KT-10, SM30 and MS2C measurements were least affected. There was no direct linkage between the observed drift and the instruments frequencies. The operating frequencies from the lowest to the highest are 0.565 kHz, 0.75 kHz, 0.93 kHz, 8 kHz and 10 kHz for the MS2C, RT-1, MS2K, SM30 and KT-10 respectively. This study found there was no observed or inferred trend that could suggest that either low or high frequencies are more susceptible to temporal drift. The variation in temporal drift amongst these instruments might be explained by other factors such as differences in the design of the instruments' coil, the electronics or some limitation of the physical phenomena being measured. Lee and Morris (2013) implied that the instruments that measure the changes in the frequency of an LRC circuit (e.g. the KT-10 and the SM30) are more susceptible to drift. Their study looked at three instruments (the KT-10, SM-30 and MS2E); however, this study finds that the LRC circuit instruments showed less drift than most of the other instruments.

Sensitivity

Another observation was that there are discrepancies in the magnitude of MS measurements from different instruments. The GDD, MS2K and MS2C have consistently given higher measurements compared to the SM30, RT-1 and KT-10. In this case there is a strong inverse correlation between the magnitude of MS readings and the instruments' operational frequencies. Both the MS2K and MS2C have the lowest frequencies of all the six instruments and give the highest measurement and the SM30 and KT-10, with the highest frequencies, give the lowest measurement. The exception is for the GDD whose operational frequency is not known.

Comparing whole and split core measurements showed that halved core consistently gives higher MS measurements when the measurement is taken on the flat side. The exceptions were the GDD (on the ultramafic sample) and the KT-10 (on the schist); in both these cases, the readings were almost similar. Higher measurements from the split core could be attributed to (1) a larger surface for coupling between the sensor and the core, (2) fine grained metal shavings or dust from the metal blade (cutting device) that might have contaminated the split surface or (3) it is due to presence of fresh (unweathered) magnetite and pyrrhotite in the cut surface.

The cartoon in figure 57 illustrated the first explanation. In this case splitting a core increases the area of contact between the flat sensor and the core sample. The increased surface area allows direct coupling between the sensor and the rock, thus reducing any diluting impact of air (with zero MS) between the sensor and more distal parts of the core that will occur in the case when the core is not split. This variation might be resolved by applying geometric correction between split core and whole core.

The second explanation is that the higher MS readings are the result of contamination of the cut surface by iron dust. As the core is cut, the steel saw blade could wear off and form a fine dust of iron that can "contaminate" the sample, which can be observed as increase in MS measurements. Because of the fine grained nature of this dust, it is not easy to clean off the surface and this might be a major source of error for split samples.

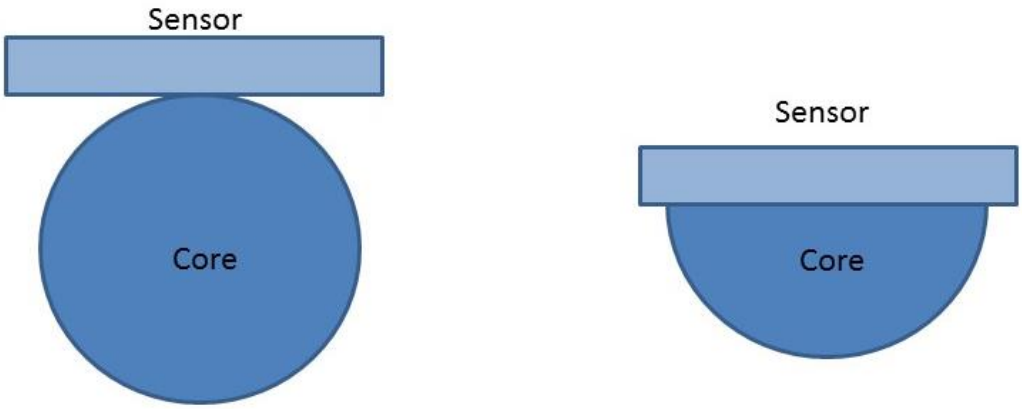

Figure 57: Schematic cartoon showing larger surface area for coupling between the sensor and the split core compared to a smaller surface area between the whole core and the sensor.

Correlations

The cross plots comparing the measurements from the different instruments show a linear relationship for high susceptibilities, but poorer relationships at lower values. When comparing the cross plots for the mean values and the median values, the median values show a stronger correlation. This is believed to be because outliers can adversely impact the mean value, whereas the median is more robust to outliers (Rainsford pers. comm., 2014). Table 24 below summarizes the fundamental observations and parameters from all the instruments used in this research.

Table 24: Summary of the findings from all the six MS instruments. MS = magnetic susceptibility, cond => conductivity, s. par = strongly paramagnetic, w. par = weakly paramagnetic.

	RT-1	KT-10	GDD	MS2K	MS2C	SM30
Lower limit of accuracy (SI)	$0.1x10^{-3}$	$0.007x10^{-3}$	$0.15x10^{-3}$	$0.005x10^{-3}$	$0.02x10^{-3}$	$0.02x10^{-3}$
Largest value measured (SI)	$280x10^{-3}$	$186x10^{-3}$	$360x10^{-3}$	$230x10^{-3}$	$220x10^{-3}$	$200x10^{-3}$
Example drift – s. par. ($x10^{-3}$ SI)	0.0014	0.0082	-0.0396	-0.0053	-0.0008	0.0058
Example drift – w. par ($x10^{-3}$ SI)	-0.0004	0.00004	0.0011	0.0001	-0.00006	-0.0014
Portability in the field	✓	✓	✓	x	x	✓
Usability on large irregular sample size	✓	✓	✓	✓	x	✓
Usability on core of diameter >72 mm	✓	✓	✓	✓	x	✓
Usability on core of diameter ≤72 mm	✓	✓	✓	✓	✓	✓
Ability for the instrument to account for split core in software	x	x	✓	x	x	x
Mode used in this research	Scan	measure	Manual	Manual	Manual	Basic mode B
Most Erratic mode	Step	Scanner	N/A	N/A	N/A	Scanning

Ease of use

Among the instruments studied, the RT-1 is the easiest to operate. It takes up to 5 seconds from the time it is turned on to the time it is ready for use. During this time, the instrument performs internal self-calibration by zeroing in air. Addition 2 – 5 minutes can be used to set the parameters and mode of operation.

The Bartington instruments are easy to record measurements in the manual mode but they require a lengthy setup. The time spent while installing Bartsoft and the setting of operational parameters ranges

between 20 – 45 minutes. However, data collected can be executed in a very short space of time once the instruments are ready to use.

The rest of the instruments are relatively easy to use but have their own peculiarities. For instance, GDD's MPP-EMS2+ probe requires 40 minutes of warm up time after turning it on. Once this step is completed and the pocket computer is connected to PC, the operation is easy. The KT-10 requires the completion of air-sample-air sequence of measurements in 7 seconds or the LCD will display "Err" and no measurements will be recorded. Last but not least, SM30 can be easily operated by following the instrument's manual. However, care must be taken to avoid mixing of modes and overriding measurements.

Price

The price of each of these instrument will play a very important role in choosing which instrument to buy. This means if other factors studied in this research are not considered, the buyer (users) of these instruments will try to reduce cost by choosing the cheapest. The price list of these instruments is given in table 25 below.

Table 25: Price list for the instrument used. Normalized price is based on the Bank of Canada Exchange Rate of November 28, 2014

Instrument	Actual Price	Normalized price
Furgo: RT-1	2850 (AUD)	US$ 2426
Terraplus: KT-10	2150 CAD	US$ 1885
GDD: MPP-EMS2+ Probe	6300 CAD	US$ 5520
Bartington: MS2K	2925 USD	US$ 2925
Bartington: MS2C	2925 USD	US$ 2925
Bartington: MS3	2520 USD	US$ 2520
ZH Instruments: SM30	1995 USD	US$ 1995

7.3 Potential sources of Errors

Although various quality control procedures were followed, there are still a possibility of unwanted external influence adversely impacting the quality of MS data. These factors include instrumental, environmental and inhomogeneity of the mineralogy of the rock specimen. Among the environmental errors include changes in the earth's ambient magnetic field and the presence of nearby magnetic materials.

8.0 Conclusion and Recommendations

8.1 Conclusion

The choice of modes of operation in each of the six hand-held MS instruments enabled the generation of high-quality data that was used with confidence to assess each instruments' susceptibility to temporal drift, resolution, lower limit of accuracies and the repeatability of measurements. This was also achieved by deploying various quality control protocols discussed in chapter 5. A comparison with downhole BSS-02B probe data shows that the data collected using the downhole probe gave measurements consistent with the hand-held instruments, except where the rock was conductive.

The drift analysis shows that the MS2K and GDD are the most affected by temporal drift whereas the KT-10 and MS2C are consistently the least affected. The results show no direct relationship between the degree of drift and the operating frequency of the instrument.

A direct relationship was observed where instruments with lower frequencies consistently recorded higher values of susceptibilities compare to those instruments that used higher frequencies. It was also observed that split core gave higher susceptibility measurements in all instruments compared to whole core. This is explained by an increase in the surface area of contact, exposure of more mineral grains and/or contamination of the cut surface by iron dust. This occurs even for the GDD and KT-10 which are able to correct for the fact that core is not split; these instruments allow the operator to enter the core diameter.

In conclusion, the instruments to be used for a given project must take into account the availability of different modes; some of which may be most suitable for the goals of the project. It is also important

to note that each instrument has it weaknesses and strengths and one has to weigh the advantages against disadvantages before deciding which instrument to use.

8.2 When is each instrument appropriate?

As mentioned earlier, the objective and the site of the investigation have a huge influence on the choice of the instruments depending on the desired accuracy, sensitivity and resilience to drift. I shall give general scenarios where each of these instruments can be used and each user has a liberty to customize their instrument choice based on specific circumstances.

Mineral Exploration

In the mineral exploration industry, the most useful instruments are those that can give information regarding the whereabout of magnetic and conductive minerals. The normal range of interest of magnetic susceptibility measurements are usually those of strong paramagnetic and ferro-/ferrimagnetic sulfides and/or ultramafic intrusion. This means diamagnetic materials are less likely to be the concern of mineral exploration geologist and geophysicists alike except perhaps when there is an interest in carbonates. Moreover, the degrees of temporal drifts observed in this research are somewhat tolerable to many exploration companies, which use MS values as constraints in the inversion of magnetic data.

Therefore, GDD's MPP-EMS2+ probe and KT-10S/C (version of KT-10 that also measures conductivity) are the most suited instruments for exploration purposes because they measured conductivity in addition to magnetic susceptibility. Other instruments recommended are RT-1, SM30 and KT-10. The Bartington Instruments' MS2C & MS2K studied in this research are not easily usable

in the field because they require set up on the computer, which might be cumbersome. Nonetheless, they can be good alternatives especially at a camp site.

Scientific expeditions and geological surveys

The magnetic susceptibility measurement is an important physical property that is currently deployed in geological and geophysical mapping to characterize variations in rock units. The tools are being used by geological surveys and expeditions across the globe (Enkin et al., 2012; Searl 2008) to log core and record readings on the outcrops in order to better understand various geological phenomena under investigation. These scientific studies require high resolution and attention to minute changes in the measurements as they might signify changes in lithology, grade of alteration, metamorphic conditions or depositional environment. For example, some of the paleo-climate studies involve weak paramagnetic or diamagnetic sediments. This eliminates RT-1 and GDD's MPP-EMS2+ probe because they cannot measure diamagnetic or very weak paramagnetic material. The MS2K is also not favoured due to high variability of its measurements. Therefore, the most appropriate instruments for these types of field mappings are the KT-10 and SM30. If the project is laboratory based, semi-sedentary camp site or aboard the ship, the best choice would be the MS2C as it can be setup semi-permanently for the duration of the studies and used to generate the most stable MS measurements.

8.3 Recommendations

There several recommendations that can be drawn from this thesis:

(i) Before selecting a MS instrument, define the type of measurements you will be undertaking and the goals of your study. For example, an exploration geologist may be interested in simultaneously collecting magnetic susceptibility and electrical conductivity. This will narrow his or her choice of the instruments to the GDD and KT-10 S/C (another version of the KT-10). Assuming that the geologist may also want repeatable data with less effect of temporal drift, this will further constraint and justify his or her choice to the KT-10 S/C (note that the KT-10 S/C can measure conductivity and MS while the KT-10 can only measure MS).

(ii) Consideration of the facilities at the research site (laboratory or field) is very important since some instruments are less portable and can be more cumbersome in the field. For example, these versions of MS2C and MS2K require power supply from main electricity or generators and a laptop and are therefore best for laboratory use, while the SM30, KT-10, RT-1 and GDD are more portable and are ideal for field work.

(iii) Select an MS instrument that has a mode of operation appropriate to the project. For example, the scan or continuous mode might be useful if the purpose is to find the most susceptible lithologies in a core tray; however, manual or single point measurements might be better for drift corrected and multiple measurements on one sample.

(iv) The operator should read the user's manual to understand the basic care and functionality of each instruments. However beware that claims are not always achievable with the instrument. For example, the smallest reading possible on an instrument is not always the lower limit of accuracy.

(v) Follow manufacturers recommendations on appropriate use of equipment as this will reduce risk of damaging the instruments or collecting poor quality data. For example, the GDD requires at least 40 minutes to warm up.

(vi) Read available literature on the use of the magnetic susceptibility meter as well as the factors that are necessary in acquiring quality data. These will give you background information on how to produce high quality data.

(vii) Test the instruments to make sure they are working properly before embarking on major projects. This will reduce time wastage. Some instruments require a software upgrade for them to measure or download MS data. Others are compatible with specific computer models that have RS-232 serial ports. Prior checking will enable users to resolve any deficiencies in due time, thus saving them time and money.

(viii) Take at least 5 measurements and calculate averages or medians. This step accounts for the inhomogeneity of the mineralogy. In this research, median is preferred as the mean value seemed to be more corrupted by outliers.

(ix) The choice for statistical or analytical method(s) is determined by the desired outcomes and the type of data to be processed. When analyzing data, try many statistical techniques applicable to your project before arriving at any conclusion as to which procedures are most appropriate. For example, plots of the CV as a function of median MS measurement could be used to estimate the lower limit of reliable measurements.

(x) Hand-held instruments provide data comparable to borehole BSS-02B data and the hand-held measurements are not biased to lower values when the rock is conductive.

9.0 REFERENCES

Airo, M.L., Säävuori, H., and Vuoriainen, S., 2011: *Petrophysical properties of the Outokumpu Deep Drill core and the surrounding bedrock; Geological survey of Finland, Spec. Paper 51, 63 – 82,*

Aldana, M., Costanzo-Alvarez, V., Guzmản, O., 2011: *Discrimination of hydrocarbon-related conditions based on a statistical analysis of magnetic parameters. Latinmag Letters, Vol. 1, Special (2011), D32, 1-6. Proceedings Tandil , Argentina*

Anderson, R.G. and Lowe, C. 2002: *Preliminary interpretations of new aeromagnetic data for the Atlin map area, British Columbia; Current Research 2002-A17. Geological Survey of Canada*

Andrews, G., Quane, S., Enkin, R.J., Russell, K., Kushnir, A., Kennedy, L., Hayward, N., Heap, M., 2011: *Rock Physical Property Measurements to aid Geophysical Surveys in the Nechako Basin Oil and Gas Region, Central British Columbia. Final Report for Geoscience BC Project 2008 – 028*

Bartington instruments: *MS2C sensor, MS2K sensor; MS3 sensor manual, www.bartington.com Bartington Instruments: user's manual*

Bleeker, W. 1991: *Evolution of the Thompson Nickel Belt and its Nickel Deposits, Manitoba Canada*

Bleil, V., and Petersen, N., 1982: *Magnetic properties of natural minerals; Paramagnetism. IN: Landolt-Boernstein, Numerical data and functional relationships in science and technology, Group V, vol. 1, subvol. b, 312-320. Springer Verlag Berlin.*

Borradaile, G.J, B. Henry, B., 1997: *Tectonic applications of magnetic susceptibility and its anisotropy; Earth-Science Reviews 42 (1997) 49-93; Elsevier*

Dearing, J.A., Hay, K.L., Baban, S.M.J., Huddleston, A.S., Wellington, E.M.H., and Loveland, P.J., 1996*: Magnetic susceptibility of soil: an evaluation of conflicting theories using a national data set; Geophys. J. Int. (1996) 127,728-734*

Deng, D. N., 2012: *Spatial Trends In Metal Tenors within Birchtree 140 Ultramafic, Thompson Nickel Belt, Manitoba Canada. University of Toronto, Dept. Earth Sciences honours thesis, 2012*

Eisenhart, C. 1963: *Realistic Evaluation of precision and accuracy of instrument calibration systems, J.Res. National Bureau of Standard 67C 161-187*

Enkin, R. J., Cowan, D. Tigner, J., Severide, A., Gilmour, D., Tkachyk, A., Kilduff, M., Vidal, B., Baker, J., 2012: *Physical Property Measurements at the GSC Paleomagnetism and Petrophysics laboratory, including Electric Impedance Spectrum Methodology and Analysis. Geological Survey of Canada, Open File 7227*

***Enkin, R.J., pers. communication, 2014**: explanation on the uses of pin option in KT-10 Instrument*

GDD user's manual – *User's manual for MPP – EMS2+ probe by GDD Inc.*

Girault, F., Poitou, C., Perrier, F., Koirala, B. P. and Bhattarai, M., 2011: *Soil characterization using patterns of magnetic susceptibility versus effective radium concentration; Nat. Hazards Earth Syst. Sci., 11, 2285–2293* ***OR*** *www.nat-hazards-earth-syst-sci.net/11/2285/2011/ doi:10.5194/nhess-11-2285-2011*

Heider, F., Zitzelsberger, A., Fabian, K., 1996: *Magnetic susceptibility and remanent coercive force in grown magnetite crystals from 0.1/xm to 6 mm; Physics of the Earth and Planetary Interiors, v. 93, p.239-256*

Hrouda, F., 1986: *The effect of quartz on the magnetic anisotropy of quartzite. Stud. Geophys. Geod., 30: 39—45*

IFG *Conductivity Logging Procedural Manual Equipment, Data Acquisition, Data Processing and Interpretation March 2004 C.C. Technical and General*

Hrouda, F., Chlupàčovà, M., Chadima, M., 2009: *The use of magnetic susceptibility of rocks in geological exploration, Brno 2009* http://kdjonesinstruments.com/Portals/121/case-study-magnetic-susceptibility.pdf

Ivakhnenko, O. P., 2012: *Magnetic Susceptibility of Petroleum Reservoir Crude Oils in Petroleum Engineering, Crude Oil Exploration in the World, Prof. Mohamed Younes (Ed.), ISBN: 978-953-51-0379-0, InTech, Available from: http://www.intechopen.com/books/crude-oil-exploration-in-the-world/magnetic-susceptibility-of-petroleum-reservoir-crude-oils-in-petroleum-engineering*

Kropaček, V., 1971: *Distribution of the values of natural remanent magnetization and magnetic susceptibility of some minerals. Studia geoph. geod., 15, 340-353.*

Krs, M and Kropaček, V, 1987: *A contribution to the magnetic properties of natural cobaltite. Phys. Earth Planet. Inter., 46, 227-232*

KT-10 user's manual, Rev. 16: *printed by Terraplus Geophysics*

Kume, H.; 1987*: Statistical methods for quality improvement*. *The Association for Overseas technical scholarship 1985; reprinted in September, 1987; 30-1, Senju-azuma 1-chome, Adachi-ku, Tokyo, 120*

Lawley, C. 2007: *Characterization of Nickel Sulfide Ores at the South Mystery Deposit, Thompson, Manitoba; Honours Bachelor of Science, the University of Western Ontario*

Layton-Matthews, D. 2001: *Metasomatism of ultramafic intrusions in the Thompson Nickel Belt, Manitoba, Canada; Laurentian University*

Layton-Metthews, D., Lesher, C.M, Burnham, O.M, Liwanag, J., Halden, N.M, Hulbert, L., Peck, D.C. 2007*: Magmatic Ni-Cu-Platinum-Group Element Deposits of the Thompson Nickel Belt*

Lee, M.D., and Morris, W.A, 2013: *Comparison of magnetic-susceptibility meters using rock samples from the Wopmay Orogen Northwest Territories, Geological Survey of Canada, Technical Note 5; Natural Resources Canada*

Lelièvre, P.G., 2003: *Forward modelling and inversion of geophysical magnetic data; master's thesis, Faculty of Graduate Studies, Department of Earth and Ocean Sciences, Geophysics; University of British Columbia, BC, Canada*

Macek, J.J. pers. communication, 2011 – *induction training on the geology and stratigraphy of Thompson Nickel Belt, Vale exploration office, 60 Seal Road, Thompson*

Macek, J.J, McGregor, C.R, Zwanzig, H.V. 2004: *Thompson Nickel Belt Project, Manitoba (part of NTS 63P): geology of the South pit, Thompson Mine. Report of Activities 2004, Manitoba Industry, Economic Development and Mines, Manitoba Geological Survey, p.135-148*

McDowell, G.M., Fenlon, K. and King, A. 2004: *Conductivity-based nickel grade estimation for grade control at Inco's Sudbury mines. SEG Int'l Exposition and 74th Annual Meeting, Denver, Colorado, 1-4.*

McDowell, G. M., Mackie, A. D., and Palkovits, M., 2007: *Grade Estimation at Inco's Canadian Sulphide Mines. 20th EEGS Symposium on the Application of Geophysics to Engineering and Environmental Problems. Session: Borehole Geophysics*

McFadden, M. and Scott, W.R., 2013: *Broadband Soil Susceptibility Measurements for EMI Applications, Journal of Applied Geophysics (2013) doi: 10.1016/j.jappgeo.2013.01.009*

Oniku, S. A., Osazuwa, I. B., and Meludu, O. C., 2008: *Preliminary report on magnetic susceptibility measurements on rocks within the Zaria granite batholith, Nigeria. Geofizika Vol. 25 No. 2 2008*

Paktunč, A.D. 1984a: *Metamorphism of the ultramafic rocks of the Thompson Mine, Thompson Nickel Belt, Northern Manitoba. The Canadian Mineralogist vol.22 77-91*

Potter, D., 2005: *Magnetic Susceptibility as a rapid non-destructive technique for improved RCAL and SCAL parameter prediction. 2005 International Symposium of the Society of Core Analysis, Toronto, Canada, Paper SCA2005-02*

Provincial Map of Manitoba*: http://geology.about.com/library/bl/maps/blmanitobaecmap.htm*

Rainsford pers. communication, 2014: *suggesting the usefulness of median over mean methods*

Retallack, G.J., Sheldon, N.D., Cogoini, M., Elmore, R.D., 2003: *Magnetic susceptibility of early Paleozoic and Precambrian paleosols, Elsevier; Palaeography, Palaeoclimatology, Palaeoecology 198 (2003)373-380*

Rochette, P, 1987b*: Metamorphic control of the magnetic mineralogy of black shales in the Swiss Alps: towards the use of "magnetic isograde*s*". Earth Planet. Sci Lett., 84, 446-456*

RT-1 user's manual, 2011 *by Fugro Instrument*

Schibler, L., Boyko, T., Ferdyn, M., Gajda, B., Höll, S., Jordanova, N., Rösler, W., y Magprox 5 Team., 2002: *Topsoil mangetic susceptibility mapping: Data reproducibility and compatibility, measurement strategy, Stud., Geophys. Geod, 46, 43 - 57*

Searl, R. C., 2008: *Magnetic Susceptibility as a Tool for Investigating Igneous Rocks – Experience from IODP Expedition 304. Scientific Drilling, No. 6, July 2008*

SM30 user manual, *2009 by ZH Instruments*

Smith, R.S., Shore, M., Rainsford, D., 2012: *How to make better use of physical properties in mineral exploration: The exploration site measurement. Special Section: Mining Geophysics*

Statistics Solutions: http://www.statisticssolutions.com/academic-solutions/resources/directory-of-statistical-analyses/measures-of-association/

UNIDO, 2006: *Role of measurement and calibration in the manufacture of products for the global market. A guide for small and medium – sized enterprises; United Nations Industrial Development Organization (UNIDO) working paper, Vienna, 2006*

Vanos, S.N. 2008: *The Association of Platinum Group Elements with Fuchsite mineralization in Thompson Mine, Thompson Manitoba.*

Wolfram Math World*: http://mathworld.wolfram.com/VariationCoefficient.html*

Zhao, X., 1996: *Magnetic signatures of peridotite rocks from sites 897 and 899 and their implications Proceedings of the Ocean Drilling Program, Scientific Results, Vol. 149*

Zwanzig, H.V, Macek, J.J, McGregor, C.R. 2007: *Lithostratigraphy and Geochemistry of the High-Grade metasedimentary rocks in the Thompson Nickel Belt and Adjacent Kisseynew Domain, Manitoba: Implications for Nickel Explorations Society of Economic Geologists, Inc. Economic Geology, v. 102 pp. 1197-1216*

10.0 APPENDICES

Appendix A: Equipment list

Table 26: List of MS instruments and their accompanying accessories.

Instrument	Parts	comments
SM30 from ZH instruments	• SM30 meter • Connecting cable • User's manual • Leather case • Instruction DVD	✓ Complete
RT-1 from Fugro Instruments	• RT-1 Mag susc meter • Blue interface • User's manual • Yellow carrying case • Memory stick	✓ Complete
KT-10 supplied by Terraplus	• KT-10 Meter • 2 orange batteries • 1 pin • GEORADiS DVD • Instruction manual • Downloading cable • Battery charger • Black carrying case	- One pin missing - No geousb.exe software for USB connection • Later supplied by the manufacturer
MPP – EMS2+ probe by GDD Inc.	• MPP Probe • 4 AA batteries with charger • Handheld computer • External power supply with international adapters • Serial communication cable (RS232) • MPP Probe's & hp instructions manuals • Charger adapter	✓ Complete

	• A/C adapter for cradle • PDA software version • Instructions manual • Standard battery with cover	
Calibration sample	• KT-10 Calibration sample manufactured by **GEORADiS**	✓
MS2C & MS2K Bartington Instruments	• MS3 Magnetic susceptibility meter • MS2C core logging sensor • MS2E High Resolution Surface Sensor • 1 Bartsoft DVD • 1 instructions Manual DVD • 4 Connecting cables • 1 Black carrying case for MS2E High Resolution Surface sensor • 1 charger	✓ Complete

Appendix B: Instruments specifications

Table 27: RT-1 specifications

RT-1 Specifications

FUGRO INSTRUMENTS

Specifications

Sensitivity (SI)	1×10^{-5}
Operating Range	1×10^{-5} to 10 SI
Units	SI or CGS
Operating Frequency	750Hz
Response Time	Less than 1 second
Operating Mode	Single or Continuous readings
Memory	More than 9800 readings and flags!
Display Type & Rate	Liquid Crystal Display, with backlight 55 mm x 28 mm Displays analogue and digital readings and menus
Audio Output	Audio output on key touch Selectable Continuous Audio Indication or relative reading values
Power Source	3 x 1.5V AA Alkaline Batteries Power down feature with auto shut-off Low battery is indicated
Battery Life	Better than 25 hours continuous use
Water Resistance rating	IP65
Coil Type	Ferrite
Temperature Range (°C)	Operating: 0°C - +50°C Storage: -40°C - +60°C
Relative Humidity	10 to 90% (non condensing)
Data Input/Output	Bluetooth

Features

- **Bluetooth interface**
- **External Sensor Attachment**
- **Continuous Reading**
- **Water Resistant (IP65 rated)**
- **Memory Flags**
- **Toggle to CGS Units**
- **Audio Output**
- **Auto Ranging**

Weight & Dimensions

Length:	**155 mm**
Width:	**84 mm**
Height:	**34 mm**
Weight:	**0.35 kg**

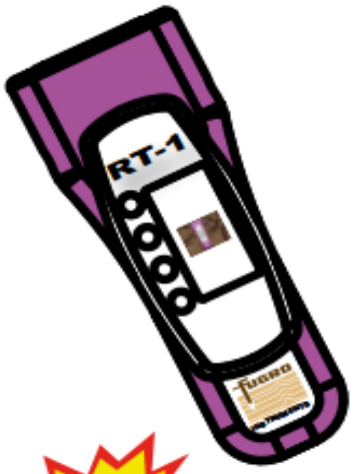

Standard System

The RT-1standard system is supplied with:

- RT-1 Console with removable sensor, and wrist strap
- Three Alkaline AA Batteries
- 1GB USB with Operating Software, Manual and Quick Start Guide
- Operations Manual and Quick Start Guide
- Sturdy, plastic, waterproof carry case with foam insert
- Leather carrying case
- Bluetooth USB and software

FUGRO INSTRUMENTS
21 Mellor Street
West Ryde 2114 NSW
Sydney Australia
Tel: +61 2 8878 9000
Fax: +61 2 8878 9012
Email: sales@fugroinstruments.com

Table 28: MS2 & MS3 specifications (http://www.ascscientific.com/MS2_MS3DS0020.pd)

Specifications	MS2 Meter	MS3 Meter
Range	0.09999 SI (volume specific)	26 SI (volume specific)
Maximum resolution	$2x10^{-6}$ SI	$2x10^{-6}$ SI
Units	SI or CGS	SI or CGS
Measurement time	1s or 10s	Selectable to 0.1s minimum
Display	Yes	No (requires PC or PDA)
Laboratory data logging	Yes (with Bartsoft or Multisus)	Yes (with Bartsoft)
Field data logging	Not available	Yes (with Bartsoft for Windows® CE)
Weight	1.9kg	0.13kg
Internal battery	0.7Ah sealed Ni-MH gives 8 hours use before recharge is required	N/A
Enclosure material	High impact ABS	White Acetal
Operating temperature	-10°C to +40°C	-10°C to +40°C
Dimensions (W x H x D)	155 x 50 x 256mm	50 x 25 x 123.5mm
Battery charger inlet	2.1mm socket, 6-18VDC, 100mA maximum, polarity protected	N/A
Battery charge	16 hours full charge	N/A
RS232 interface to PC	1200/9600 baud rate selected on rear panel Pin assignment: 1 = Ground Ov, 2 = MS2 Tx, 3 = MS2 Rx	N1200/9600 baud rate – software selectable
Interface connector	4-way rear panel Fischer socket TNC-TNC	Hirose HR10-7R-6P

MS2C

Table 29: MS2C instrument specifications (http://www.ascscientific.com/MS2_MS3DS0020.pd)

Specification	
Loop internal diameter	30, 36, 40, 45, 47, 50, 60, 70, 72, 80, 85, 90, 93, 100, 110, 120, 125, 130, 135, 140, 145, 146, 150, 160 or 162mm (Intermediate sizes can be provided at an additional charge)
Calibration accuracy	5% (calibration sample provided)
Measurement period (MS2)*: x 1 range x 0.1range	1.1s SI (0.9s CGS) 11s SI (9s CGS)
Operating frequency	0.565kHz
Spatial resolution	20mm
Drift at room temperature	<2 x 10^{-5} SI (vol) (<2 x 10^{-6} CGS) in 10 minutes (after 5 minutes' warm-up)
Dimensions (W x H x D)	200 x 290 x 162mm (with feet)
Weight	2 to 2.7kg depending on diameter
Enclosure material	White polyacetal

Table 30: Specifications of MS2K (http://www.ascscientific.com/MS2_MS3DS0020.pd)

Specification	
Calibration accuracy	1% (calibration sample provided)
Area of response	25.4mm diameter (full-width, half-maximum)
Depth of response	50% at 3mm, 10% at 8mm
Measurement period (MS2)*: x 1 range x 0.1 range	1.2s SI (1s CGS) 12s SI (10s CGS)
Operating frequency	0.93kHz
Drift at room temperature	<2 x 10^{-5} SI (vol) (<2 x 10^{-6} CGS) in 5 minutes (after 5 minutes' warm-up)
Environmental	May be used under wet conditions: not suitable for immersion
Dimensions (W x H x D)	50 x 170 x 165mm
Weight	0.32kg (1.20kg with carrying case)

* MS3 measurement period is software selectable

Table 31: SM30 specifications, user manual

1.2 Specification

SENSITIVITY.....x10-7 SI Units
MAX MEASURED VALUE.....10^{-1}SI
DIMENSIONS.....100 x 65 x 25 mm
WEIGHT.....0.180 kg
OPERATING FREQUENCY.....9kHz
MEASUREMENT TIME
- .....basic mode approx. 5s
- .....drift correction modes approx. 8s

DIGITAL DISPLAY.....LCD 4digit,10mm high
CONTROLS.....3 push buttons
DATA MEMORY.....up to 250 measurements
PICK-UP COIL SIZE 50 mm in diameter
OPERATING TEMPERATURE.....-20°C to +50°C
BATTERY.....2 Lithium 3V type CR2430
BATTERY LIFE.....typically 80 hours
COMMUNICATION WITH COMPUTER.....RS232

Table 32: KT-10 meter and calibration sample specifications

Terraplus

Specifications:

Sensitivity:	$1x10^{-6}$ SI Units
Measurement range:	$0.001x10^{-3}$ to $9999.99 X 10^{-3}$ SI Units Auto-Ranging (10 SI Units)
Operating frequency:	10 kHz
Measurement frequency:	20 times per second (in Scan mode, 5 readings averaged together and 4 readings /second stored)
Calibration Curves:	1 Calibration Curve is included for magnetite with another 2 additional calibration curves to be programmed by the operator
Display:	High Contrast LCD Graphic Display with 104 x 88 pixels
Memory:	Up to 3000 measurements or 2000 measurements with one minute of comments per reading.
Control:	1 button with up / down function & pin for rough surfaces
Data Input/Output:	USB, Bluetooth with GPS link via Bluetooth
Power Supply:	2 AA Alkaline Batteries or 2 optional AA Rechargeable Batteries
Battery life:	Approximately 100 hours without voice recorder
Operating temperature:	-20 °C to 60 °C
Dimensions:	200mm x 57mm X 30mm
Coil Diameter:	65 mm with a 45 degree angle
Weight:	0.30 kg

Optional:

Magnetic Susceptibility Standard

A magnetic susceptibility standard is now available as an option for either the KT-10 or the KT-10 Plus. The standard is manufactured from Mn-Zn ferrite compacted with mudstone. Its purpose is to confirm that the KT-10 or the KT-10 Plus is operating properly or to recalibrate the unit.

Nominal susceptibility will vary between standards

Typically:	34×10^{-3} SI
Diameter:	145 mm
Height :	70mm
Density:	2.36g/ccm
Weight:	2.65kg

Specifications subject to change without notice # -03-10 5

Terraplus Inc.
52 West Beaver Cr. Rd. #12, Richmond Hill, ON. Canada L4B 1L9
Tel: 905-764-5505
Fax: 905-764-8093
Email: sales@terraplus.ca
Website: www.terraplus.ca

GEORADiS

Magnetic Susceptibility Calibration Pad

Serial Number:	**2011/50**
Nominal Value:	**36.2 +/- 0.5 x 10^{-3} SI at 22 ^{0}C**
Density:	**2.36 g/ccm**

Standard is manufactured of Mn Zn ferrite mixed in mudstone. Susceptibility of the standard and its homogeneity was tested independently by Advanced Geoscience Instruments Company, Inc.

Testing instrument:	MFK1-FA Kappabridge
Sensitivity:	2 x 10^{-5} [SI]
Accuracy of Absolute Calibration:	+/- 3%
Measuring Field:	200 A/m
Field Homogeneity:	0.5%
Operating Frequency:	4 kHz

Homogeneity test:

36.2
35.9
36.0
36.1
35.9
36.1
36.1

Test pattern:

Tested by: Jiri Bartosek

Date: October 12, 2011

Figure 58: The latest test performed to determine the MS value of the KT-10 calibration in 2011 by Terraplus Geophysics' employee

Appendix C: Auxiliary Diagrams

Figure 59: Picture of the six MS instruments used in this study. They include (from left to right) GDD's MPP EMS2+ probe, KT-10, RT-1, SM30, MS2C, MS2K and the two calibration samples.

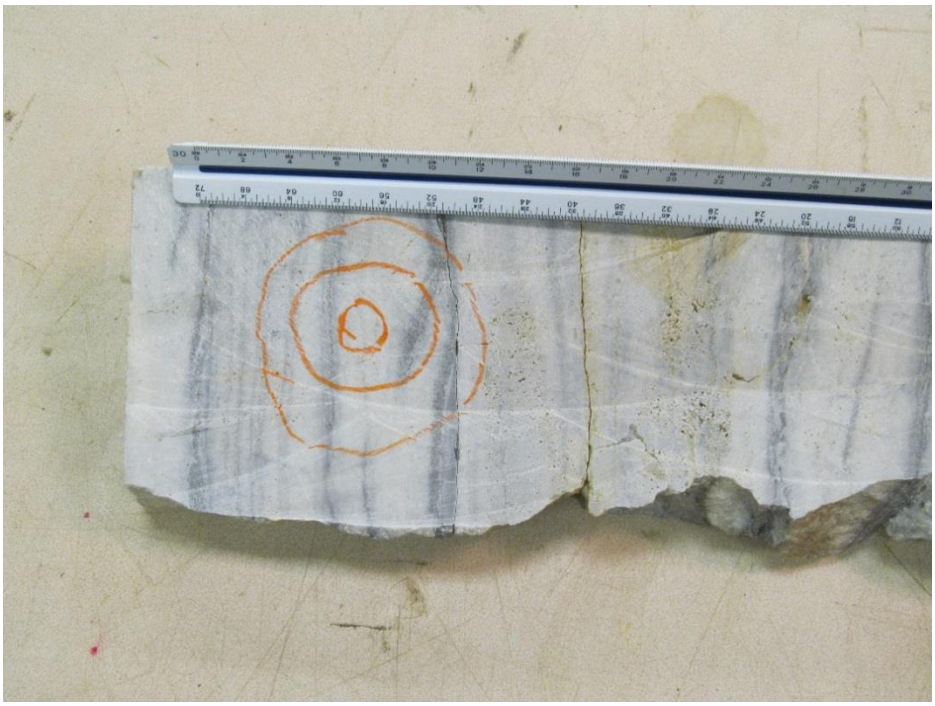

Figure 60: Dolomite sample used in this research

Figure 61: Shows how BSS-02B continuous down-hole data was collected by lowering the sensor and controlled by winch

Appendix D: Research Data

Table 33: Raw magnetic susceptibility data from Borehole 1301020

Drillhole#	Depth	Lithology	RT1	KT10	GDD	MS2K	MS2C	SM30 B
	(ft)		(x10-3SI)	(x10-3SI)	(x10-3SI)	(x10-3SI)	(x10-3SI)	(x10-3SI)
1301020	613.5	Gneiss	0	0.119	0	0.102	0.221	0.085
1301020	613.5	Gneiss	0	0.119	0	0.123	0.268	0.082
1301020	613.5	Gneiss	0	0.12	0	0.121	0.326	0.082
1301020	613.5	Gneiss	0	0.117	0	0.116	0.365	0.082
1301020	613.5	Gneiss	0	0.12	0	0.108	0.401	0.082
1301020	613.5	Gneiss	0	0.121	0	0.110	0.431	0.081
1301020	613.5	Gneiss	0	0.12	0	0.110	0.463	0.079
1301020	613.5	Gneiss	0	0.123	0	0.106	0.514	0.08
1301020	613.5	Gneiss	0	0.12	0	0.103	0.550	0.083
1301020	613.5	Gneiss	0	0.12	0	0.099	0.590	0.08
1301020	613.5	Gneiss	0	0.116	0	0.094	0.623	0.084
1301020	613.5	Gneiss	0	0.122	0	0.081	0.657	0.081
1301020	613.5	Gneiss	0	0.12	0	0.110	0.675	0.081
1301020	613.5	Gneiss	0	0.118	0	0.110	0.703	0.081
1301020	613.5	Gneiss	0	0.114	0	0.102	0.729	0.081
1301020	613.5	Gneiss	0	0.117	0	0.096	0.755	0.082
1301020	613.5	Gneiss	0	0.12	0	0.099	0.802	0.082
1301020	613.5	Gneiss	0	0.116	0	0.114	0.843	0.081
1301020	613.5	Gneiss	0	0.12	0	0.113	0.880	0.08
1301020	629.9	Amphibolite	0.44	0.425	0.22	0.715	2.127	0.447
1301020	629.9	Amphibolite	0.43	0.417	0.12	0.711	2.158	0.432
1301020	629.9	Amphibolite	0.44	0.427	0.05	0.710	2.187	0.423
1301020	629.9	Amphibolite	0.43	0.439	0	0.706	2.217	0.431
1301020	629.9	Amphibolite	0.43	0.447	0	0.705	2.250	0.424
1301020	629.9	Amphibolite	0.43	0.433	0	0.679	2.315	0.429
1301020	629.9	Amphibolite	0.42	0.431	0	0.727	2.339	0.429
1301020	629.9	Amphibolite	0.41	0.444	0	0.728	2.380	0.423
1301020	629.9	Amphibolite	0.42	0.45	0	0.729	2.395	0.427
1301020	629.9	Amphibolite	0.41	0.431	0	0.729	2.440	0.429
1301020	629.9	Amphibolite	0.44	0.431	0	0.724	2.474	0.424
1301020	629.9	Amphibolite	0.44	0.432	0	0.733	2.513	0.417
1301020	629.9	Amphibolite	0.44	0.431	0	0.733	2.534	0.424
1301020	629.9	Amphibolite	0.44	0.436	0	0.733	2.558	0.43
1301020	629.9	Amphibolite	0.43	0.426	0	0.734	2.571	0.428
1301020	629.9	Amphibolite	0.43	0.439	0	0.732	2.600	0.426
1301020	629.9	Amphibolite	0.43	0.446	0	0.731	2.620	0.411
1301020	629.9	Amphibolite	0.43	0.445	0	0.733	2.642	0.427
1301020	629.9	Amphibolite	0.42	0.453	0	0.733	2.662	0.426
1301020	629.9	Amphibolite	0.43	0.445	0	0.732	2.716	0.424
1301020	629.9	Amphibolite	0.42	0.455	0	0.730	2.741	0.429
1301020	836.6	M. Peridotite	8.84	9.442	10	8.334	27.493	9.3
1301020	836.6	M. Peridotite	8.85	9.354	10	8.352	27.487	8.41
1301020	836.6	M. Peridotite	8.87	8.858	9.97	8.347	27.482	8.43
1301020	836.6	M. Peridotite	8.85	8.649	9.92	8.833	27.474	8.15
1301020	836.6	M. Peridotite	8.86	9.266	9.94	8.742	27.470	8.29

1301020	836.6	M. Peridotite	8.85	9.432	9.89	8.873	27.472	8.4
1301020	836.6	M. Peridotite	8.85	9.404	9.87	8.854	27.470	8.22
1301020	836.6	M. Peridotite	8.87	9.003	9.82	8.850	27.468	8.33
1301020	836.6	M. Peridotite	8.88	9.432	9.77	8.848	27.478	9.78
1301020	836.6	M. Peridotite	8.87	8.972	9.74	8.754	27.476	8.9
1301020	836.6	M. Peridotite	8.85	9.494	9.72	8.742	27.470	8.35
1301020	836.6	M. Peridotite	8.83	9.438	9.65	8.741	27.476	8.33
1301020	836.6	M. Peridotite	8.84	9.436	9.6	8.739	27.463	8.3
1301020	836.6	M. Peridotite	8.87	9.747	9.52	8.741	27.474	8.16
1301020	836.6	M. Peridotite	8.86	9.274	9.47	8.739	27.463	8.22
1301020	836.6	M. Peridotite	8.84	9.432	9.45	8.717	27.470	8.64
1301020	836.6	M. Peridotite	8.84	9.403	9.42	8.684	27.470	8.21
1301020	836.6	M. Peridotite	8.83	9.379	9.37	8.690	27.463	8.57
1301020	836.6	M. Peridotite	8.82	9.781	9.35	8.630	27.463	8.51
1301020	841.5	M. Serpentinite	55.81	36.676	93	65.152	96.695	35.7
1301020	841.5	M. Serpentinite	55.79	36.841	92.5	62.574	96.287	36.4
1301020	841.5	M. Serpentinite	55.55	37.078	92.5	64.018	95.897	36.2
1301020	841.5	M. Serpentinite	55.55	37.132	92.4	63.783	95.672	35.2
1301020	841.5	M. Serpentinite	55.49	37.134	92.1	64.630	95.470	36.5
1301020	841.5	M. Serpentinite	55.54	37.014	91.7	65.241	95.122	36.4
1301020	841.5	M. Serpentinite	55.61	37.188	91.7	65.367	75.222	35.8
1301020	841.5	M. Serpentinite	55.63	37.296	91.6	65.360	74.710	36.2
1301020	841.5	M. Serpentinite	55.64	37.205	91.2	65.343	74.505	35.3
1301020	841.5	M. Serpentinite	55.65	37.105	91	65.230	74.222	35.5
1301020	841.5	M. Serpentinite	55.66	37.167	90.6	65.117	74.039	36.2
1301020	841.5	M. Serpentinite	55.7	37.141	90.3	65.101	73.840	36
1301020	841.5	M. Serpentinite	55.67	37.044	90	64.132	73.670	36.7
1301020	841.5	M. Serpentinite	53.99	36.777	90	64.738	73.398	35.9
1301020	841.5	M. Serpentinite	53.06	37.242	90	64.318	73.234	36.3
1301020	841.5	M. Serpentinite	53.08	36.484	89.9	63.256	73.056	35.6
1301020	841.5	M. Serpentinite	53.13	36.998	89.8	64.925	72.721	35.9
1301020	841.5	M. Serpentinite	52.66	37.029	89.5	64.873	72.567	36.5
1301020	841.5	M. Serpentinite	52.46	36.972	89.4	64.739	72.380	35.8
1301020	841.5	M. Serpentinite	52.86	37.042	89.2	64.800	72.202	36.3
1301020	846.5	M. Peridotite	3.9	5.032	6.29	4.107	14.285	4.75
1301020	846.5	M. Peridotite	3.94	5.18	6.24	4.034	14.281	4.75
1301020	846.5	M. Peridotite	3.95	5.109	6.22	4.297	14.279	4.82
1301020	846.5	M. Peridotite	3.93	5.153	6.12	4.312	14.281	4.55
1301020	846.5	M. Peridotite	3.92	5.005	6.04	4.365	14.281	4.55
1301020	846.5	M. Peridotite	3.92	5.056	5.99	4.360	14.279	4.62
1301020	846.5	M. Peridotite	3.92	5.09	5.97	4.365	14.281	4.49
1301020	846.5	M. Peridotite	3.93	5.293	5.89	4.369	14.277	4.62
1301020	846.5	M. Peridotite	3.91	4.587	5.85	4.373	14.267	4.47
1301020	846.5	M. Peridotite	3.91	5.509	5.77	4.380	14.266	4.93
1301020	846.5	M. Peridotite	3.91	5.226	5.72	4.379	14.267	4.43
1301020	846.5	M. Peridotite	3.92	5.045	5.62	4.382	14.269	4.75
1301020	846.5	M. Peridotite	3.92	5.299	5.62	4.383	14.264	4.61
1301020	846.5	M. Peridotite	3.92	5.214	5.55	4.384	14.265	5.05
1301020	846.5	M. Peridotite	3.93	5.784	5.52	4.383	14.267	4.92
1301020	846.5	M. Peridotite	3.93	4.634	5.5	4.388	14.264	4.35
1301020	846.5	M. Peridotite	3.93	5.503	5.4	4.387	14.267	4.56

1301020	846.5	M. Peridotite	3.93	5.374	5.35	4.388	14.262	4.48
1301020	846.5	M. Peridotite	3.93	5.827	5.3	4.394	14.263	4.56
1301020	846.5	M. Peridotite	3.93	4.405	5.15	4.398	14.267	4.78
1301020	850.4	Serpentinite	42.4	31.035	70.8	52.154	83.220	29.3
1301020	850.4	Serpentinite	42.29	30.186	70.7	52.234	83.214	28.9
1301020	850.4	Serpentinite	42.31	30.74	70.7	52.374	83.212	29.2
1301020	850.4	Serpentinite	42.24	30.654	70.6	52.350	83.212	29.3
1301020	850.4	Serpentinite	42.11	29.341	70.5	52.339	83.212	29.4
1301020	850.4	Serpentinite	42	30.753	70.5	52.444	83.214	28.8
1301020	850.4	Serpentinite	42.01	30.587	70.5	52.407	83.212	29.1
1301020	850.4	Serpentinite	42.01	30.056	70.4	51.636	83.214	29.1
1301020	850.4	Serpentinite	42.02	30.739	70.4	52.089	83.214	29.6
1301020	850.4	Serpentinite	42.03	28.761	70.3	51.317	83.210	29.4
1301020	850.4	Serpentinite	42.01	30.327	70.3	50.067	83.216	29.4
1301020	850.4	Serpentinite	41.94	31.125	70.2	48.810	83.206	29.2
1301020	850.4	Serpentinite	41.9	30.417	70.1	48.399	83.208	29.3
1301020	850.4	Serpentinite	41.95	29.812	70.1	44.931	83.205	29.4
1301020	850.4	Serpentinite	41.99	30.946	70.1	52.384	83.206	29.6
1301020	850.4	Serpentinite	42.01	30.9	70.1	52.689	83.210	29.3
1301020	850.4	Serpentinite	42.01	30.418	70.1	52.897	83.212	28.9
1301020	850.4	Serpentinite	42	30.767	70	53.100	83.212	29.4
1301020	850.4	Serpentinite	41.99	31.047	70	53.467	83.208	29.4
1301020	850.4	Serpentinite	41.97	30.802	69.9	53.553	83.206	29.3
1301020	866.8	Amphibolite	0.17	0.369	0.1	0.507	1.225	0.32
1301020	866.8	Amphibolite	0.18	0.367	0.07	0.560	1.211	0.332
1301020	866.8	Amphibolite	0.18	0.346	0.02	0.552	1.211	0.329
1301020	866.8	Amphibolite	0.18	0.365	0	0.562	1.194	0.33
1301020	866.8	Amphibolite	0.17	0.368	0	0.567	1.184	0.329
1301020	866.8	Amphibolite	0.17	0.363	0	0.569	1.175	0.331
1301020	866.8	Amphibolite	0.17	0.364	0	0.572	1.180	0.325
1301020	866.8	Amphibolite	0.18	0.37	0	0.571	1.163	0.324
1301020	866.8	Amphibolite	0.18	0.358	0	0.572	1.164	0.324
1301020	866.8	Amphibolite	0.17	0.367	0	0.574	1.149	0.328
1301020	866.8	Amphibolite	0.17	0.367	0	0.574	1.017	0.324
1301020	866.8	Amphibolite	0.16	0.37	0	0.576	1.022	0.327
1301020	866.8	Amphibolite	0.16	0.365	0	0.575	1.004	0.329
1301020	866.8	Amphibolite	0.16	0.363	0	0.575	1.006	0.329
1301020	866.8	Amphibolite	0.16	0.372	0	0.576	1.000	0.325
1301020	866.8	Amphibolite	0.16	0.371	0	0.577	0.986	0.323
1301020	866.8	Amphibolite	0.16	0.363	0	0.576	0.985	0.326
1301020	866.8	Amphibolite	0.16	0.37	0	0.580	0.977	0.324
1301020	866.8	Amphibolite	0.16	0.37	0	0.579	0.979	0.323
1301020	866.8	Amphibolite	0.16	0.363	0	0.580	0.973	0.329
1301020	883.9	Iron formation	4.95	5.736	19.8	17.644	21.536	5.38
1301020	883.9	Iron formation	4.96	5.693	19.4	17.770	21.540	5.36
1301020	883.9	Iron formation	4.96	5.689	19.4	17.820	21.536	5.49
1301020	883.9	Iron formation	4.98	5.722	19.3	17.826	21.538	5.35
1301020	883.9	Iron formation	4.99	5.859	19.2	17.844	21.532	5.43
1301020	883.9	Iron formation	4.99	5.733	19.1	17.851	21.536	5.45
1301020	883.9	Iron formation	5	5.825	19.1	17.855	21.536	5.48
1301020	883.9	Iron formation	5	5.921	19	17.847	21.536	5.52

1301020	883.9	Iron formation	5	5.789	18.9	17.840	21.534	5.55
1301020	883.9	Iron formation	5	5.771	18.9	17.741	21.534	5.53
1301020	883.9	Iron formation	5	5.924	18.8	17.844	21.534	5.48
1301020	883.9	Iron formation	5	5.737	18.8	17.756	21.534	5.48
1301020	883.9	Iron formation	5	5.872	18.8	17.824	21.536	5.22
1301020	883.9	Iron formation	5	5.722	18.7	17.804	21.536	5.33
1301020	883.9	Iron formation	5	5.766	18.6	17.785	21.536	5.34
1301020	883.9	Iron formation	5	5.717	18.6	17.748	21.534	5.29
1301020	883.9	Iron formation	5	5.728	18.6	17.795	21.536	5.32
1301020	883.9	Iron formation	5	5.902	18.5	17.775	21.538	5.34
1301020	883.9	Iron formation	5	5.745	18.5	17.740	21.532	5.08
1301020	883.9	Iron formation	5.01	5.789	18.3	17.730	21.534	5.2
1301020	915.4	Pegmatite	0	0.095	0	0.079	0.201	0.05
1301020	915.4	Pegmatite	0	0.073	0	0.081	0.195	0.046
1301020	915.4	Pegmatite	0	0.071	0	0.081	0.198	0.048
1301020	915.4	Pegmatite	0	0.069	0	0.081	0.195	0.046
1301020	915.4	Pegmatite	0	0.069	0	0.081	0.194	0.047
1301020	915.4	Pegmatite	0	0.065	0	0.081	0.192	0.048
1301020	915.4	Pegmatite	0	0.073	0	0.081	0.187	0.05
1301020	915.4	Pegmatite	0	0.068	0	0.081	0.186	0.045
1301020	915.4	Pegmatite	0	0.071	0	0.081	0.187	0.047
1301020	915.4	Pegmatite	0	0.065	0	0.081	0.190	0.048
1301020	915.4	Pegmatite	0	0.068	0	0.081	0.190	0.05
1301020	915.4	Pegmatite	0	0.071	0	0.081	0.188	0.049
1301020	915.4	Pegmatite	0	0.071	0	0.081	0.187	0.05
1301020	915.4	Pegmatite	0	0.072	0	0.081	0.186	0.049
1301020	915.4	Pegmatite	0	0.066	0	0.081	0.183	0.05
1301020	996.1	Quartzite	0	0.007	0	-0.007	-0.021	-0.007
1301020	996.1	Quartzite	0	0.005	0	-0.007	-0.027	-0.004
1301020	996.1	Quartzite	0	0.007	0	-0.007	-0.029	-0.001
1301020	996.1	Quartzite	0	0.005	0	-0.007	-0.029	0
1301020	996.1	Quartzite	0	0.007	0	-0.007	-0.019	-0.001
1301020	996.1	Quartzite	0	0.005	0	-0.007	-0.029	-0.002
1301020	996.1	Quartzite	0	0.002	0	-0.007	-0.021	-0.002
1301020	996.1	Quartzite	0	0.006	0	-0.007	-0.019	-0.002
1301020	996.1	Quartzite	0	0.01	0	-0.007	-0.019	-0.002
1301020	996.1	Quartzite	0	0.009	0	-0.007	-0.030	-0.001
1301020	996.1	Quartzite	0	0.01	0	-0.007	-0.021	-0.002
1301020	996.1	Quartzite	0	0.008	0	-0.007	-0.025	-0.001
1301020	996.1	Quartzite	0	0.007	0	-0.007	-0.021	-0.001
1301020	996.1	Quartzite	0	0.005	0	-0.008	-0.027	-0.001
1301020	996.1	Quartzite	0	0.008	0	-0.007	-0.029	-0.001
1301020	996.1	Quartzite	0	0.008	0	-0.007	-0.028	0
1301020	996.1	Quartzite	0	0.006	0	-0.007	-0.021	-0.002
1301020	996.1	Quartzite	0	0.008	0	-0.007	-0.025	-0.003
1301020	996.1	Quartzite	0	0.005	0	-0.008	-0.021	-0.002
1301020	996.1	Quartzite	0	0.011	0	-0.008	-0.030	0

Table 34: Raw magnetic susceptibility data from borehole 1301080

Drillhole#	Depth	Lithology	RT1	KT10	GDD	MS2K	MS2C	SM30 B
	(ft)		(x10-3SI)	(x10-3SI)	(x10-3SI)	(x10-3SI)	(x10-3SI)	(x10-3SI)
1301080	731	GNAM	0.34	0.283	0.54	0.471	1.005	0.258
1301080	731	GNAM	0.33	0.274	0.57	0.471	1.005	0.257
1301080	731	GNAM	0.33	0.287	0.57	0.472	1.007	0.262
1301080	731	GNAM	0.33	0.288	0.59	0.472	1.009	0.261
1301080	731	GNAM	0.32	0.287	0.57	0.472	1.007	0.258
1301080	735	GN	0	0.077	0.2	0.165	0.200	0.063
1301080	735	GN	0	0.076	0.15	0.163	0.202	0.069
1301080	735	GN	0	0.083	0.17	0.165	0.198	0.07
1301080	735	GN	0	0.085	0.15	0.165	0.202	0.066
1301080	735	GN	0	0.085	0.15	0.165	0.202	0.07
1301080	764	PEG	0	0.064	0.02	0.032	0.087	0.036
1301080	764	PEG	0	0.064	0.02	0.032	0.087	0.038
1301080	764	PEG	0	0.063	0.02	0.032	0.087	0.038
1301080	764	PEG	0	0.061	0.02	0.032	0.087	0.038
1301080	764	PEG	0	0.063	0.02	0.033	0.087	0.04
1301080	773	AMPT	0	0.383	0.81	0.636	0.668	0.334
1301080	773	AMPT	0	0.370	0.81	0.634	0.668	0.334
1301080	773	AMPT	0	0.382	0.79	0.631	0.668	0.339
1301080	773	AMPT	0	0.382	0.81	0.634	0.670	0.335
1301080	773	AMPT	0	0.382	0.79	0.633	0.666	0.336
1301080	787	P2 SCH	0	0.369	0.79	0.690	1.140	0.33
1301080	787	P2 SCH	0	0.356	0.74	0.688	1.138	0.331
1301080	787	P2 SCH	0	0.371	0.74	0.687	1.144	0.347
1301080	787	P2 SCH	0	0.373	0.76	0.686	1.144	0.333
1301080	787	P2 SCH	0	0.372	0.76	0.697	1.142	0.336
1301080	792	PEG	0	0.136	0.1	0.045	0.373	0.117
1301080	792	PEG	0	0.105	0.07	0.046	0.373	0.103
1301080	792	PEG	0	0.113	0.1	0.045	0.371	0.127
1301080	792	PEG	0	0.099	0.05	0.045	0.377	0.146
1301080	792	PEG	0	0.100	0.05	0.044	0.369	0.129
1301080	800	P2 SCH	0	0.485	0.79	0.669	1.342	0.417
1301080	800	P2 SCH	0	0.525	0.76	0.677	1.342	0.415
1301080	800	P2 SCH	0	0.463	0.79	0.681	1.340	0.426
1301080	800	P2 SCH	0	0.480	0.79	0.681	1.342	0.453
1301080	800	P2 SCH	0	0.453	0.81	0.685	1.338	0.431
1301080	833	AMPT	0.02	0.807	1.53	1.670	2.755	0.725
1301080	833	AMPT	0.03	0.729	1.68	1.661	2.747	0.699
1301080	833	AMPT	0.03	0.747	1.68	1.661	2.745	0.715
1301080	833	AMPT	0.02	0.784	1.7	1.661	2.743	0.674
1301080	833	AMPT	0.01	0.814	1.7	1.658	2.737	0.675
1301080	838	P2 MSCH	12.99	5.975	25	22.915	24.488	6.5
1301080	838	P2 MSCH	12.99	6.247	24.8	25.746	24.458	6.5
1301080	838	P2 MSCH	13.02	7.220	24.8	25.464	24.435	6.49

1301080	838	P2 MSCH	13.07	6.520	24.7	25.381	24.421	6.27
1301080	838	P2 MSCH	13.08	6.453	24.6	25.738	24.401	6.23
1301080	843	P2 PSCH	0	0.444	0.2	0.114	0.595	0.267
1301080	843	P2 PSCH	0	0.409	0.27	0.112	0.595	0.406
1301080	843	P2 PSCH	0	0.433	0.25	0.113	0.593	0.367
1301080	843	P2 PSCH	0	0.394	0.2	0.112	0.587	0.39
1301080	843	P2 PSCH	0	0.410	0.25	0.113	0.589	0.465
1301080	854	P2 SUMX	18.64	12.694	37	24.570	95.999	11.7
1301080	854	P2 SUMX	18.71	12.450	37	24.543	95.822	11.1
1301080	854	P2 SUMX	18.67	12.617	37.1	24.688	95.751	11.1
1301080	854	P2 SUMX	18.62	12.394	37.1	24.391	95.668	11.1
1301080	854	P2 SUMX	18.59	12.250	37.2	24.048	95.606	10.9
1301080	858	P2? SCH	0	0.149	0.57	0.058	0.190	0.13
1301080	858	P2? SCH	0	0.129	0.57	0.057	0.188	0.107
1301080	858	P2? SCH	0	0.129	0.57	0.057	0.190	0.108
1301080	858	P2? SCH	0	0.134	0.54	0.056	0.190	0.122
1301080	858	P2? SCH	0	0.123	0.52	0.057	0.186	0.118
1301080	863	AMPT	0	0.377	0.69	0.540	1.237	0.358
1301080	863	AMPT	0	0.388	0.72	0.540	1.233	0.36
1301080	863	AMPT	0	0.383	0.69	0.538	1.237	0.355
1301080	863	AMPT	0	0.392	0.69	0.536	1.235	0.355
1301080	863	AMPT	0	0.381	0.69	0.538	1.239	0.362
1301080	873	SF QTE	0	0.250	0	0.016	0.020	0.123
1301080	873	SF QTE	0	0.193	0	0.016	0.020	0.339
1301080	873	SF QTE	0	0.306	0	0.016	0.022	0.147
1301080	873	SF QTE	0	0.161	0	0.016	0.020	0.384
1301080	873	SF QTE	0	0.136	0	0.016	0.018	0.212
1301080	882	SF SCH	0	0.259	0.32	0.200	0.815	0.217
1301080	882	SF SCH	0	0.300	0.32	0.201	0.813	0.232
1301080	882	SF SCH	0	0.262	0.32	0.200	0.817	0.232
1301080	882	SF SCH	0	0.293	0.35	0.200	0.817	0.233
1301080	882	SF SCH	0	0.285	0.37	0.200	0.813	0.245
1301080	902	PEG	0	0.026	0	0.031	0.067	0.022
1301080	902	PEG	0	0.029	0.02	0.030	0.065	0.023
1301080	902	PEG	0	0.043	0	0.028	0.066	0.025
1301080	902	PEG	0	0.040	0	0.030	0.065	0.028
1301080	902	PEG	0	0.029	0	0.028	0.062	0.029
1301080	912	AMPT	0	0.353	0.67	0.551	1.275	0.333
1301080	912	AMPT	0	0.351	0.64	0.561	1.273	0.334
1301080	912	AMPT	0	0.349	0.64	0.564	1.273	0.337
1301080	912	AMPT	0	0.348	0.84	0.564	1.274	0.317
1301080	912	AMPT	0	0.348	0.84	0.567	1.275	0.336
1301080	920	SF PSCH	0	0.256	0.32	0.321	0.700	0.248
1301080	920	SF PSCH	0	0.256	0.35	0.320	0.698	0.262
1301080	920	SF PSCH	0	0.260	0.35	0.318	0.698	0.267
1301080	920	SF PSCH	0	0.244	0.37	0.319	0.698	0.261
1301080	920	SF PSCH	0	0.248	0.37	0.319	0.694	0.237
1301080	935	SF QTE	0	0.113	0.1	0.052	0.103	0.093
1301080	935	SF QTE	0	0.113	0.07	0.052	0.103	0.104
1301080	935	SF QTE	0	0.106	0.1	0.051	0.103	0.096

1301080	935	SF QTE	0	0.115	0.07	0.049	0.107	0.093
1301080	935	SF QTE	0	0.109	0.1	0.046	0.105	0.101
1301080	937	AMPT	0	0.119	0.69	0.549	1.158	0.326
1301080	937	AMPT	0	0.109	0.74	0.565	1.162	0.313
1301080	937	AMPT	0	0.111	0.79	0.567	1.160	0.326
1301080	937	AMPT	0	0.107	0.76	0.570	1.159	0.331
1301080	937	AMPT	0	0.114	0.76	0.569	1.160	0.321
1301080	943	SF PSCH	0	0.373	0.07		0.149	0.04
1301080	943	SF PSCH	0	0.365	0.1		0.145	0.037
1301080	943	SF PSCH	0	0.364	0.1		0.149	0.041
1301080	943	SF PSCH	0	0.354	0.1		0.145	0.038
1301080	943	SF PSCH	0	0.360	0.12		0.153	0.05
1301080	953	P3 IF	5.02	3.366	9.57	3.818	79.978	4.27
1301080	953	P3 IF	5.08	3.063	9.7	3.792	79.976	3.32
1301080	953	P3 IF	5.12	2.950	9.7	3.822	79.978	4.78
1301080	953	P3 IF	5.12	3.074	9.67	3.818	79.976	3.54
1301080	953	P3 IF	5.1	3.050	9.67	3.828	79.976	4.15
1301080	991	PEG	0	0.117	0.17	0.112	0.204	0.11
1301080	991	PEG	0	0.123	0.2	0.111	0.204	0.093
1301080	991	PEG	0	0.114	0.17	0.112	0.208	0.096
1301080	991	PEG	0	0.126	0.17	0.109	0.210	0.11
1301080	991	PEG	0	0.119	0.2	0.107	0.208	0.095
1301080	1010	P3 IF (MT)	282.11	190.222	358	223.885	611.313	201
1301080	1010	P3 IF (MT)	281.95	186.039	359	226.710	611.303	201
1301080	1010	P3 IF (MT)	281.09	188.473	360	227.085	611.303	204
1301080	1010	P3 IF (MT)	279.87	187.296	360	227.321	611.303	193
1301080	1010	P3 IF (MT)	279.01	194.259	360	226.880	611.301	208
1301080	1020	P3 IF-GRNT	59.18	58.008	70	43.177	221.476	40.4
1301080	1020	P3 IF-GRNT	59.4	44.093	69.9	43.323	221.474	47.2
1301080	1020	P3 IF-GRNT	59.2	42.420	69.8	43.494	221.482	36.5
1301080	1020	P3 IF-GRNT	59.03	45.679	69.7	43.601	221.474	40.7
1301080	1020	P3 IF-GRNT	58.93	42.069	69.6	43.751	221.466	53.4
1301080	1030	AMPT	0	14.966	2.42	1.368	2.642	5.88
1301080	1030	AMPT	0	11.343	2.42	1.365	2.642	4.39
1301080	1030	AMPT	0	11.202	2.39	1.364	2.640	4.59
1301080	1030	AMPT	0	11.767	2.42	1.360	2.640	4.81
1301080	1030	AMPT	0	10.179	2.44	1.356	2.644	4.91
1301080	1041	AMPT - GAR	5.89	0.793	1.26	0.981	2.577	0.739
1301080	1041	AMPT - GAR	5.97	1.006	1.28	0.981	2.575	0.815
1301080	1041	AMPT - GAR	5.93	1.001	1.26	0.980	2.577	0.708
1301080	1041	AMPT - GAR	5.92	0.961	1.26	0.977	2.575	0.709
1301080	1041	AMPT - GAR	5.94	0.915	1.26	0.975	2.577	0.671
1301080	1056	APLITE	0	0.017	0	0.005	0.038	0.009
1301080	1056	APLITE	0	0.023	0	0.005	0.042	0.012
1301080	1056	APLITE	0	0.034	0	0.005	0.046	0.01
1301080	1056	APLITE	0	0.025	0	0.005	0.048	0.012
1301080	1056	APLITE	0	0.032	0	0.005	0.038	0.012

Table 35: Raw magnetic susceptibility data from borehole 1301240

Drillhole#	Depth (ft)	Lithology	KT10 (x10-3SI)	RT1 (x10-3SI)	GDD (x10-3SI)	MS2K (x10-3SI)	MS2C (x10-3SI)	SM30 B (x10-3SI)
1301240	1368.5	Gneiss	0.093	0.06	0.12	0.093	0.200	0.074
1301240	1368.5	Gneiss	0.097	0.06	0.1	0.093	0.200	0.077
1301240	1368.5	Gneiss	0.097	0	0.12	0.093	0.202	0.077
1301240	1368.5	Gneiss	0.093	0	0.12	0.093	0.200	0.077
1301240	1368.5	Gneiss	0.102	0	0.12	0.093	0.204	0.079
1301240	1381	Amphibolite	0.293	0.31	0.59	0.473	1.060	0.295
1301240	1381	Amphibolite	0.306	0.3	0.64	0.474	1.065	0.268
1301240	1381	Amphibolite	0.304	0.3	0.61	0.473	1.062	0.278
1301240	1381	Amphibolite	0.304	0.3	0.64	0.473	1.067	0.277
1301240	1381	Amphibolite	0.317	0.3	0.64	0.473	1.067	0.278
1301240	1388.2	Gneiss	0.139	0.14	0.27	0.104	0.454	0.149
1301240	1388.2	Gneiss	0.14	0.12	0.27	0.104	0.452	0.168
1301240	1388.2	Gneiss	0.135	0.08	0.27	0.103	0.454	0.161
1301240	1388.2	Gneiss	0.138	0.05	0.27	0.103	0.454	0.154
1301240	1388.2	Gneiss	0.132	0.04	0.27	0.104	0.450	0.153
1301240	1390.5	Amphibolite	0.897	1.48	2.87	1.533	4.529	0.906
1301240	1390.5	Amphibolite	0.894	1.45	2.87	1.535	4.514	0.948
1301240	1390.5	Amphibolite	0.865	1.42	2.87	1.537	4.504	0.957
1301240	1390.5	Amphibolite	0.889	1.4	2.85	1.536	4.495	0.947
1301240	1390.5	Amphibolite	0.897	1.4	2.85	1.534	4.489	0.96
1301240	1409	Gneiss	0.165	0.09	0.25	0.393	0.686	0.152
1301240	1409	Gneiss	0.158	0.08	0.25	0.396	0.686	0.148
1301240	1409	Gneiss	0.164	0.08	0.22	0.395	0.686	0.156
1301240	1409	Gneiss	0.154	0.07	0.22	0.395	0.686	0.154
1301240	1409	Gneiss	0.151	0.07	0.22	0.395	0.688	0.145
1301240	1410	Amphibolite	0.373	0.05	0.64	0.462	0.646	0.11
1301240	1410	Amphibolite	0.346	0.05	0.64	0.459	0.644	0.11
1301240	1410	Amphibolite	0.357	0.04	0.61	0.457	0.644	0.109
1301240	1410	Amphibolite	0.348	0.03	0.64	0.455	0.644	0.111
1301240	1410	Amphibolite	0.33	0.03	0.64	0.454	0.642	0.11
1301240	1418.5	Gneiss	0.167	0.31	0.27	0.242	1.241	0.331
1301240	1418.5	Gneiss	0.165	0.3	0.29	0.243	1.239	0.328
1301240	1418.5	Gneiss	0.169	0.3	0.32	0.242	1.239	0.326
1301240	1418.5	Gneiss	0.165	0.3	0.32	0.242	1.237	0.326
1301240	1418.5	Gneiss	0.166	0.3	0.32	0.242	1.241	0.324
1301240	1428	Granitized Gneiss	0.073	0.08	0.15	0.108	0.170	0.182
1301240	1428	Granitized Gneiss	0.076	0.07	0.17	0.107	0.175	0.183
1301240	1428	Granitized Gneiss	0.079	0.06	0.17	0.107	0.181	0.176
1301240	1428	Granitized Gneiss	0.082	0.05	0.17	0.107	0.175	0.186
1301240	1428	Granitized Gneiss	0.084	0.05	0.17	0.107	0.177	0.187
1301240	1437.5	Granitized Gneiss	0.129	0.04	0.2	0.188	0.217	0.085
1301240	1437.5	Granitized Gneiss	0.123	0	0.22	0.186	0.206	0.083
1301240	1437.5	Granitized Gneiss	0.128	0	0.22	0.187	0.219	0.083
1301240	1437.5	Granitized Gneiss	0.123	0	0.22	0.186	0.219	0.082
1301240	1437.5	Granitized Gneiss	0.123	0	0.22	0.187	0.208	0.08
1301240	1447	Granitized Gneiss	0.101	0	0.15	0.082	0.255	0.118
1301240	1447	Granitized Gneiss	0.118	0	0.17	0.081	0.244	0.117
1301240	1447	Granitized Gneiss	0.136	0	0.17	0.081	0.246	0.124
1301240	1447	Granitized Gneiss	0.124	0	0.17	0.081	0.250	0.127
1301240	1447	Granitized Gneiss	0.116	0	0.17	0.080	0.246	0.122
1301240	1457	Pegmatite	0.088	0	0.12	0.090	0.589	0.15

1301240	1457	Pegmatite	0.086	0	0.12	0.090	0.581	0.138
1301240	1457	Pegmatite	0.09	0	0.12	0.090	0.589	0.138
1301240	1457	Pegmatite	0.09	0	0.1	0.090	0.587	0.13
1301240	1457	Pegmatite	0.089	0	0.12	0.090	0.579	0.139
1301240	1466.8	Amphibolite	0.281	0	0.56	0.441	0.200	0.067
1301240	1466.8	Amphibolite	0.28	0	0.56	0.440	0.202	0.066
1301240	1466.8	Amphibolite	0.272	0	0.56	0.440	0.202	0.062
1301240	1466.8	Amphibolite	0.272	0	0.59	0.440	0.206	0.064
1301240	1466.8	Amphibolite	0.282	0	0.59	0.440	0.198	0.065
1301240	1470.7	Granitized Gneiss	0.125	0.13	0.25	0.126	0.976	0.245
1301240	1470.7	Granitized Gneiss	0.121	0.08	0.25	0.126	0.985	0.22
1301240	1470.7	Granitized Gneiss	0.119	0.17	0.25	0.127	0.982	0.227
1301240	1470.7	Granitized Gneiss	0.13	0.16	0.27	0.127	0.980	0.231
1301240	1470.7	Granitized Gneiss	0.123	0.16	0.25	0.129	0.978	0.242
1301240	1480	Amphibolite	0.203	0.16	0.34	0.416	0.347	0.111
1301240	1480	Amphibolite	0.2	0.15	0.34	0.414	0.354	0.108
1301240	1480	Amphibolite	0.198	0.14	0.34	0.413	0.354	0.108
1301240	1480	Amphibolite	0.199	0.14	0.32	0.414	0.356	0.11
1301240	1480	Amphibolite	0.216	0.14	0.32	0.413	0.358	0.108
1301240	1489.4	Pegmatite	0.06	0	0.07	0.052	0.901	0.17
1301240	1489.4	Pegmatite	0.056	0	0.07	0.052	0.900	0.178
1301240	1489.4	Pegmatite	0.058	0	0.07	0.052	0.900	0.18
1301240	1489.4	Pegmatite	0.067	0	0.1	0.053	0.905	0.183
1301240	1489.4	Pegmatite	0.068	0	0.07	0.054	0.903	0.179
1301240	1498	Pegmatite	0.059	0.05	0.12	0.115	0.255	0.033
1301240	1498	Pegmatite	0.054	0.04	0.15	0.115	0.252	0.035
1301240	1498	Pegmatite	0.067	0.04	0.15	0.115	0.257	0.033
1301240	1498	Pegmatite	0.071	0.04	0.15	0.116	0.255	0.036
1301240	1498	Pegmatite	0.075	0.04	0.15	0.116	0.259	0.035
1301240	1503	M1 Quartzite	0.021	0	0.1	0.090	0.158	0.044
1301240	1503	M1 Quartzite	0.026	0	0.12	0.090	0.158	0.046
1301240	1503	M1 Quartzite	0.037	0	0.1	0.089	0.164	0.045
1301240	1503	M1 Quartzite	0.057	0	0.1	0.090	0.160	0.046
1301240	1503	M1 Quartzite	0.039	0	0.12	0.090	0.162	0.045
1301240	1507	Pegmatite	0.087	0	0.15	0.151	0.259	0.034
1301240	1507	Pegmatite	0.083	0	0.15	0.150	0.255	0.037
1301240	1507	Pegmatite	0.085	0	0.15	0.152	0.261	0.034
1301240	1507	Pegmatite	0.08	0	0.17	0.152	0.255	0.034
1301240	1507	Pegmatite	0.083	0	0.17	0.151	0.259	0.035
1301240	1511.3	Skarn	0.177	0	0.34	0.262	0.698	0.055
1301240	1511.3	Skarn	0.186	0	0.37	0.262	0.699	0.055
1301240	1511.3	Skarn	0.181	0	0.37	0.261	0.699	0.052
1301240	1511.3	Skarn	0.271	0	0.34	0.261	0.696	0.055
1301240	1511.3	Skarn	0.259	0	0.37	0.262	0.698	0.054
1301240	1517	Skarn	0.267	0	0.37	0.472	0.698	0.161
1301240	1517	Skarn	0.269	0	0.59	0.475	0.421	0.172
1301240	1517	Skarn	0.258	0	0.61	0.474	0.414	0.175
1301240	1517	Skarn	0.267	0	0.61	0.476	0.408	0.171
1301240	1517	Skarn	0.135	0	0.61	0.478	0.419	0.162
1301240	1526.6	Skarn	0.13	0	0.34	0.479	0.322	0.241
1301240	1526.6	Skarn	0.134	0	0.37	0.478	0.328	0.232
1301240	1526.6	Skarn	0.126	0	0.34	0.482	0.326	0.232
1301240	1526.6	Skarn	0.131	0	0.34	0.479	0.328	0.236
1301240	1526.6	Skarn	0.125	0.04	0.34	0.200	0.318	0.241
1301240	1534.8	Skarn	0.208	0.03	0.47	0.202	0.673	0.12

1301240	1534.8	Skarn	0.207	0.02	0.47	0.200	0.677	0.117
1301240	1534.8	Skarn	0.201	0.02	0.44	0.200	0.684	0.118
1301240	1534.8	Skarn	0.207	0.02	0.47	0.201	0.679	0.118
1301240	1534.8	Skarn	0.202	0.01	0.47	0.201	0.686	0.121
1301240	1536	Pegmatite	0.066	0.01	0.34	0.295	0.158	0.171
1301240	1536	Pegmatite	0.066	0	0.39	0.297	0.162	0.176
1301240	1536	Pegmatite	0.066	0	0.39	0.295	0.158	0.178
1301240	1536	Pegmatite	0.07	0	0.39	0.295	0.160	0.172
1301240	1536	Pegmatite	0.076	0	0.39	0.293	0.154	0.172
1301240	1545.5	Pegmatite	0.074	0	0.29	0.097	0.151	0.118
1301240	1545.5	Pegmatite	0.073	0	0.29	0.097	0.149	0.117
1301240	1545.5	Pegmatite	0.074	0	0.29	0.098	0.145	0.118
1301240	1545.5	Pegmatite	0.075	0	0.29	0.097	0.149	0.118
1301240	1545.5	Pegmatite	0.077	0	0.29	0.098	0.149	0.12
1301240	1564.6	Pegmatite	0.077	0	0	0.035	0.042	0.075
1301240	1564.6	Pegmatite	0.074	0	0	0.036	0.044	0.077
1301240	1564.6	Pegmatite	0.073	0	0	0.036	0.046	0.076
1301240	1564.6	Pegmatite	0.071	0	0	0.036	0.046	0.08
1301240	1564.6	Pegmatite	0.824	0	0.02	0.036	0.044	0.083
1301240	1573.5	Pegmatite	1.389	0	0.22	0.060	0.101	0.027
1301240	1573.5	Pegmatite	0.884	0	0.25	0.060	0.099	0.028
1301240	1573.5	Pegmatite	1.002	0	0.22	0.060	0.099	0.028
1301240	1573.5	Pegmatite	0.779	0	0.22	0.059	0.099	0.027
1301240	1573.5	Pegmatite	0.646	0	0.22	0.059	0.101	0.033
1301240	1576	Pegmatite	4.272	0	6.9	40.903	41.118	2.67
1301240	1576	Pegmatite	5.498	0	9.43	40.379	41.059	2.96
1301240	1576	Pegmatite	5.03	0	9.58	40.287	41.034	2.75
1301240	1576	Pegmatite	4.335	0	9.6	40.011	41.011	3.05
1301240	1576	Pegmatite	4.393	0	9.62	39.856	41.004	3.39
1301240	1578	M. Pegmatite	16.189	4.52	41.9	48.686	135.145	13.7
1301240	1578	M. Pegmatite	18.746	4.56	51.6	48.788	135.071	11.1
1301240	1578	M. Pegmatite	18.777	4.59	51.9	48.718	134.987	12.5
1301240	1578	M. Pegmatite	14.398	4.61	52.1	48.699	134.928	13.3
1301240	1578	M. Pegmatite	16.729	4.63	52.6	48.646	134.877	13.4
1301240	1580	Schist	3.691	4.65	10	6.117	27.666	5.28
1301240	1580	Schist	3.95	2.01	10.8	6.114	27.639	4.8
1301240	1580	Schist	3.834	2	10.9	6.130	27.615	4.83
1301240	1580	Schist	3.963	1.99	11	6.123	27.590	5.07
1301240	1580	Schist	4.19	1.98	11	6.110	27.559	4.91
1301240	1581.8	M. Schist	5.983	27.81	10.6	16.206	32.845	4.61
1301240	1581.8	M. Schist	5.695	27.91	11	16.167	32.788	4.12
1301240	1581.8	M. Schist	6.223	27.94	11	16.269	32.756	4.04
1301240	1581.8	M. Schist	5.165	27.97	10.7	16.296	32.723	4.84
1301240	1581.8	M. Schist	5.307	27.99	10.8	16.256	32.668	4.51
1301240	1584	Schist	1.402	9.02	1.84	2.497	7.390	1.26
1301240	1584	Schist	1.731	9.02	1.87	2.521	7.375	1.08
1301240	1584	Schist	1.321	9.03	1.87	2.524	7.352	1.05
1301240	1584	Schist	1.635	9.04	1.87	2.520	7.343	1.36
1301240	1584	Schist	1.507	9.05	1.87	2.520	7.329	1.27
1301240	1585.6	Massive sulphide	27.785	44.88	119	70.544	206.093	26.5
1301240	1585.6	Massive sulphide	28.094	44.84	119	70.571	205.620	26.5
1301240	1585.6	Massive sulphide	28.05	44.83	119	70.593	205.357	27.2
1301240	1585.6	Massive sulphide	27.719	44.82	118	70.627	205.136	26.8
1301240	1585.6	Massive sulphide	27.693	44.83	117	70.658	204.936	26.7
1301240	1587.3	Massive sulphide	25.533	59.13	72.8	60.693	137.892	20.6

1301240	1587.3	Massive sulphide	24.325	59.25	72.9	59.883	137.705	20
1301240	1587.3	Massive sulphide	25.507	59.4	72.5	59.501	137.601	20.4
1301240	1587.3	Massive sulphide	24.727	59.58	72.1	59.054	137.484	20.9
1301240	1587.3	Massive sulphide	23.93	59.63	71.8	58.896	137.378	21.6
1301240	1588.2	M. Schist	0.86	1.27	1.94	0.976	5.263	0.901
1301240	1588.2	M. Schist	0.838	1.24	1.92	0.976	5.246	0.86
1301240	1588.2	M. Schist	0.839	1.24	1.94	0.977	5.236	0.885
1301240	1588.2	M. Schist	0.836	1.23	1.96	0.976	5.229	0.801
1301240	1588.2	M. Schist	0.84	1.23	1.94	0.976	5.221	0.927
1301240	1589.6	Sulphide Matrix	13.644	46.14	84	74.386	83.927	20.5
1301240	1589.6	Sulphide Matrix	14.474	45.69	83.4	74.776	83.818	19.2
1301240	1589.6	Sulphide Matrix	14.377	45.68	82.8	75.224	83.713	20.3
1301240	1589.6	Sulphide Matrix	14.469	45.67	82.7	75.696	83.635	20.8
1301240	1589.6	Sulphide Matrix	14.122	45.68	81.6	75.908	83.528	20
1301240	1596.6	Pegmatite	0.364	0.28	1.96	0.177	0.509	0.489
1301240	1596.6	Pegmatite	0.362	0.26	1.94	0.178	0.505	0.475
1301240	1596.6	Pegmatite	0.343	0.26	1.94	0.177	0.505	0.452
1301240	1596.6	Pegmatite	0.333	0.26	1.92	0.177	0.503	0.444
1301240	1596.6	Pegmatite	0.364	0.26	1.92	0.177	0.505	0.473
1301240	1605.7	Quartzite	0.126	0	0.02	0.040	0.313	0.45
1301240	1605.7	Quartzite	0.141	0	0.02	0.041	0.309	0.081
1301240	1605.7	Quartzite	0.12	0	0	0.041	0.305	0.099
1301240	1605.7	Quartzite	0.136	0	0	0.041	0.305	0.099
1301240	1605.7	Quartzite	0.122	0	0	0.041	0.301	0.098
1301240	1615.4	Quartzite	0.088	0	0.1	0.119	0.160	0.085
1301240	1615.4	Quartzite	0.088	0	0.1	0.119	0.174	0.04
1301240	1615.4	Quartzite	0.088	0	0.07	0.119	0.164	0.043
1301240	1615.4	Quartzite	0.086	0	0.07	0.119	0.164	0.047
1301240	1615.4	Quartzite	0.083	0	0.07	0.119	0.160	0.04
1301240	1624.6	Quartzite	0.102	0	0.15	0.156	0.286	0.044
1301240	1624.6	Quartzite	0.1	0	0.15	0.157	0.282	0.061
1301240	1624.6	Quartzite	0.107	0	0.15	0.156	0.288	0.052
1301240	1624.6	Quartzite	0.106	0	0.15	0.156	0.280	0.049
1301240	1624.6	Quartzite	0.1	0	0.15	0.156	0.288	0.055
1301240	1634	Quartzite	0.131	0	0.1	0.088	0.227	0.05
1301240	1634	Quartzite	0.151	0	0.1	0.088	0.221	0.074
1301240	1634	Quartzite	0.132	0	0.07	0.088	0.227	0.062
1301240	1634	Quartzite	0.129	0	0.1	0.088	0.225	0.074
1301240	1634	Quartzite	0.145	0	0.12	0.088	0.223	0.076

Table 36: Raw magnetic susceptibility measurements on KT-10 calibration sample

Calibration	RT1	KT10	GDD	MS2K	MS2C	SM30 B
Standard	(x10^-3SI)	(x10^-3SI)	(x10^-3SI)	(x10^-3SI)	(x10^-3SI)	(x10^-3SI)
KT10 cal sample	35.22	35.608	35.3	39.914	*	33.4
KT10 cal sample	35.4	35.584	35.2	39.617	*	33.3
KT10 cal sample	35.4	35.635	34.8	39.594	*	33.3
KT10 cal sample	35.37	35.638	34.7	39.053	*	33.3
KT10 cal sample	35.33	35.643	34.6	37.399	*	33.1
KT10 cal sample	35.29	35.64	35.2	37.811	*	33.2
KT10 cal sample	35.25	35.612	35.4	37.979	*	33.1
KT10 cal sample	35.21	35.702	35.4	37.932	*	33.4
KT10 cal sample	35.17	35.638	35.4	38.383	*	33.3
KT10 cal sample	35.16	35.682	35.4	37.632	*	33.2
KT10 cal sample	35.16	35.674	35.3	37.601	*	33.2
KT10 cal sample	35.13	35.712	35.3	38.037	*	33.4
KT10 cal sample	35.13	35.662	35.3	38.956	*	33.4
KT10 cal sample	35.1	35.702	35.3	38.993	*	33.4
KT10 cal sample	35.08	35.727	35.4	38.747	*	33.3
KT10 cal sample	35.07	35.669	35.4	38.380	*	33.3
KT10 cal sample	35.07	35.736	35.4	38.501	*	33.3
KT10 cal sample	35.06	35.73	35.4	37.765	*	33.3
KT10 cal sample	35.06	35.718	35.1	37.340	*	33.4
KT10 cal sample	35.05	35.748	34.8	38.067	*	33.3
KT10 cal sample	35.05	35.725	34.9	38.491	*	33.2
KT10 cal sample	34.93	35.757	35.1	36.391	*	33.3
KT10 cal sample	34.9	35.715	35.2	36.109	*	33.2
KT10 cal sample	34.86	35.717	34.9	37.977	*	33.3
KT10 cal sample	34.83	35.781	34.7	38.112	*	33.3
KT10 cal sample	34.84	35.735	35.1	37.974	*	33.3
KT10 cal sample	34.79	35.764	35.2	37.690	*	33.4

KT10 cal sample	34.74	35.787	35.3	37.413	*	33.4
KT10 cal sample	34.7	35.72	35.5	38.758	*	33.4
KT10 cal sample	34.64	35.735	35.5	38.677	*	33.2
KT10 cal sample	34.55	35.714	35.3	38.697	*	33.4
KT10 cal sample	34.42	35.687	35.3	38.561	*	33.3
KT10 cal sample	34.37	35.727	35.4	38.596	*	33.4
KT10 cal sample	34.34	35.771	35.3	38.768	*	33.4
KT10 cal sample	34.34	35.734	35.1	39.092	*	33.4
KT10 cal sample	34.42	35.781	34.9	38.245	*	33.4
Average readings	**34.956**	**35.703**	**35.189**	**38.257**	*****	**33.311**

Table 37: Raw magnetic susceptibility data on MS2C calibration sample

Calibration	RT1	KT10	GDD	MS2K	MS2C	SM30 B
Standard	(x10^-3SI)	(x10^-3SI)	(x10^-3SI)	(x10^-3SI)	(x10^-3SI)	(x10?^-3SI)
MS2C cal sample	3.83	4.401	4.15	4.196	11.039	4.24
MS2C cal sample	3.83	4.393	4.12	4.195	11.035	4.24
MS2C cal sample	3.79	4.353	4.1	4.196	11.040	4.25
MS2C cal sample	3.78	4.374	4.07	4.190	11.038	4.25
MS2C cal sample	3.77	4.31	4.05	4.187	11.035	4.23
MS2C cal sample	3.73	4.397	4.05	4.186	11.036	4.24
MS2C cal sample	3.70	4.329	4.07	4.186	11.035	4.22
MS2C cal sample	3.70	4.313	4.04	4.186	11.036	4.17
MS2C cal sample	3.70	4.108	4.02	4.189	11.038	4.22
MS2C cal sample	3.71	4.405	3.97	4.181	11.040	4.21
MS2C cal sample	3.70	4.354	3.96	4.172	11.036	4.2
MS2C cal sample	3.76	3.97	3.99	4.171	11.036	4.2
MS2C cal sample	3.76	4.38	3.97	4.166	11.035	4.02
MS2C cal sample	3.76	4.174	3.96	4.164	11.035	4.23
MS2C cal sample	3.75	4.345	3.94	4.159	11.037	4.24
MS2C cal sample	3.74	4.291	3.94	4.151	11.035	4.15
MS2C cal sample	3.73	4.418	3.92	4.139	11.036	4.24
MS2C cal sample	3.73	4.396	3.91	4.129	11.039	4.24
MS2C cal sample	3.74	4.36	3.91	4.121	11.035	4.22
MS2C cal sample	3.74	4.346	3.91	4.122	11.037	4.22
MS2C cal sample	3.72	4.408	3.92	4.136	11.035	4.24
MS2C cal sample	3.71	4.376	3.94	4.122	11.039	4.14
MS2C cal sample	3.70	4.408	3.94	4.111	11.039	4.24
MS2C cal sample	3.70	4.401	3.99	4.077	11.039	4.22
MS2C cal sample	3.71	4.343	3.97	4.151	11.039	4.24
MS2C cal sample	3.72	4.398	3.96	4.070	11.034	4.18
MS2C cal sample	3.70	4.039	3.94	4.083	11.036	4.24
MS2C cal sample	3.69	4.391	3.94	4.053	11.038	4.22
MS2C cal sample	3.69	3.848	3.94	4.097	11.039	4.22
MS2C cal sample	3.69	4.325	3.94	4.107	11.039	4.24
MS2C cal sample	3.69	4.411	3.94	4.078	11.045	4.24
MS2C cal sample	3.69	4.332	3.92	4.067	11.046	4.24
MS2C cal sample	3.68	4.4	3.94	4.064	11.045	4.22
MS2C cal sample	3.69	4.393	3.92	4.027	11.041	4.24
MS2C cal sample	3.70	4.406	3.88	4.045	11.046	4.24
Average readings	**3.727**	**4.323**	**3.975**	**4.134**	**11.038**	**4.217**

Table 38: Raw magnetic susceptibility measurements on NQ whole core - semi-massive sulfide

Sample ID	Depth	Lithology	RT1	KT10	GDD	MS2K	MS2C	SM30 B
	(ft)		(x10^-3SI)	(x10^-3SI)	(x10^-3SI)	(x10^-3SI)	(x10^-3SI)	(x10^-3SI)
NQ Whole core	6122.5	Sumx	73.76	47.69	87	97.87	136.5	44.8
NQ Whole core	6122.5	Sumx	73.9	47.77	87.5	98	136.39	44.7
NQ Whole core	6122.5	Sumx	74.03	47.14	87.5	98.05	136.36	44.6
NQ Whole core	6122.5	Sumx	74.04	47.76	87.1	98.06	136.34	44.6
NQ Whole core	6122.5	Sumx	74.05	47.41	87.3	98.15	136.32	44.5
NQ Whole core	6122.5	Sumx	74.07	48.01	87.6	98.16	136.3	44.5
NQ Whole core	6122.5	Sumx	74.1	46.69	87.9	98.24	136.29	44.6
NQ Whole core	6122.5	Sumx	74.1	46.55	88.8	98.25	136.27	44.6
NQ Whole core	6122.5	Sumx	74.07	47.87	90.5	98.01	136.26	44.6
NQ Whole core	6122.5	Sumx	74.05	45.77	92.9	98.22	136.24	44.5
NQ Whole core	6122.5	Sumx	74.05	47.24	94.7	98.24	136.23	44.5
NQ Whole core	6122.5	Sumx	74.08	47.8	95.2	98.16	136.21	44.5
NQ Whole core	6122.5	Sumx	74.1	47.78	96.5	98.21	136.2	44.5
NQ Whole core	6122.5	Sumx	74.11	47.12	98	98.26	136.19	44.4
NQ Whole core	6122.5	Sumx	74.13	47.95	99.5	98.26	136.17	44.4
NQ Whole core	6122.5	Sumx	74.13	47.75	99.8	98.36	136.16	44.4
NQ Whole core	6122.5	Sumx	74.16	47.67	99.5	98.31	136.15	44.4
NQ Whole core	6122.5	Sumx	74.16	47.72	99.3	98.35	136.14	44.3
NQ Whole core	6122.5	Sumx	74.15	47.71	98.4	98.23	136.13	44.3
NQ Whole core	6122.5	Sumx	74.14	47.36	97.8	97.58	136.13	44.3
NQ Whole core	6122.5	Sumx	74.14	48.02	97.8	97.85	136.12	44
NQ Whole core	6122.5	Sumx	74.13	45.78	98	97.88	136.1	44.1
NQ Whole core	6122.5	Sumx	74.12	48.06	98.1	97.97	136.09	44.2
NQ Whole core	6122.5	Sumx	74.14	47.82	99.3	97.65	136.09	44.2
NQ Whole core	6122.5	Sumx	74.16	47.56	101	97.98	136.08	44.2
NQ Whole core	6122.5	Sumx	74.17	47.58	102	97.88	136.07	44.2
NQ Whole core	6122.5	Sumx	74.17	47.99	102	97.99	136.07	44.2
NQ Whole core	6122.5	Sumx	74.21	47.76	102	97.9	136.06	44.3
NQ Whole core	6122.5	Sumx	74.22	47.63	102	97.87	136.05	44.3
NQ Whole core	6122.5	Sumx	74.22	47.91	102	98.03	136.05	44.3
NQ Whole core	6122.5	Sumx	74.22	47.81	101	98.11	136.04	44.3
NQ Whole core	6122.5	Sumx	74.22	47.91	99.3	98.1	136.03	44.3
NQ Whole core	6122.5	Sumx	74.22	47.66	97.7	98.14	136.03	44.3
NQ Whole core	6122.5	Sumx	74.23	47.49	105	98.16	136.02	44.3
NQ Whole core	6122.5	Sumx	74.23	47.66	105	98.19	136.02	44.2
NQ Whole core	6122.5	Sumx	74.23	47.91	104	98.18	136.01	44.3
NQ Whole core	6122.5	Sumx	74.24	47.39	104	98.25	136	44.4
NQ Whole core	6122.5	Sumx	74.24	47.6	104	98.25	136	44.4
NQ Whole core	6122.5	Sumx	74.25	47.84	104	98.25	135.99	44.4
NQ Whole core	6122.5	Sumx	74.26	47.62	104	98.37	135.99	44.4
NQ Whole core	6122.5	Sumx	74.26	47.82	104	98.34	135.98	43.5
NQ Whole core	6122.5	Sumx	74.26	47.7	104	98.36	135.98	43.7
NQ Whole core	6122.5	Sumx	74.25	47.58	105	98.32	135.96	43.7
NQ Whole core	6122.5	Sumx	74.25	47.63	105	98.34	135.96	43.9
NQ Whole core	6122.5	Sumx	74.24	47.26	105	98.29	135.96	43.8
NQ Whole core	6122.5	Sumx	74.24	47.56	105	98.31	135.95	44

NQ Whole core	6122.5	Sumx	74.23	47.6	105	98.38	135.95	44.1
NQ Whole core	6122.5	Sumx	74.22	47.5	105	98.31	135.94	44.2
NQ Whole core	6122.5	Sumx	74.22	47.05	105	98.31	135.94	44.3
NQ Whole core	6122.5	Sumx	74.22	47.61	105	98.27	135.93	44.3
NQ Whole core	6122.5	Sumx	74.22	47.33	105	98.27	135.93	44.3
NQ Whole core	6122.5	Sumx	74.23	47.35	105	98.31	135.93	44.3
NQ Whole core	6122.5	Sumx	74.23	47.43	104	98.33	135.93	44.3
NQ Whole core	6122.5	Sumx	74.23	47.45	104	98.35	135.92	44.3
NQ Whole core	6122.5	Sumx	74.22	47.55	104	98.35	135.92	44.2
NQ Whole core	6122.5	Sumx	74.21	47.55	104	98.27	135.92	44.3
NQ Whole core	6122.5	Sumx	74.22	47.52	104	98.17	135.91	44.3
NQ Whole core	6122.5	Sumx	74.21	46.96	105	97.98	135.91	44.3
NQ Whole core	6122.5	Sumx	74.21	47.59	105	98.25	135.9	44.3
NQ Whole core	6122.5	Sumx	74.21	47.54	105	98.27	135.9	44.3
NQ Whole core	6122.5	Sumx	74.19	47.56	105	98.5	135.89	44
NQ Whole core	6122.5	Sumx	74.18	47.48	105	98.95	135.89	44.1
NQ Whole core	6122.5	Sumx	74.16	47.57	105	98.9	135.88	44.1
NQ Whole core	6122.5	Sumx	74.16	47.5	105	97.23	135.88	44.1
NQ Whole core	6122.5	Sumx	74.16	47.31	105	97.39	135.87	44.2
NQ Whole core	6122.5	Sumx	74.18	47.5	105	97.32	135.87	44.2
NQ Whole core	6122.5	Sumx	74.17	47.47	105	97.3	135.87	44.2
NQ Whole core	6122.5	Sumx	74.18	47.53	105	97.27	135.87	44.2
NQ Whole core	6122.5	Sumx	74.18	47.63	105	97.26	135.86	44.2
NQ Whole core	6122.5	Sumx	74.18	47.59	105	97.29	135.86	44.3
NQ Whole core	6122.5	Sumx	74.17	47.58	104	97.32	135.85	44.2
NQ Whole core	6122.5	Sumx	74.17	47.68	104	97.41	135.85	44.2
NQ Whole core	6122.5	Sumx	74.17	47.56	104	97.35	135.84	44.3
NQ Whole core	6122.5	Sumx	74.18	47.13	104	97.27	135.84	44.3
NQ Whole core	6122.5	Sumx	74.19	47.44	103	97.3	135.83	44.3
NQ Whole core	6122.5	Sumx	74.21	47.49	102	97.32	135.83	44.3
NQ Whole core	6122.5	Sumx	74.22	46.15	101	97.21	135.82	44.3
NQ Whole core	6122.5	Sumx	74.22	47.34	102	97.05	135.82	44.3
NQ Whole core	6122.5	Sumx	74.22	47.4	102	97.15	135.82	44.2
NQ Whole core	6122.5	Sumx	74.2	47.27	102	97.18	135.81	
NQ Whole core	6122.5	Sumx	74.18	47.42	102	97.17	135.81	
NQ Whole core	6122.5	Sumx	74.17	47.45	102	97.15	135.81	
NQ Whole core	6122.5	Sumx	74.16	47.34	102	97.09	135.8	
NQ Whole core	6122.5	Sumx	74.15	47.47	102	97.13	135.8	
NQ Whole core	6122.5	Sumx	74.15	47.29	102	97.18	135.8	
NQ Whole core	6122.5	Sumx	74.15	47.49	105	97.22	135.79	
NQ Whole core	6122.5	Sumx	74.15	47.16	105	97.18	135.79	
NQ Whole core	6122.5	Sumx	74.15	47.47	105	97.17	135.79	
NQ Whole core	6122.5	Sumx	74.17	47.39	105	97.19	135.79	
NQ Whole core	6122.5	Sumx	74.18	47.19	105	97.23	135.78	
NQ Whole core	6122.5	Sumx	74.23	47.39	105	97.27	135.78	
NQ Whole core	6122.5	Sumx	74.23	47.39	105	97.3	135.78	
NQ Whole core	6122.5	Sumx	74.26	47.35	105	97.29	135.77	
NQ Whole core	6122.5	Sumx	74.27	46.89	105	97.48	135.77	
NQ Whole core	6122.5	Sumx	74.3	47.26	106	97.52	135.76	
NQ Whole core	6122.5	Sumx	74.31	47.27	107	97.59	135.76	

NQ Whole core	6122.5	Sumx	74.33	47.09	108	97.57	135.76	
NQ Whole core	6122.5	Sumx	74.34	47.4	109	97.55	135.76	
NQ Whole core	6122.5	Sumx	74.38	47.4	109	97.5	135.76	
NQ Whole core	6122.5	Sumx	74.43	47.09	107	97.54	135.76	
NQ Whole core	6122.5	Sumx	74.44	45.02	106	97.61	135.75	
NQ Whole core	6122.5	Sumx	74.46	46.54	105	97.58	135.75	
NQ Whole core	6122.5	Sumx	74.48	47.51	105	97.66	135.74	
NQ Whole core	6122.5	Sumx	74.5	46.96	105	97.66	135.75	
NQ Whole core	6122.5	Sumx	74.51	46.91	105	97.67	135.74	
NQ Whole core	6122.5	Sumx	74.54	47.35	105	97.62	135.74	
NQ Whole core	6122.5	Sumx	74.55	47.18	105	97.68	135.74	
NQ Whole core	6122.5	Sumx	74.56	47.38	106	97.69	135.73	
NQ Whole core	6122.5	Sumx	74.56	45.88	106	97.76	135.73	
NQ Whole core	6122.5	Sumx	74.56	47.34	106	97.72	135.73	
NQ Whole core	6122.5	Sumx	74.56	47.43	106	97.68	135.72	
NQ Whole core	6122.5	Sumx	74.59	47.25	106	97.91	135.73	
NQ Whole core	6122.5	Sumx	74.62	45.82	107	97.7	135.72	
NQ Whole core	6122.5	Sumx	74.66	47.1	107	97.77	135.72	
NQ Whole core	6122.5	Sumx	74.67	47.12	107	97.77	135.72	
NQ Whole core	6122.5	Sumx	74.66	47.16	107	97.74	135.72	
NQ Whole core	6122.5	Sumx	74.64	47.12	107	97.8	135.72	
NQ Whole core	6122.5	Sumx	74.67	47.3	107	97.81	135.71	
NQ Whole core	6122.5	Sumx		47.21	106	97.87	135.71	
NQ Whole core	6122.5	Sumx		47.2	106	97.92	135.71	
NQ Whole core	6122.5	Sumx		47.31	98.1	97.93	135.71	
NQ Whole core	6122.5	Sumx		47.33	108	97.91	135.69	
NQ Whole core	6122.5	Sumx		47.04	108	98	135.7	
NQ Whole core	6122.5	Sumx		47.33	108	98	135.7	
NQ Whole core	6122.5	Sumx			107	97.99	135.69	
NQ Whole core	6122.5	Sumx			107	98.14	135.69	
NQ Whole core	6122.5	Sumx			99.9	98.05	135.69	
NQ Whole core	6122.5	Sumx			100	98.47	135.69	
NQ Whole core	6122.5	Sumx			99.9	98.12	135.69	
NQ Whole core	6122.5	Sumx			98.5	98.02	135.68	
Average readings			74.24	47.37	102.47	97.86	135.91	44.27

Table 39: Raw magnetic susceptibility data measured on NQ half core sample - semi-massive sulfide

Sample ID	Depth	Lithology	RT1	KT10	GDD	MS2K	MS2C	SM30 B
NQ Half core	6122.5	Sumx	79.35	56.5	102.000	105.042	138.695	61.8
NQ Half core	6122.5	Sumx	77.09	57.016	102.000	105.130	138.66	61.2
NQ Half core	6122.5	Sumx	76.43	56.837	101.000	105.141	138.632	60.7
NQ Half core	6122.5	Sumx	75.68	56.736	101.000	105.169	138.607	59.3
NQ Half core	6122.5	Sumx	74.91	57.479	101.000	105.177	138.584	61.7
NQ Half core	6122.5	Sumx	74.8	58.179	101.000	105.184	138.563	61.3
NQ Half core	6122.5	Sumx	75.11	56.666	100.000	105.200	138.544	60.7
NQ Half core	6122.5	Sumx	75.67	56.75	99.600	105.013	138.531	60.2
NQ Half core	6122.5	Sumx	75.8	56.546	98.000	104.846	138.515	61.4
NQ Half core	6122.5	Sumx	76.05	57.764	98.200	104.832	138.502	60
NQ Half core	6122.5	Sumx	76.15	55.978	102.000	104.893	138.487	57.7
NQ Half core	6122.5	Sumx	76.1	58.008	102.000	104.849	138.477	60.1
NQ Half core	6122.5	Sumx	76.02	58.128	102.000	104.560	138.47	60.1
NQ Half core	6122.5	Sumx	75.86	58.522	102.000	104.355	138.456	58.7
NQ Half core	6122.5	Sumx	76.01	58.185	102.000	104.620	138.445	59.3
NQ Half core	6122.5	Sumx	76.33	56.565	102.000	104.557	138.437	59.2
NQ Half core	6122.5	Sumx	77.07	57.603	102.000	104.579	138.437	57.5
NQ Half core	6122.5	Sumx	77.43	58.137	101.000	104.712	138.424	57.7
NQ Half core	6122.5	Sumx	77.54	57.434	100.000	104.772	138.416	57.5
NQ Half core	6122.5	Sumx	77.38	57.555	101.000	104.785	138.411	54.9
NQ Half core	6122.5	Sumx	77.06	58.16	102.000	104.784	138.399	58.1
NQ Half core	6122.5	Sumx	77	57.678	102.000	104.746	138.39	54.9
NQ Half core	6122.5	Sumx	77.03	57.482	102.000	104.696	138.386	57.9
NQ Half core	6122.5	Sumx	77.1	56.497	102.000	104.729	138.384	57.2
NQ Half core	6122.5	Sumx	77.88	55.471	102.000	104.708	138.38	56.8
NQ Half core	6122.5	Sumx	77.87	56.279	102.000	104.702	138.369	55.2
NQ Half core	6122.5	Sumx	77.98	57.396	102.000	104.560	138.369	56.3
NQ Half core	6122.5	Sumx	77.99	56.616	102.000	104.559	138.363	54.3
NQ Half core	6122.5	Sumx	78	56.769	102.000	104.509	138.357	55.2
NQ Half core	6122.5	Sumx	78	56.235	102.000	104.654	138.348	57.9
NQ Half core	6122.5	Sumx	77.97	56.363	102.000	104.635	138.342	53.9
NQ Half core	6122.5	Sumx	77.98	55.661	102.000	104.479	138.346	55.3
NQ Half core	6122.5	Sumx	78	56.689	102.000	104.440	138.342	54.6
NQ Half core	6122.5	Sumx	78.01	56.149	102.000	104.559	138.327	55.6
NQ Half core	6122.5	Sumx	78.03	56.208	101.000	104.434	138.334	56
NQ Half core	6122.5	Sumx	78.07	55.474	101.000	103.395	138.323	56.1
NQ Half core	6122.5	Sumx	78.1	55.865	102.000	100.623	138.319	56.6
NQ Half core	6122.5	Sumx	78.12	55.399	102.000	103.827	138.319	57.3
NQ Half core	6122.5	Sumx	78.12	54.252	102.000	103.720	138.306	53.4
NQ Half core	6122.5	Sumx	78.12	58.006	102.000	103.738	138.306	55.3
NQ Half core	6122.5	Sumx	78.13	57.615	102.000	103.546	138.3	55.8
NQ Half core	6122.5	Sumx	78.11	54.824	102.000	103.660	138.302	56
NQ Half core	6122.5	Sumx	78.11	57.955	102.000	103.706	138.29	55.3
NQ Half core	6122.5	Sumx	78.12	57.23	102.000	103.064	138.292	55.4
NQ Half core	6122.5	Sumx	78.12	56.339	102.000	102.371	138.289	54.5
NQ Half core	6122.5	Sumx	78.12	54.44	102.000	102.552	138.281	56.9
NQ Half core	6122.5	Sumx	78.13	51.73	102.000	100.267	138.281	55.1
NQ Half core	6122.5	Sumx	78.14	55.161	102.000	99.293	138.275	52.9
NQ Half core	6122.5	Sumx	78.13	55.176	102.000	96.944	138.275	55.1

NQ Half core	6122.5	Sumx	78.13	56.481	102.000	107.131	138.268	53.5
NQ Half core	6122.5	Sumx	78.12	55.853	102.000	106.966	138.268	53.6
NQ Half core	6122.5	Sumx	78.11	52.829	102.000	106.765	138.262	56.4
NQ Half core	6122.5	Sumx	78.09	53.991	102.000	106.719	138.262	52.5
NQ Half core	6122.5	Sumx	78.08	57.637	101.000	106.615	138.254	51.4
NQ Half core	6122.5	Sumx	78.07	57.644	101.000	106.428	138.25	56.4
NQ Half core	6122.5	Sumx	78.06	58.044	101.000	106.209	138.252	53.7
NQ Half core	6122.5	Sumx	78.02	55.674	101.000	105.968	138.254	54.6
NQ Half core	6122.5	Sumx	77.91	55.661	102.000	105.661	138.247	53.5
NQ Half core	6122.5	Sumx	77.85	57.788	101.000	105.385	138.241	53.8
NQ Half core	6122.5	Sumx	77.85	55.878	101.000	105.664	138.237	53
NQ Half core	6122.5	Sumx	77.85	55.314	102.000	106.468	138.241	55.5
NQ Half core	6122.5	Sumx	77.95	54.694	102.000	106.486	138.231	55.1
NQ Half core	6122.5	Sumx	77.99	55.434	102.000	106.540	138.228	55.4
NQ Half core	6122.5	Sumx	77.98	54.532	102.000	106.547	138.224	58.4
NQ Half core	6122.5	Sumx	78	54.709	102.000	106.550	138.233	58.4
NQ Half core	6122.5	Sumx	77.99	54.99	102.000	106.490	138.224	57.7
NQ Half core	6122.5	Sumx	78.01	51.21	102.000	106.411	138.22	58.2
NQ Half core	6122.5	Sumx	78.03	52.501	102.000	106.414	138.222	57.3
NQ Half core	6122.5	Sumx	78.07	56.989	102.000	106.406	138.222	51.1
NQ Half core	6122.5	Sumx	78.11	58.138	102.000	106.341	138.212	59.6
NQ Half core	6122.5	Sumx	78.12	57.056	101.000	106.226	138.22	60.3
NQ Half core	6122.5	Sumx	78.14	55.52	101.000	106.278	138.212	58.7
NQ Half core	6122.5	Sumx	78.12	56.575	102.000	106.244	138.21	59.7
NQ Half core	6122.5	Sumx	78.1	57.142	102.000	106.122	138.207	59.7
NQ Half core	6122.5	Sumx	78.1	57.703	102.000	106.157	138.205	59.1
NQ Half core	6122.5	Sumx	78.09	58.129	102.000	106.165	138.199	56.9
NQ Half core	6122.5	Sumx	78.13	56.44	102.000	106.153	138.201	58.5
NQ Half core	6122.5	Sumx	78.16	56.74	102.000	106.087	138.203	57.6
NQ Half core	6122.5	Sumx	78.2	56.957	102.000	105.949	138.201	59
NQ Half core	6122.5	Sumx	78.03	56.952	102.000	105.840	138.203	57
NQ Half core	6122.5	Sumx	78.03	57.968	102.000	105.917	138.195	52.6
NQ Half core	6122.5	Sumx	78.07	57.865	101.000	106.063	138.193	58.4
NQ Half core	6122.5	Sumx	77.93	57.711	103.000	106.055	138.189	59.8
NQ Half core	6122.5	Sumx	77.83	57.998	103.000	106.020	138.195	58.5
NQ Half core	6122.5	Sumx	77.83	58.021	103.000	105.973	138.186	58.8
NQ Half core	6122.5	Sumx	77.81	58.073	103.000	105.908	138.184	57.7
NQ Half core	6122.5	Sumx	77.85	57.662	102.000	105.984	138.186	56.9
NQ Half core	6122.5	Sumx	78.01	57.927	102.000	105.907	138.186	59.4
NQ Half core	6122.5	Sumx	78.05	57.143	103.000	104.661	138.182	58.7
NQ Half core	6122.5	Sumx	78.06	57.848	102.000	104.973	138.182	59.4
NQ Half core	6122.5	Sumx	78.02	57.931	102.000	105.126	138.182	59
NQ Half core	6122.5	Sumx	78.02	56.961	102.000	102.521	138.176	59.9
NQ Half core	6122.5	Sumx	78.02	57.053	102.000	105.606	138.176	59.6
NQ Half core	6122.5	Sumx	78.12	57.524	102.000	105.623	138.172	58.9
NQ Half core	6122.5	Sumx	78.12	56.911	102.000	104.013	138.17	59.8
NQ Half core	6122.5	Sumx	78.13	57.26	102.000	105.409	138.172	60.1
NQ Half core	6122.5	Sumx	78.11	55.736	102.000	105.390	138.168	60
NQ Half core	6122.5	Sumx	78.09	57.076	102.000	103.041	138.163	58.2
NQ Half core	6122.5	Sumx	78.08	53.963	102.000	105.590	138.167	57.7
NQ Half core	6122.5	Sumx	78.06	57.936	102.000	105.474	138.163	58.3
NQ Half core	6122.5	Sumx	78.07	57.51	102.000	105.493	138.165	58.6
NQ Half core	6122.5	Sumx	78.08	57.31	102.000	105.549	138.157	58.4

NQ Half core	6122.5	Sumx	78.07	57.192	102.000	105.570	138.161	52.2
NQ Half core	6122.5	Sumx	78.05	53.743	102.000	105.563	138.159	55.1
NQ Half core	6122.5	Sumx	78.02	56.753	102.000	105.588	138.155	58.8
NQ Half core	6122.5	Sumx	78	55.651	102.000	105.588	138.151	59.2
NQ Half core	6122.5	Sumx	78.01	55.422	102.000	105.581	138.153	58.4
NQ Half core	6122.5	Sumx	78.01	55.853	102.000	105.625	138.146	59.8
NQ Half core	6122.5	Sumx	78.06	56.831	102.000	105.635	138.148	59.9
NQ Half core	6122.5	Sumx	78.01	56.85	102.000	105.649	138.146	59.8
NQ Half core	6122.5	Sumx	77.98	56.781	102.000	105.656	138.144	57.6
NQ Half core	6122.5	Sumx	77.97	57.606	102.000	105.684	138.149	60.1
NQ Half core	6122.5	Sumx	77.96	56.94	102.000	105.686	138.142	59.7
NQ Half core	6122.5	Sumx	78	57.257	101.000	105.676	138.14	60.1
NQ Half core	6122.5	Sumx	78.01	55.78	101.000	105.780	138.144	59.6
NQ Half core	6122.5	Sumx	77.96	58.036	102.000	105.813	138.142	59.9
NQ Half core	6122.5	Sumx	77.53	56.355	102.000	105.805	138.14	58.1
NQ Half core	6122.5	Sumx	77.3	56.763	102.000	105.801	138.138	60.4
NQ Half core	6122.5	Sumx	77.05	56.083	102.000	105.815	138.14	60.1
NQ Half core	6122.5	Sumx	76.88	55.636	102.000	105.812	138.138	59.9
NQ Half core	6122.5	Sumx	76.83	53.692	101.000	105.827	138.136	59.4
NQ Half core	6122.5	Sumx	76.43	56.942	101.000	105.756	138.132	59.8
NQ Half core	6122.5	Sumx	76.12	54.679	101.000	105.422	138.13	59.6
NQ Half core	6122.5	Sumx	76.11	57.331	100.000	105.522	138.132	59.8
NQ Half core	6122.5	Sumx	76.37	57.931	102.000	104.529	138.13	58.4
NQ Half core	6122.5	Sumx	76.65	56.213	101.000	104.109	138.132	
NQ Half core	6122.5	Sumx	76.73	54.812	102.000	105.809	138.13	
NQ Half core	6122.5	Sumx	76.78	53.195	102.000	105.703	138.125	
NQ Half core	6122.5	Sumx		54.174	102.000	103.643	138.13	
NQ Half core	6122.5	Sumx		56.582	101.000	105.758	138.123	
Average readings			**77.61766**	**56.48755**	**101.729**	**105.103**	**138.268**	**57.5672**

Table 40: Raw magnetic susceptibility measurements on whole NQ core - schist

Sample ID	Depth	Lithology	RT1	KT10	GDD	MS2K	MS2C	SM30 B
	(ft)		(x10^-3SI)	(x10^-3SI)	(x10^-3SI)	(x10^-3SI)	(x10^-3SI)	(x10^-3SI)
NQ Whole core	6105.6	P2 Schist	0	0.305	0.4	0.739	0.500	0.273
NQ Whole core	6105.6	P2 Schist	0	0.26	0.44	0.741	0.500	0.273
NQ Whole core	6105.6	P2 Schist	0	0.304	0.44	0.715	0.498	0.273
NQ Whole core	6105.6	P2 Schist	0	0.327	0.44	0.695	0.500	0.273
NQ Whole core	6105.6	P2 Schist	0	0.28	0.44	0.694	0.499	0.272
NQ Whole core	6105.6	P2 Schist	0	0.318	0.42	0.695	0.498	0.273
NQ Whole core	6105.6	P2 Schist	0	0.291	0.4	0.695	0.499	0.273
NQ Whole core	6105.6	P2 Schist	0	0.292	0.44	0.696	0.500	0.273
NQ Whole core	6105.6	P2 Schist	0	0.323	0.47	0.698	0.499	0.273
NQ Whole core	6105.6	P2 Schist	0	0.32	0.47	0.714	0.499	0.273
NQ Whole core	6105.6	P2 Schist	0	0.292	0.44	0.712	0.500	0.274
NQ Whole core	6105.6	P2 Schist	0	0.349	0.42	0.722	0.498	0.273
NQ Whole core	6105.6	P2 Schist	0	0.28	0.44	0.724	0.498	0.272
NQ Whole core	6105.6	P2 Schist	0	0.353	0.47	0.729	0.499	0.273
NQ Whole core	6105.6	P2 Schist	0	0.266	0.47	0.731	0.498	0.274
NQ Whole core	6105.6	P2 Schist	0	0.287	0.49	0.748	0.497	0.273
NQ Whole core	6105.6	P2 Schist	0	0.329	0.49	0.750	0.499	0.273
NQ Whole core	6105.6	P2 Schist	0	0.286	0.47	0.752	0.497	0.273
NQ Whole core	6105.6	P2 Schist	0	0.309	0.51	0.753	0.498	0.273
NQ Whole core	6105.6	P2 Schist	0	0.346	0.51	0.756	0.500	0.272
NQ Whole core	6105.6	P2 Schist	0	0.398	0.53	0.761	0.498	0.263
NQ Whole core	6105.6	P2 Schist	0	0.321	0.56	0.763	0.499	0.263
NQ Whole core	6105.6	P2 Schist	0	0.348	0.51	0.764	0.500	0.262
NQ Whole core	6105.6	P2 Schist	0	0.301	0.56	0.763	0.498	0.262
NQ Whole core	6105.6	P2 Schist	0	0.347	0.56	0.763	0.498	0.264
NQ Whole core	6105.6	P2 Schist	0	0.332	0.51	0.763	0.498	0.263
NQ Whole core	6105.6	P2 Schist	0	0.282	0.53	0.759	0.498	0.263
NQ Whole core	6105.6	P2 Schist	0	0.344	0.53	0.761	0.498	0.263
NQ Whole core	6105.6	P2 Schist	0	0.309	0.53	0.762	0.498	0.264
NQ Whole core	6105.6	P2 Schist	0	0.303	0.56	0.763	0.499	0.264
NQ Whole core	6105.6	P2 Schist	0	0.354	0.58	0.760	0.498	0.263
NQ Whole core	6105.6	P2 Schist	0	0.442	0.58	0.760	0.499	0.263
NQ Whole core	6105.6	P2 Schist	0	0.3	0.58	0.760	0.500	0.263
NQ Whole core	6105.6	P2 Schist	0	0.289	0.6	0.760	0.500	0.263
NQ Whole core	6105.6	P2 Schist	0	0.305	0.6	0.762	0.495	0.261
NQ Whole core	6105.6	P2 Schist	0	0.277	0.6	0.761	0.499	0.261
NQ Whole core	6105.6	P2 Schist	0	0.344	0.6	0.757	0.497	0.26
NQ Whole core	6105.6	P2 Schist	0	0.312	0.58	0.757	0.500	0.26
NQ Whole core	6105.6	P2 Schist	0	0.268	0.58	0.761	0.496	0.259
NQ Whole core	6105.6	P2 Schist	0	0.305	0.62	0.759	0.499	0.26
NQ Whole core	6105.6	P2 Schist	0	0.34	0.62	0.760	0.498	0.259
NQ Whole core	6105.6	P2 Schist	0	0.285	0.6	0.757	0.495	0.258
NQ Whole core	6105.6	P2 Schist	0	0.314	0.6	0.763	0.497	0.257

NQ Whole core	6105.6	P2 Schist	0	0.337	0.64	0.761	0.497	0.256
NQ Whole core	6105.6	P2 Schist	0	0.293	0.64	0.767	0.498	0.255
NQ Whole core	6105.6	P2 Schist	0	0.344	0.62	0.764	0.498	0.252
NQ Whole core	6105.6	P2 Schist	0	0.328	0.64	0.768	0.499	0.25
NQ Whole core	6105.6	P2 Schist	0	0.381	0.67	0.763	0.496	0.249
NQ Whole core	6105.6	P2 Schist	0	0.374	0.67	0.768	0.496	0.25
NQ Whole core	6105.6	P2 Schist	0	0.31	0.67	0.764	0.498	0.249
NQ Whole core	6105.6	P2 Schist	0	0.342	0.67	0.770	0.499	0.249
NQ Whole core	6105.6	P2 Schist	0	0.335	0.69	0.770	0.498	0.25
NQ Whole core	6105.6	P2 Schist	0	0.304	0.69	0.768	0.498	0.256
NQ Whole core	6105.6	P2 Schist	0	0.317	0.69	0.768	0.497	0.256
NQ Whole core	6105.6	P2 Schist	0	0.372	0.69	0.763	0.497	0.254
NQ Whole core	6105.6	P2 Schist	0	0.294	0.71	0.769	0.498	0.254
NQ Whole core	6105.6	P2 Schist	0	0.382	0.71	0.761	0.499	0.253
NQ Whole core	6105.6	P2 Schist	0	0.357	0.71	0.765	0.499	0.254
NQ Whole core	6105.6	P2 Schist	0	0.351	0.71	0.759	0.497	0.252
NQ Whole core	6105.6	P2 Schist	0	0.312	0.71	0.769	0.498	0.255
NQ Whole core	6105.6	P2 Schist	0	0.335	0.73	0.765	0.498	0.264
NQ Whole core	6105.6	P2 Schist	0	0.345	0.73	0.772	0.497	0.265
NQ Whole core	6105.6	P2 Schist	0	0.323	0.73	0.764	0.497	0.266
NQ Whole core	6105.6	P2 Schist	0	0.346	0.73	0.770	0.497	0.265
NQ Whole core	6105.6	P2 Schist	0	0.36	0.73	0.764	0.498	0.265
NQ Whole core	6105.6	P2 Schist	0	0.328	0.76	0.770	0.498	0.264
NQ Whole core	6105.6	P2 Schist	0	0.341	0.76	0.764	0.498	0.265
NQ Whole core	6105.6	P2 Schist	0	0.376	0.78	0.767	0.496	0.265
NQ Whole core	6105.6	P2 Schist	0	0.347	0.8	0.761	0.497	0.265
NQ Whole core	6105.6	P2 Schist	0	0.345	0.8	0.768	0.499	0.265
NQ Whole core	6105.6	P2 Schist	0	0.335	0.78	0.767	0.498	0.263
NQ Whole core	6105.6	P2 Schist	0	0.346	0.8	0.773	0.498	0.263
NQ Whole core	6105.6	P2 Schist	0	0.337	0.8	0.770	0.497	0.263
NQ Whole core	6105.6	P2 Schist	0	0.33	0.8	0.774	0.498	0.264
NQ Whole core	6105.6	P2 Schist	0	0.321	0.8	0.772	0.497	0.264
NQ Whole core	6105.6	P2 Schist	0	0.351	0.8	0.772	0.497	0.265
NQ Whole core	6105.6	P2 Schist	0	0.346	0.82	0.772	0.499	0.265
NQ Whole core	6105.6	P2 Schist	0	0.318	0.82	0.768	0.497	0.265
NQ Whole core	6105.6	P2 Schist	0	0.346	0.8	0.773	0.499	0.266
NQ Whole core	6105.6	P2 Schist	0	0.331	0.82	0.769	0.498	0.266
NQ Whole core	6105.6	P2 Schist	0	0.338	0.84	0.772	0.498	0.251
NQ Whole core	6105.6	P2 Schist	0	0.336	0.84	0.771	0.497	0.252
NQ Whole core	6105.6	P2 Schist	0	0.336	0.84	0.772	0.497	0.252
NQ Whole core	6105.6	P2 Schist	0	0.338	0.84	0.772	0.497	0.252
NQ Whole core	6105.6	P2 Schist	0	0.343	0.87	0.776	0.498	0.253
NQ Whole core	6105.6	P2 Schist	0	0.345	0.84	0.777	0.498	0.253
NQ Whole core	6105.6	P2 Schist	0	0.331	0.87	0.778	0.498	0.253
NQ Whole core	6105.6	P2 Schist	0	0.333	0.89	0.778	0.498	0.253
NQ Whole core	6105.6	P2 Schist	0	0.34	0.91	0.778	0.498	0.254

NQ Whole core	6105.6	P2 Schist	0	0.337	0.89	0.776	0.498	0.254
NQ Whole core	6105.6	P2 Schist	0	0.328	0.87	0.780	0.496	0.254
NQ Whole core	6105.6	P2 Schist	0	0.35	0.87	0.772	0.498	0.254
NQ Whole core	6105.6	P2 Schist	0	0.328	0.89	0.778	0.497	0.256
NQ Whole core	6105.6	P2 Schist	0	0.344	0.91	0.778	0.499	0.255
NQ Whole core	6105.6	P2 Schist	0	0.355	0.91	0.778	0.499	0.254
NQ Whole core	6105.6	P2 Schist	0	0.348	0.91	0.771	0.497	0.255
NQ Whole core	6105.6	P2 Schist	0	0.349	0.93	0.774	0.497	0.255
NQ Whole core	6105.6	P2 Schist	0	0.32	0.91	0.768	0.498	0.255
NQ Whole core	6105.6	P2 Schist	0	0.325	0.91	0.770	0.498	0.255
NQ Whole core	6105.6	P2 Schist	0	0.333	0.93	0.766	0.497	0.256
NQ Whole core	6105.6	P2 Schist	0	0.34	0.93	0.768	0.497	0.263
NQ Whole core	6105.6	P2 Schist	0	0.319	0.93	0.768	0.497	0.263
NQ Whole core	6105.6	P2 Schist	0	0.319	0.93	0.764	0.496	0.263
NQ Whole core	6105.6	P2 Schist	0	0.329	0.93	0.766	0.497	0.264
NQ Whole core	6105.6	P2 Schist	0	0.336	0.98	0.752	0.497	0.264
NQ Whole core	6105.6	P2 Schist	0	0.32	0.96	0.732	0.497	0.264
NQ Whole core	6105.6	P2 Schist	0	0.337	0.96	0.736	0.498	0.266
NQ Whole core	6105.6	P2 Schist	0	0.342	0.98	0.724	0.498	0.265
NQ Whole core	6105.6	P2 Schist	0	0.328	0.98	0.710	0.497	0.266
NQ Whole core	6105.6	P2 Schist	0	0.324	1	0.699	0.497	0.265
NQ Whole core	6105.6	P2 Schist	0	0.317	1	0.704	0.499	0.266
NQ Whole core	6105.6	P2 Schist	0	0.322	1.02	0.695	0.496	0.264
NQ Whole core	6105.6	P2 Schist	0	0.322	1.02	0.697	0.497	0.264
NQ Whole core	6105.6	P2 Schist	0	0.32	1	0.690	0.497	0.265
NQ Whole core	6105.6	P2 Schist	0	0.344	1.02	0.698	0.498	0.265
NQ Whole core	6105.6	P2 Schist	0	0.346	1.04	0.686	0.497	0.266
NQ Whole core	6105.6	P2 Schist	0	0.338	1.04	0.691	0.498	0.267
NQ Whole core	6105.6	P2 Schist	0	0.328	1.04	0.670	0.498	0.267
NQ Whole core	6105.6	P2 Schist	0	0.307	1.04	0.690	0.498	0.267
NQ Whole core	6105.6	P2 Schist	0	0.295	1.02	0.666	0.498	0.267
NQ Whole core	6105.6	P2 Schist	0	0.357	1.04	0.682	0.497	0.258
NQ Whole core	6105.6	P2 Schist	0	0.349	1.07	0.672	0.497	0.257
NQ Whole core	6105.6	P2 Schist	0	0.329	1.07	0.683	0.497	0.257
NQ Whole core	6105.6	P2 Schist	0	0.332	1.09	0.667	0.497	0.257
NQ Whole core	6105.6	P2 Schist	0	0.323	1.09	0.689	0.498	0.257
NQ Whole core	6105.6	P2 Schist	0		1.09	0.681	0.498	0.257
NQ Whole core	6105.6	P2 Schist	0		1.09	0.691	0.499	0.257
NQ Whole core	6105.6	P2 Schist	0		1.11	0.682	0.497	0.257
Average readings			**0.000**	**0.328**	**0.746**	**0.747**	**0.498**	**0.262**

Table 41: Raw magnetic susceptibility measurements collected on NQ half core – schist

Sample ID	Depth	Lithology	RT1	KT10	GDD	MS2K	MS2C	SM30 B
NQ Half core	6105.6	P2 Schist	0.37	0.328	0.720	0.379	0.662	0.648
NQ Half core	6105.6	P2 Schist	0.37	0.333	0.770	0.379	0.665	0.678
NQ Half core	6105.6	P2 Schist	0.37	0.384	0.770	0.379	0.663	0.742
NQ Half core	6105.6	P2 Schist	0.38	0.408	0.770	0.380	0.663	0.698
NQ Half core	6105.6	P2 Schist	0.37	0.345	0.790	0.381	0.665	0.777
NQ Half core	6105.6	P2 Schist	0.37	0.385	0.26	0.381	0.667	0.684
NQ Half core	6105.6	P2 Schist	0.37	0.368	0.37	0.382	0.667	0.702
NQ Half core	6105.6	P2 Schist	0.37	0.356	0.35	0.382	0.663	0.727
NQ Half core	6105.6	P2 Schist	0.37	0.355	0.37	0.381	0.663	0.696
NQ Half core	6105.6	P2 Schist	0.37	0.351	0.39	0.378	0.66	0.736
NQ Half core	6105.6	P2 Schist	0.37	0.361	0.39	0.385	0.663	0.704
NQ Half core	6105.6	P2 Schist	0.37	0.346	0.39	0.385	0.665	0.679
NQ Half core	6105.6	P2 Schist	0.37	0.347	0.39	0.386	0.665	0.692
NQ Half core	6105.6	P2 Schist	0.37	0.4	0.39	0.388	0.665	0.742
NQ Half core	6105.6	P2 Schist	0.37	0.371	0.39	0.388	0.663	0.695
NQ Half core	6105.6	P2 Schist	0.37	0.37	0.39	0.390	0.665	0.64
NQ Half core	6105.6	P2 Schist	0.36	0.392	0.4	0.393	0.667	0.749
NQ Half core	6105.6	P2 Schist	0.36	0.335	0.39	0.394	0.663	0.698
NQ Half core	6105.6	P2 Schist	0.36	0.367	0.39	0.395	0.663	0.831
NQ Half core	6105.6	P2 Schist	0.36	0.336	0.4	0.395	0.667	0.969
NQ Half core	6105.6	P2 Schist	0.35	0.347	0.4	0.395	0.665	0.933
NQ Half core	6105.6	P2 Schist	0.36	0.349	0.42	0.396	0.665	0.927
NQ Half core	6105.6	P2 Schist	0.36	0.342	0.4	0.396	0.669	0.938
NQ Half core	6105.6	P2 Schist	0.36	0.378	0.4	0.396	0.665	1.01
NQ Half core	6105.6	P2 Schist	0.36	0.35	0.4	0.396	0.665	0.904
NQ Half core	6105.6	P2 Schist	0.37	0.341	0.42	0.400	0.669	0.963
NQ Half core	6105.6	P2 Schist	0.37	0.362	0.42	0.401	0.662	0.909
NQ Half core	6105.6	P2 Schist	0.36	0.313	0.42	0.402	0.667	0.936
NQ Half core	6105.6	P2 Schist	0.37	0.353	0.42	0.403	0.665	0.905
NQ Half core	6105.6	P2 Schist	0.36	0.357	0.42	0.403	0.667	0.958
NQ Half core	6105.6	P2 Schist	0.36	0.359	0.44	0.402	0.667	0.986
NQ Half core	6105.6	P2 Schist	0.36	0.397	0.44	0.403	0.669	0.857
NQ Half core	6105.6	P2 Schist	0.36	0.389	0.42	0.402	0.665	0.881
NQ Half core	6105.6	P2 Schist	0.36	0.337	0.42	0.402	0.665	0.881
NQ Half core	6105.6	P2 Schist	0.36	0.346	0.42	0.402	0.656	0.954
NQ Half core	6105.6	P2 Schist	0.36	0.314	0.42	0.403	0.679	0.878
NQ Half core	6105.6	P2 Schist	0.36	0.375	0.44	0.402	0.66	1.04
NQ Half core	6105.6	P2 Schist	0.36	0.387	0.44	0.402	0.658	0.894
NQ Half core	6105.6	P2 Schist	0.36	0.353	0.44	0.403	0.66	1.03
NQ Half core	6105.6	P2 Schist	0.36	0.373	0.44	0.403	0.662	1.16
NQ Half core	6105.6	P2 Schist	0.35	0.334	0.44	0.403	0.656	0.99
NQ Half core	6105.6	P2 Schist	0.35	0.371	0.46	0.402	0.665	0.971
NQ Half core	6105.6	P2 Schist	0.35	0.343	0.46	0.402	0.658	0.892
NQ Half core	6105.6	P2 Schist	0.36	0.347	0.46	0.403	0.658	1
NQ Half core	6105.6	P2 Schist	0.36	0.362	0.46	0.402	0.654	1.09
NQ Half core	6105.6	P2 Schist	0.36	0.388	0.48	0.402	0.654	1.14
NQ Half core	6105.6	P2 Schist	0.35	0.399	0.48	0.402	0.663	0.675

NQ Half core	6105.6	P2 Schist	0.35	0.354	0.48	0.402	0.667	0.626
NQ Half core	6105.6	P2 Schist	0.35	0.355	0.48	0.402	0.658	0.636
NQ Half core	6105.6	P2 Schist	0.35	0.368	0.46	0.401	0.656	0.672
NQ Half core	6105.6	P2 Schist	0.34	0.357	0.46	0.402	0.663	0.618
NQ Half core	6105.6	P2 Schist	0.35	0.339	0.48	0.401	0.665	0.598
NQ Half core	6105.6	P2 Schist	0.34	0.328	0.48	0.401	0.656	0.607
NQ Half core	6105.6	P2 Schist	0.34	0.358	0.48	0.401	0.66	0.619
NQ Half core	6105.6	P2 Schist	0.34	0.343	0.46	0.401	0.663	0.627
NQ Half core	6105.6	P2 Schist	0.34	0.336	0.46	0.401	0.654	0.637
NQ Half core	6105.6	P2 Schist	0.33	0.368	0.48	0.402	0.66	0.601
NQ Half core	6105.6	P2 Schist	0.33	0.373	0.48	0.402	0.665	0.604
NQ Half core	6105.6	P2 Schist	0.33	0.373	0.48	0.403	0.652	0.626
NQ Half core	6105.6	P2 Schist	0.33	0.338	0.48	0.402	0.662	0.652
NQ Half core	6105.6	P2 Schist	0.33	0.372	0.48	0.403	0.654	0.62
NQ Half core	6105.6	P2 Schist	0.34	0.331	0.49	0.402	0.662	0.624
NQ Half core	6105.6	P2 Schist	0.33	0.372	0.49	0.401	0.658	0.704
NQ Half core	6105.6	P2 Schist	0.33	0.364	0.49	0.402	0.66	0.666
NQ Half core	6105.6	P2 Schist	0.34	0.311	0.49	0.401	0.662	0.69
NQ Half core	6105.6	P2 Schist	0.34	0.325	0.48	0.401	0.66	0.67
NQ Half core	6105.6	P2 Schist	0.34	0.335	0.48	0.401	0.656	0.706
NQ Half core	6105.6	P2 Schist	0.34	0.378	0.49	0.401	0.66	0.688
NQ Half core	6105.6	P2 Schist	0.34	0.35	0.49	0.402	0.665	0.731
NQ Half core	6105.6	P2 Schist	0.34	0.352	0.49	0.396	0.662	0.723
NQ Half core	6105.6	P2 Schist	0.34	0.343	0.49	0.395	0.66	0.694
NQ Half core	6105.6	P2 Schist	0.34	0.353	0.49	0.402	0.656	0.661
NQ Half core	6105.6	P2 Schist	0.34	0.356	0.49	0.401	0.665	0.658
NQ Half core	6105.6	P2 Schist	0.34	0.384	0.49	0.403	0.662	0.625
NQ Half core	6105.6	P2 Schist	0.34	0.356	0.49	0.403	0.654	0.7
NQ Half core	6105.6	P2 Schist	0.34	0.372	0.510	0.403	0.658	0.681
NQ Half core	6105.6	P2 Schist	0.34	0.392	0.510	0.403	0.658	0.654
NQ Half core	6105.6	P2 Schist	0.34	0.352	0.49	0.403	0.656	0.627
NQ Half core	6105.6	P2 Schist	0.33	0.351	0.510	0.403	0.662	0.688
NQ Half core	6105.6	P2 Schist	0.33	0.395	0.530	0.403	0.662	0.687
NQ Half core	6105.6	P2 Schist	0.33	0.371	0.510	0.403	0.66	0.607
NQ Half core	6105.6	P2 Schist	0.33	0.346	0.510	0.403	0.658	0.648
NQ Half core	6105.6	P2 Schist	0.33	0.335	0.510	0.403	0.656	0.622
NQ Half core	6105.6	P2 Schist	0.34	0.369	0.510	0.403	0.662	0.605
NQ Half core	6105.6	P2 Schist	0.34	0.356	0.530	0.403	0.66	0.628
NQ Half core	6105.6	P2 Schist	0.33	0.353	0.530	0.403	0.662	0.638
NQ Half core	6105.6	P2 Schist	0.33	0.357	0.510	0.403	0.658	0.587
NQ Half core	6105.6	P2 Schist	0.33	0.363	0.510	0.403	0.658	0.589
NQ Half core	6105.6	P2 Schist	0.33	0.323	0.530	0.403	0.658	0.605
NQ Half core	6105.6	P2 Schist	0.33	0.361	0.530	0.404	0.663	0.558
NQ Half core	6105.6	P2 Schist	0.34	0.383	0.550	0.403	0.665	0.612
NQ Half core	6105.6	P2 Schist	0.34	0.398	0.550	0.403	0.656	0.628
NQ Half core	6105.6	P2 Schist	0.34	0.355	0.550	0.403	0.667	0.605
NQ Half core	6105.6	P2 Schist	0.35	0.396	0.550	0.403	0.658	0.65
NQ Half core	6105.6	P2 Schist	0.35	0.346	0.550	0.403	0.656	0.619
NQ Half core	6105.6	P2 Schist	0.35	0.34	0.530	0.403	0.66	0.65
NQ Half core	6105.6	P2 Schist	0.35	0.372	0.530	0.403	0.654	0.586

NQ Half core	6105.6	P2 Schist	0.35	0.375	0.530	0.403	0.658	0.634
NQ Half core	6105.6	P2 Schist	0.35	0.354	0.530	0.403	0.66	0.627
NQ Half core	6105.6	P2 Schist	0.34	0.372	0.55	0.404	0.66	0.626
NQ Half core	6105.6	P2 Schist	0.34	0.343	0.53	0.403	0.658	0.603
NQ Half core	6105.6	P2 Schist	0.34	0.296	0.53	0.404	0.656	0.632
NQ Half core	6105.6	P2 Schist	0.34	0.387	0.55	0.404	0.658	0.67
NQ Half core	6105.6	P2 Schist	0.34	0.343	0.56	0.403	0.656	0.654
NQ Half core	6105.6	P2 Schist	0.34	0.338	0.55	0.404	0.66	0.742
NQ Half core	6105.6	P2 Schist	0.34	0.386	0.55	0.404	0.66	0.846
NQ Half core	6105.6	P2 Schist	0.34	0.382	0.55	0.404	0.656	0.806
NQ Half core	6105.6	P2 Schist	0.33	0.339	0.55	0.404	0.662	0.826
NQ Half core	6105.6	P2 Schist	0.33	0.381	0.55	0.404	0.658	0.676
NQ Half core	6105.6	P2 Schist	0.33	0.385	0.56	0.404	0.662	0.726
NQ Half core	6105.6	P2 Schist	0.33	0.357	0.58	0.404	0.662	0.801
NQ Half core	6105.6	P2 Schist	0.33	0.369	0.56	0.404	0.656	0.745
NQ Half core	6105.6	P2 Schist	0.33	0.335	0.55	0.403	0.656	0.692
NQ Half core	6105.6	P2 Schist	0.32	0.342	0.560	0.404	0.658	0.693
NQ Half core	6105.6	P2 Schist	0.32	0.384	0.58	0.405	0.662	0.768
NQ Half core	6105.6	P2 Schist	0.32	0.348	0.58	0.405	0.66	0.679
NQ Half core	6105.6	P2 Schist	0.32	0.346	0.56	0.404	0.656	0.752
NQ Half core	6105.6	P2 Schist	0.32	0.318	0.56	0.405	0.656	0.729
NQ Half core	6105.6	P2 Schist	0.32	0.391	0.58	0.405	0.658	0.769
NQ Half core	6105.6	P2 Schist	0.32	0.378	0.60	0.405	0.66	0.745
NQ Half core	6105.6	P2 Schist	0.32	0.347	0.60	0.405	0.658	0.71
NQ Half core	6105.6	P2 Schist	0.31	0.372	0.60	0.405	0.658	0.741
NQ Half core	6105.6	P2 Schist	0.31	0.373	0.58	0.405	0.662	0.76
NQ Half core	6105.6	P2 Schist	0.31	0.413	0.58	0.404	0.66	0.688
NQ Half core	6105.6	P2 Schist	0.31	0.378	0.58	0.404	0.66	0.692
Average readings			**0.35**	**0.359**	**0.495**	**0.400**	**0.661**	**0.738224**

Table 42: Raw magnetic susceptibility data collected on dolomite (freshly cut outcrop) sample.

Rock-type	RT1	KT10	GDD	MS2K	MS2C	SM30 B
	(x10-3SI)	(x10-3SI)	(x10-3SI)	(x10-3SI)	(x10-3SI)	(x10-3SI)
Dolomite	0	0.108	0	0.073		0.09
Dolomite	0	0.112	0	0.086		0.09
Dolomite	0	0.112	0	0.078		0.09
Dolomite	0	0.112	0	0.086		0.09
Dolomite	0	0.11	0	0.085		0.09
Dolomite	0	0.112	0	0.087		0.09
Dolomite	0	0.112	0	0.087		0.09
Dolomite	0	0.111	0	0.086		0.091
Dolomite	0	0.11	0	0.086		0.091
Dolomite	0	0.11	0	0.084		0.09
Dolomite	0	0.113	0	0.087		0.089
Dolomite	0	0.111	0	0.088		0.089
Dolomite	0	0.113	0	0.088		0.09
Dolomite	0	0.111	0	0.085		0.09
Dolomite	0	0.111	0	0.088		0.09
Dolomite	0	0.11	0	0.088		0.09
Dolomite	0	0.111	0	0		0.087
Dolomite	0	0.113	0	0.083		0.087
Dolomite	0	0.11	0	0.088		0.088
Dolomite	0	0.117	0	0.088		0.089
Dolomite	0	0.11	0	0.088		0.088
Dolomite	0	0.111	0	0.088		0.09
Dolomite	0	0.112	0	0.088		0.089
Dolomite	0	0.111	0	0.087		0.088
Dolomite	0	0.117	0	0.087		0.088
Dolomite	0	0.117	0	0.089		0.087
Dolomite	0	0.116	0	0.086		0.087
Dolomite	0	0.109	0	0.087		0.087
Dolomite	0	0.109	0	0.085		0.088
Dolomite	0	0.117	0	0.084		0.088
Dolomite	0	0.107	0	0.082		0.087
Dolomite	0	0.107	0	0.087		0.087
Dolomite	0	0.113	0	0.088		0.088
Dolomite	0	0.115	0	0.087		0.088
Dolomite	0	0.111	0	0.088		0.087
Dolomite	0	0.108	0	0.088		0.087
Dolomite	0	0.108	0	0.088		0.087
Dolomite	0	0.113	0	0.088		0.087
Dolomite	0	0.117	0	0.086		0.086
Dolomite	0	0.11	0	0.088		0.086
Dolomite	0	0.111	0	0.087		0.087

Dolomite	0	0.109	0	0.087		0.087
Dolomite	0	0.112	0	0.084		0.088
Dolomite	0	0.113	0	0.04		0.089
Dolomite	0	0.113	0	0.086		0.09
Dolomite	0	0.115	0	0.088		0.091
Dolomite	0	0.109	0	0.086		0.091
Dolomite	0	0.111	0	0.085		0.09
Dolomite	0	0.116	0	0.087		0.092
Dolomite	0	0.118	0	0.085		0.093
Dolomite	0	0.112	0	0.081		0.092
Dolomite	0	0.113	0	0.085		0.092
Average readings	**0.000**	**0.112**	**0.000**	**0.083**		**0.089**

Table 43: Raw magnetic susceptibility data collected on ultramafic picrite (freshly cut) sample

Rock-type	RT1	KT10	GDD	MS2K	MS2C	SM30 B
	(x10-3SI)	(x10-3SI)	(x10-3SI)	(x10-3SI)	(x10-3SI)	(x10-3SI)
Ultramafic	42.98	47.447	47.1	47.675		45.7
Ultramafic	42.94	47.339	47.2	45.315		45.7
Ultramafic	42.71	47.987	47.2	42.692		45.7
Ultramafic	42.98	47.214	47.2	45.109		45.7
Ultramafic	42.7	47.404	47.2	43.876		45.7
Ultramafic	42.65	47.411	47.1	46.047		45.7
Ultramafic	42.59	47.538	47.1	43.575		45.7
Ultramafic	42.51	47.022	47.1	41.751		45.7
Ultramafic	42.38	47.28	47.2	53.479		45.7
Ultramafic	42.31	47.414	47.1	48.808		45.7
Ultramafic	42.22	47.809	47.3	46.413		45.7
Ultramafic	42.44	47.443	47.3	44.722		45.7
Ultramafic	43.5	47.572	47.1	46.603		45.7
Ultramafic	43.38	47.23	47.1	48.203		45.7
Ultramafic	43.2	47.767	47.3	48.237		45.7
Ultramafic	42.98	47.683	47.3	48.284		45.8
Ultramafic	42.65	47.467	47.3	50.147		45.8
Ultramafic	42.51	47.81	47.3	52.504		45.8
Ultramafic	42.53	47.226	47.3	49.531		45.7
Ultramafic	42.46	47.52	47.3	51.891		45.5
Ultramafic	42.65	47.093	47.3	51.809		45.5
Ultramafic	42.83	47.474	47.3	48.236		45.5
Ultramafic	42.92	47.202	47.4	52.684		45.5
Ultramafic	42.99	47.673	47.4	46.134		45.9
Ultramafic	42.03	47.374	47.4	51.165		46.1
Ultramafic	42.18	47.455	47.4	53.424		46
Ultramafic	42.07	47.404	47.4	48.823		46.1
Ultramafic	42.06	47.213	47.4	47.906		46.1
Ultramafic	42.09	47.196	47.4	50.194		46.1
Ultramafic	42.41	47.329	47.4	54.000		46.1
Ultramafic	42.28	47.434	47.4	52.246		46.1
Ultramafic	42.21	47.634	47.4	49.507		46.1
Ultramafic	42.2	47.435	47.4	50.906		45.9
Ultramafic	42.29	46.978	47.4	49.725		45.9
Ultramafic	42.49	47.535	47.4	52.541		45.9
Ultramafic	42.73	47.029	47.4	52.035		45.9
Ultramafic	42.82	47.459	47.5	49.752		45.9
Ultramafic	42.95	47.298	47.5	52.614		45.9
Ultramafic	42.85	47.48	47.5	51.227		45.9
Ultramafic	42.68	47.318	47.5	53.653		45.9
Ultramafic	42.48	47.476	47.3	50.341		45.9
Ultramafic	42.44	47.484	46.8	49.087		45.9
Ultramafic	42.49	47.482	47.4	50.531		45.9
Ultramafic	42.59	47.464	47.5	52.816		46

Ultramafic	42.73	47.783	47.5	48.342		46.3
Ultramafic	42.82	47.228	47.4	47.702		46.3
Ultramafic	42.85	47.266	47.4	50.044		46.3
Ultramafic	42.89	47.623	47.4	48.577		46.3
Ultramafic	42.91	47.416	47.4	53.363		46.2
Ultramafic	42.94	47.077	47.4	51.180		46.3
Ultramafic	42.99	47.444	47.5			46.2
Ultramafic	42.98	47.578	47.5			46.3
Ultramafic	42.94	46.967	47.5			46.4
Ultramafic	42.91	47.245	47.5			46.4
Ultramafic	42.89	47.525	47.5			46.5
Ultramafic	42.91	47.732	47.5			46.5
Ultramafic	42.9	47.139	47.5			46.5
Ultramafic	42.87	46.914	47.5			46.5
Ultramafic	42.83	47.15	47.5			46.5
Ultramafic	42.73	47.376	47.6			46.5
Ultramafic	42.59	47.782	47.6			46.5
Ultramafic	42.45	47.324	47.6			46.5
Ultramafic	42.36	47.34	47.6			46.5
Ultramafic	42.29	47.242	47.6			46.5
Ultramafic	42.31	47.281	47.5			46.5
Ultramafic	42.35	47.582	47.5			46.5
Ultramafic	42.4	47.434	47.6			46.5
Ultramafic	42.46	47.274	47.6			46.5
Ultramafic	42.52	47.043	47.5			46.5
Ultramafic	42.58	47.479	47.5			46.5
Ultramafic	42.55	47.265	47.5			46.5
Ultramafic	42.45	47.199	47.5			46.5
Ultramafic	42.24	46.998	47.6			46.5
Ultramafic	42.07	47.199	47.6			46.5
Ultramafic	42.05	47.024	47.6			46.5
Ultramafic	42.57	47.478	47.6			46.5
Ultramafic	42.69	47.391	47.6			46.5
Ultramafic	42.73	47.616	47.6			46.5
Ultramafic	42.79	47.247	47.6			46.5
Ultramafic	42.86	47.127	47.6			46.5
Ultramafic	42.85	47.201	47.6			46.5
Ultramafic	42.81	47.279	47.6			46.5
Ultramafic	42.79	47.347	47.6			46.5
Ultramafic	42.75	47.219	47.5			46.5
Ultramafic	42.71	47.155	47.5			46.1
Ultramafic	42.66	47.623	47.6			46.1
Ultramafic	42.63	47.145	47.6			46.1
Ultramafic	42.64	47.507	47.6			46.1
Ultramafic	42.61	47.089	47.6			46.1
Ultramafic	42.67	47.349	47.6			46.1
Ultramafic	42.65	47.448	47.6			46.1
Ultramafic	42.58	47.284	47.6			46.1

Ultramafic	42.54	47.332	47.7			46.1
Ultramafic	42.41	47.26	47.7			46.1
Ultramafic	42.27	47.264	47.7			46.1
Ultramafic	42.27	47.124	47.7			46.1
Ultramafic	42.29	47.211	47.7			46.1
Ultramafic	42.31	47.249	47.6			46.1
Ultramafic	42.35	47.839	47.5			46.1
Ultramafic	42.33	47.059	47.5			46.1
Ultramafic	42.31	47.408	47.6			46.1
Ultramafic	42.24	47.252	47.6			46.1
Ultramafic	42.18	47.744	47.7			46.1
Ultramafic	42.09	47.137	47.7			46.1
Ultramafic	42.06	47.688	47.6			45.9
Ultramafic	42.3	47.227	47.6			45.9
Ultramafic	42.6	47.275	47.7			46.2
Ultramafic	42.74	47.139	47.5			46.2
Ultramafic	42.79	47.746	47.4			46.2
Ultramafic	42.76	47.204	47.3			46.2
Ultramafic	42.72	47.598	47.3			46.2
Ultramafic	42.67	47.227	47.4			46.2
Ultramafic	42.59	47.323	47.4			46.2
Ultramafic	42.42	47.739	47.3			46.2
Ultramafic	42.2	47.273	47.3			46.2
Ultramafic	42.95	47.378	47.3			46.3
Ultramafic	42.9	47.253	47.3			46.3
Ultramafic	42.87	47.005	47.2			46.3
Ultramafic	42.78	47.228	47.1			46.3
Ultramafic	42.73	47.12	47.8			46.3
Average Readings	**42.598**	**47.360**	**47.446**	**49.308**		**46.127**

Table 44: Shows computed averages from all instruments in their chosen mode of operation

Sample ID	Depth	Lithology	RT1	KT10	GDD	MS2K	MS2C	SM30 B
	(ft)		(x10^-3 SI)	(x10^-3 SI)	(x10^-3 SI)	(x10^-3 SI)	(x10^-3 SI)	(x10^-3 SI)
1301080	731	GNAM	0.330	0.284	0.568	0.472	1.007	0.259
1301080	735	GN	0.000	0.081	0.164	0.165	0.201	0.068
1301080	764	PEG	0.000	0.063	0.020	0.032	0.087	0.038
1301080	773	AMPT	0.000	0.380	0.802	0.634	0.668	0.336
1301080	787	P2 SCH	0.000	0.368	0.758	0.690	1.142	0.335
1301080	792	PEG	0.000	0.111	0.074	0.045	0.373	0.124
1301080	800	P2 SCH	0.000	0.481	0.788	0.678	1.341	0.428
1301080	833	AMPT	0.022	0.776	1.658	1.662	2.745	0.698
1301080	838	P2 MSCH	13.030	6.483	24.780	25.049	24.440	6.398
1301080	843	P2 PSCH	0.000	0.418	0.234	0.113	0.592	0.379
1301080	854	P2 SUMX	18.646	12.481	37.080	24.448	95.769	11.180
1301080	858	P2? SCH	0.000	0.133	0.554	0.057	0.189	0.117
1301080	863	AMPT	0.000	0.384	0.696	0.538	1.236	0.358
1301080	873	SF QTE	0.000	0.209	0.000	0.016	0.020	0.241
1301080	882	SF SCH	0.000	0.280	0.336	0.200	0.815	0.232
1301080	902	PEG	0.000	0.033	0.004	0.030	0.065	0.025
1301080	912	AMPT	0.000	0.350	0.726	0.562	1.274	0.331
1301080	920	SF PSCH	0.000	0.253	0.352	0.319	0.698	0.255
1301080	935	SF QTE	0.000	0.111	0.088	0.050	0.104	0.097
1301080	937	AMPT	0.000	0.112	0.748	0.564	1.160	0.323
1301080	943	SF PSCH	0.000	0.363	0.098	*	0.149	0.041
1301080	953	P3 IF	5.088	3.101	9.662	3.815	79.977	4.012
1301080	991	PEG	0.000	0.120	0.182	0.110	0.207	0.101
1301080	1010	P3 IF (MT)	280.806	189.258	359.400	226.376	611.304	201.400
1301080	1020	IF-GRNT	59.148	46.454	69.800	43.469	221.474	43.640
1301080	1030	AMPT	0.000	11.891	2.418	1.362	2.642	4.916
1301080	1041	AMPT	5.930	0.935	1.264	0.979	2.576	0.728
1301080	1056	APLITE	0.000	0.026	0.000	0.005	0.043	0.011
1301020	613.5	Gneiss	0.000	0.119	0.000	0.106	0.568	0.082
1301020	629.9	AMPT	0.429	0.437	0.019	0.723	2.449	0.427
1301020	836.6	MPRD	8.851	9.326	9.709	8.695	27.473	8.500
1301020	841.5	M. SRPT	54.727	37.028	90.920	64.635	80.245	36.020
1301020	846.5	MPRD	3.924	5.166	5.756	4.341	14.272	4.652
1301020	850.4	Serpentinite	42.060	30.471	70.315	51.582	83.211	29.265
1301020	866.8	AMPT	0.168	0.366	0.010	0.569	1.090	0.327
1301020	883.9	IF	4.992	5.782	18.915	17.792	21.535	5.381
1301020	915.4	Pegmatite	0.000	0.071	0.000	0.081	0.191	0.048
1301020	996.1	Quartzite	0	0.007	0	-0.0074	-0.0253	-0.0018
Rock		Ultramafic	42.598	47.360	47.446	49.308		46.127

Rock		Dolomite	0.000	0.112	0.000	0.083		0.089
Whole NQ		Sulphide	74.242	47.367	102.472	97.856	135.913	44.275
Whole NQ		P2 schist	0.000	0.328	0.746	0.747	0.498	0.262
Half NQ		Sulphide	77.618	56.488	101.729	105.103	138.268	57.567
Half NQ		P2 schist	0.345	0.359	0.497	0.400	0.661	0.738
KT-10 cal		sample	34.956	35.703	35.189	38.257		33.311
MS2C cal		sample	3.727	4.323	3.975	4.134	11.038	4.217
1301240	1369	Gneiss	3.727	4.323	3.975	4.134	11.038	4.217
1301240	1381	Amphibolite	0.024	0.096	0.116	0.093	0.201	0.077
1301240	1388	Gneiss	0.302	0.305	0.624	0.473	1.064	0.279
1301240	1391	Amphibolite	0.086	0.137	0.270	0.104	0.453	0.157
1301240	1409	Gneiss	1.430	0.888	2.862	1.535	4.506	0.944
1301240	1410	Amphibolite	0.078	0.158	0.232	0.395	0.686	0.151
1301240	1419	Gneiss	0.040	0.351	0.634	0.458	0.644	0.110
1301240	1428	Gneiss	0.302	0.166	0.304	0.242	1.239	0.327
1301240	1438	Gneiss	0.062	0.079	0.166	0.107	0.176	0.183
1301240	1447	Gneiss	0.008	0.125	0.216	0.187	0.214	0.083
1301240	1457	Pegmatite	0.000	0.119	0.166	0.081	0.248	0.122
1301240	1467	Amphibolite	0.000	0.089	0.116	0.090	0.585	0.139
1301240	1471	Gneiss	0.000	0.277	0.572	0.440	0.202	0.065
1301240	1480	Amphibolite	0.140	0.124	0.254	0.127	0.980	0.233
1301240	1489	Pegmatite	0.146	0.203	0.332	0.414	0.353	0.109
1301240	1498	Pegmatite	0.000	0.062	0.076	0.053	0.902	0.178
1301240	1503	Quartzite	0.042	0.065	0.144	0.115	0.255	0.034
1301240	1507	Pegmatite	0.000	0.036	0.108	0.090	0.160	0.045
1301240	1511	Skarn	0.000	0.084	0.158	0.151	0.258	0.035
1301240	1517	Skarn	0.000	0.215	0.358	0.262	0.698	0.054
1301240	1527	Skarn	0.000	0.239	0.558	0.475	0.472	0.168
1301240	1535	Skarn	0.008	0.129	0.346	0.424	0.324	0.236
1301240	1536	Pegmatite	0.020	0.205	0.464	0.201	0.680	0.119
1301240	1546	Pegmatite	0.002	0.069	0.380	0.295	0.158	0.174
1301240	1565	Pegmatite	0.000	0.075	0.290	0.097	0.149	0.118
1301240	1574	Pegmatite	0.000	0.224	0.004	0.036	0.045	0.078
1301240	1576	Pegmatite	0.000	0.940	0.226	0.059	0.100	0.029
1301240	1578	M. Peg	0.000	4.706	9.026	40.287	41.045	2.964
1301240	1580	Schist	4.582	16.968	50.020	48.707	135.001	12.800
1301240	1582	M. Schist	2.526	3.926	10.740	6.119	27.614	4.978
1301240	1584	Schist	27.924	5.675	10.820	16.239	32.756	4.424
1301240	1586	sulphide	9.032	1.519	1.864	2.516	7.358	1.204
1301240	1587	sulphide	44.840	27.868	118.400	70.599	205.428	26.740
1301240	1588	M. Schist	59.398	24.804	72.420	59.605	137.612	20.700
1301240	1590	Sulphide	1.242	0.843	1.940	0.976	5.239	0.875
1301240	1597	Pegmatite	45.772	14.217	82.900	75.198	83.724	20.160

1301240	1606	Quartzite	0.264	0.353	1.936	0.177	0.505	0.467
1301240	1615	Quartzite	0.000	0.129	0.008	0.041	0.307	0.165
1301240	1625	Quartzite	0.000	0.087	0.082	0.119	0.164	0.051
1301240	1634	Quartzite	0.000	0.103	0.150	0.157	0.285	0.052

Table 45: Shows log10 values calculated from mean values shown in table 40 above

Sample ID	Depth		RT1	KT10	GDD	MS2K	MS2C	SM30 B
1301080	731	GNAM	-0.4815	-0.5470	-0.2457	-0.3264	0.0029	-0.5864
1301080	735	GN	*	-1.0904	-0.7852	-0.7830	-0.6977	-1.1701
1301080	764	PEG	*	-1.2007	-1.6990	-1.4892	-1.0618	-1.4202
1301080	773	AMPT	*	-0.4204	-0.0958	-0.1982	-0.1752	-0.4742
1301080	787	P2 SCH	*	-0.4339	-0.1203	-0.1613	0.0576	-0.4744
1301080	792	PEG	*	-0.9562	-1.1308	-1.3474	-0.4284	-0.9052
1301080	800	P2 SCH	*	-0.3177	-0.1035	-0.1685	0.1274	-0.3682
1301080	833	AMPT	-1.6576	-0.1100	0.2196	0.2207	0.4386	-0.1564
1301080	838	P2 MSCH	1.1149	0.8118	1.3941	1.3988	1.3881	0.8060
1301080	843	P2 PSCH	*	-0.3788	-0.6308	-0.9471	-0.2276	-0.4214
1301080	854	P2 SUMX	1.2706	1.0962	1.5691	1.3882	1.9812	1.0484
1301080	858	P2? SCH	*	-0.8768	-0.2565	-1.2442	-0.7247	-0.9318
1301080	863	AMPT	*	-0.4154	-0.1574	-0.2689	0.0921	-0.4461
1301080	873	SF QTE	*	-0.6794	*	-1.8008	-1.6969	-0.6180
1301080	882	SF SCH	*	-0.5532	-0.4737	-0.6982	-0.0886	-0.6349
1301080	902	PEG	*	-1.4763	-2.3979	-1.5285	-1.1875	-1.5952
1301080	912	AMPT	*	-0.4562	-0.1391	-0.2506	0.1052	-0.4796
1301080	920	SF PSCH	*	-0.5972	-0.4535	-0.4957	-0.1562	-0.5935
1301080	935	SF QTE	*	-0.9539	-1.0555	-1.3003	-0.9825	-1.0114
1301080	937	AMPT	*	-0.9508	-0.1261	-0.2487	0.0645	-0.4903
1301080	943	SF PSCH	*	-0.4399	-1.0088	*	-0.8283	-1.3851
1301080	953	P3 IF	0.7065	0.4914	0.9851	0.5815	1.9030	0.6034
1301080	991	PEG	*	-0.9215	-0.7399	-0.9575	-0.6848	-0.9965
1301080	1010	P3 IF (MT)	2.4484	2.2771	2.5556	2.3548	2.7863	2.3041
1301080	1020	IF-GRNT	1.7719	1.6670	1.8439	1.6382	2.3453	1.6399
1301080	1030	AMPT	*	1.0752	0.3835	0.1343	0.4219	0.6916
1301080	1041	AMPT	0.7731	-0.0291	0.1017	-0.0093	0.4110	-0.1376
1301080	1056	APLITE	*	-1.5817	*	-2.3344	-1.3690	-1.9586
1301020	613.5	Gneiss	*	-0.9243	*	-0.9737	-0.2455	-1.0887
1301020	629.9	AMPT	-0.3675	-0.3592	-1.7312	-0.1408	0.3891	-0.3699
1301020	836.6	MPRD	0.9470	0.9697	0.9872	0.9393	1.4389	0.9294
1301020	841.5	M. SRPT	1.7382	1.5685	1.9587	1.8105	1.9044	1.5565
1301020	846.5	MPRD	0.5937	0.7132	0.7601	0.6376	1.1545	0.6676
1301020	850.4	Serpentinite	1.6239	1.4839	1.8470	1.7125	1.9202	1.4663
1301020	866.8	AMPT	-0.7747	-0.4371	-2.0223	-0.2451	0.0375	-0.4861
1301020	883.9	IF	0.6983	0.7621	1.2768	1.2502	1.3332	0.7309
1301020	915.4	Pegmatite	*	-1.1479	*	-1.0914	-0.7197	-1.3170
1301020	996.1	Quartzite	*	-2.1549	*	*	*	*

Rock sample		Ultramafic	1.6294	1.6754	1.6762	1.6929	*	1.6640
Rock sample		Dolomite	*	-0.9512	*	-1.0785	*	-1.0511
Whole NQ		Sulphide	1.8707	1.6755	2.0106	1.9906	2.1333	1.6462
Whole NQ		P2 schist	*	-0.4835	-0.1274	-0.1268	-0.3031	-0.5822
Half NQ		Sulphide	1.8900	1.7520	2.0074	2.0216	2.1407	1.7602
Half NQ		P2 schist	-0.4626	-0.4453	-0.3033	-0.3982	-0.1799	-0.1318
KT-10 cal		sample	1.5435	1.5527	1.5464	1.5827	*	1.5226
MS2C cal		sample	0.5714	0.6359	0.5993	0.6164	1.0429	0.6250
1301240	1368.5	Gneiss	0.5713	0.6358	0.5994	0.6163	1.0429	0.6250
1301240	1381	Amphibolite	-1.6198	-1.0159	-0.9355	-1.0322	-0.6964	-1.1146
1301240	1388.2	Gneiss	-0.5200	-0.5160	-0.2048	-0.3249	0.0270	-0.5541
1301240	1390.5	Amphibolite	-1.0655	-0.8639	-0.5686	-0.9848	-0.3437	-0.8041
1301240	1409	Gneiss	0.1553	-0.0514	0.4567	0.1861	0.6538	-0.0252
1301240	1410	Amphibolite	-1.1079	-0.8002	-0.6345	-0.4038	-0.1635	-0.8210
1301240	1418.5	Gneiss	-1.3979	-0.4549	-0.1979	-0.3395	-0.1913	-0.9586
1301240	1428	Gneiss	-0.5200	-0.7788	-0.5171	-0.6156	0.0932	-0.4855
1301240	1437.5	Gneiss	-1.2076	-1.1035	-0.7799	-0.9697	-0.7557	-0.7380
1301240	1447	Gneiss	-2.0969	-0.9024	-0.6655	-0.7292	-0.6700	-1.0830
1301240	1457	Pegmatite	*	-0.9245	-0.7799	-1.0912	-0.6051	-0.9151
1301240	1466.8	Amphibolite	*	-1.0526	-0.9355	-1.0454	-0.2330	-0.8570
1301240	1470.7	Gneiss	*	-0.5569	-0.2426	-0.3566	-0.6955	-1.1884
1301240	1480	Amphibolite	-0.8539	-0.9080	-0.5952	-0.8961	-0.0086	-0.6326
1301240	1489.4	Pegmatite	-0.8356	-0.6921	-0.4789	-0.3829	-0.4516	-0.9626
1301240	1498	Pegmatite	*	-1.2090	-1.1192	-1.2782	-0.0449	-0.7496
1301240	1503	Quartzite	-1.3768	-1.1858	-0.8416	-0.9378	-0.5927	-1.4634
1301240	1507	Pegmatite	*	-1.4437	-0.9666	-1.0477	-0.7948	-1.3449
1301240	1511.3	Skarn	*	-1.0778	-0.8013	-0.8207	-0.5891	-1.4584
1301240	1517	Skarn	*	-0.6680	-0.4461	-0.5821	-0.1561	-1.2660
1301240	1526.6	Skarn	*	-0.6212	-0.2534	-0.3234	-0.3260	-0.7742
1301240	1534.8	Skarn	-2.0969	-0.8887	-0.4609	-0.3729	-0.4888	-0.6264
1301240	1536	Pegmatite	-1.6990	-0.6882	-0.3335	-0.6969	-0.1676	-0.9252
1301240	1545.5	Pegmatite	-2.6990	-1.1624	-0.4202	-0.5301	-0.8010	-0.7600
1301240	1564.6	Pegmatite	*	-1.1273	-0.5376	-1.0111	-0.8272	-0.9274
1301240	1573.5	Pegmatite	*	-0.6501	-2.3979	-1.4456	-1.3512	-1.1068
1301240	1576	Pegmatite	*	-0.0269	-0.6459	-1.2270	-1.0017	-1.5436
1301240	1578	M. Peg	*	0.6726	0.9555	1.6052	1.6133	0.4719
1301240	1580	Schist	0.6611	1.2296	1.6991	1.6876	2.1303	1.1072
1301240	1581.8	M. Schist	0.4024	0.5939	1.0310	0.7867	1.4411	0.6971
1301240	1584	Schist	1.4460	0.7539	1.0342	1.2106	1.5153	0.6458
1301240	1585.6	sulphide	0.9558	0.1816	0.2704	0.4008	0.8667	0.0806

1301240	1587.3	sulphide	1.6517	1.4451	2.0734	1.8488	2.3127	1.4272
1301240	1588.2	M. Schist	1.7738	1.3945	1.8599	1.7753	2.1387	1.3160
1301240	1589.6	Sulphide	0.0941	-0.0744	0.2878	-0.0104	0.7192	-0.0581
1301240	1596.6	Pegmatite	1.6606	1.1528	1.9186	1.8762	1.9229	1.3045
1301240	1605.7	Quartzite	-0.5784	-0.4520	0.2869	-0.7513	-0.2965	-0.3311
1301240	1615.4	Quartzite	*	-0.8894	-2.0969	-1.3897	-0.5133	-0.7815
1301240	1624.6	Quartzite	*	-1.0625	-1.0862	-0.9246	-0.7840	-1.2924
1301240	1634	Quartzite	*	-0.9872	-0.8239	-0.8054	-0.5455	-1.2823

Table 46: Calculated medians from the raw magnetic susceptibility raw data tables

Sample ID	Depth	Lithology	RT1	KT10	GDD	MS2K	MS2C	SM30 B
	(ft)		(x10-3SI)	(x10-3SI)	(x10-3SI)	(x10-3SI)	(x10-3SI)	(x10-3SI)
1301080	731.0	GNAM	0.330	0.287	0.570	0.472	1.007	0.258
1301080	735.0	GN	0.000	0.083	0.150	0.165	0.202	0.069
1301080	764.0	PEG	0.000	0.063	0.020	0.032	0.087	0.038
1301080	773.0	AMPT	0.000	0.382	0.810	0.634	0.668	0.335
1301080	787.0	P2 SCH	0.000	0.371	0.760	0.688	1.142	0.333
1301080	792.0	PEG	0.000	0.105	0.070	0.045	0.373	0.127
1301080	800.0	P2 SCH	0.000	0.480	0.790	0.681	1.342	0.426
1301080	833.0	AMPT	0.020	0.784	1.680	1.661	2.745	0.699
1301080	838.0	P2 MSCH	13.020	6.453	24.800	25.464	24.435	6.490
1301080	843.0	P2 PSCH	0.000	0.410	0.250	0.113	0.593	0.390
1301080	854.0	P2 SUMX	18.640	12.450	37.100	24.543	95.751	11.100
1301080	858.0	P2? SCH	0.000	0.129	0.570	0.057	0.190	0.118
1301080	863.0	AMPT	0.000	0.383	0.690	0.538	1.237	0.358
1301080	873.0	SF QTE	0.000	0.193	0.000	0.016	0.020	0.212
1301080	882.0	SF SCH	0.000	0.285	0.320	0.200	0.815	0.232
1301080	902.0	PEG	0.000	0.029	0.000	0.030	0.065	0.025
1301080	912.0	AMPT	0.000	0.349	0.670	0.564	1.274	0.334
1301080	920.0	SF PSCH	0.000	0.256	0.350	0.319	0.698	0.261
1301080	935.0	SF QTE	0.000	0.113	0.100	0.051	0.103	0.096
1301080	937.0	AMPT	0.000	0.111	0.760	0.567	1.160	0.326
1301080	943.0	SF PSCH	0.000	0.364	0.100	*	0.149	0.040
1301080	953.0	P3 IF	5.100	3.063	9.670	3.818	79.976	4.150
1301080	991.0	PEG	0.000	0.119	0.170	0.111	0.208	0.096
1301080	1010.0	P3 IF (MT)	281.090	188.473	360.000	226.880	611.303	201.000
1301080	1020.0	IF-GRNT	59.180	44.093	69.800	43.494	221.474	40.700
1301080	1030.0	AMPT	0.000	11.343	2.420	1.364	2.642	4.810
1301080	1041.0	AMPT	5.930	0.961	1.260	0.980	2.577	0.709
1301080	1056.0	APLITE	0.000	0.025	0.000	0.005	0.042	0.012
1301020	613.5	Gneiss	0.000	0.120	0.000	0.108	0.590	0.081
1301020	629.9	AMPT	0.430	0.438	0.000	0.730	2.494	0.427
1301020	836.6	MPRD	8.850	9.404	9.730	8.740	27.470	8.340
1301020	841.5	M. SRPT	55.550	37.061	90.800	64.837	74.131	36.100
1301020	846.5	MPRD	3.925	5.167	5.745	4.380	14.267	4.615
1301020	850.4	Serpentinite	42.010	30.697	70.300	52.345	83.212	29.300
1301020	866.8	AMPT	0.170	0.367	0.000	0.574	1.086	0.327
1301020	883.9	IF	5.000	5.756	18.850	17.800	21.536	5.370
1301020	915.4	Pegmatite	0.000	0.071	0.000	0.081	0.193	0.050
1301020	996.1	Quartzite	0.000	0.007	0.000	-0.007	-0.025	-0.002
Rock		Ultramafic	42.620	47.331	47.500	49.628		46.100
Rock		Dolomite	0.000	0.112	0.000	0.087		0.089
Whole NQ		Sulphide	74.210	47.440	105.000	97.910	135.870	44.300
Whole NQ		P2 schist	0.000	0.331	0.730	0.763	0.498	0.263
Half NQ		Sulphide	78.000	56.769	102.000	105.549	138.224	58.150
Half NQ		P2 schist	0.340	0.356	0.490	0.402	0.660	0.692
KT-10 cal		sample	35.060	35.716	35.300	38.313		33.300
MS2C cal		sample	3.710	4.374	3.940	4.139	11.038	4.230
1301240	1369.0	Gneiss	0.097	0.000	0.120	0.093	0.200	0.077

1301240	1381.0	Amphibolite	0.304	0.300	0.640	0.473	1.065	0.278
1301240	1388.0	Gneiss	0.138	0.080	0.270	0.104	0.454	0.154
1301240	1391.0	Amphibolite	0.894	1.420	2.870	1.535	4.504	0.948
1301240	1409.0	Gneiss	0.158	0.080	0.220	0.395	0.686	0.152
1301240	1410.0	Amphibolite	0.348	0.040	0.640	0.457	0.644	0.110
1301240	1419.0	Gneiss	0.166	0.300	0.320	0.242	1.239	0.326
1301240	1428.0	Gneiss	0.079	0.060	0.170	0.107	0.175	0.183
1301240	1438.0	Gneiss	0.123	0.000	0.220	0.187	0.217	0.083
1301240	1447.0	Gneiss	0.118	0.000	0.170	0.081	0.246	0.122
1301240	1457.0	Pegmatite	0.089	0.000	0.120	0.090	0.587	0.138
1301240	1467.0	Amphibolite	0.280	0.000	0.560	0.440	0.202	0.065
1301240	1471.0	Gneiss	0.123	0.160	0.250	0.127	0.980	0.231
1301240	1480.0	Amphibolite	0.200	0.140	0.340	0.414	0.354	0.108
1301240	1489.0	Pegmatite	0.060	0.000	0.070	0.052	0.901	0.179
1301240	1498.0	Pegmatite	0.067	0.040	0.150	0.115	0.255	0.035
1301240	1503.0	Quartzite	0.037	0.000	0.100	0.090	0.160	0.045
1301240	1507.0	Pegmatite	0.083	0.000	0.150	0.151	0.259	0.034
1301240	1511.0	Skarn	0.186	0.000	0.370	0.262	0.698	0.055
1301240	1517.0	Skarn	0.267	0.000	0.610	0.475	0.419	0.171
1301240	1527.0	Skarn	0.130	0.000	0.340	0.479	0.326	0.236
1301240	1535.0	Skarn	0.207	0.020	0.470	0.201	0.679	0.118
1301240	1536.0	Pegmatite	0.066	0.000	0.390	0.295	0.158	0.172
1301240	1546.0	Pegmatite	0.074	0.000	0.290	0.097	0.149	0.118
1301240	1565.0	Pegmatite	0.074	0.000	0.000	0.036	0.044	0.077
1301240	1574.0	Pegmatite	0.884	0.000	0.220	0.060	0.099	0.028
1301240	1576.0	Pegmatite	4.393	0.000	9.580	40.287	41.034	2.960
1301240	1578.0	M. Peg	16.729	4.590	51.900	48.699	134.987	13.300
1301240	1580.0	Schist	3.950	2.000	10.900	6.117	27.615	4.910
1301240	1582.0	M. Schist	5.695	27.940	10.800	16.256	32.756	4.510
1301240	1584.0	Schist	1.507	9.030	1.870	2.520	7.352	1.260
1301240	1586.0	sulphide	27.785	44.830	119.000	70.593	205.357	26.700
1301240	1587.0	sulphide	24.727	59.400	72.500	59.501	137.601	20.600
1301240	1588.0	M. Schist	0.839	1.240	1.940	0.976	5.236	0.885
1301240	1590.0	Sulphide	14.377	45.680	82.800	75.224	83.713	20.300
1301240	1597.0	Pegmatite	0.362	0.260	1.940	0.177	0.505	0.473
1301240	1606.0	Quartzite	0.126	0.000	0.000	0.041	0.305	0.099
1301240	1615.0	Quartzite	0.088	0.000	0.070	0.119	0.164	0.043
1301240	1625.0	Quartzite	0.102	0.000	0.150	0.156	0.286	0.052
1301240	1634.0	Quartzite	0.132	0.000	0.100	0.088	0.225	0.074

Table 47: Shows log10 values calculated from the median values shown in table 46 above

Sample ID	Depth (ft)	Lithology	RT1 (x10-3SI)	KT10 (x10-3SI)	GDD (x10-3SI)	MS2K (x10-3SI)	MS2C (x10-3SI)	SM30 B (x10-3SI)
1301080	731.0	GNAM	-0.4815	-0.5421	-0.2441	-0.3261	0.0030	-0.5884
1301080	735.0	GN	*	-1.0809	-0.8239	-0.7825	-0.6946	-1.1612
1301080	764.0	PEG	*	-1.2007	-1.6990	-1.4949	-1.0605	-1.4202
1301080	773.0	AMPT	*	-0.4179	-0.0915	-0.1979	-0.1752	-0.4750
1301080	787.0	P2 SCH	*	-0.4306	-0.1192	-0.1624	0.0577	-0.4776
1301080	792.0	PEG	*	-0.9788	-1.1549	-1.3468	-0.4283	-0.8962
1301080	800.0	P2 SCH	*	-0.3188	-0.1024	-0.1669	0.1278	-0.3706
1301080	833.0	AMPT	-1.6990	-0.1057	0.2253	0.2204	0.4385	-0.1555
1301080	838.0	P2 MSCH	1.1146	0.8098	1.3945	1.4059	1.3880	0.8122
1301080	843.0	P2 PSCH	*	-0.3872	-0.6021	-0.9469	-0.2269	-0.4089
1301080	854.0	P2 SUMX	1.2704	1.0952	1.5694	1.3899	1.9811	1.0453
1301080	858.0	P2? SCH	*	-0.8894	-0.2441	-1.2441	-0.7212	-0.9281
1301080	863.0	AMPT	*	-0.4168	-0.1612	-0.2692	0.0924	-0.4461
1301080	873.0	SF QTE	*	-0.7144	*	-1.7959	-1.6990	-0.6737
1301080	882.0	SF SCH	*	-0.5452	-0.4949	-0.6990	-0.0888	-0.6345
1301080	902.0	PEG	*	-1.5376	*	-1.5229	-1.1871	-1.6021
1301080	912.0	AMPT	*	-0.4572	-0.1739	-0.2487	0.1052	-0.4763
1301080	920.0	SF PSCH	*	-0.5918	-0.4559	-0.4962	-0.1561	-0.5834
1301080	935.0	SF QTE	*	-0.9469	-1.0000	-1.2924	-0.9872	-1.0177
1301080	937.0	AMPT	*	-0.9547	-0.1192	-0.2464	0.0645	-0.4868
1301080	943.0	SF PSCH	*	-0.4389	-1.0000	*	-0.8268	-1.3979
1301080	953.0	P3 IF	0.7076	0.4861	0.9854	0.5818	1.9030	0.6180
1301080	991.0	PEG	*	-0.9245	-0.7696	-0.9547	-0.6819	-1.0177
1301080	1010.0	P3 IF (MT)	2.4488	2.2752	2.5563	2.3558	2.7863	2.3032
1301080	1020.0	IF-GRNT	1.7722	1.6444	1.8439	1.6384	2.3453	1.6096
1301080	1030.0	AMPT	*	1.0547	0.3838	0.1348	0.4219	0.6821
1301080	1041.0	AMPT	0.7731	-0.0173	0.1004	-0.0088	0.4111	-0.1494
1301080	1056.0	APLITE	*	-1.6021	*	-2.3010	-1.3768	-1.9208
1301020	613.5	Gneiss	*	-0.9208	*	-0.9666	-0.2291	-1.0915
1301020	629.9	AMPT	-0.3665	-0.3590	*	-0.1370	0.3968	-0.3701
1301020	836.6	MPRD	0.9469	0.9733	0.9881	0.9415	1.4389	0.9212
1301020	841.5	M. SRPT	1.7447	1.5689	1.9581	1.8118	1.8700	1.5575
1301020	846.5	MPRD	0.5938	0.7132	0.7593	0.6414	1.1543	0.6642
1301020	850.4	Serpentinite	1.6234	1.4871	1.8470	1.7189	1.9202	1.4669
1301020	866.8	AMPT	-0.7696	-0.4353	*	-0.2411	0.0356	-0.4861
1301020	883.9	IF	0.6990	0.7601	1.2753	1.2504	1.3332	0.7300
1301020	915.4	Pegmatite	*	-1.1487	*	-1.0915	-0.7144	-1.3054
1301020	996.1	Quartzite	*	-2.1549	*	*	*	*
Rock		Ultramafic	1.6296	1.6751	1.6767	1.6957	*	1.6637
Rock		Dolomite	*	-0.9527	*	-1.0605	*	-1.0506
Whole NQ		Sulphide	1.8705	1.6761	2.0212	1.9908	2.1331	1.6464
Whole NQ		P2 schist	*	-0.4802	-0.1367	-0.1178	-0.3028	-0.5800
Half NQ		Sulphide	1.8921	1.7541	2.0086	2.0235	2.1406	1.7645
Half NQ		P2 schist	-0.4685	-0.4486	-0.3098	-0.3958	-0.1805	-0.1599
KT-10 cal		sample	1.5448	1.5529	1.5478	1.5833	*	1.5224
MS2C cal		sample	0.5694	0.6409	0.5955	0.6169	1.0429	0.6263

1301240	1369.0	Gneiss	-1.0132	*	-0.9208	-1.0315	-0.6990	-1.1135
1301240	1381.0	Amphibolite	-0.5171	-0.5229	-0.1938	-0.3251	0.0273	-0.5560
1301240	1388.0	Gneiss	-0.8601	-1.0969	-0.5686	-0.9830	-0.3429	-0.8125
1301240	1391.0	Amphibolite	-0.0487	0.1523	0.4579	0.1861	0.6536	-0.0232
1301240	1409.0	Gneiss	-0.8013	-1.0969	-0.6576	-0.4034	-0.1637	-0.8182
1301240	1410.0	Amphibolite	-0.4584	-1.3979	-0.1938	-0.3401	-0.1911	-0.9586
1301240	1419.0	Gneiss	-0.7799	-0.5229	-0.4949	-0.6162	0.0931	-0.4868
1301240	1428.0	Gneiss	-1.1024	-1.2218	-0.7696	-0.9706	-0.7570	-0.7375
1301240	1438.0	Gneiss	-0.9101	*	-0.6576	-0.7282	-0.6635	-1.0809
1301240	1447.0	Gneiss	-0.9281	*	-0.7696	-1.0915	-0.6091	-0.9136
1301240	1457.0	Pegmatite	-1.0506	*	-0.9208	-1.0458	-0.2314	-0.8601
1301240	1467.0	Amphibolite	-0.5528	*	-0.2518	-0.3565	-0.6946	-1.1871
1301240	1471.0	Gneiss	-0.9101	-0.7959	-0.6021	-0.8962	-0.0088	-0.6364
1301240	1480.0	Amphibolite	-0.6990	-0.8539	-0.4685	-0.3830	-0.4510	-0.9666
1301240	1489.0	Pegmatite	-1.2218	*	-1.1549	-1.2840	-0.0453	-0.7471
1301240	1498.0	Pegmatite	-1.1739	-1.3979	-0.8239	-0.9393	-0.5935	-1.4559
1301240	1503.0	Quartzite	-1.4318	*	-1.0000	-1.0458	-0.7959	-1.3468
1301240	1507.0	Pegmatite	-1.0809	*	-0.8239	-0.8210	-0.5867	-1.4685
1301240	1511.0	Skarn	-0.7305	*	-0.4318	-0.5817	-0.1561	-1.2596
1301240	1517.0	Skarn	-0.5735	*	-0.2147	-0.3233	-0.3778	-0.7670
1301240	1527.0	Skarn	-0.8861	*	-0.4685	-0.3197	-0.4868	-0.6271
1301240	1535.0	Skarn	-0.6840	-1.6990	-0.3279	-0.6968	-0.1681	-0.9281
1301240	1536.0	Pegmatite	-1.1805	*	-0.4089	-0.5302	-0.8013	-0.7645
1301240	1546.0	Pegmatite	-1.1308	*	-0.5376	-1.0132	-0.8268	-0.9281
1301240	1565.0	Pegmatite	-1.1308	*	*	-1.4437	-1.3565	-1.1135
1301240	1574.0	Pegmatite	-0.0535	*	-0.6576	-1.2218	-1.0044	-1.5528
1301240	1576.0	Pegmatite	0.6428	*	0.9814	1.6052	1.6131	0.4713
1301240	1578.0	M. Peg	1.2235	0.6618	1.7152	1.6875	2.1303	1.1239
1301240	1580.0	Schist	0.5966	0.3010	1.0374	0.7865	1.4411	0.6911
1301240	1582.0	M. Schist	0.7555	1.4462	1.0334	1.2110	1.5153	0.6542
1301240	1584.0	Schist	0.1781	0.9557	0.2718	0.4014	0.8664	0.1004
1301240	1586.0	sulphide	1.4438	1.6516	2.0755	1.8488	2.3125	1.4265
1301240	1587.0	sulphide	1.3932	1.7738	1.8603	1.7745	2.1386	1.3139
1301240	1588.0	M. Schist	-0.0762	0.0934	0.2878	-0.0106	0.7190	-0.0531
1301240	1590.0	Sulphide	1.1577	1.6597	1.9180	1.8764	1.9228	1.3075
1301240	1597.0	Pegmatite	-0.4413	-0.5850	0.2878	-0.7520	-0.2967	-0.3251
1301240	1606.0	Quartzite	-0.8996	*	*	-1.3872	-0.5157	-1.0044
1301240	1615.0	Quartzite	-1.0555	*	-1.1549	-0.9245	-0.7852	-1.3665
1301240	1625.0	Quartzite	-0.9914	*	-0.8239	-0.8069	-0.5436	-1.2840
1301240	1634.0	Quartzite	-0.8794	*	-1.0000	-1.0555	-0.6478	-1.1308

Table 48: Calculated standard deviations from the magnetic susceptibilities raw data tables above.

Sample ID	Depth	Lithology	RT1	KT10	GDD	MS2K	MS2C	SM30 B
1301080	731	GNAM	0.007	0.006	0.018	0.001	0.002	0.002
1301080	735	GN	0.000	0.004	0.020	0.001	0.002	0.003
1301080	764	PEG	0.000	0.001	0.000	0.000	0.000	0.001
1301080	773	AMPT	0.000	0.005	0.011	0.002	0.001	0.002
1301080	787	P2 SCH	0.000	0.007	0.020	0.004	0.003	0.007
1301080	792	PEG	0.000	0.015	0.025	0.000	0.003	0.016
1301080	800	P2 SCH	0.000	0.028	0.018	0.006	0.002	0.015
1301080	833	AMPT	0.008	0.037	0.072	0.005	0.007	0.023
1301080	838	P2 MSCH	0.043	0.463	0.148	1.204	0.033	0.136
1301080	843	P2 PSCH	0.000	0.020	0.032	0.001	0.004	0.072
1301080	854	P2 SUMX	0.046	0.177	0.084	0.247	0.152	0.303
1301080	858	P2? SCH	0.000	0.010	0.023	0.001	0.002	0.010
1301080	863	AMPT	0.000	0.006	0.013	0.001	0.002	0.003
1301080	873	SF QTE	0.000	0.069	0.000	0.000	0.001	0.116
1301080	882	SF SCH	0.000	0.018	0.023	0.000	0.002	0.010
1301080	902	PEG	0.000	0.008	0.009	0.001	0.002	0.003
1301080	912	AMPT	0.000	0.002	0.105	0.006	0.001	0.008
1301080	920	SF PSCH	0.000	0.007	0.020	0.001	0.002	0.012
1301080	935	SF QTE	0.000	0.004	0.016	0.003	0.002	0.005
1301080	937	AMPT	0.000	0.005	0.037	0.009	0.002	0.007
1301080	943	SF PSCH	0.000	0.007	0.018	*	0.003	0.005
1301080	953	P3 IF	0.041	0.156	0.054	0.014	0.001	0.587
1301080	991	PEG	0.000	0.005	0.016	0.002	0.003	0.008
1301080	1010	P3 IF (MT)	1.341	3.192	0.894	1.411	0.005	5.505
1301080	1020	IF-GRNT	0.179	6.618	0.158	0.226	0.006	6.672
1301080	1030	AMPT	0.000	1.815	0.018	0.005	0.002	0.575
1301080	1041	AMPT	0.029	0.088	0.009	0.003	0.001	0.054
1301080	1056	APLITE	0.000	0.007	0.000	0.000	0.005	0.001
1301020	613.5	Gneiss	0.000	0.002	0.000	0.010	0.197	0.001
1301020	629.9	AMPT	0.009	0.010	0.054	0.014	0.190	0.007
1301020	836.6	MPRD	0.016	0.280	0.225	0.169	0.008	0.417
1301020	841.5	M. SRPT	1.305	0.200	1.198	0.754	10.518	0.419
1301020	846.5	MPRD	0.011	0.356	0.336	0.097	0.008	0.185
1301020	850.4	Serpentinite	0.137	0.601	0.266	2.077	0.004	0.216
1301020	866.8	AMPT	0.008	0.006	0.027	0.016	0.100	0.003
1301020	883.9	IF	0.016	0.076	0.375	0.054	0.002	0.123
1301020	915.4	Pegmatite	0.000	0.007	0.000	0.001	0.005	0.002
1301020	996.1	Quartzite	0.000	0.002	0.000	0.000	0.004	0.002
Rock sample		Ultramafic	0.293	0.219	0.173	3.071	*	0.294
Rock sample		Dolomite	0.000	0.003	0.000	0.014	*	0.002
Whole NQ		Sulphide	0.162	0.472	5.010	0.429	0.185	0.213
Whole NQ		P2 schist	0.000	0.027	0.201	0.032	0.001	0.007
Half NQ		Sulphide	0.813	1.419	0.724	1.430	0.131	2.452
Half NQ		P2 schist	0.017	0.022	0.084	0.007	0.004	0.135

KT-10 Cal		sample	0.314	0.053	0.246	0.804	*	0.089
MS2C Cal		sample	0.0389	0.1337	0.0664	0.0509	0.0033	0.0434
1301240	1369	Gneiss	0.033	0.004	0.009	0.000	0.002	0.002
1301240	1381	Amphibolite	0.004	0.009	0.023	0.001	0.003	0.010
1301240	1388	Gneiss	0.043	0.003	0.000	0.000	0.002	0.008
1301240	1391	Amphibolite	0.035	0.013	0.011	0.001	0.016	0.022
1301240	1409	Gneiss	0.008	0.006	0.016	0.001	0.001	0.004
1301240	1410	Amphibolite	0.010	0.016	0.013	0.003	0.001	0.001
1301240	1419	Gneiss	0.004	0.002	0.023	0.000	0.002	0.003
1301240	1428	Gneiss	0.013	0.004	0.009	0.000	0.004	0.004
1301240	1438	Gneiss	0.018	0.003	0.009	0.001	0.006	0.002
1301240	1447	Gneiss	0.000	0.013	0.009	0.001	0.004	0.004
1301240	1457	Pegmatite	0.000	0.002	0.009	0.000	0.005	0.007
1301240	1467	Amphibolite	0.000	0.005	0.016	0.001	0.003	0.002
1301240	1471	Gneiss	0.037	0.004	0.009	0.001	0.003	0.010
1301240	1480	Amphibolite	0.009	0.007	0.011	0.001	0.004	0.001
1301240	1489	Pegmatite	0.000	0.005	0.013	0.001	0.002	0.005
1301240	1498	Pegmatite	0.004	0.009	0.013	0.000	0.002	0.001
1301240	1503	Quartzite	0.000	0.014	0.011	0.000	0.003	0.001
1301240	1507	Pegmatite	0.000	0.003	0.011	0.001	0.003	0.001
1301240	1511	Skarn	0.000	0.046	0.016	0.000	0.001	0.001
1301240	1517	Skarn	0.000	0.058	0.105	0.002	0.127	0.006
1301240	1527	Skarn	0.018	0.004	0.013	0.125	0.005	0.005
1301240	1535	Skarn	0.007	0.003	0.013	0.001	0.005	0.002
1301240	1536	Pegmatite	0.004	0.004	0.022	0.001	0.003	0.003
1301240	1546	Pegmatite	0.000	0.002	0.000	0.000	0.002	0.001
1301240	1565	Pegmatite	0.000	0.336	0.009	0.001	0.002	0.003
1301240	1574	Pegmatite	0.000	0.283	0.013	0.000	0.001	0.003
1301240	1576	Pegmatite	0.000	0.538	1.191	0.403	0.046	0.283
1301240	1578	M. Peg	0.043	1.851	4.554	0.052	0.108	1.049
1301240	1580	Schist	1.187	0.184	0.422	0.008	0.042	0.199
1301240	1582	M. Schist	0.071	0.445	0.179	0.052	0.067	0.337
1301240	1584	Schist	0.013	0.167	0.013	0.011	0.025	0.133
1301240	1586	sulphide	0.023	0.190	0.894	0.045	0.450	0.288
1301240	1587	sulphide	0.213	0.711	0.466	0.721	0.199	0.600
1301240	1588	M. Schist	0.016	0.010	0.014	0.000	0.016	0.048
1301240	1590	Sulphide	0.206	0.351	0.894	0.630	0.156	0.611
1301240	1597	Pegmatite	0.009	0.014	0.017	0.001	0.002	0.018
1301240	1606	Quartzite	0.000	0.009	0.011	0.001	0.005	0.159
1301240	1615	Quartzite	0.000	0.002	0.016	0.000	0.006	0.019
1301240	1625	Quartzite	0.000	0.003	0.000	0.000	0.004	0.006
1301240	1634	Quartzite	0.000	0.010	0.018	0.000	0.003	0.011

Table 49: Shows calculated coefficient of variation from the three selected holes, rocks samples, two NQ core samples (whole & split sumx & schist) and calibration samples

Sample ID	Depth	Lithology	RT1	KT10	GDD	MS2K	MS2C	SM30 B
1301080	731	GNAM	0.007	0.006	0.018	0.001	0.002	0.002
1301080	735	GN	0.000	0.004	0.020	0.001	0.002	0.003
1301080	764	PEG	0.000	0.001	0.000	0.000	0.000	0.001
1301080	773	AMPT	0.000	0.005	0.011	0.002	0.001	0.002
1301080	787	P2 SCH	0.000	0.007	0.020	0.004	0.003	0.007
1301080	792	PEG	0.000	0.015	0.025	0.000	0.003	0.016
1301080	800	P2 SCH	0.000	0.028	0.018	0.006	0.002	0.015
1301080	833	AMPT	0.008	0.037	0.072	0.005	0.007	0.023
1301080	838	P2 MSCH	0.043	0.463	0.148	1.204	0.033	0.136
1301080	843	P2 PSCH	0.000	0.020	0.032	0.001	0.004	0.072
1301080	854	P2 SUMX	0.046	0.177	0.084	0.247	0.152	0.303
1301080	858	P2? SCH	0.000	0.010	0.023	0.001	0.002	0.010
1301080	863	AMPT	0.000	0.006	0.013	0.001	0.002	0.003
1301080	873	SF QTE	0.000	0.069	0.000	0.000	0.001	0.116
1301080	882	SF SCH	0.000	0.018	0.023	0.000	0.002	0.010
1301080	902	PEG	0.000	0.008	0.009	0.001	0.002	0.003
1301080	912	AMPT	0.000	0.002	0.105	0.006	0.001	0.008
1301080	920	SF PSCH	0.000	0.007	0.020	0.001	0.002	0.012
1301080	935	SF QTE	0.000	0.004	0.016	0.003	0.002	0.005
1301080	937	AMPT	0.000	0.005	0.037	0.009	0.002	0.007
1301080	943	SF PSCH	0.000	0.007	0.018	#DIV/0!	0.003	0.005
1301080	953	P3 IF	0.041	0.156	0.054	0.014	0.001	0.587
1301080	991	PEG	0.000	0.005	0.016	0.002	0.003	0.008
1301080	1010	P3 IF (MT)	1.341	3.192	0.894	1.411	0.005	5.505
1301080	1020	IF-GRNT	0.179	6.618	0.158	0.226	0.006	6.672
1301080	1030	AMPT	0.000	1.815	0.018	0.005	0.002	0.575
1301080	1041	AMPT	0.029	0.088	0.009	0.003	0.001	0.054
1301080	1056	APLITE	0.000	0.007	0.000	0.000	0.005	0.001
1301020	613.5	Gneiss	0.009	0.010	0.054	0.014	0.190	0.007
1301020	629.9	AMPT	0.016	0.280	0.225	0.169	0.008	0.417
1301020	836.6	MPRD	1.305	0.200	1.198	0.754	10.518	0.419
1301020	841.5	M. SRPT	0.011	0.356	0.336	0.097	0.008	0.185
1301020	846.5	MPRD	0.137	0.601	0.266	2.077	0.004	0.216
1301020	850.4	Serpentinite	0.008	0.006	0.027	0.016	0.100	0.003
1301020	866.8	AMPT	0.016	0.076	0.375	0.054	0.002	0.123
1301020	883.9	IF	0.000	0.007	0.000	0.001	0.005	0.002
1301020	915.4	PEGMATITE	*	0.075	*	0.007	0.108	0.035
1301020	996.1	Quartzite	*	0.311	0	-0.067	-0.159	-0.906
Rock sample		Ultramafic	0.293	0.219	0.173	3.071	*	0.294
Rock sample		Dolomite	0.000	0.003	0.000	0.014	*	0.002
Whole NQ		Sumx	0.162	0.472	5.010	0.429	0.185	0.213
Whole NQ		P2 schist	0.000	0.027	0.201	0.032	0.001	0.007
Half NQ		Sumx	0.813	1.419	0.724	1.430	0.131	2.452

Half NQ		P2 Schist	0.017	0.022	0.084	0.007	0.004	0.135
KT-10 Cal		sample	0.314	0.053	0.246	0.804	*	0.089
MS2C Cal		Sample	0.010	0.031	0.017	0.012	0.003	0.010
1301240	1369	Gneiss	0.033	0.004	0.009	0.000	0.002	0.002
1301240	1381	Amphibolite	0.004	0.009	0.023	0.001	0.003	0.010
1301240	1388	Gneiss	0.043	0.003	0.000	0.000	0.002	0.008
1301240	1391	Amphibolite	0.035	0.013	0.011	0.001	0.016	0.022
1301240	1409	Gneiss	0.008	0.006	0.016	0.001	0.001	0.004
1301240	1410	Amphibolite	0.010	0.016	0.013	0.003	0.001	0.001
1301240	1419	Gneiss	0.004	0.002	0.023	0.000	0.002	0.003
1301240	1428	Gneiss	0.013	0.004	0.009	0.000	0.004	0.004
1301240	1438	Gneiss	0.018	0.003	0.009	0.001	0.006	0.002
1301240	1447	Gneiss	0.000	0.013	0.009	0.001	0.004	0.004
1301240	1457	Pegmatite	0.000	0.002	0.009	0.000	0.005	0.007
1301240	1467	Amphibolite	0.000	0.005	0.016	0.001	0.003	0.002
1301240	1471	Gneiss	0.037	0.004	0.009	0.001	0.003	0.010
1301240	1480	Amphibolite	0.009	0.007	0.011	0.001	0.004	0.001
1301240	1489	Pegmatite	0.000	0.005	0.013	0.001	0.002	0.005
1301240	1498	Pegmatite	0.004	0.009	0.013	0.000	0.002	0.001
1301240	1503	Quartzite	0.000	0.014	0.011	0.000	0.003	0.001
1301240	1507	Pegmatite	0.000	0.003	0.011	0.001	0.003	0.001
1301240	1511	Skarn	0.000	0.046	0.016	0.000	0.001	0.001
1301240	1517	Skarn	0.000	0.058	0.105	0.002	0.127	0.006
1301240	1527	Skarn	0.018	0.004	0.013	0.125	0.005	0.005
1301240	1535	Skarn	0.007	0.003	0.013	0.001	0.005	0.002
1301240	1536	Pegmatite	0.004	0.004	0.022	0.001	0.003	0.003
1301240	1546	Pegmatite	0.000	0.002	0.000	0.000	0.002	0.001
1301240	1565	Pegmatite	0.000	0.336	0.009	0.001	0.002	0.003
1301240	1574	Pegmatite	0.000	0.283	0.013	0.000	0.001	0.003
1301240	1576	Pegmatite	0.000	0.538	1.191	0.403	0.046	0.283
1301240	1578	M. Peg	0.043	1.851	4.554	0.052	0.108	1.049
1301240	1580	Schist	1.187	0.184	0.422	0.008	0.042	0.199
1301240	1582	M. Schist	0.071	0.445	0.179	0.052	0.067	0.337
1301240	1584	Schist	0.013	0.167	0.013	0.011	0.025	0.133
1301240	1586	sulphide	0.023	0.190	0.894	0.045	0.450	0.288
1301240	1587	sulphide	0.213	0.711	0.466	0.721	0.199	0.600
1301240	1588	M. Schist	0.016	0.010	0.014	0.000	0.016	0.048
1301240	1590	Sumx	0.206	0.351	0.894	0.630	0.156	0.611
1301240	1597	Pegmatite	0.009	0.014	0.017	0.001	0.002	0.018
1301240	1606	Quartzite	0.000	0.009	0.011	0.001	0.005	0.159
1301240	1615	Quartzite	0.000	0.002	0.016	0.000	0.006	0.019
1301240	1625	Quartzite	0.000	0.003	0.000	0.000	0.004	0.006
1301240	1634	Quartzite	0.000	0.010	0.018	0.000	0.003	0.011

Table 50: Shows calculated log_{10} from the coefficient of variations from the three selected holes, rock samples, two NQ core samples (whole & split sumx & schist) and calibration samples

Sample ID	Depth	Lithology	RT1	KT10	GDD	MS2K	MS2C	SM30 B
1301080	731	GNAM	-2.1549	-2.2218	-1.7447	-3.0000	-2.6990	-2.6990
1301080	735	GN		-2.3979	-1.6990	-3.0000	-2.6990	-2.5229
1301080	764	PEG		-3.0000				-3.0000
1301080	773	AMPT		-2.3010	-1.9586	-2.6990	-3.0000	-2.6990
1301080	787	P2 SCH		-2.1549	-1.6990	-2.3979	-2.5229	-2.1549
1301080	792	PEG		-1.8239	-1.6021		-2.5229	-1.7959
1301080	800	P2 SCH		-1.5528	-1.7447	-2.2218	-2.6990	-1.8239
1301080	833	AMPT	-2.0969	-1.4318	-1.1427	-2.3010	-2.1549	-1.6383
1301080	838	P2 MSCH	-1.3665	-0.3344	-0.8297	0.0806	-1.4815	-0.8665
1301080	843	P2 PSCH		-1.6990	-1.4949	-3.0000	-2.3979	-1.1427
1301080	854	P2 SUMX	-1.3372	-0.7520	-1.0757	-0.6073	-0.8182	-0.5186
1301080	858	P2? SCH		-2.0000	-1.6383	-3.0000	-2.6990	-2.0000
1301080	863	AMPT		-2.2218	-1.8861	-3.0000	-2.6990	-2.5229
1301080	873	SF QTE		-1.1612			-3.0000	-0.9355
1301080	882	SF SCH		-1.7447	-1.6383		-2.6990	-2.0000
1301080	902	PEG		-2.0969	-2.0458	-3.0000	-2.6990	-2.5229
1301080	912	AMPT		-2.6990	-0.9788	-2.2218	-3.0000	-2.0969
1301080	920	SF PSCH		-2.1549	-1.6990	-3.0000	-2.6990	-1.9208
1301080	935	SF QTE		-2.3979	-1.7959	-2.5229	-2.6990	-2.3010
1301080	937	AMPT		-2.3010	-1.4318	-2.0458	-2.6990	-2.1549
1301080	943	SF PSCH		-2.1549	-1.7447		-2.5229	-2.3010
1301080	953	P3 IF	-1.3872	-0.8069	-1.2676	-1.8539	-3.0000	-0.2314
1301080	991	PEG		-2.3010	-1.7959	-2.6990	-2.5229	-2.0969
1301080	1010	P3 IF (MT)	0.1274	0.5041	-0.0487	0.1495	-2.3010	0.7408
1301080	1020	IF-GRNT	-0.7471	0.8207	-0.8013	-0.6459	-2.2218	0.8243
1301080	1030	AMPT		0.2589	-1.7447	-2.3010	-2.6990	-0.2403
1301080	1041	AMPT	-1.5376	-1.0555	-2.0458	-2.5229	-3.0000	-1.2676
1301080	1056	APLITE		-2.1549			-2.3010	-3.0000
1301020	613.5	Gneiss	-2.0458	-2.0000	-1.2676	-1.8539	-0.7212	-2.1549
1301020	629.9	AMPT	-1.7959	-0.5528	-0.6478	-0.7721	-2.0969	-0.3799
1301020	836.6	MPRD	0.1156	-0.6990	0.0785	-0.1226	1.0219	-0.3778
1301020	841.5	M. SRPT	-1.9586	-0.4486	-0.4737	-1.0132	-2.0969	-0.7328
1301020	846.5	MPRD	-0.8633	-0.2211	-0.5751	0.3174	-2.3979	-0.6655
1301020	850.4	Serpentinite	-2.0969	-2.2218	-1.5686	-1.7959	-1.0000	-2.5229
1301020	866.8	AMPT	-1.7959	-1.1192	-0.4260	-1.2676	-2.6990	-0.9101
1301020	883.9	IF		-2.1549		-3.0000	-2.3010	-2.6990
1301020	915.4	PEGMATITE		-1.1249		-2.1549	-0.9666	-1.4559
1301020	996.1	Quartzite		-0.5072				
Rock sample		Ultramafic	-0.5331	-0.6596	-0.7620	0.4873		-0.5317
Rock sample		Dolomite		-2.5229		-1.8539		-2.6990
Whole NQ		Sumx	-0.7905	-0.3261	0.6998	-0.3675	-0.7328	-0.6716
Whole NQ		P2 schist		-1.5686	-0.6968	-1.4949	-3.0000	-2.1549
Half NQ		Sumx	-0.0899	0.1520	-0.1403	0.1553	-0.8827	0.3895
Half NQ		P2 Schist	-1.7696	-1.6576	-1.0757	-2.1549	-2.3979	-0.8697

KT-10 Cal		sample	-0.5031	-1.2757	-0.6091	-0.0947		-1.0506
MS2C Cal		Sample	-2.0000	-1.5086	-1.7696	-1.9208	-2.5229	-2.0000
1301240	1369	Gneiss	-1.4815	-2.3979	-2.0458		-2.6990	-2.6990
1301240	1381	Amphibolite	-2.3979	-2.0458	-1.6383	-3.0000	-2.5229	-2.0000
1301240	1388	Gneiss	-1.3665	-2.5229			-2.6990	-2.0969
1301240	1391	Amphibolite	-1.4559	-1.8861	-1.9586	-3.0000	-1.7959	-1.6576
1301240	1409	Gneiss	-2.0969	-2.2218	-1.7959	-3.0000	-3.0000	-2.3979
1301240	1410	Amphibolite	-2.0000	-1.7959	-1.8861	-2.5229	-3.0000	-3.0000
1301240	1419	Gneiss	-2.3979	-2.6990	-1.6383		-2.6990	-2.5229
1301240	1428	Gneiss	-1.8861	-2.3979	-2.0458		-2.3979	-2.3979
1301240	1438	Gneiss	-1.7447	-2.5229	-2.0458	-3.0000	-2.2218	-2.6990
1301240	1447	Gneiss		-1.8861	-2.0458	-3.0000	-2.3979	-2.3979
1301240	1457	Pegmatite		-2.6990	-2.0458		-2.3010	-2.1549
1301240	1467	Amphibolite		-2.3010	-1.7959	-3.0000	-2.5229	-2.6990
1301240	1471	Gneiss	-1.4318	-2.3979	-2.0458	-3.0000	-2.5229	-2.0000
1301240	1480	Amphibolite	-2.0458	-2.1549	-1.9586	-3.0000	-2.3979	-3.0000
1301240	1489	Pegmatite		-2.3010	-1.8861	-3.0000	-2.6990	-2.3010
1301240	1498	Pegmatite	-2.3979	-2.0458	-1.8861		-2.6990	-3.0000
1301240	1503	Quartzite		-1.8539	-1.9586		-2.5229	-3.0000
1301240	1507	Pegmatite		-2.5229	-1.9586	-3.0000	-2.5229	-3.0000
1301240	1511	Skarn		-1.3372	-1.7959		-3.0000	-3.0000
1301240	1517	Skarn		-1.2366	-0.9788	-2.6990	-0.8962	-2.2218
1301240	1527	Skarn	-1.7447	-2.3979	-1.8861	-0.9031	-2.3010	-2.3010
1301240	1535	Skarn	-2.1549	-2.5229	-1.8861	-3.0000	-2.3010	-2.6990
1301240	1536	Pegmatite	-2.3979	-2.3979	-1.6576	-3.0000	-2.5229	-2.5229
1301240	1546	Pegmatite		-2.6990			-2.6990	-3.0000
1301240	1565	Pegmatite		-0.4737	-2.0458	-3.0000	-2.6990	-2.5229
1301240	1574	Pegmatite		-0.5482	-1.8861		-3.0000	-2.5229
1301240	1576	Pegmatite		-0.2692	0.0759	-0.3947	-1.3372	-0.5482
1301240	1578	M. Peg	-1.3665	0.2674	0.6584	-1.2840	-0.9666	0.0208
1301240	1580	Schist	0.0745	-0.7352	-0.3747	-2.0969	-1.3768	-0.7011
1301240	1582	M. Schist	-1.1487	-0.3516	-0.7471	-1.2840	-1.1739	-0.4724
1301240	1584	Schist	-1.8861	-0.7773	-1.8861	-1.9586	-1.6021	-0.8761
1301240	1586	sulphide	-1.6383	-0.7212	-0.0487	-1.3468	-0.3468	-0.5406
1301240	1587	sulphide	-0.6716	-0.1481	-0.3316	-0.1421	-0.7011	-0.2218
1301240	1588	M. Schist	-1.7959	-2.0000	-1.8539		-1.7959	-1.3188
1301240	1590	Sumx	-0.6861	-0.4547	-0.0487	-0.2007	-0.8069	-0.2140
1301240	1597	Pegmatite	-2.0458	-1.8539	-1.7696	-3.0000	-2.6990	-1.7447
1301240	1606	Quartzite		-2.0458	-1.9586	-3.0000	-2.3010	-0.7986
1301240	1615	Quartzite		-2.6990	-1.7959		-2.2218	-1.7212
1301240	1625	Quartzite		-2.5229			-2.3979	-2.2218
1301240	1634	Quartzite		-2.0000	-1.7447		-2.5229	-1.9586

Table 51: Calculated means, standard deviations, percent coefficient of variations, range and variance that were used in assessing the suitable modes in each instrument; data was obtained from borehole 1301020.

Gneiss @ 613.5 ft						
	Mean	**Units**	**StD**	**%CV**	**Range**	**Variance**
RT 1	0	10-3SI	0	*	0	0.00E+00
SM30 Mode A	0.0878	10-3SI	0.0013	1.5247	0.005	1.79E-06
SM30 Mode B	0.0817	10-3SI	0.0015	1.8328	0.006	2.24E-06
SM30 Extrapolation	0.1087	10-3SI	0.0013	1.1671	0.005	1.61E-06
SM30 Interpolation	0.1076	10-3SI	0.0018	1.6896	0.007	3.31E-06
SM30 Scanning mode	0.1091	10-3SI	0.0011	1.0259	0.004	1.25E-06
MS2C	-0.8161	10-3SI	0.3351	-41.0557	1.1846	1.12E-01
MS2K	0.1124	10-3SI	0.0108	9.6207	0.0469	1.17E-04
GDD	0	10-3SI	0	*	0	0.00E+00
KT 10	0.1186	10-3SI	0.0027	2.2736	0.01	7.27E-06
Amphibolite @ 629.9 ft						
	Mean		**StD**	**%CV**	**Range**	**Variance**
RT 1	0.422	x10-3 SI	0.0121	2.8621	0.0004	
SM30 Mode A	0.4046	x10-3 SI	0.0061	1.5098	0.034	3.73E-05
SM30 Mode B	0.4267	x10-3 SI	0.0067	1.5641	0.036	4.45E-05
SM30 Extrapolation	0.4231	x10-3 SI	0.0105	2.475	0.055	1.10E-04
SM30 Interpolation	0.4257	x10-3 SI	0.0057	1.3334	0.024	3.22E-05
Scanning mode	0.4259	x10-3 SI	0.0013	0.3074	0.006	1.71E-06
MS2C	-2.6483		0.2959	-11.172	1.0259	8.75E-02
MS2K	0.7177	x10-3 SI	0.0139	1.9373	0.0549	1.93E-04
GDD	0	x10-3 SI	0	*	0	0.00E+00
KT 10	0.4399	x10-3 SI	0.0097	2.1999	0.038	9.36E-05
Mineralized peridotite @ 836.6 ft						
	Mean		**StD**	**%CV**	**Range**	**Variance**
RT 1	8.8415	x10-3 SI	0.0258	0.2922	0.11	
SM30 Mode A	9.076	x10-3 SI	0.5554	6.119	2.14	3.08E-01
SM30 Mode B	8.5	x10-3 SI	0.417	4.9054	1.63	1.74E-01
SM30 Extrapolation	8.742	x10-3 SI	0.4263	4.8768	1.42	1.82E-01
SM30 Interpolation	8.6215	x10-3 SI	0.5775	6.6984	2.1	3.34E-01
SM30 Scanning	9.8075	x10-3 SI	0.0013	0.0133	2.1	1.71E-06
MS2C	27.4685	x10-3 SI	0.0086	0.0314	0.034	7.44E-05
MS2K	8.5826	x10-3 SI	0.2901	3.38	1.5945	8.42E-02
GDD Probe	9.7285	x10-3 SI	0.2361	2.4268	0.75	5.57E-02
KT 10	9.3393	x10-3 SI	0.2286	2.4474	1.132	5.22E-02
Mineralized serpentinite @ 841.5 ft						
	Mean		**StD**	**%CV**	**Range**	**Variance**
RT 1	55.4123	x10-3 SI	1.076	1.9418	3.88	
SM30 Mode A	35.375	x10-3 SI	0.2511	0.7097	0.9	6.30E-02
SM30 Mode B	36.02	x10-3 SI	0.4188	1.1626	1.5	1.75E-01
SM30 Extrapolation	35.95	x10-3 SI	0.4818	1.3401	1.5	2.32E-01
SM30 Interpolation	35.47	x10-3 SI	0.6891	1.9427	2.2	4.75E-01
SM30 Scanning	35.9278	x10-3 SI	0.274	0.7626	1	7.51E-02
MS2C	75.8126	x10-3 SI	9.4776	12.5014	28.836	8.98E+01
MS2K	64.6689	x10-3 SI	0.5752	0.8895	2.793	3.31E-01
GDD Probe	90.92	x10-3 SI	1.1981	1.3177	3.8	1.44E+00

KT 10	36.9339	x10-3 SI	0.3466	0.9384	1.661	1.20E-01
Mineralized Peridotite @ 846.5 ft						
	Mean		**StD**	**%CV**	**Range**	**Variance**
RT 1	3.9385	x10-3 SI	0.1574	0.3996	0.06	
SM30 Mode A	4.7455	x10-3 SI	0.1273	2.6825	0.39	1.62E-02
SM30 Mode B	4.652	x10-3 SI	0.1852	3.9818	0.7	3.43E-02
SM30 Extrapolation	4.702	x10-3 SI	0.1972	4.1941	0.73	3.89E-02
SM30 Interpolation	5.5505	x10-3 SI	0.4659	8.3933	1.76	2.17E-01
SM30 Scanning	4.775	x10-3 SI	0.2003	4.1943	0.7	4.01E-02
MS2C	14.2675	x10-3 SI	0.0077	0.0539	0.027	5.91E-05
MS2K	4.3117	x10-3 SI	0.1248	2.8952	0.6111	1.56E-02
GDD Probe	5.7555	x10-3 SI	0.3359	5.8366	1.14	1.13E-01
KT 10	5.0967	x10-3 SI	0.3261	6.399	1.422	1.06E-01
Serpentinite @ 850.4 ft						
	Mean		**StD**	**%CV**	**Range**	**Variance**
RT 1	41.9963	x10-3 SI	0.134	0.319	0.64	
SM30 Mode A	29.2176	x10-3 SI	0.1015	0.3473	0.4	1.03E-02
SM30 Mode B	29.265	x10-3 SI	0.2159	0.7377	0.8	4.66E-02
SM30 Extrapolation	29.18	x10-3 SI	0.1361	0.4665	0.5	1.85E-02
SM30 Interpolation	29.165	x10-3 SI	0.2681	0.9192	1	7.19E-02
Scanning mode	28.355	x10-3 SI	0.5549	1.9568	1.7	3.08E-01
MS2C	83.2085	x10-3 SI	0.005	0.006	0.019	2.53E-05
MS2K	52.4556	x10-3 SI	1.9066	3.6346	9.073	3.63E+00
GDD	70.315	x10-3 SI	0.2661	0.3785	0.9	7.08E-02
KT 10	30.5903	x10-3 SI	0.5515	1.8027	2.474	3.04E-01
Amphibolite @ 866.8 ft						
	Mean		**StD**	**%CV**	**Range**	**Variance**
RT 1	0.1691	x10-3 SI	0.0085	5.0435	0.02	
SM30 Mode A	0.3323	x10-3 SI	0.0044	1.3136	0.02	1.91E-05
SM30 Mode B	0.3266	x10-3 SI	0.0032	0.9759	0.012	1.02E-05
SM30 Extrapolation	0.3275	x10-3 SI	0.0026	0.7956	0.011	6.79E-06
SM30 Interpolation	0.3289	x10-3 SI	0.0036	1.0998	0.014	1.31E-05
SM30 Scanning	0.3311	x10-3 SI	0.0036	1.1022	0.012	1.33E-05
MS2C	1.0378	x10-3 SI	0.1114	10.7301	0.3346	1.24E-02
MS2K	0.5723	x10-3 SI	0.0141	2.4639	0.0747	1.99E-04
GDD Probe	0	x10-3 SI	0	*	0	0.00E+00
KT 10	0.3657	x10-3 SI	0.0053	1.4369	0.027	2.76E-05
Iron formation @ 883.9 ft						
	Mean		**StD**	**%CV**	**Range**	**Variance**
RT 1	4.9965	x10-3 SI	0.0139	0.2782	0.06	
SM30 Mode A	5.3645	x10-3 SI	0.1063	1.9817	0.39	1.13E-02
SM30 Mode B	5.3532	x10-3 SI	0.1297	2.4223	0.47	1.68E-02
SM30 Extrapolation	5.1435	x10-3 SI	0.1061	2.0636	0.45	1.13E-02
SM30 Interpolation	5.268	x10-3 SI	0.1123	2.1322	0.45	1.26E-02
SM30 Scanning	5.355	x10-3 SI	0.0248	0.4634	0.09	6.16E-04
MS2C	21.5352	x10-3 SI	0.0021	0.0096	0.008	4.30E-06
MS2K	17.7231	x10-3 SI	0.0964	0.5439	0.348	9.29E-03
GDD Probe	18.915	x10-3 SI	0.3746	1.9802	1.5	1.40E-01
KT 10	5.7885	x10-3 SI	0.0843	1.4562	0.293	7.11E-03
Pegmatite @ 915.4 ft						

	Mean		StD	%CV	Range	Variance
RT 1	0	x10-3 SI	0	*	0	0.00E+00
SM30 Mode A	0.0481	x10-3 SI	0.0017	3.6275	0.007	3.05E-06
SM30 Mode B	0.0482	x10-3 SI	0.0017	3.5244	0.005	2.89E-06
SM30 Extrapolation	0.0471	x10-3 SI	0.0024	5.1434	0.0119	5.87E-06
SM30 Interpolation	0.0446	x10-3 SI	0.0012	2.783	0.0039	1.54E-06
SM30 Scanning	0.0451	x10-3 SI	0.001	2.1461	0.003	9.37E-07
MS2C	0.171	x10-3 SI	0.0184	10.785	0.0578	3.40E-04
MS2K	0.0808	x10-3 SI	0.0006	0.7271	0.002	3.45E-07
GDD	0	x10-3 SI	0	*	0	0.00E+00
KT 10	0.0706	x10-3 SI	0.0053	7.5236	0.03	2.82E-05
Quartzite @ 996.1 ft						
	Mean		**StD**	**%CV**	**Range**	**Variance**
RT 1	0	x10-3 SI	0	*	0	0.00E+00
SM30 Mode A	-0.0023	x10-3 SI	0.0011	-49.6904	0.004	1.25E-06
SM30 Mode B	-0.0018	x10-3 SI	0.0016	-90.5882	0.007	2.51E-06
SM30 Extrapolation	-0.0033	x10-3 SI	0.0018	-53.4795	0.0084	3.16E-06
SM30 Interpolation	-0.0023	x10-3 SI	0.0018	-78.6866	0.0085	3.25E-06
SM30 Scanning	-0.0014	x10-3 SI	0.001	-71.0516	0.003	9.89E-07
MS2C	-0.0253	x10-3 SI	0.004	-15.9269	0.0126	1.62E-05
MS2K	-0.0074	x10-3 SI	0.0005	-6.7265	0.002	2.50E-07
GDD	0	x10-3 SI	0	*	0	0.00E+00
KT 10	0.007	x10-3 SI	0.0022	31.1323	0.009	4.68E-06

Table 52: Shows the averaged MS data collected on KT-10 calibration sample using all instruments, except MS2C because of the shape and size of the sample

Date	RT-1	KT-10	GDD	MS2K	SM30
	($x10^{-3}$)	($x10^{-3}$)	($x10^{-3}$)	($x10^{-3}$)	($x10^{-3}$)
25/05/2013	36.48	35.7	34.97	38.25	33.27
02/06/2013	35.8	35.73	35.12	37.31	33.28
17/06/2013	35.6	35.8	35.38	38.9	33.31
23/06/2013	35.34	35.63	35.21	37.91	33.24
12/07/2013	35.76	35.66	35.01	38.5	33.29
16/07/2013	35.59	35.68	35.19	38.62	33.36
17/07/2013	35.95	35.78	35.34	38.03	33.36
18/07/2013	35.79	36.05	35.36	38.65	33.38

Table 53: Shows data collected using the six hand-held MS instruments and the BSS-02B probe used with the IFG interface box.

Depth	Lithology	BSS-02B	RT1	KT10	GDD	MS2K	MS2C	SM30 B
1368.49	Gneiss	0.366	0.024	0.096	0.116	0.093	0.201	0.077
1381.04	Amphibolite	2.359	0.302	0.305	0.624	0.473	1.064	0.279
1388.19	Gneiss	0.402	0.086	0.137	0.270	0.104	0.453	0.157
1390.49	Amphibolite	0.246	1.430	0.888	2.862	1.535	4.506	0.944
1408.99	Gneiss	0.326	0.078	0.158	0.232	0.395	0.686	0.151
1410.04	Amphibolite	0.290	0.040	0.351	0.634	0.458	0.644	0.110
1418.49	Gneiss	0.093	0.302	0.166	0.304	0.242	1.239	0.327
1428.04	Granitized Gneiss	0.093	0.062	0.079	0.166	0.107	0.176	0.183
1437.49	Granitized Gneiss	0.122	0.008	0.125	0.216	0.187	0.214	0.083
1447.04	Granitized Gneiss	0.218	0.000	0.119	0.166	0.081	0.248	0.122
1457.04	Pegmatite	0.327	0.000	0.089	0.116	0.090	0.585	0.139
1466.79	Amphibolite	0.207	0.000	0.277	0.572	0.440	0.202	0.065
1470.69	Granitized Gneiss	0.187	0.140	0.124	0.254	0.127	0.980	0.233
1480.04	Amphibolite	0.175	0.146	0.203	0.332	0.414	0.353	0.109
1489.39	Pegmatite	0.393	0.000	0.062	0.076	0.053	0.902	0.178
1498.04	Pegmatite	0.265	0.042	0.065	0.144	0.115	0.255	0.034
1503.04	M1 Quartzite	0.200	0.000	0.036	0.108	0.090	0.160	0.045
1507.04	Pegmatite	0.257	0.000	0.084	0.158	0.151	0.258	0.035
1511.29	Skarn	0.073	0.000	0.215	0.358	0.262	0.698	0.054
1517.04	Skarn	0.049	0.000	0.239	0.558	0.475	0.472	0.168
1526.59	Skarn	0.366	0.008	0.129	0.346	0.424	0.324	0.236
1534.79	Skarn	0.104	0.020	0.205	0.464	0.201	0.680	0.119
1535.99	Pegmatite	0.360	0.002	0.069	0.380	0.295	0.158	0.174
1545.49	Pegmatite	0.265	0.000	0.075	0.290	0.097	0.149	0.118
1564.59	Pegmatite	0.088	0.000	0.224	0.004	0.036	0.045	0.078
1573.49	Pegmatite	0.239	0.000	0.940	0.226	0.059	0.100	0.029
1575.99	Pegmatite	0.167	0.000	4.706	9.026	40.287	41.045	2.964
1577.99	M. Pegmatite	0.305	4.582	16.968	50.020	48.707	135.001	12.800
1579.99	Schist	1.222	2.526	3.926	10.740	6.119	27.614	4.978
1581.79	M. Schist	0.629	27.924	5.675	10.820	16.239	32.756	4.424
1583.99	Schist	0.221	9.032	1.519	1.864	2.516	7.358	1.204
1585.59	Massive sulphide	-2.096	44.840	27.868	118.400	70.599	205.428	26.740

Table 54: Show MS measurements collected using KT-10 meter on KT-10 calibration sample. The data was used to assess the two modes and the pin option.

Measure mode with Pin	Measure mode without pin	Scanner mode without pin
37.516	35.608	35.703
40.216	35.584	35.703
37.718	35.635	31.404
37.184	35.638	30.118
38.947	35.643	35.353
38.045	35.64	35.333
37.417	35.612	35.46
37.705	35.702	35.703
38.02	35.638	35.486
37.915	35.682	35.26
37.847	35.674	35.583
37.552	35.712	35.382
37.19	35.662	35.457
36.956	35.702	35.504
37.766	35.727	35.552
37.751	35.669	34.877
38.409	35.736	35.092
38.144	35.73	34.717
37.101	35.718	35.325
37.611	35.748	34.236
37.772	35.725	32.153
37.546	35.757	33.787
37.962	35.715	35.401
37.672	35.717	35.518
37.793	35.781	35.528
38.052	35.735	35.459
38.148	35.764	35.529
37.201	35.787	35.475
36.673	35.72	35.582
37.593	35.735	35.487
38.2	35.714	33.947
38.425	35.687	35.011
37.955	35.727	35.542
37.763	35.771	35.669
37.753	35.734	35.512
37.925	35.781	35.376

AUTHOR'S PROFILE

- **Name:** Deng Ngang Deng
- **Place of Birth**: Cueiker, Kolnyang Payam, Bor county, Jonglei State, Republic of South Sudan
- **Date of Birth**: May 06, 1984

Schools Attended

- **Raja Primary School**, Kakuma Refugee camp, Kenya from 2000 to 2002, KCPE Certificate. **Courses**: English, Kiswahili, Mathematics, Geography, History and Government combined with Christian Religious Education and Science (339 marks out of 500 marks)
- **Kakuma Refugee Secondary School**, Kenya; from 2003 to 2005 after completion of grade 11. **Courses**: English, Kiswahili, Mathematics, Chemistry, Physics, Biology, Business Studies, History and Government, Christian Religious Education, Geography and Agriculture
- **Arnesen's Secondary School**, Kenya; Kenya Certificate of Secondary Education. Scoring a mean grade of **A-** from eight courses: English (B-), Kiswahili (B-), Mathematics (A), Chemistry (A), Physics (A), Biology (A-), Christian Religious Education (A) and Business Studies (A-)
- **Windle Trust Kenya**, Kakuma Kenya; Advanced Communicative English Course (A-), 2005

Universities Attended

- **Laurentian University**, Department of Earth Sciences, Sudbury Ontario, Canada; Thesis Masters of Geology 2012 – 2014
- **University of Toronto**, Department of Earth Sciences, Toronto Ontario, Canada; Honours BSc. Geology (with Distinction), 2008 – 2012

Scholarships & Awards

- The University of Toronto - The James P. Nowlan Explorers Awards (2012)
- Geological Association of Canada- Best student's prize (2011)
- The University of Toronto - Dr. Anderson Abbott Scholarship (2010)
- World University Service of Canada (WUSC) Scholarship (2008/2009)

Work Experiences

- **Mine Geologist (G.I.T II) –** Vale, Thompson, MB (Nov. 2013 – present)
- **Exploration Geologist (G.I.T I)-** Vale, Thompson, MB (Aug, 2012 - Nov. 2013)
- **Exploration casual Geologist (contract) –** Vale, Thompson, MB (Oct.2011 – Aug. 2012)
- **Jr. geologist (contract) –** Rencore Resources Ltd (10th June – 7th July, 2011)
- **Geophysical Research Assistant:** Tell Ta'yinat Archaeological Project, Turkey (2010 - 2011)
- **Geophysical Research Assistant**, Whitefish Falls, Ontario Canada,(2009-2010)
- **Chemistry & Physics teacher** – Kakuma Secondary, Kenya (2007 - 2008)
- **Mathematics teacher** – Imatong primary school, Kenya (January – May 2007)

Professional Affiliations

- Association of Professional Geoscientists of Ontario
- Geological Survey of Africa (GSAF)

Book

- Genealogy of my grandfather – Anuet Thodoh. Still in the press at the time of this thesis submission